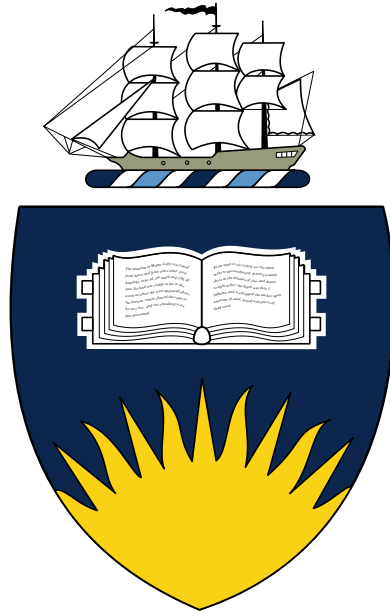


**Validating dipeptidyl peptidase (DP) 8 and DP9
potential substrates and investigating the effects of DP8
and DP9 overexpression and silencing on adenylate
kinase (AK) 2 in ovarian cancer cells**



**School of Biological Sciences
Flinders University of South Australia**

Dono Indarto

2013

**Thesis submitted in fulfillment of the requirement for the degree of
Doctor of Philosophy**

DECLARATION

I certify that this thesis does not incorporate without acknowledgment any material previously submitted for a degree or diploma in any university; and that to the best of my knowledge and belief it does not contain any material previously published or written by another person except where due reference is made in the text.



.....
Dono Indarto

.....
Date

I hereby certify that this statement is correct, that this thesis is properly presented and is of sufficient standard, *prima facie*, worthy examination.

Ass. Prof. Catherine A. Abbott
(Principal Supervisor of this study)

Ass. Prof. Robert I. Menz
(Co-Supervisor of this study)

TABLE OF CONTENTS

Declaration	i
Table of Contents	ii
List of Figures	ix
List of Tables.....	xii
Acknowledgments.....	xiii
Publication derived from this thesis at time of submission.....	xvi
Abstract	xvii
Abbreviations	xx
1. Introduction	1
1.1. DP family	2
1.1.1. DP4.....	2
1.1.2.1. DP4 structure.....	2
1.1.2.2. DP4 expression	4
1.1.2.3. Clinical aspects of DP4	6
1.1.2. FAP	10
1.1.2.1. FAP structure and its proteolytic activity	10
1.1.2.2. FAP expression	12
1.1.2.3. Clinical Aspects of FAP.....	13
1.1.3. DP8 and DP9.....	15
1.1.3.1. DP8 and DP9 structures	15

1.1.3.2. DP8 and DP9 expression.....	17
1.1.3.3. DP8 and DP9 substrate specificity and its function.....	18
1.1.3.4. The potential functions of DP8 and DP9	20
1.1.3.5. Using proteomics to determine DP8/DP9 substrates	21
1.2. Hypothesis.....	24
1.3. Project aims.....	24
2. Materials and Methods.....	26
2.1. Distilled water	26
2.2. Buffers and solutions	26
2.2.1. Phosphate buffered saline (PBS).....	26
2.2.2. 1 M Tris-HCl pH 7.4.....	26
2.2.3. 1 M NaCl.....	27
2.2.4. Tris buffer (50 mM Tris-HCl pH 7.4 and 150 mM NaCl).....	27
2.2.5. 100 mM EDTA	27
2.2.6. 1 M DTT	27
2.2.7. 1 M Sucrose	28
2.2.8. 150 mM MgCl ₂	28
2.2.9. 100 mM EGTA	28
2.2.10. 1 M KCl	28
2.2.11. 200 mM HEPES pH 7.5	28
2.2.12. Buffer and solution for flow cytometry analysis	28

2.2.13. Buffers and solutions for cell extraction	29
2.2.14. Buffers and solutions for AK assay	30
2.2.15. Buffers and solutions for SDS-PAGE and Western blotting	33
2.3. Methods.....	37
2.3.1. Cell stocks used.....	37
2.3.2. Growing cancer cell lines.....	37
2.3.3. Harvesting cancer cell lines	38
2.3.4. Counting cell number using trypan blue exclusion assay	39
2.3.5. Preserving cancer cell lines.....	39
2.3.6. Protein analysis	40
2.3.6.1. Cell extraction	40
2.3.6.2. Bicinchoninic acid (BCA) protein assay.....	40
2.3.6.3. DP enzyme activity	41
2.3.7. Western Blotting	42
2.3.7.1. SDS-PAGE.....	42
2.3.7.2. Blotting the gels on the polyvinyl difluoride (PVDF) membrane	42
2.3.7.3. Ponceau staining.....	43
2.3.7.4. Immunoblotting.....	44
2.3.7.5. Stripping and reprobing the membrane.....	46
2.3.8. Statistical analysis	46
3. Validating DP8 and DP9 potential substrates with biochemical and <i>in vitro</i> assays	47

3.1. Introduction	47
3.2. Materials and methods	50
3.2.1. MALDI-TOF mass spectrometry analysis	50
3.2.2. Cell Culture	52
3.2.3. Flow cytometry analysis	52
3.2.4. Immunocytochemistry.....	53
3.2.5. Western Blotting	54
3.2.6. DP enzyme activity	55
3.3. Results	55
3.3.1. Characteristics of stable SKOV3 cell line.....	55
3.3.2. Co-localization of DP8/DP9 and AK2/calreticulin in SKOV3 cells	57
3.3.3. Validation of potential DP8 and DP9 substrates.....	61
3.4. Discussion	75
3.4.1. AK2 and calreticulin are natural substrates for DP8 and DP9.....	75
3.4.2. Validation of potential substrates for DP8 and DP9.....	78
3.4.3. Proteins with a signal sequence:	79
3.4.4. Substrates which contain a Met that is removed.....	80
3.4.5. Proteolytic activity rate of DP8 and DP9.....	84
3.4.6. Limitation of these assays	84
4. Investigation of the effects of DP8 and DP9 overexpression on AK2 expression and activity in SKOV3 cells.....	88
4.1. Introduction	88

4.2. Materials and Methods	90
4.2.1. Cell culture	90
4.2.2. Cell proliferation assay	91
4.2.3. Adenylate energy charge (AEC) assay	91
4.2.4. Mitochondria isolation	92
4.2.5. BCA protein assay	93
4.2.6. DP enzyme activity	94
4.2.7. LDH assay	94
4.2.8. AK assay	95
4.2.9. Western Blotting	95
4.2.10. Statistical analysis	96
4.3. Results	97
4.3.1. Characterization of SKOV3 cells overexpressing wt and mt DP8/DP9	97
4.3.2. Purity of mitochondria extracted from SKOV3 cells with DP8 and DP9 overexpression.....	99
4.3.3. AK2 activity in SKOV3 cells with DP8 and DP9 overexpression	102
4.3.4. Adenine nucleotide levels in DP8 and DP9-overexpressing SKOV3 cells	106
4.4. Discussion	109
5. Investigation of the effect of DP8 and DP9 silencing on AK2 protein expression and enzyme activity in ovarian cancer cell lines.....	115

5.1. Introduction	115
5.2. Material and Methods	118
5.2.1. Cell culture of ovarian cancer cell lines	118
5.2.2. siRNA transfection.....	118
5.2.3. Cell extraction and protein quantification.....	119
5.2.4. Measuring adenine levels and AEC values.....	120
5.2.5. DP enzyme activity assay	120
5.2.6. AK activity assay	120
5.2.7. Western Blotting	121
5.2.8. Statistical analysis	121
5.3. Results	122
5.3.1. Characteristics of the three ovarian cancer lines.....	122
5.3.2. Validation of DP8, DP9 and AK2 siRNAs in ovarian cancer cell lines	124
5.3.3. Effects of DP8 and DP9 siRNA silencing on AK2, AMPK and AEC levels	127
5.4. Discussion	131
6. General discussion and conclusion	135
6.1. Potential natural substrates for DP8 and DP9.....	135
6.2. AK2 processing by DP8.....	139
6.3. DP8 protein is a potential target for inhibition of ovarian cancer cells	139
6.4. DP9 promotes cancer progression.....	142

6.5. Limitation of this study	145
6.6. Conclusions and future directions	149
7. References	150
8. Appendices	174

LIST OF FIGURES

Figure 1.1. Schematic of the DP4 homodimeric form with its transmembrane domains.....	4
Figure 1.2. Superposition of FAP with DP4 using USCF chimera program (Pettersen et al., 2004).....	12
Figure 1.3. N terminal peptides of nine potential substrates for DP8 and DP9 identified by TAILS (Wilson, 2011).....	22
Figure 3.1. Characterization of SKOV3 cells overexpressing wt and mt DP8 and DP9 proteins.....	56
Figure 3.2. Protein expression in SKOV3 cells overexpressing wt and mt DP8 and DP9.....	58
Figure 3.3. Co-localization of AK2 with DP8 and DP9 in stable SKOV3 cells.....	59
Figure 3.4. Co-localization of calreticulin with DP8 and DP9 in SKOV3 cells.....	60
Figure 3.5. DP8, DP9 and DP4 cleavage activity toward the N- terminus bifunctional purine biosynthesis protein PURH.....	67
Figure 3.6. DP8, DP9 and DP4 cleavage activity toward the N- terminus of C-1-tetrahydrofolate synthase, cytoplasmic.....	68
Figure 3.7. DP8, DP9 and DP4 cleavage activity toward the N – terminus of cathepsin Z/X.....	69
Figure 3.8. DP8, DP9 and DP4 cleavage activity toward the N- terminus of dihydropyrimidine dehydrogenase [NADP ⁺].....	70
Figure 3.9. DP8, DP9 and DP4 cleavage activity towards the N-terminus of mitochondrial import receptor subunit TOM34.....	72
Figure 3.10. DP8, DP9 and DP4 cleavage activity toward the N- terminus of obg-like ATPase 1.....	73

Figure 3.11. DP8, DP9 and DP4 cleavage activity towards the N- terminus of serine/threonine-protein phosphatase 6.....	74
Figure 4.1. Characteristics of SKOV3 cells overexpressing wt and mt DP8/DP9 proteins.....	99
Figure 4.2. Cell viability of SKOV3 cells overexpressing wt and mt DP8/DP9 proteins.....	100
Figure 4.3. Characterization of purified mitochondria from wt and mt DP8/DP9 over-expressing SKOV3 cells.	101
Figure 4.4. AK kinetic profiles in cytoplasmic and mitochondrial fractions from SKOV3 cells overexpressing wt and mt DP8/DP9.	105
Figure 4.5. Specific AK enzyme activity in cytoplasmic and mitochondrial fractions from SKOV3 cells overexpressing wt and mt DP8/DP9.	106
Figure 4.6. Adenylate energy charge of SKOV3 cells overexpressing wt and mt DP8/DP9.	108
Figure 5.1. Characteristics of the three ovarian cancer cell lines.....	123
Figure 5.2. Immunoblot analysis of ovarian cancer lines transfected with DP8, DP9 and AK2 siRNAs.	124
Figure 5.3. DP enzyme activity in ovarian cancer cell lines transfected with 50 nM DP8, DP9 and AK2 siRNA.....	126
Figure 5.4. Relative protein expression of DP8 and DP9 in ovarian cancer lines transfected with DP8, DP9 and AK2 siRNAs.....	127
Figure 5.5. AK specific enzyme activity in ovarian cancer cell lines transfected with 50 nM DP8, DP9 and AK2 siRNA.	129

Figure 5.6. Relative protein expression of AK2, total AMPK and phosphorylated AMPK in ovarian cancer lines transfected with 50 nM DP8, DP9 and AK2 siRNA.	130
Figure 5.7. Adenylate energy charge of SKOV3 cells 72h after transfection with 50 nM DP8, DP9 and AK2 siRNAs.....	131
Figure 6.1. A model for the regulation of AK2 activity by DP8. Modified from (Luo et al., 2010; Hardie, 2011a).....	143
Figure 8.1. DP8, DP9 and DP4 cleavage activity towards the N terminus acetyl-CoA acetyltransferase.....	174
Figure 8.2. DP8, DP9 and DP4 cleavage activity towards the N terminus of AK2.	175
Figure 8.3. DP8, DP9 and DP4 cleavage activity towards the N terminus of calreticulin.....	176
Figure 8.4. DP8, DP9 and DP4 cleavage activity towards the N terminus of collagen-binding protein 2 (Serpin H-1).....	177
Figure 8.5. DP8, DP9 and DP4 cleavage activity towards the N terminus of endoplasmin.	178
Figure 8.6. DP8, DP9 and DP4 cleavage activity towards the N terminus of enoyl-CoA hydratase.....	179
Figure 8.7. DP8, DP9 and DP4 cleavage activity towards the N terminus of heat shock 70 kDa protein 1L.	180
Figure 8.8. Glucose and fatty acid metabolism in SKOV3 cells with DP8 and DP9 overexpression.....	181
Figure 8.9. Protein expression of AK2 in cell fractions from SKOV3 cells with wt and mt DP8/DP9 overexpression.	182

LIST OF TABLES

Table 2.1. Propagation of ovarian cancer cells	38
Table 2.2. Primary and secondary antibodies used for Western blotting.....	45
Table 3.1. Cleavage of DP8 and DP9 potential substrates.....	63
Table 4.1. AK assay mixture modified from Bergmeyer (1974).	96
Table 4.2. AK binding affinity to AMP and maximum reaction rate of SKOV3 cells overexpressing wt and mt DP8/DP9.	104

ACKNOWLEDGMENTS

In the name of Allah, the most Gracious and the most Merciful. All praise is due to Allah, the Lord of all creatures existing in the universe.

At first, I would like to thank my supervisor Associate Professor Catherine A. Abbott for giving me an opportunity to perform this PhD research project in her laboratory and for her guidance, critical thinking and time during the study and for broadening my horizon about dipeptidyl peptidase knowledge and writing a standard thesis. I would also like to thank her for helping me to obtain a travel grant to present part of my thesis at an International conference and a tuition waiver for my 6 month study.

I would like to thank my co-supervisor Associate Professor Robert Ian Menz for discussing the research project and kinetic profiles of adenylate kinase activity and helping purify recombinant human DP8 protein.

I would particularly like to thank Dr. Claire H. Wilson for providing SKOV3 cells overexpressing DP8 and DP9 proteins and an opportunity to become second author on her publication. I would like to thank Lisa Pogson for helping me to conduct matrix-assisted laser desorption ionization time of flight mass spectrometry (MALDI-TOF MS) analysis, to create figures using computer programs, Power point 2010 and Bio-Rad Image Lab and editing this thesis. Dr. Hanna Krysinska is thanked for providing an alternative technique to isolate mitochondria and helping edit this thesis. Michele Squirt and her friend (PhD student at the University of South Australia) are thanked for helping perform the breath test. Thanks to past and present

students in the Abbott laboratory (Dr Samsu U. Nurdin, Babek Esmeelian, Dr Melissa Pitman, Kym McNicholas, Usma Munawara and Robert Xiao) for their immeasurable comments throughout my study.

Associate Professor Peta Macardle is thanked for allowing me to perform flow cytometry in her laboratory. Dr. Daniel Jardine and Jason Young are thanked for helping analyze adenylate nucleotide levels, discussing problems arising during HPLC analysis and allowing me to perform MALDI-TOF MS analysis in the Flinders Analytical laboratory. Dr. Jennifer Clarke is thanked for her training in the use of fluorescence and confocal microscopes.

I would also like to thank Dr. Tong Chen and Dr. Roger Yazbeck for their assistance in explaining the experimental protocols such as immunocytochemistry, cell culture, Western blotting and breath test.

Special thanks should be given to my Indonesian brothers in the Muslim Society in South Australia who helped analyze the experimental data with the SPSS program and gave me the spiritual support that allowed me to complete my studies.

Finally, I would like thank my parents, sisters and brothers for your financial and spiritual support throughout my study and my life. For my beloved wife, Desianna Kusumadewi thank you for your dedication to look after our sons in Indonesia on your own while I have been working on my PhD at Flinders University here in Australia. My sons (Denobia Faishal Kusindarto, Dofito Hanifah Kusindarto and

Daustriid Shafwan Kusindarto), I will always remember your support and motivation by saying “when I go back to Indonesia”.

PUBLICATION DERIVED FROM THIS THESIS AT TIME OF SUBMISSION

Full publication

Wilson, C. H., **Indarto, D.**, Doucet, A., Pogson, L. D., Pitman, M. R., McNicholas, K., Menz, R. I., Overall, C. M. and Abbott, C. A. (2013) Identifying natural substrates for dipeptidyl peptidase 8 and 9 using terminal amine isotopic labeling of substrates (TAILS) reveals in vivo roles in cellular homeostasis and energy metabolism. *Journal of Biological Chemistry* 288: 13936-13949 (part of this publication derived from Chapter 3 in this thesis). Images from chapter 3 were also used to construct the cover image for this edition.

Conference Abstracts

Indarto, D., Wilson, C. H., Pogson, L., Menz, I. R. and Abbott, C. A. (2012) Bio-molecular function of dipeptidyl peptidase 8 and 9 in ovarian cancer cell line (SKOV3). **Poster** at Gordon Research Conference on Proteolytic Enzymes & Their Inhibitors. Proteolysis: the most important post translational modification regulating biology, life and death of every cell, Lucca, Barga, Italy, 17 – 22 June 2012

Indarto, D., Wilson, C. H., Menz, I. R. and Abbott, C. A. (2012) Co-expression of Dipeptidyl peptidase 9 and adenylate kinase 2 may be involved in cell tumor inhibition of ovarian cancer cell line (SKOV3). **Oral presentation** at the Australian Society of Medical research conference, Adelaide, South Australia, 6 June 2012

ABSTRACT

The dipeptidyl peptidase (DP) 4 gene family is a serine protease family that cleaves various biopeptides at the post-prolyl bond. DP4 is the most studied member of the family and is involved in regulating metabolism, the immune system and cell signaling. Fibroblast activation protein (FAP) is another member of the DP4 gene family that contributes to tissue proliferation during cell malignancy and wound healing. In contrast to DP4 and FAP, the biological functions of DP8 and DP9 are still under investigation although their mRNA and protein are ubiquitously expressed in human tissues. Previous work in the laboratory using a proteomics approach identified adenylate kinase 2 (AK2) and other proteins as potential *in vivo* DP8 and DP9 substrates and revealed a role for DP8 and DP9 in cell metabolism. AK2 is an enzyme that is localized in the intermembrane space of mitochondria. This enzyme has a pivotal role in catalyzing reversibly ATP and AMP to 2ADP, maintaining cellular energy homeostasis. The major aim of this study was to further validate the substrates identified and to investigate the role of these proteases in cellular metabolism, in particular in regulating the function of AK2.

Immunocytochemistry and western blotting were used for studying DP8 and DP9 co-localization with AK2 and calreticulin in ovarian cancer cell lines (SKOV3) overexpressing DP8 and DP9, which were tagged with enhanced green fluorescent protein (EGFP). MALDI-TOF mass spectrometry (MS) was then used to test a further 12 substrates for cleavage by DP8 and DP9 that were previously identified using a recent proteomics approach. Cleavage activity of DP8 and DP9 towards AK2 in these SKOV3 cells was evaluated using proliferation rate and AK assays. Changes in adenine nucleotide levels (ATP, ADP and AMP) and cellular energy charge were

assessed by using high performance liquid chromatography (HPLC). DP8 and DP9 small interfering RNA (siRNA) were used to silence these proteases in OVCA 429, OVCA 432 and SKOV3 cell lines in order to test the effects of each DP gene on AK2 protein and enzyme activity.

Immunofluorescence confocal microscopy was used to demonstrate that DP8 and DP9 and their substrates AK2 and calreticulin are in close proximity. No difference in substrate localization was observed in cells expressing wt or mt proteases. The work also revealed that N-terminal oligopeptides of seven of 12 potential substrates are cleaved by DP8, DP9 and DP4. However cleavage rates differed between the three enzymes, reflecting differences in their active sites. These differences reflect different amino acids that line entry to the catalytic site and the site itself between the three proteases. In the first six hrs after sub culture in a 96 well plate cells expressing wt and mt DP8 had increased viability compared to vector expressing cells, while the proliferation rate of SKOV3 cells with wt and mt DP9 overexpression was lower. In contrast in a T75 flask it was observed that both wt and mt DP8 took longer to reach confluence and that vector and wt and mt DP9 expressing cells (four days compared to seven). In these SKOV3 cells overexpressing wt and mt DP9, ATP levels and adenylate energy charge decreased significantly, compared to those in SKOV3 cells overexpressing vector control. Meanwhile, ADP and AMP levels in SKOV3 cells overexpressing wt and mt DP9 increased but a significant increase in AMP level was only observed in SKOV3 cells overexpressing wt DP9. ADP/ATP and AMP/ATP ratios also increased in wt and mt DP9 overexpression. This data combined suggests opposite roles for both DP8 and DP9 in cell growth and proliferation that are independent of their enzyme activity.

DP8 and DP9 were silenced in three different ovarian cancer cell lines. The results were more similar in OVCA 423 and SKOV3 cells than in OVCA 429 cells, this difference probably reflects the different phenotypes of these cells to start with. Intriguing data was obtained using silencing that suggests that *in vivo* in SKOV3 cells that AK2 is a substrate of DP8 but not DP9. DP8 silencing led to a decrease in AK specific activity and an increase in AMPK phosphorylation. A similar result was observed when AK2 was silenced in these cells. In contrast DP9 silencing had no significant effect on AK specific activity but did appear to increase the expression of AK2 and had no effect on AMPK phosphorylation

In summary this work has provided additional evidence for the role of DP8 and DP9 in maintaining cellular metabolism. However, further work is required. Important questions that need to be answered is what effect does DP9 and or DP8 overexpression have on activated AMPK and the pathways downstream including glucose uptake and lactate production. In addition more work needs to be performed to investigate the effect of DP8 and DP9 silencing on genes downstream of AMPK. DP8 and DP9 may modulate AMPK an important player in both cellular metabolism and cancer growth. Further understanding of this role may lead to development of DP8/DP9 inhibitors or activators that may be used to treat cancers such as ovarian cancer.

ABBREVIATIONS

ADA	adenosine deaminase
AK	adenylate kinase
AK2	adenylate kinase 2
ADP	adenosine diphosphate
AMP	adenosine monophosphate
AMPK	adenosine monophosphate kinase
ANOVA	analysis of variance
ATCC	American type tissue collection
ATP	adenosine triphosphate
APS	ammonium persulphate
BCA	bicinchoninic acid
BSA	bovine serum albumin
C	celsius
Ca	calcium
cAMP	cyclic adenosine monophosphate
cDNA	complementary deoxyribonucleic acid
CD3	cluster of differentiation 3
CD4	cluster of differentiation 4
CD26	cluster of differentiation 26
CD47	cluster of differentiation 47
CD91	cluster of differentiation 91
CHAPS	3-[(3-cholamidopropyl) dimethylammonio]-1propanesulfonate
CO ₂	carbon dioxide
C terminus	carboxyl terminus
CXCL12	chemokine ligand 12
DAPI	4'-6-diaminidino-2-phenylindole
DMEM	Dulbecco's modified eagle medium
DMSO	dimethylsulfoxide
DNA	deoxyribonucleic acid
DP	dipeptidyl peptidase
DP8	dipeptidyl peptidase 8
DP9	dipeptidyl peptidase 9

DP6	dipeptidyl peptidase 6
DP4	dipeptidyl peptidase 4
DP10	dipeptidyl peptidase 10
DPD	dihydropyrimidine dehydrogenase
DTT	dithiothreitol
ECL	enhanced chemiluminescence
ECM	extracellular matrix
EDTA	ethylene diamine tetraacetic acid
EGFP	enhanced green fluorescent protein
EGF	epithelial growth factor
EGTA	ethylene glycol tetraacetic acid
FACS	fluorescence activated cell sorter
FAP	fibroblast activation protein
FBS	foetal bovine serum
FDA	food and drug administration
g	gram
GIP	gastric inhibitory polypeptide
GLP-1	glucagon like peptide 1
GLP-2	glucagon like peptide 2
GLUT	glucose transporter
h	hour
HCl	hydrochloric acid
HEK 293	human embryonic kidney cell line
HEPES	4-(2-hydroxyethyl)-1-piperazineethanesulfonic acid
HPLC	high performance liquid chromatography
HRP	horse radish peroxidase
HT-29	human colon adenocarcinoma grade II cell line
IBC	Institutional Biosafety Committee
IL-1	interleukin-1
IL-2	interleukin-2
IgG	immunoglobulin G
IP10	inflammatory protein-10
ITAC	interferon-inducible T cell chemo-attractant
K ₂ HPO ₄	dipotassium hydrogen phosphate

K_3PO_4	potassium phosphate
KCl	potassium chloride
kDa	kilo dalton
KH_2PO_4	monopotassium phosphate
KOH	potassium hydroxide
LDH	lactate dehydrogenase
M	molar
mAb F19	monoclonal antibody against the human FAP antigen
MALDI-TOF	matrix-assisted laser desorption ionization time of flight
Mg	magnesium
$MgCl_2$	magnesium chloride
$MgSO_4$	magnesium sulphate
MHC	major histocompatibility complex
min	minutes
ml	milliliter
mm	millimeter
mM	millimolar
Mn	manganese
mU	milliunit
mt	mutant
mRNA	messenger ribonucleic acid
MS	mass spectrometry
MTT	3-(4,5-dimethylthiazol-2yl)-2,5-diphenyl tetrazolium bromide
Na_2HPO_4	disodium hydrogen phosphate
NaCl	sodium chloride
NADP	nicotinamide adenine dinucleotide phosphate
NADH	nicotinamide adenine dinucleotide
NaOH	sodium hydroxide
NaN_3	sodium azide
nM	nanomolar
NK	natural killer
NPY	neuropeptide Y
N terminus	amino terminus
OD	optical density

OVCA 429	ovarian cancer cell line
OVCA 432	ovarian cancer cell line
SDS-PAGE	SDS polyacrylamide gel electrophoresis
pAMPK	phosphorylated adenosine monophosphate kinase
PBS	phosphate buffered saline
pEGFPN1	cloning vector containing EGFP
PEP	phosphoenol pyruvate
PK	pyruvate kinase
PKA	protein kinase A
PVDF	polyvinylidene difluoride
PYY	peptide YY
RANTES	regulated on activation normal T cell expressed and secreted
RFU	relative fluorescence intensity
RNA	ribonucleic acid
RPMI 1640	Roswell Park Memorial Institute 1640
RT	room temperature
RT-PCR	reverse transcript polymerase chain reaction
SDF 1 α and β	stromal cell-derived factors 1 α and 1 β
SCID	severe combined immunodeficient
SDS	sodium dodecyl sulphate
SEM	standard error mean
siRNA	small interfering RNA
SKOV3	ovarian cancer cell line
SOD	superoxide dismutase
SPSS	statistical package for the social science
TAILS	terminal amine isotopic labelling of substrates
TFA	trifluoroacetic acid
THF	tetrahydrofolate
TNF α	tumor necrosis factor α
TSP-1	thrombospondin-1
TEMED	N,N,N,N tetramethylenediamine
μ M	micromolar
UCSF	University of California, San Francisco
UK	United Kingdom

USA	United States of America
TIM	translocase of the inner membrane
TOM	translocase of the outer membrane
wt	wildtype

1. INTRODUCTION

In the last decade, the dipeptidyl peptidase (DP) gene family has been extensively studied because several members have become potential targets for the development of drugs to treat human diseases. This enzyme family is different from other serine proteases because dipeptidyl peptidases are exopeptidases that cleave various biopeptides and proteins at the post-prolyl bond. This family consists of four proteins, the extracellular proteins DP4 and fibroblast activation protein (FAP) and the cytoplasmic proteins DP8 and DP9. DP4 was the first member of the gene family discovered whose structure was determined (Engel *et al.*, 2003; Hiramatsu *et al.*, 2003; Oefner *et al.*, 2003; Rasmussen *et al.*, 2003). DP4 is involved in regulating metabolism, the immune system, cell signaling, the endocrine system and cancer biology (Yu *et al.*, 2010). FAP is another member of the DP gene family which has an identical three dimensional (3D) structure to DP4 (Scanlan *et al.*, 1994; Niedermeyer *et al.*, 1998; Aertgeerts *et al.*, 2005). FAP contributes to degrading extracellular matrix tissues during cell malignancy and scar formation (Scanlan *et al.*, 1994; Park *et al.*, 1999). FAP is also involved in stromagenesis and angiogenesis during tumor proliferation (Santos *et al.*, 2009) and in blood clotting formation (Lee *et al.*, 2006b). In contrast to DP4 and FAP, the biological functions of DP8 and DP9 are still under investigation although their mRNA and protein are widely expressed in human tissues. Therefore, the aim of this thesis is to validate DP8 and DP9 natural substrates in order to unravel their physiological roles in normal and abnormal conditions. In this chapter, each DP family member will be discussed in detail regarding their structure, expression and some advances in the clinical setting. Because DP8 and DP9 structures have not been solved, this literature review focuses on their expression and possible natural substrates and functions.

1.1. DP family

The DP family is an atypical serine protease family which belongs to the S9b subfamily. Four members (DP4, FAP, DP8, and DP9) have the distinctive ability to cleave proline or alanine in the second position from the N-terminus. The two remaining members (DP6 and DP10) lack the catalytic serine residue and thus serine protease activity. Although the enzyme members of the DP family are serine proteases, their catalytic motif (Ser- Asp- His) is the reverse of the classical serine proteases (His-Asp-Ser) like trypsin and chymotrypsin (Neurath, 1984; David *et al.*, 1993; Lambeir *et al.*, 2003b). Additionally, the catalytic serine site is flanked by Gly-Trp and Tyr-Gly-Gly residues, this is different to the sequences found in classical proteases (Gly-Asp-Ser-Gly-Gly-Pro) (Lambeir *et al.*, 2003b). The Gly-Trp-Ser-Tyr-Gly-Gly motif is split between two exons for DP4 and FAP but resides in one exon for DP8 and DP9 (Abbott *et al.*, 1994; Abbott *et al.*, 2000; Olsen and Wagtmann, 2002). Two glutamic acid residues in the propeller domain are also conserved in all members of the DP gene family and essential for substrate entry into the enzyme active site (Abbott *et al.*, 1999; Ajami *et al.*, 2003; Engel *et al.*, 2003; Aertgeerts *et al.*, 2005).

1.1.1. DP4

1.1.2.1. DP4 structure

DP4 is a 766 amino acid (aa) membrane-bound proteolytic enzyme which has a unique expression pattern in different tissues, cell types and cellular compartments of all organisms (Šedo and Malik, 2001). This enzyme was firstly identified in 1966 as glycylproline naphthylamidase (Hopsu-Havu and Glenner, 1966). Since this identification, many studies have been performed to elucidate its structure and

function in both physiological and pathological conditions. The *DP4* gene was initially cloned and sequenced from rat liver (Ogata *et al.*, 1989). With advances in molecular biology techniques, the complete DNA and aa sequences for DP4 were cloned from human lymphocytes (Misumi *et al.*, 1992) and murine thymocytes (Marguet *et al.*, 1992). In humans, *DP4* is located on the long arm of chromosome 2 locus 24.2 and contains 26 exons (Abbott *et al.*, 1994).

The DP4 protein sequence contains a transmembrane domain and immunostaining with DP4 antibodies has demonstrated that DP4 is expressed at the cell surface. DP4 contains a short N-terminus (1-6 aa) that acts a cytoplasmic tail (Engel *et al.*, 2003; Lambeir *et al.*, 2003b). This is linked to hydrophobic segment (7-28 aa) and the remaining extracellular sequences are attached to the membrane by a flexible stalk (29-48 aa). The DP4 extracellular component consists of a 49-289 aa glycosylated domain, a 290-510 aa cysteine domain and a 511-766 aa catalytic domain (Figure 1.1). A soluble form of DP4 exists that lacks the hydrophobic and N-terminus segments but the DP activity remains unchanged (Durinx *et al.*, 2000). The DP4 extracellular segment appears to have biological functions separate from the enzyme activity and is involved in cell signaling, binds to adenosine deaminase (ADA), caveolin-1 and extracellular matrix such as fibronectin (De Meester *et al.*, 1999; Lambeir *et al.*, 2003a; Ohnuma *et al.*, 2006).

X-ray crystallographic analysis indicates that the DP4 molecule consists of an α/β hydrolase domain and an eight bladed β -propeller domain (Engel *et al.*, 2003; Hiramatsu *et al.*, 2003; Rasmussen *et al.*, 2003). β sheets are predominantly found in the formation of the propeller and each propeller is linked together in the complex by

cysteine residues (Hiramatsu *et al.*, 2003). The DP4 protein forms homodimers, which are connected with several hydrogen bonds in order to retain the folded

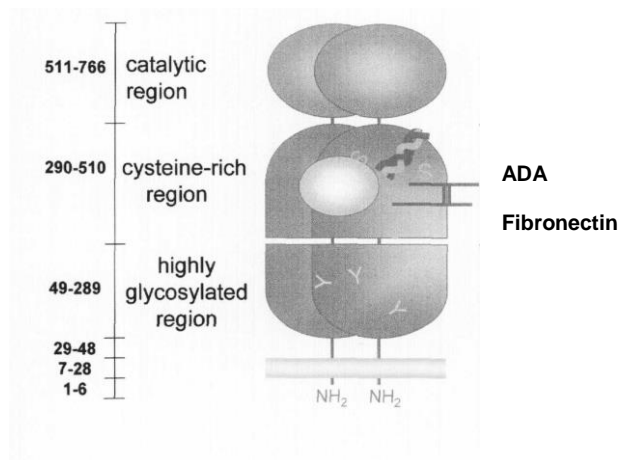


Figure 1.1. Schematic of the DP4 homodimeric form with its transmembrane domains. A majority of DP4 aa residues are located in the extracellular compartment. The remaining domains are the hydrophobic transmembrane domain and the cytoplasmic tail domain. Adapted from (Lambeir *et al.*, 2003).

structure (Engel *et al.*, 2003). Because the β propeller domain covers the catalytic site of DP4, which is situated in the α/β hydrolase domain, the enzyme's substrates are likely to reach the active site through a side opening that is constructed by blade 1 and the carboxyl terminus on the side of β propeller (Engel *et al.*, 2003; Hiramatsu *et al.*, 2003).

1.1.2.2. DP4 expression

DP4 is widely distributed in mammalian tissues and highly expressed on the surface of epithelial, endothelial, and immune cells (De Meester *et al.*, 1999). In mice, the highest levels of the DP activity of DP4 are found in liver, kidney, lung, immune system, and small intestine (Ansorge *et al.*, 2009). Whilst, in rat and human tissues, the kidney has the highest DP activity, followed by lung, adrenal gland, small intestine, and liver (Mentlein, 1999). The discrepancy is probably caused by use of different species. Surprisingly, both authors reported that only a small proportion of

the DP activity in brain and pancreas is coming from DP4 (Mentlein, 1999; Ansoorge *et al.*, 2009). There is no further information that clearly explains why those organs have the lowest DP activity.

DP4 or CD26 as it is also known is expressed at different levels in several cells of the immune system. Originally, CD26 was recognized as a molecule expressed by activated T cells that was induced by IL-2 (Fox *et al.*, 1984), anti CD3, antigen and mitogenic agents (Fleischer, 1987). Basically, most peripheral blood T cells express CD26/DP4 constitutively and the lowest amount of CD26/DP4 expression is found on resting cells (Fox *et al.*, 1984; Fleischer, 1987). After stimulation by pokeweed mitogen, CD26/DP4 seems to regulate development of CD4⁺ T and natural killer (NK) cells, cytokine secretion, and immunoglobulin G (IgG) production activated by T cells (Yan *et al.*, 2003). In term of expression on B lymphocytes and NK cells, there are different patterns between resting and activated forms. CD26/DP4 is detected at low levels or zero levels on resting B cells but it increases considerably after stimulation (Gorrell *et al.*, 1991; Bühling *et al.*, 1995). Meanwhile, cytokine-activated NK cells expressed prominently CD26/DP4 while resting NK cells are negative for CD26 (Bühling *et al.*, 1994). It is also reported that some populations of dendritic cells in skin and intestinal lymph nodes are positive for CD26/DP4 expression (Gliddon and Howard, 2002). Thus, coexpression of CD26/DP4 in activated- immune cells is implicated in regulation of cell proliferation (Bühling *et al.*, 1994).

1.1.2.3. Clinical aspects of DP4

Because the specific function and natural substrates of DP4 protein will be tissue-dependent, inhibition of DP activity will have different clinical implications. During food intake, for instance, the DP activity of DP4 modulates the expression of gastric inhibitory polypeptide (GIP) and glucagon like peptide-1 (GLP-1) peptides to maintain normal levels of plasma glucose (Drucker and Nauck, 2006). In healthy people, both incretin hormones are responsible for more than 50% of insulin secretion after oral administration of glucose (Nauck *et al.*, 1986). In type-2 diabetic patients, however, bioactive GLP-1 levels are remarkably decreased resulting in a loss of the incretin effect (Holst and Gromada, 2004).

Sitagliptin, a DP4 inhibitor, is now approved by the food and drug administration (FDA) for treating patients who suffer type-2 diabetes. The inhibitor works by enhancing circulating levels of GIP and GLP-1 and is therefore a useful treatment for improvement of insulin deficiency (Mu *et al.*, 2009). However, several studies have indicated that a daily use of sitagliptin by type-2 diabetes patients might increase infections of respiratory, alimentary and urinary tracts (Amori *et al.*, 2007; Richter *et al.*, 2008). From these studies, it is necessarily noted that the researchers do not take consideration of individual immune status and history of illness before treatment with the DP4 inhibitor. White and coworkers (2010) also reported that CD4⁺ T cells isolated from peripheral blood patients, who suffer type-2 diabetes treated with sitagliptin, remain inactive after induction by phytohaemagglutinin and a similar result was also observed in CD4⁺ T cells of diabetic patients who were treated with sitagliptin. Therefore, the increased infections in the meta-analysis studies above may not be associated with T cell inhibition but perhaps other cells of the immune

system are involved (White *et al.*, 2010). Thus, in terms of patient safety, the immune system of patients on long term treatment with DP4 inhibitors should be monitored regularly since recent evidence has shown that the composition of lymphocytes like T and B and NK cells are significantly decreased in diabetic mice treated with sitagliptin (Kim *et al.*, 2009) and DP4 deficient rats (Klemann *et al.*, 2009). As described in Kim *et al.* (2009), a higher soluble DP activity was observed in type-1 diabetic mice that received islet transplantation compared to control mice and the increased DP activity is correlated with increased CD4⁺ T cell migration from spleen. Whereas, administration of sitagliptin during the islet graft in those mice decreased the DP activity and the CD4⁺ T cell migration. Thus, the sitagliptin might modulate T cell activity and the mechanism of action is probably via cyclic adenosine triphosphate (cAMP) and or protein kinase A (PKA) pathways (Kim *et al.*, 2009). From cAMP and PKA activity assays, incubation of splenic CD4⁺ T cells isolated from diabetic mice with porcine DP4 enzyme increases cAMP and PKA levels significantly, compared to control and sitagliptin administration abolishes the DP activity (Kim *et al.*, 2009). Although Kim's findings seem convincing, further research is required to check whether immune changes occur in patients with type-2 diabetes during long term sitagliptin treatment. Another study performed by Klemann *et al.* (2008) reveals that older rats lacking the DP4 gene have a lower number of CD4⁺ and memory T cells in thymus and B cells and NK cells in blood circulation than their counterparts. These findings indicate that CD26/DP4 plays an essential role in T cell maturation and migration through interacting with a specific site on antigen presenting cells (APCs). Furthermore, the decreased levels of B and NK cells may be related to low levels of DP activity of CD26/DP4 which influences B cell maturation in bone marrow and NK activity against pathogens respectively

(Ohnuma *et al.*, 2008; Klemann *et al.*, 2009). Other data collected from *in vitro* studies confirm a role for CD26/DP4 in T cell migration but that T cell mobility requires further cell signaling which up-regulates thrombospondin-1 (TSP-1), CD91 and CD47 expression (Liu *et al.*, 2009). Furthermore, the presence of vildagliptin (another DP4 inhibitor) in T cell culture activated by anti CD3 down-regulates TSP-1, CD47 and CD91 expression, leading to inhibition of lymphocyte migration and adhesion (Liu *et al.*, 2009). In addition, it should be noted that the type-2 diabetes commonly found in older people results from insulin deficiency. So far, obesity, genetic factors, lifestyle and physical activity have been considered as the main risk factor for type 2 diabetes (Zhao *et al.*, 2011; Zhao *et al.*, 2013). Recent studies in animal models and human subjects have showed that there is a causative direction between type-2 diabetes, inflammation and autoimmune disease (Donath and Shoelson, 2011; Nikolajczyk *et al.*, 2011; DeFuria *et al.*, 2013; Pedicino *et al.*, 2013). Thus, vildagliptin administration in patients with diabetes may also modulate the immune system.

Another application of DP4 inhibitors that has been proposed is to use them to treat autoimmune and inflammatory diseases. Rheumatoid arthritis is a human disease with a combination of chronic inflammation and autoimmune disorders, characterized by persistent activation of CD4⁺ T cells, macrophage and B cells (Firestein, 2003; Rodrigues *et al.*, 2009). In rheumatoid arthritis, CD26/DP4 might activate T lymphocytes and modify some chemokines (Busso *et al.*, 2005). Liu *et al.* (2009) support Busso's hypothesis by giving clear evidence that CD26/DP4 is involved in processing of chemokines CXCL12 and RANTES to stimulate T cell migration through induction of TSP-1, CD47 and CD91 expression. Other studies

also reported that the membrane-bound proteolytic enzyme of CD26/DP4 is increased in the synovial fluids and peripheral blood of patients with rheumatoid arthritis (Muscat *et al.*, 1994; Gerli *et al.*, 1996). The increased CD26/DP4 enzyme activity evidently correlates with severity of rheumatoid disease and is implicated in inflammatory progression (Muscat *et al.*, 1994; Gerli *et al.*, 1996; Ohnuma *et al.*, 2006).

Starting from these viewpoints, several research centers have tried to apply some DP4 inhibitors for treating rheumatoid arthritis. Tanaka and coworkers (1997), for example, used DP4 inhibitors, Ala-boroPro, Lys-[Z(NO₂)]-thiazolidide and Ala-Pro-nitro-benzoylhydroxylamine to treat arthritis rat models, induced by a type II collagen or alkyldiamine. The competitive DP4 inhibitor (Lys-[Z(NO₂)]-thiazolidide) seems to be more potent and reduced hind paw swelling as an arthritis indicator, compared to other DP4 inhibitors (Tanaka *et al.*, 1997). Interestingly, weight loss was also observed in both chemically induced-arthritis rats and was restored after subcutaneously injection of Ala-boroPro and Lys-[Z(NO₂)]-thiazolidide (Tanaka *et al.*, 1998). The mechanism of action underlying these effects is not well understood because administration of the DP4 inhibitors similarly inhibits mitogen- and antigen-activated lymphocytes from spleen and lymph node of normal and DP4 deficient rats (Tanaka *et al.*, 1997). Additionally, the Lys-[Z(NO₂)]-thiazolidide perhaps inhibits DP8 and DP9 activities as well because this inhibitor is not specific for DP4 (Reinhold *et al.*, 2009; Yazbeck *et al.*, 2009). To clarify these findings, further studies are needed to determine the involvement of other members of the DP gene family either in animal models or humans. Later, Tanaka et al developed another candidate therapeutic agent, a tetrahydroisoquinoline compound

that was isolated from *Aspergillus oryzae*. This antibiotic shows similar results to the previous DP4 inhibitors when administered to arthritis rats induced by alkyldiamine but uncompetitive inhibition to synthetic DP4 substrates with a $K_i = 5.3\mu\text{M}$ (Tanaka *et al.*, 1998). The DP inhibitory effect of tetrahydroisoquinoline is also observed in normal human serum and in a T cell line with IC_{50} values less than $10\mu\text{M}$ (Williams *et al.*, 2003). The anti-arthritic effect of this DP4 inhibitor is possibly via inhibition of lymphocyte proliferation since human and mouse lymphocytes induced by CD3 antibody and a bacterial antigen have a low proliferative response when co-incubated with tetrahydroisoquinoline (Williams *et al.*, 2003). However, further clinical studies are required to support the inhibitory effect of this antibiotic in patients who suffer rheumatoid arthritis.

1.1.2. FAP

1.1.2.1. FAP structure and its proteolytic activity

FAP is another member of the DP gene family that is an integral plasma membrane protein. However like for DP4, Lee *et al.* (2006) suggest that a soluble form of FAP is present in human plasma. This soluble FAP was initially recognized as an anti-plasmin protease, which inhibits fibrin degradation during blood clotting (Lee *et al.*, 2004; Lee *et al.*, 2006b). In general, FAP is similar to DP4. It shares DP activity and 50% aa identity to DP4, consists of 26 exons, and is located at 2q24.2 adjacent to DP4. Homodimerization is essential for its DP activity and a heterodimeric form that binds to DP4 is found in migratory cells in response to connective tissue repair (Gherzi *et al.*, 2002; Aertgeerts *et al.*, 2005). The DP activity of FAP is similar to that of DP4, it is able to cleave some peptide substrates with Gly-Pro residues in the N terminus. However, its catalytic activity is 100 fold weaker than the DP4 catalytic

activity (Aertgeerts *et al.*, 2005). As can be seen in the FAP structure, each monomeric FAP protein consists of an α/β hydrolase domain and an eight bladed β propeller domain as well (Figure 1.2) (Aertgeerts *et al.*, 2005). The catalytic residues of FAP, Ser⁶²⁴, Asp⁷⁰² and His⁷³⁴ are located in the α/β hydrolase domain but buried between the two domains (Aertgeerts *et al.*, 2005). Therefore like described for DP4 above, the active site can be accessed by FAP substrates through a central hole formed by eight blades of the propeller and/or by the side cavity between the α/β hydrolase and eight bladed β propeller domains (Aertgeerts *et al.*, 2005). Moreover, the FAP sequence also has five potential glycosylation sites, most of which are present in the β propeller sequence but their contribution to FAP biology is not understood (Aertgeerts *et al.*, 2005).

Even though FAP and DP4 are structurally very similar and share 50% aa identity (Aertgeerts *et al.*, 2005), FAP also has an endopeptidase activity and promotes tissue remodeling only in fetal and pathological conditions (Garin-Chesa *et al.*, 1990; Park *et al.*, 1999; Niedermeyer *et al.*, 2000; Aertgeerts *et al.*, 2005). Its endopeptidase activity results from a change of residue Asp⁶⁶³ instead of residue Ala⁶⁵⁷ as in DP4 (Aertgeerts *et al.*, 2005). From structural analysis and enzyme kinetic studies, this residue decreases negative charges in the active site and affinity for N terminal biopeptides, allowing FAP to operate as an endopeptidase (Aertgeerts *et al.*, 2005).



Figure 1.2. Superposition of FAP with DP4 using USCF chimera program (Pettersen *et al.*, 2004). The blue color is the human DP4 structure with 1PFQ PDB code (Oefner *et al.*, 2003) and human FAP is purple with 1Z68 PDB code (Aertgeerts *et al.*, 2005).

1.1.2.2. FAP expression

Originally, FAP was identified as an epitope of stromal fibroblasts expressed in epithelial cancers and granulation tissue of healing wounds (Garin-Chesa *et al.*, 1990; Scanlan *et al.*, 1994). Since this finding, FAP expression has also been observed during fetal tissue development (Niedermeyer *et al.*, 2000), chronic inflammation like liver cirrhosis (Levy *et al.*, 1999; Wang *et al.*, 2008) and other types of malignancy such as melanoma (Huber *et al.*, 2003), multiple myeloma (Ge *et al.*, 2006), soft tissue sarcoma and bone sarcoma (Dohi *et al.*, 2009). In contrast, FAP protein expression is absent from stromal fibroblasts of benign lesions and adult normal tissues (Rettig *et al.*, 1988; Garin-Chesa *et al.*, 1990).

In addition to FAP expression, several studies have been performed to elucidate its functions and endogenous substrates. It is postulated that FAP has a vital role in the promotion of tumor growth through release of some growth factors (Bhowmick *et al.*, 2004; Cheng *et al.*, 2005), and regulating cell adhesion and migration (Wang *et al.*, 2005), and angiogenesis (Huang *et al.*, 2004). The mechanism underlying these

functions is not well understood. Recent findings give evidence that FAP promotes tumor proliferation indirectly by up regulating degradation of extracellular matrix, stromagenesis, and formation of new blood vessels in a mouse model with lung and colon cancers (Santos *et al.*, 2009). However is unclear whether its effect on cancer promotion is via its enzyme activity or its interaction with other proteins. Other data taken from patients who suffer colon cancer indicate that FAP up regulation is also associated with cancer progression and recurrence (Henry *et al.*, 2007). Meanwhile, so far α_2 -antiplasmin is the only natural substrate identified for FAP. α_2 -antiplasmin, a peptide with an additional 12 residues in the N terminus (X-Pro₁₂-Asn₁₃- α_2 -antiplasmin) is cleaved by FAP to become Asn₁₃- α_2 -antiplasmin, which binds to fibrin during clotting formation (Lee *et al.*, 2004; Lee *et al.*, 2006b).

1.1.2.3. Clinical Aspects of FAP

Because FAP expression seems to be a critical mediator of tumor growth, inhibition of FAP expression is a promising target for development of a novel tumor treatment. In recent years, several therapeutic techniques to inhibit FAP protein expression, FAP proteolytic activity, and FAP cell signaling have been developed (Kelly, 2005). Initially, a mouse monoclonal antibody (mAb) against the human FAP antigen (mAb F19) was used to treat patients with FAP-expressing colorectal cancer and soft tissue sarcoma (Tanswell *et al.*, 2001). Modifications of some regions of the mAb F19 were developed to avoid generation of anti-mouse antibodies during treatment and then used to treat FAP positive carcinomas such as colon, lung, breast, head, and neck (Scott *et al.*, 2003; Kloft *et al.*, 2004). Nevertheless, the results were disappointing and no clinical advantages were observed although pharmacologically these FAP unconjugated antibodies were found to be safe, tumor-selective, and well

tolerated. In the near future, the next generation FAP monoclonal antibody will be conjugated to anti-tumor agents like anti mitotic molecules (Ostermann *et al.*, 2008) and/or single chain antibody fragments will be incorporated into liposomes as a drug delivery system (Baum *et al.*, 2007) in order to provide an effective method to eliminate FAP positive tumors.

Another method of inhibiting tumor growth may be via attenuation of the DP activity of FAP. As reported by Cheng *et al.* (2005), all severe combined immunodeficient (SCID) mice developed tumors when inoculated with HEK293 cells expressing wild type (wt) FAP compared to their counterpart SCID mice with mutated FAP. These results demonstrate that FAP protease activity plays an important role in promotion of tumor growth (Cheng *et al.*, 2005). In addition to these findings, inoculation of HT-29 colon cancer cells without FAP expression into SCID mice could induce FAP expression on tumor stroma and administration of a DP4 inhibitor (Val-boroPro) for 21 days seemed to inhibit expression of FAP protease and to reduce tumor size (Cheng *et al.*, 2005). However, a further clinical investigation using Val-boroPro to treat advanced colorectal cancer revealed little clinical response (Narra *et al.*, 2007) as Val-BoroPro is not a selective FAP inhibitor and is quite toxic to cells. Therefore, a more selective FAP inhibitor may give more promising results. Another possibility to inhibit DP activity in FAP-positive cancers is to construct a protoxin peptide that is activated by FAP selectively (LeBeau *et al.*, 2009) and to generate photosensitive molecules (Lo *et al.*, 2009). LeBeau and coworkers synthesized promellitin (inactivated toxic venom of European honeybee *Apis mellifera*) and modified the promellitin N terminus with the FAP substrate site. They injected 250 nM of the FAP-promellitin intra tumorally in animal models with human prostate and breast

cancers. The data show that the FAP-promellitin is more effective to kill tumor cells than the control group. However, FAP-promellitin is toxic to normal cells when given by other injection routes (LeBeau *et al.*, 2009). Meanwhile, another research center developed fluorescence molecules linked to a synthetic peptide containing Pro-Asn α_2 -antiplasmin sequence in order to inhibit cell tumor growth (Lo *et al.*, 2009). A greater reduction in tumor size (50%) was observed in mice inoculated with HEK293 and HT29 cells which were injected with 8 μ M of the fluorescence molecule, compared to those injected with 4 μ M of the molecule or media only (40% and 0% respectively) (Lo *et al.*, 2009). Nevertheless, this therapeutic approach is not effective for long time treatment and other routes of drug administration are required.

Disruption of signal transduction involving FAP and other molecules in/on tumor cells is another potential method for killing tumor cells (Kelly, 2005). However, the interaction of FAP with other cell signaling proteins has not yet been defined and extra research is required to elucidate the signaling pathways and FAP protein domains that interact with other molecules to propagate signaling events (Abbott *et al.*, 2000; Gorrell, 2005; Kelly, 2005).

1.1.3. DP8 and DP9

1.1.3.1. DP8 and DP9 structures

DP8 and DP9 are newer members of the DP gene family and so far their structures have not yet been determined. The human *DP8* gene encodes 882 aa, consists of 20 exons and resides at 15q22 (Abbott *et al.*, 2000; Gorrell, 2005). Originally, DP8 protein was identified as monomer with molecular size nearly 100 kDa and situated

in the cytoplasm (Abbott *et al.*, 2000). However, more recent studies with purified recombinant DP8 have revealed that DP8 like DP4 and FAP also forms homodimers (Bjelke *et al.*, 2006; Lee *et al.*, 2006a). In recent years, another DP8 isoform was identified from human testis cDNA and this isoform has 22 exons that encode 898 aa (Zhu *et al.*, 2005). Based on the aa sequence, DP8 shares 51% sequence identity to DP4 but does not contain any glycosylation sites (Abbott *et al.*, 2000). The catalytic residues in DP8 are found at Ser⁷³⁹, Asp⁸¹⁷ and His⁸⁴⁹ and two Glu residues at positions 256 and 257 also contribute to the DP activity, corresponding to the Glu position in DP4 (Glu²⁰⁵ and Glu²⁰⁶) (Abbott *et al.*, 2000; Ajami *et al.*, 2003).

DP9, initially identified *in silico* like DP8, is homologous to DP8 with 62% aa identity. DP8 and DP9 have probably evolved from gene duplication (Abbott *et al.*, 2000; Olsen and Wagtmann, 2002). The human *DP9* gene consists of 22 exons and 21 introns, which span 48.7 kb (Olsen and Wagtmann, 2002; Ajami *et al.*, 2004). This gene is located on 19p13 and encodes two protein one 863 and the other 892 amino acids (Olsen and Wagtmann, 2002; Ajami *et al.*, 2004; Bjelke *et al.*, 2006). It was originally reported that the shorter form is an in-active monomer with molecular size 98 kDa (Olsen and Wagtmann, 2002) but later, some research centers found that the DP9_{863aa} is active (Qi *et al.*, 2003; Ajami *et al.*, 2004; Pitman *et al.*, 2009). Recent studies indicate that the longer form of DP9 is more active and more stable (Bjelke *et al.*, 2006) whilst natural DP9 protein purified from bovine testes has similar biochemical properties to the recombinant DP9 shorter form (Dubois *et al.*, 2008; Dubois *et al.*, 2010). Similar to DP8, the consensus motif in DP9 surrounding the serine catalytic residue (GWSYGG) is encoded by one exon (Olsen and Wagtmann, 2002). Because the two glutamic acid residues have a critical role in DP

activity of the DP gene family, those residues are conserved in DP9 as well (Olsen and Wagtmann, 2002; Ajami *et al.*, 2004).

DP8 and DP9 protein lack a transmembrane domain and a targeted signal sequence and therefore should be expressed in the cytoplasm (Abbott *et al.*, 2000; Olsen and Wagtmann, 2002). Expression studies have shown that both proteins are not detected in cell culture supernatant and cell membrane, using DP8 and DP9 antibodies (Ajami *et al.*, 2004; Lee *et al.*, 2006a). There is some additional evidence that DP9 protein does not have glycosylation sites. An *in vitro* translation study demonstrates the similar mobility of DP9 protein products in SDS PAGE with and without canine microsomal membranes (Olsen and Wagtmann, 2002). Tang and coworkers (2009) also reported that the N-glycosidase antibody does not recognize any glycosylation site in purified recombinant DP9 protein. In contrast to DP4 and FAP, DP8 and DP9 also have a larger β -propeller domain in the N terminus which may selectively affect their binding to DP substrates.

1.1.3.2. DP8 and DP9 expression

DP8 like DP4 appears to be ubiquitously expressed. Using Northern blot analysis, DP8 mRNA is widely expressed in human fetal and adult tissues and higher expression was observed in testis, placenta, and leucocytes (Abbott *et al.*, 2000) whereas DP8_{892aa} is only detected in four human tissues with higher expression found in testis and pancreas using Southern blot analysis (Zhu *et al.*, 2005). By further investigation using reverse transcriptase polymerase chain reaction (RT-PCR), adult testis highly expresses DP8_{892aa} compared to fetal testis and it is postulated that this DP8 form may be involved in sperm production via immuno-

modulation (Zhu *et al.*, 2005). Other data generated from human and baboon tissues by using *in situ* hybridization confirmed that both organisms have similar DP8 gene mRNA expression. A similar pattern of DP8 protein expression is also observed (Yu *et al.*, 2009). By measuring DP activity in DP4 deficient mice high levels of DP activity were observed in the liver, and medium activity levels were observed in the pancreas, lymphocytes, lung, uterus and brain (Ansorge *et al.*, 2009; Yu *et al.*, 2009). At this point it is not possible to distinguish whether this activity is contributed equally by DP8 and DP9 or predominantly by one of the two enzymes. Interestingly despite the high expression of DP8 mRNA in the testes when Dubois and coworkers (2009) purified a natural non-DP4 proteolytic activity from testes, they demonstrated that this protein is DP9 using antibodies and mass spectrometry (Dubois *et al.*, 2009).

DP9 mRNA expression resembles DP8 mRNA expression. Almost all human tissues from early life to adult express DP9 mRNA and the highest expression is noted in skeletal muscle, liver and heart (Olsen and Wagtmann, 2002; Ajami *et al.*, 2004). Some cancer cells such as melanoma, lung carcinoma, leukemia, and colorectal carcinoma also express the DP9 mRNA (Olsen and Wagtmann, 2002). Interestingly, although leucocytes express DP9 mRNA, their expression does not change after stimulation with a mitogen agent (phytohaemagglutinin), in contrast to DP4 mRNA expression (Tang *et al.*, 2009).

1.1.3.3. DP8 and DP9 substrate specificity and its function

Although DP8 mRNA expression is found in many human cells, there is nearly no knowledge about its endogenous substrates and the biological functions of DP8 *in*

vivo. Because all members of the DP4 gene family have the same catalytic motif, DP8 protein can hydrolyze many of the hormones and chemokines that contain a P₁ prolyl bond and are cleaved by DP4. From kinetic assays *in vitro*, the recombinant DP8 protein is able to cleave artificial substrates with Ala, Gly, and Arg at the P₂ position (Abbott *et al.*, 2000). Neuropeptide Y (NPY), peptide YY (PYY), GLP-1, and GLP-2 are all enteropeptides that are cleaved by DP8, however DP8 cleavage rates are slower than that observed for DP4 (Bjelke *et al.*, 2006). Several chemokines inactivated by DP4: stromal cell-derived factors 1 α and 1 β (SDF1 α and β), inflammatory protein-10 (IP10), and interferon-inducible T cell chemo-attractant (ITAC) are also cleaved by DP8 *in vitro*. However, these are unlikely to be endogenous substrates as they are located in a different cellular component to DP8 (Ajami *et al.*, 2008). Overall, DP8-cleaved substrates are likely to be active compounds in the alimentary and immune system where high DP8 mRNA levels are observed.

So far DP9 appears to have very similar biochemical properties to DP8. As reported for all other DP members, a homodimeric form of DP9 is required for its enzyme activity, which has pH optimum around 7.5 (Bjelke *et al.*, 2006; Tang *et al.*, 2009). Similar to DP8, the cleavage activity of DP9 reaches optimum when artificial substrates contain basic or hydrophobic residues in the P₂ site (Abbott *et al.*, 2000; Ajami *et al.*, 2004; Tang *et al.*, 2009). The carboxyl terminus of DP8 and DP9 also plays a vital role in their DP enzyme activity because single point mutation at the carboxyl terminus results in elimination of the enzyme activity even though their quaternary structure does not change at all (Lee *et al.*, 2006a; Tang *et al.*, 2009). For biological substrates, Bjelke and colleagues (2006) showed that several

enteropeptides like GLP-1, GLP-2, NPY, and PYY are cleaved by DP9 with similar rates to the cleavage activity of DP8 but lower than that of DP4. As a consequence, DP8 and DP9 may play a small role in N terminal processing of the incretin hormones, however they are not found in the same cellular location (Bjelke *et al.*, 2006). A recent study has demonstrated that an antigenic peptide VPYGSFKHV presented to MHC class I is a DP9 substrate (Geiss-Friedlander *et al.*, 2009). The authors also stated that DP9 enzyme activity is probably involved in degradation of proteosomal products and antigen presentation.

1.1.3.4. The potential functions of DP8 and DP9

Most studies investigating DP8 and DP9 function have relied on DP4 family or selective DP8/DP9 inhibitors since knockout mice for DP8 and DP9 are unavailable (Geiss-Friedlander *et al.*, 2009). As described above like DP4, DP8 and DP9 are widely expressed in human tissues (Abbott *et al.*, 2000; Olsen and Wagtmann, 2002; Ajami *et al.*, 2004; Tang *et al.*, 2009; Yu *et al.*, 2009). *In vivo* enzyme activity of DP8 and DP9 was firstly identified in human lymphocytes (Maes *et al.*, 2007). Their activity may be related to lymphocyte activation and apoptosis because DP8 and DP9 expression is up regulated in mouse lymphocytes, which were induced by pokeweed mitogen and lipopolysaccharide (Chowdhury *et al.*, 2013). Other studies demonstrated that a selective DP8 and DP9 inhibitor, (2S,3R)-2-(2-amino-3-methyl-1-oxopentan-1-yl)-1,3-dihydro-2H-isoindole hydrochloride, attenuates lymphocyte proliferation in animal models (Lankas *et al.*, 2005; Reinhold *et al.*, 2009). In addition to immunological function, DP9, but not DP8, is involved in processing the RU134-42 antigenic peptide, presenting to MHC class I (Geiss-Friedlander *et al.*, 2009). DP8 and DP9 overexpression in human embryonic kidney cell lines increases

apoptosis (Yu *et al.*, 2006). It suggests that DP8 and DP9 might have a role in cell growth, proliferation and differentiation. In the same cell line, overexpression of DP9 down-regulates Akt protein kinase B of Ras cell signalling, resulting in inhibition of cell proliferation (Yao *et al.*, 2011). Therefore, it is difficult to discriminate which biological events are influenced by DP8 or DP9 (Yu *et al.*, 2010). Further knowledge regarding the natural biological substrates of DP8 and DP9 is required in order to delineate the functions of DP8 and DP9

1.1.3.5. Using proteomics to determine DP8/DP9 substrates

During her PhD Dr Claire Wilson used terminal amine isotopic labelling of substrates (TAILS), an N-terminal positional proteomic approach, for the discovery of *in vivo* DP8 and DP9 substrates (Wilson, 2011). This work revealed *in vivo* roles for DP8 and DP9 in cellular metabolism and homeostasis via the identification of more than 29 candidate natural substrates and pathways affected by DP8/DP9 overexpression. Using MALDI-TOFMS Dr Wilson was able to confirm cleavage of two of these substrates, calreticulin and adenylate kinase 2 (AK2). The remaining substrates have not been validated.

Calreticulin or calcium binding protein is found at high levels in the endoplasmic reticulum of every cell in living organisms (Krause and Michalak, 1997). Structurally, calreticulin is encoded by a single gene which contains 9 exons and 8 introns and is located on chromosome 19 (McCauliffe *et al.*, 1992). The calreticulin protein sequence consists of a 17 aa signal sequence, a N terminus with 180 aa, a 181-290 aa P domain rich in Pro residues and a 291-400 aa C terminus (Johnson *et al.*, 2001; Michalak *et al.*, 2009). This protein has many biological roles, which vary

from protein processing, anti-apoptotic, cell development, immunity, to cell regeneration (Johnson *et al.*, 2001; Michalak *et al.*, 2009). Dr Wilson's thesis showed that DP8 and DP9 are capable of cleaving a N- terminal peptide of calreticulin protein. This peptide contained the N terminus of calreticulin after the signal sequence was removed.

AK2	
	M¹AP↓<u>SVPAAEPEYPKGIR</u>AVLLGPPGAGKGTQAPRLAENFCVCHLA ⁴⁵ ²³⁹
Bifunctional purine biosynthesis protein PURH	
	M¹APGQLALFSVSDKTGLVEFARNL TALGLNLVASGGTAKALRDAGL ⁴⁶ . ⁵⁹²
C-1 tetrahydrofolate synthase, cytoplasmic	
	M¹APAEILNGKEISAQIR ARLKNQVTQLKEQVPGFTPRLAILQVGNRD ⁴⁵ ⁹³⁵
Calreticulin	
	M¹LLSVPLLGLLGLAVA EP↓ AVYFKEOFLDGDGWTSRWIESKHKSD ⁴⁶ ⁴¹⁷
Cathepsin Z/X	
	M¹ARRGPGWRPLLLVLLAGAAQGGLYFRRGQTCYRPLRGDGLAPLGRSTYPRPHEYL S PADLPKSWDWRNVDG ⁷² ³⁰³
Dihydropyrimidine dehydrogenase [NADP ⁺]	
	M¹APVLSKDSADIESILALNPRTQ THATLCSTSAKKLDKHKHWKRNPDK ⁴⁷ ¹⁰²⁵
Mitochondrial import receptor subunit TOM34	
	M¹APKFPDSVEELR AAGNESFRNGQYAEASALYGRALRVLQAQGSS ⁴⁵ ³⁰⁹
Obg-like ATPase	
	M¹PPKKGGDGIKPPPIGR FGTSLKIGIVGLPNVGKSTFFNVLNSQAS ⁴⁸ ³⁹⁶
Serine/threonine-protein phosphatase 6	
	M¹APLDLDKYVEIAR LCKYLPENDLKRLCDYVCDLLEESNVQPVSTP ⁴⁷ ³⁰⁵

Figure 1.3. N terminal peptides of nine potential substrates for DP8 and DP9 identified by TAILS (Wilson, 2011). Bold, underlined text indicates peptides identified using MS/MS. Blue bold text indicates the first residue of mature protein that is removed by aminopeptidases. Red bold text indicates aa residues that are

potentially cleaved by DP8 and DP9. Black arrow indicates cleavage site by DP8 and DP9.

The second substrate of DP8 and DP9 that was validated was AK2. AKs are a family of bioenergetic enzymes that convert ATP to 2ADP in the presence of AMP and Mg^{2+} in order to maintain energy supply for various cell activities (Noma *et al.*, 2001). To date, nine subtypes of these enzymes have been identified and these are distributed in a tissue specific manner (Ren *et al.*, 2005; Panayiotou *et al.*, 2011; Amiri *et al.*, 2013). AK1 is found in the cytosol of brain, skeletal muscle and red blood cells but AK2 is located in the cytosol and mitochondrial matrix of several human tissues like liver, kidney, heart and spleen (Khoo and Russell, 1972; Noma *et al.*, 2001). Moreover, there are two isoforms of AK2 which were successfully cloned and these isoforms encode 239 and 232 aa sequences respectively (Noma *et al.*, 1998). From mRNA and protein analysis, liver and heart have the strongest expression of both AK2 isoforms while weaker expression was found in brain. In kidney and skeletal muscle although RNA levels are high the protein levels are low (Noma *et al.*, 1998). The different expression of AK2 isoforms in some human tissues might be the result of post-transcriptional and -translational modifications (Noma *et al.*, 1998). Naturally in bovine liver tissue two forms of AK2 were isolated, one form was missing the Met residue only and the other form was missing Met-Ala-Pro, and this later form of AK2 was found to be two fold active. The *in vitro* identification of DP8 and DP9 proteases having the ability to process the N-terminus of AK2, suggest that DP8 and DP9 may play a role in regulating AK2 function.

As discussed in the background above, while DP8 and DP9 are widely distributed in human tissues very little is still known about their physiological function. In our laboratory, 22 potential substrates of DP8 and DP9 were identified but to date only calreticulin and AK2 have been validated. This thesis aims to validate 12 more substrates and to focus on investigating the role of DP8 and DP9 overexpression and silencing on AK2 expression and enzyme activity.

1.2. Hypothesis

Although DP8 and DP9 are similar to DP4 in terms of structure, expression and enzyme activity, up to now their endogenous substrates and biological functions remain mostly unknown. For better understanding of DP8 and DP9 actions in pathological conditions, the characterization of their natural substrates is definitely required, which may give further clues and insights into their biological roles. One of the main substrates identified as a DP8 substrate from a proteomics study was AK2. AK2 plays key roles in cellular energy and nucleotide homeostasis. Many other substrates identified in Dr Wilson's study are involved in regulating metabolism and energy homeostasis in the cell. The major hypothesis that is being tested in this thesis is that DP8 and DP9 are essential modulators of metabolism and energy homeostasis via their ability to cleave substrates involved in regulating these processes.

1.3. Project aims

Thus the aims of this study are

1. For AK2 and calreticulin to be *in vivo* substrates for DP8 and DP9, both substrate and proteases need to be in the same cellular compartment. In aim 1 it will be

- determined whether DP8 and DP9 co-localize with AK2 and calreticulin in an ovarian cancer cell line (SKOV3) overexpressing DP8 and DP9 proteins (**Chapter 3**).
2. Dr. Claire Wilson's thesis identified a further 27 potential DP8 and DP9 substrates. In aim 2, 12 further potential substrates of DP8 and DP9 will be tested and compared to DP4 using MALDI-TOF (**Chapter 3**).
 3. Current findings have showed that up regulation of DP8 and DP9 expression is involved in several pathological processes (Yu *et al.*, 2006; Yao *et al.*, 2011). Thus, in aim 3, the effects of DP8 and DP9 overexpression on AK2 activity *in vivo* will be examined (**Chapter 4**). Phenotypical changes and proliferation rates of SKOV3 cells overexpressing DP8 and DP9 will also be evaluated. Kinetic profiles of AK activity in the cytoplasm and mitochondria will determine whether DP8 or DP9 overexpression effects AK2 or not. Moreover, adenine nucleotide levels will be measured in order to identify the effects of DP8 and DP9 overexpression on the SKOV3 cells.
 4. Ovarian cancer cells have different mRNA and protein levels of DP8 and DP9. In **Chapter 5**, DP8 and DP9 in three OVCA 429, OVCA 432 and SKOV3 cell lines will be silenced using siRNA to see whether DP8 and DP9 silencing effects AK2 enzyme levels and downstream effects. AK2 expression and AK enzyme activity in the three cancer cells will also be investigated.

2. MATERIALS AND METHODS

Most chemicals used during this PhD were purchased from Sigma-Aldrich (St. Louis, MO, USA) unless otherwise stated. To make buffers and solutions, standard techniques were used (Sambrook *et al.*, 1989).

2.1. Distilled water

All water used in this thesis was provided by the School of Biological Sciences, Flinders University, South Australia and used for dissolving and diluting all chemicals throughout this thesis after purification. Tap water was distilled three times using Millipore equipment (Millipore Q Gard[®]1, Australia, Cat#QGARD00L1).

2.2. Buffers and solutions

2.2.1. Phosphate buffered saline (PBS)

8 g NaCl (APS Ajax Finechem, New South Wales, Australia)

0.2 g KCl (Chem-Supply, South Australia)

1.44 g Na₂HPO₄ (Scharlau, Chemie SA, Barcelona, Spain)

0.24 g KH₂PO₄ (Chem-Supply)

were dissolved in 800 ml water. The solution was adjusted with 32% volume/volume (v/v) HCl (Merck, KGaA, Darmstadt, Germany) to give pH 7.4. The remaining volume was added with water to reach 1,000 ml solution. For washing cells, PBS solution was sterilized in an autoclave at 103 kPa for 15 minutes (min) at 121°C.

2.2.2. 1 M Tris-HCl pH 7.4

121.14 g Tris base (Amresco[®], Solon, Ohio, USA)

was dissolved in 800 ml water. The solution was adjusted with concentrated HCl to give pH 7.4. The remaining volume was added with distilled water to reach 1,000 ml solution.

2.2.3. 1 M NaCl

58.44 g NaCl (APS Ajax Finechem)

was dissolved in 800 ml water. The solution was sterilized in an autoclave at 103 kPa for 15 minutes (min) at 121°C.

2.2.4. Tris buffer (50 mM Tris-HCl pH 7.4 and 150 mM NaCl)

50 ml 1 M Tris-HCl pH 7.4

150 ml 1 M NaCl

were diluted in 800 ml water.

2.2.5. 100 mM EDTA

3.722 g EDTA

was dissolved in 50ml water. This solution was adjusted with 10M KOH to dissolve completely and to give pH 8.0.

2.2.6. 1 M DTT

1.542 g DTT was dissolved in 10 ml water. The solution was filtered using a 0.20µm syringe filter (Sartorius stedim biotech, Goettingen, Germany) and stored in 1ml aliquots at -20°C before use.

2.2.7. 1 M Sucrose

342.30 g Sucrose (BDH AnalaR[®], Victoria, Australia)

was dissolved in 500 ml water.

2.2.8. 150 mM MgCl₂

3.049 g MgCl₂ (BDH AnalaR[®], Victoria, Australia)

was dissolved in 100 ml water.

2.2.9. 100 mM EGTA

3.804 g EGTA (Sigma-Aldrich)

was dissolved in 50ml water. This solution was adjusted with 10M KOH to dissolve completely and to give pH 8.0.

2.2.10. 1 M KCl

7.455 g KCl (Chem-Supply)

was dissolved in 100ml water.

2.2.11. 200 mM HEPES pH 7.5

4.766 g HEPES (BDH Biochemical, Poole, England)

was dissolved in 80ml water. This solution was adjusted with 10M KOH to dissolve completely and to give pH 7.5.

2.2.12. Buffer and solution for flow cytometry analysis

2.2.12.1. 10 % weight/volume (w/v) Sodium azide (NaN₃)

1g NaN₃

was dissolved in 10 ml water and filtered using a 0.20 µm filter.

2.2.12.2. Fluorescence Activated Cell Sorter (FACS) buffer

1 g	Glucose (Ajax Finechem, New South Wales, Australia)
1.3 ml	40 % Formaldehyde (Merck KGaA, Darmstadt, Germany)
0.25 ml	10% NaN ₃

were dissolved in 40 ml of PBS pH 7.4. The solution was adjusted to 50 mls.

2.2.13. Buffers and solutions for cell extraction

2.2.13.1. Lysis buffer modified from Ahn et. al. (2004)

50 mM	Tris-HCl pH 7.4
150 mM	NaCl
1 mM	EDTA
1 mM	DTT

1x protease inhibitor cocktails (Sigma-Aldrich, Cat# P8849)

were freshly prepared and stored at 4°C before use.

2.2.13.2. Lysis buffer modified from Rezaul et. al. (2005)

250 mM	Sucrose
20 mM	HEPES pH 7.5
10 mM	KCl
1.5 mM	MgCl ₂
1 mM	EDTA
1 mM	EGTA
1 mM	DTT

1x protease inhibitor cocktails (Sigma-Aldrich, Cat# P8849)

were freshly prepared and stored at 4°C before use.

2.2.13.3. Sucrose buffer

250 mM Sucrose

10 mM Tris-HCl pH 7.4

1 mM EDTA

were prepared and stored at 4°C before use.

2.2.13.4. 4 % (w/v) 3-[(3-cholamidopropyl) dimethylammonio]-1-propanesulfonate

CHAPS solution

1g CHAPS (Boehringer Mannheim, Germany)

was dissolved in 25ml water.

2.2.13.5. Mitochondrial buffer

50 mM Tris-HCl pH 7.4

150 mM NaCl

4 % CHAPS

1 mM EDTA

1x protease inhibitor cocktails (Sigma-Aldrich, Cat# P8849)

were freshly prepared and stored at 4°C before use.

2.2.14. Buffers and solutions for AK assay

2.2.14.1. 10 mM ATP

55.11 mg ATP was dissolved in 10ml water and stored at -20°C.

2.2.14.2. 10 mM ADP

42.72 mg ADP

was dissolved in 10ml water and stored at -20°C.

2.2.14.3. 40 mM AMP

69.44 mg AMP

was dissolved in 50 ml water and stored in 10 ml aliquots at -20°C.

2.2.14.4. 40 mM MgSO₄

0.986 g MgSO₄ (BDH AnalaR[®], Victoria, Australia)

was dissolved in 100 ml water.

2.2.14.5. 200 mM Triethanolamine-HCl pH 7.6

18.57 g Triethanolamine

was dissolved in 400 ml water. The solution was adjusted with concentrated HCl to give pH 7.6. The remaining volume was added with water to reach 500 ml solution.

2.2.14.6. 25 mM Tris-HCl pH 8.0

0.303 g Tris

was dissolved in 80 ml water. The solution was adjusted with concentrated HCl to give pH 8.0. The remaining volume was added with water to reach 100 ml solution.

2.2.14.7. 10 mM Tris-HCl pH 8.5

0.121g Tris

was dissolved in 80 ml water. The solution was adjusted with concentrated HCl to give pH 8.5. The remaining volume was added with water to reach 100 ml solution.

2.2.14.8. 10.92 mM Phosphoenol pyruvate (PEP) solution

25 mg PEP

was dissolved in 5 ml of 25 mM Tris-HCl pH 8.0 and stored in 1 ml aliquots at -20°C.

2.2.14.9. Pyruvate Kinase (PK) solution

3.3 mg PK

was dissolved in 1 ml water and stored in 100 µl aliquots at -20°C.

2.2.14.10. Lactate dehydrogenase (LDH) solution

1.66 mg LDH

was dissolved in 1 ml water and stored in 100 µl aliquots at -20°C.

2.2.14.11. 13.48 mM Nicotinamide adenine dinucleotide (NADH) solution

20 mg NADH

was dissolved in 2 ml of 10 mM Tris-HCl pH 8.5 and stored at -80°C .

2.2.14.12. 50 mM K₃PO₄ pH 7.0 adapted from Li et. al. (2007)

5.23 g K₂HPO₄ (Chem-Supply)

2.72 g KH₂PO₄ (Chem-Supply)

were dissolved in 800 ml water. The solution was adjusted with 1M HCl to give pH 7.0. The remaining volume was added with water to reach 1,000 ml solution. For

HPLC elution buffer, K_3PO_4 solution was filtered using Millipore glass filter device (Merck Millipore, Billerica, MA, USA).

2.2.14.13. 0.6 M Perchloric acid

1.732 ml 70% Perchloric acid

was diluted in 18.278 ml water. The solution was stored at 4°C before use.

2.2.15. Buffers and solutions for SDS-PAGE and Western blotting

2.2.15.1. 1.5 M Tris-HCl pH 8.8

181.71 g Tris base

was dissolved in 800 ml water. The solution was adjusted with concentrated HCl to give pH 8.8. The remaining volume was added with distilled water to reach 1,000 ml solution.

2.2.15.2. 1 M Tris-HCl pH 6.8

12.114 g Tris base

was dissolved in 80 ml water. The solution was adjusted with concentrated HCl to give pH 6.8. The remaining volume was added with distilled water to reach 100 ml solution.

2.2.15.3. 0.5 M Tris-HCl pH 6.8

60.57 g Tris base

was dissolved in 800 ml water. The solution was adjusted with concentrated HCl to give pH 6.8. The remaining volume was added with distilled water to reach 1,000 ml solution.

2.2.15.4. 10% (w/v) sodium dodecyl sulphate (SDS)

20 g SDS

was dissolved in 200ml water.

2.2.15.5. 10% (w/v) Ammonium persulphate (APS)

1 g APS (BDH AnalaR)

was dissolved in 10ml water and stored in 1ml aliquots at -20°C.

2.2.15.6. 5% volume/volume (v/v) Acetic acid

5ml glacial acetic acid

was diluted in 95ml water.

2.2.15.7. Stripping buffer (200 mM NaOH)

8 g NaOH (BDH AnalaR)

was dissolved in 1,000 ml water.

2.2.15.8. SDS-PAGE gels

2.2.15.8.1. 10% Resolving gel

4.840 ml water

2.500 ml 1.5 M Tris-HCl pH 8.8

2.500 ml acrylamide-bis (40%: 0.8%) (Amresco)

0.100 ml 10 % SDS

0.040 ml N,N,N,N tetramethylenediamine (TEMED)

0.050 ml 10% APS

2.2.15.8.2. 4% Stacking gel

3.170 ml	water
1.250 ml	0.5 M Tris-HCl pH 6.8
0.500 ml	acrylamide-bis (40%: 0.8%)
0.050 ml	10 % SDS
0.010 ml	TEMED
0.025 ml	10% APS

2.2.15.9. 3x SDS-PAGE sample buffer adapted from (Laemmli, 1970)

4.687 ml	1M Tris-HCl pH 6.8
15 ml	10% SDS
18.75 ml	Glycerol
1.5 ml	0.5% (w/v) Bromophenol blue
3.75 ml	2-Mercaptoethanol
6.312 ml	water

were mixed thoroughly.

2.2.15.10. 10x Tris Glycine buffer pH 8.3-9.0

30.285 g	Tris base
144.134 g	Glycine (Amresco)

were dissolved in 800 ml water. The solution was adjusted if pH was more than 9.0.

The remaining volume was added with distilled water to reach 1,000 ml solution.

2.2.15.11. Running buffer

100 ml 10x Tris Glycine buffer

10 ml 10% SDS

were diluted in 890 ml water.

2.2.15.12. Transfer buffer

100 ml 10x Tris Glycine buffer

100 ml 100% Methanol (Merck)

were diluted in 890 ml water.

2.2.15.13. Washing buffer (Tris buffer with 0.1% (v/v) Tween-20)

999 ml Tris buffer pH 7.4

1 ml Tween-20

were mixed thoroughly.

2.2.15.14. Blocking buffer, 5% (w/v) skim milk in washing buffer

10g Skim milk (Black and Gold, Australia)

was dissolved in 200 ml washing buffer

2.2.15.15. Ponceau staining

0.05g Ponceau powder (Sigma-Aldrich)

was dissolved in 50 ml of 5% acetic acid and wrapped with Aluminium foil.

2.3. Methods

2.3.1. Cell stocks used

The SKOV3 cell line was obtained from stocks at the School of Biological Sciences, Flinders University. SKOV3 cells overexpressing wt or mt DP8 and DP9 as well as vector only were developed by Dr. Claire H. Wilson during her PhD. Briefly, DP8 and DP9 genes, which encoded 882 and 863 amino acid sequences, respectively were cloned into a plasmid vector with EGFP tag (pEGFPN1) whilst DP8 and DP9 genes with inactive enzyme activity were generated by mutation of Ser⁷³⁹ and 729 residues in their catalytic site into Ala residue and cloned into the same plasmid vector (Yu *et al.*, 2006; Wilson *et al.*, 2013). These DNA constructs were then transfected into SKOV3 cells using a liposome reagent, Fugene HD (Roche, USA) and positive clones were selected by addition of gentamycin. To generate stable-transfected SKOV3 cells, all positive clones were sorted using FACS device (BD Pharmingen, San Diego, USA) (Wilson, 2011). All cells were finally kept in liquid nitrogen storage at the School of Biological Sciences, Flinders University. Cultures of all ovarian cancer cells were approved by Institutional Biosafety Committee (IBC) (2006-06 EXEMPT).

2.3.2. Growing cancer cell lines

Cells were thawed while still in cryovials at room temperature (RT) and the vials were disinfected with 70% ethanol (School of Biological Sciences, Flinders University). The thawed cells were directly transferred into T25 cell culture flasks (Greiner Bio-one GmbH, Frickenhause, Germany) containing 5 ml of RPMI 1640 or DMEM supplemented with 10% heat inactivated foetal bovine serum (FBS), 100 U penicillin and 100 µg/ml streptomycin with or without 500 µg/ml gentamycin. The

resuspended cells were incubated at 37°C in a 5% CO₂ incubator (MCO-18AIC, Sanyo, Japan). Every second day, the media were replaced with fresh media and the cells were re-incubated until reaching confluence. Once the cells had reached confluence, cells were seeded by detaching with 1% trypsin-EDTA solution. Before adding the trypsin solution, cells were washed with sterile PBS pH 7.4 (1.76 mM KH₂PO₄, 10.14 mM Na₂HPO₄, 137 mM NaCl and 2.68 mM KCl) to remove FBS and cell debris. To ensure that all cells were completely detached, the flask was incubated at 37°C for 5-10 min with 5% CO₂. Activity of trypsin solution was quenched by resuspending cells in complete cell media. To provide sufficient enough cells during the experiments, cells were split into cell culture flasks as described in Table 2.1.

Table 2.1. Propagation of ovarian cancer cells

Cell culture vessel	Surface area (cm²)	Cell number (x 10⁶)	Volume of medium (ml)
96-well	0.3	0.1	0.1
6-well	2	0.2	2
25	25	0.5	5
75	75	1	15

2.3.3. Harvesting cancer cell lines

After cells reached confluence, the cells were harvested by addition of 1 ml trypsin-EDTA as described above. The resuspended cells were centrifuged at 1,500 x g in a table top centrifuge (Hermle Z 400K, Germany) for 5 min at RT. Depending on cell application, cell pellets could be resuspended in just media, complete media or PBS pH 7.4. For example, cell pellets were dissolved in complete media without antibiotics for small interfering (si) RNA transfection whereas cell pellets were

dissolved in PBS pH 7.4 for flow cytometry analysis. Total cell number was then determined by using trypan blue exclusion assay (described in the next section). Solubilized cells were centrifuged again at the same speed and washed twice with PBS pH 7.4. Cell pellets were finally kept in the -80°C freezer (Thermo Fisher Scientific, Asherville, NC, USA) before further analysis.

2.3.4. Counting cell number using trypan blue exclusion assay

For seeding and other cell applications, the cell suspension described in the section above was equally mixed with 0.4% (w/v) trypan blue solution and pipetted up and down several times. Ten µl of the mixed solution was loaded into the edge of a Neubauer chamber haemocytometer which had previously been affixed with a cover slip. To calculate total cell number, viable (unstained) and dead (stained) cells were counted in four individual 1 mm square sections. Total cell number was determined by dividing the total cell count by four to give the average count for one cell and then multiplying this number by 10^4 cells/ml. The percentage of cell viability was then determined by dividing viable cells by total cells (Reed *et al.*, 2007).

2.3.5. Preserving cancer cell lines

All cancer cell lines were regularly stored at liquid nitrogen to maintain cell stocks throughout this study. After trypsination, harvested cells were resuspended in fresh complete media and the cell viability was counted as described in the section above. Cells were then centrifuged at 1,500 xg for 5 min at RT and cell pellets were washed with PBS pH 7.4. Finally cell pellets were dissolved in fresh complete media which contained 10% (v/v) dimethylsulfoxide (DMSO). Cell suspensions were gradually

frozen at 4°C for 30 min, -20°C for 60 min, -80°C for overnight (o/n) and then put into liquid nitrogen for long term storage.

2.3.6. Protein analysis

2.3.6.1. Cell extraction

Most cancer cells were extracted using a modified lysis buffer (Ahn *et al.*, 2004). After short centrifugation (detailed in the section above), cell pellets were washed twice with cold PBS pH 7.4 and centrifuged at 400 x g for 10 min at 4°C. The cell pellets were then dissolved in a cold lysis buffer which contained 50 mM Tris-HCl pH 7.4, 150 mM NaCl. The modifications were the addition of 1 mM EDTA, 1 mM DTT and 1x protease inhibitor cocktail (Sigma-Aldrich, Cat# P8849). Cell integrity was disturbed using a probe sonicator (S-4000, Misonic-ultrasonic liquid processor, USA) for 10 sec on an ice box. To remove cell debris, the cell lysate was centrifuged twice at 650 x g for 10 min at 4°C. The cleared supernatant was transferred into a fresh eppendorf tube and retained as a cell lysate. To obtain a cytosol fraction, the cell lysate was centrifuged at 16,000 x g for 30 min at 4°C. All sample fractions were kept at -80°C before further analysis.

2.3.6.2. Bicinchoninic acid (BCA) protein assay

In order to estimate protein concentration of whole or fractionated cells, a serial dilution of bovine serum albumin (BSA) standard was needed. 200 mg/ml BSA stock solution was diluted with water to make final concentrations: 2, 1.5, 1.0, 0.75, 0.5, 0.25 and 0.125 mg/ml. 10µl of diluted BSA, water and diluted samples, which ranged from 2 to 10, was transferred into a 96 well plate (Sarstedt AG & Co, Numbrecht, Germany). A 50 part quantity of solution A of BCA protein assay kit was well mixed with an 1 part quantity of solution B. 200µl of mixed BCA solution

were added into the each well of the 96 well plate. The microplate was shaken on an orbital shaker for 30 sec at RT, followed by incubation at 37°C for 30 min. Before measuring absorbance values, the microplate was cooled down for 10-15 min at RT. The protein absorbance was measured using a microplate reader (FLUOstar omega, BMG lab tech GmbH, Offenburg, Germany) at 562 nm, equipped with BMG lab tech software version 3.00 R2. The protein concentration of diluted samples was calculated by using a standard curve of diluted BSA standard and its OD₅₆₂ values.

2.3.6.3. DP enzyme activity

This assay was utilised to monitor whether recombinant DP8 and DP9 proteins were still active after storage and the DP activity after cell extractions. Thawed recombinant protein (various concentrations), or 10µl of cell lysate, cytosol or mitochondrial fractions from cell lines were loaded into a 96 well plate. All experimental samples were tested in triplicate. Samples were diluted with 40µl of Tris-buffer solution which consisted of 50 mM Tris-HCl pH 7.4 and 150 mM NaCl. 50 µl of 1mM H-Ala-Pro-pNA substrate also dissolved in Tris-buffer pH 7.4 was added into each well. The temperature of the Fluorostar spectrophotometer was set at 37°C and the machine was configured to take continual readings every 5 min for 60 min. Every 5 min, the microplate was shaken at 500 rpm for 30 sec and the absorbance values were directly measured with 405 nm and 600 nm to reduce background. The specific enzyme activity was determined using the Beer-Lambert formula $A = \epsilon Cl$, where A = absorbance, ϵ = μ molar extinction coefficient (9.45 litres. $\mu\text{mol}^{-1}.\text{cm}^{-1}$ for pNA at 405 nm), C = concentration ($\mu\text{mol}.\text{litre}^{-1}$) and l = length of light path (2.94 cm for Sarstedt 96 well plate). Before calculating enzyme activity, the absorbance values of samples were normalized with the values taken for a Tris-

buffer control. Δ absorbance was calculated by subtracting absorbance values at two different time points during the exponential phase of enzyme activity. The Δ absorbance per minute was then determined by

$$\Delta \text{ absorbance/minute} = (\text{A t2 point} - \text{A t1 point})/\text{time (minute)}$$

Specific enzyme activity was presented in U/min/mg protein samples where 1 U was equal to 1 μ mol.

2.3.7. Western Blotting

2.3.7.1. SDS-PAGE

Samples (15 or 25 μ g of protein) were mixed with 3x sample buffer (93 mM Tris-HCl pH 6.8, 3% (w/v) SDS, 7.5% 2- β mercaptoethanol, 0.015% bromophenol blue, and 37.5% glycerol) and boiled at 100°C for 5 min in a dry block heater (Thermoline, Australia). The denatured samples and 5 μ l protein marker (Bio-Rad, Hercules, CA, USA) were loaded on to 10% SDS-PAGE gel which contains 1.5 mM Tris pH 8.8, 30% (w/v) Polyacrylamide [29:1 (3.3%C) Acrylamide :N,N'-Methylene-bis Acrylamide, 10% (w/v) SDS, 0.5% (v/v) TEMED and 10% (w/v) APS. The gel was run with running buffer (192 mM glycine, 25 mM Tris, and 0.1% SDS pH 8.3) in a Mini-Protean[®] II electrophoresis system (Bio-Rad) at 170V, 400 mA for 60 min.

2.3.7.2. Blotting the gels on the polyvinyl difluoride (PVDF) membrane

Separated protein samples from gels were transferred on to PVDF membranes with wet and semidry transfer methods. The wet transfer method was used in Western blotting in Chapter 3 using PVDF membrane from Thermo Fisher Scientific. A sandwich was made from chromatography paper (Whatman[®], Maidstone, England)

and filter pads. Before the blotting process began, the membrane was soaked in 100% methanol and the sandwich supports were completely wet in the transfer buffer. Once the transfer sandwich was set up in a chamber, a magnetic stirrer and a frozen ice block were put into the chamber in order to achieve even transfer process and to prevent protein degradation. The chamber was then filled with transfer buffer up to the top of the transfer sandwich. The blotting process was performed at 60V, 400 mA for 90 min. After that, the blotted membrane was incubated in blocking buffer at 4°C for o/n with shaking.

Meanwhile in Chapter 4 and 5, the semi-dry method was used to transfer separated protein samples from gels on to Hybond-P PVDF membrane (GE Healthcare, Buckinghamshire, UK). The membrane was soaked in to 100% methanol for at least 5 min, rinsed briefly with water and equilibrated in transfer buffer. At the same time, three pieces of 3 mm Whatmann chromatography paper were soaked in transfer buffer (25 mM Tris and 192 mM Glycine and 10% (v/v) methanol). The set up for transfer was to place the wetted filter paper on the tray of the transfer apparatus followed by PVDF membrane, gel containing proteins, and finally three more pieces of filter paper on the top. The sandwich transfer was run in a Trans-Blot[®]Turbo[™] transfer system from Bio-Rad at 25V, 1A for 30 min.

2.3.7.3. Ponceau staining

Once the blotted samples were completely transferred on to PVDF membrane, the membrane was briefly washed with water and allowed to dry at RT. The dried membrane was re-activated in 100% methanol and rinsed with water for a few min. After that, the membrane was dipped in Ponceau red solution (0.1% (w/v) in 5%

acetic acid) with shaking in an orbital shaker (Biodancer, New Brunswick Scientific, Edison, NJ, USA) for 5 min. Destaining of the membrane was achieved by washing with water at least three times. Red-coloured bands were then visualized using a ChemiDoc™ MP system (Bio-Rad, Hercules, CA, USA) equipped with Image Lab™ software version 4.0.

2.3.7.4. Immunoblotting

For detecting specific bands, Ponceau stained membrane was blocked with blocking buffer at RT for 60 min with shaking in an orbital shaker. The blocked membrane was briefly washed with washing buffer and then incubated with diluted primary antibody in blocking buffer. The primary antibody dilution was dependent on antibody types as stated in Table 2.2. Incubation was performed at 4°C o/n with shaking. Unbound antibody was washed with washing buffer three times for 10 min at RT. To detect antigen-antibody binding complexes, the membrane was incubated with diluted secondary antibodies coupled with horse radish peroxidase (HRP) in blocking buffer at RT for 60 min. Application of the secondary antibody was based on the host primary antibody. The excess secondary antibody was washed with washing buffer three times for 10 min. The washed membrane was then exposed to the substrate solution (equal mixture of peroxide solution ECL and luminol solution ECL) for 5 min at RT with shaking in an orbital shaker. Initially, some blotted membranes in Chapter 3 were exposed with a Pierce ECL reagent (Pierce Biotechnology, Rockford, USA) but the remaining Western blotting performed throughout this study used another ECL reagent (GE Healthcare, Buckinghamshire, UK). The substrate solution, which was not bound to the HRP, was removed by tapping on tissue paper. The ChemiDoc™ imaging system was used to develop

signals resulting from enzymatic reaction between protein targets and their antibodies. Exposure time began at 1 sec until 1200 sec and the resulting image of protein bands was quantified using Image lab™ software package program from Bio-Rad. Image quantification was presented in volume pixel intensity per mm² area, normalized with background and band intensity of wild type cancer cell line.

Table 2.2. Primary and secondary antibodies used for Western blotting. All antibodies were diluted in blocking buffer

Antibody	Source	Catalog number	Dilution
<i>Primary antibodies</i>			
AK2 (Rabbit polyclonal anti human)	Abcam plc (Cambridge, UK)	ab37594	1 : 2,500
AMPK α (Rabbit polyclonal anti human)	Cell Signalling Technology (Danver, MA, USA)	#2532	1 : 2,000
Calregulin (N-19) (Goat polyclonal anti human)	Santa Cruz Biotechnology (CA, USA)	sc-6468	1 : 10,000
Phospho-AMPK (Thr172) (Rabbit polyclonal anti human)	Cell Signalling Technology	#2535	1 : 1,000
RP1- DPP8 (Rabbit polyclonal anti human)	Triple Point Biologics Inc (Forest Grove, OR, USA)		1 : 2,500 and 1 : 5,000
RP1-DPP9 (Rabbit polyclonal anti human)	Triple Point Biologics Inc		1 : 5,000
β -Actin (Mouse monoclonal anti human)	Sigma-Aldrich	A1978	1 : 10,000
Human Mitochondrial Mn Superoxide Dismutase (SOD2) (Rabbit polyclonal anti human)	Antibody Technology Australia (Daw Park, South Australia)		1 : 10,000
<i>Secondary antibodies</i>			
Donkey anti goat IgG HRP	Santa Cruz Biotechnology	sc 2020	1 : 10,000
Swine anti rabbit IgG HRP	Dako (Glostrup,	P 0217	1 : 5,000 and 1 : 10,000

	Denmark)		
Rabbit anti mouse IgG HRP	Dako	P 0260	1 : 20,000

2.3.7.5. Stripping and reprobing the membrane

After immunoblotted membranes were visualized in the Bio-Rad ChemiDoc device, primary-secondary antibody binding complexes in the membrane could be stripped off. The presence of different proteins in the membrane could be detected using a set of their specific antibodies. The membranes were dipped and incubated with stripping buffer (section 2.4.7.7) for 60 min at RT with shaking. At the end of incubation, the membrane was washed with Tris buffer four times for 10 min at RT and then blocked with blocking buffer for 60 min at RT (in section above). Reprobing the membrane was performed as same as described in immunoblotting (section 2.5.7.4). Stripping was performed on DP8, DP9 or AK2 immunoblotted membranes and then followed by reprobing with anti β -actin or anti SOD2.

2.3.8. Statistical analysis

IBM SPSS statistics software version 20 (SPSS Inc, Chicago, Illinois, USA) was used to statistically analyse all experimental data generated in this study. For comparing means of individual sample groups to control sample group, parametric statistics (student's *t test* and one way ANOVA) were used if the sample distribution is normal. Meanwhile, non-parametric statistics (Mann-Whitney U and Kruskal Wallis tests) were used to compare means of data samples, which were not normally distributed. The significance value was set at $P < 0.05$.

3. VALIDATING DP8 AND DP9 POTENTIAL SUBSTRATES WITH BIOCHEMICAL AND *IN VITRO* ASSAYS

Work described in this chapter was partially published in the Journal of Biological Chemistry volume 20, no. 20, pp. 13936-13949, May 2013. The published paper describes the generation of the stable SKOV3 cell lines overexpressing wt and mt DP8 or DP9, the identification of potential substrates for DP8 and DP9 in these cells using terminal amine isotopic labelling of substrates (TAILS) technique, validation of amino peptides from 14 selected substrates using MALDI-TOF analysis and co-localization between the substrates AK2 and calreticulin and DP8 or DP9 protein using confocal microscopy and Western blotting. Dr. Claire Wilson performed the first two studies and validated AK2 and calreticulin as DP8 and DP9 substrates during her PhD. The remaining work validates a further 12 potential substrates and verifies the co-localization of AK2 and calreticulin in SKOV3 cells overexpressing wt and mt DP8 or DP9 protein was performed by me and is described in detail in this chapter.

3.1. Introduction

Since the completion of the human genome around 550 human proteases or proteolytic enzymes have been identified (Puente *et al.*, 2003), many of them have become drug targets. Physiologically, most proteases contribute to various biological functions such as immunity, cell division, apoptosis, cell signalling, cellular metabolism and metabolite recycling. Recent findings also suggest that proteases are implicated in many human diseases such as cancer, diabetes, cardiovascular and

neurodegenerative disorders. Therefore, it is essential to understand for each human protease: what are their endogenous substrates, cleavage products, activators, and inhibitors in order to unravel the physiological processes in which each protease is involved (Klingler and Hardt, 2012; Turk *et al.*, 2012). Originally, proteases were divided into two groups which were based on their ability to cleave internal peptide bonds (endopeptidases) or peptide bonds at amino and or carboxyl termini (exopeptidases) (Lopez-Otin and Bond, 2008). Recently, proteases have been classified into six groups based on their catalytic sites. Those are serine, cysteine, threonine, metallo, aspartic and glutamic proteases (Lopez-Otin and Bond, 2008).

DP8 and DP9 proteases are serine proteases that belong to the DP4 gene family (Chen *et al.*, 2004). However, their catalytic motif is different from other classical serine proteases (for details see Chapter 1 general introduction). Even though DP8 and DP9 proteins were discovered over a decade ago, their biological functions are still under investigation and mostly unknown. From the predicted primary structure, DP8 protein is similar to DP9 protein sharing 62% aa identity and both proteins are located in the cytoplasm (Abbott *et al.*, 2000; Olsen and Wagtmann, 2002). Previous studies have reported that amino peptides derived from neurohormones, enterohormones and chemokines are biochemically cleaved by DP8 and DP9 (Bjelke *et al.*, 2006; Ajami *et al.*, 2008). Only one endogenous substrate has been identified for DP9 which is involved in antigen presentation to MHC class I (Geiss-Friedlander *et al.*, 2009).

Many experimental methods have been developed to study protease activity (Agard and Wells, 2009; auf dem Keller and Schilling, 2010). The techniques to identify

protease active sites were developed first, including substrate phage and bacterial displays, peptide microarrays and peptide libraries (auf dem Keller and Schilling, 2010). The researchers used genetic and biochemical screenings to characterize the protease cleavage sequence. The second technique that was developed aimed to identify not only protease active sites but also the cleavage products. This technique utilises protein separation, combined with mass spectrometry (MS). Uncleaved and cleaved products of proteases are separated using either 1-dimensional or 2-dimensional gel electrophoresis. Proteolytic products are analysed separately or together using MS. Nevertheless, this technique has some limitations such as sensitivity, throughput and numerous MS runs (Agard and Wells, 2009). Another technique was developed to monitor protease activity that generally occurs at amino or carboxyl termini. The basic concept of this technique is based on reactive nitrogen atoms as all proteins have those reactive atoms in lysine ϵ - and NH terminal α -amines (Agard and Wells, 2009). In general, there are three steps to perform identification of cleavage sites. The initial step is to isolate amino terminus of untreated and protease treated potential substrates, using chemicals or enzymes (Gevaert *et al.*, 2003; Agard and Wells, 2009). The next step is to remove internal cleavage products (negative selection) or to enrich amino terminus of cleavage products (positive selection) with specific reagent, followed by solid phase extraction or affinity chromatography. Isolated amino termini of cleavage products are finally analysed using MS, accompanied by statistical analysis.

TAILS is one of the applicable techniques and it was used by Dr Claire Wilson during her PhD to successfully identify 29 potential substrates for DP8 and DP9 (Agard and Wells, 2009; Kleifeld *et al.*, 2010; Kleifeld *et al.*, 2011; Lange and

Overall, 2013; Wilson *et al.*, 2013). At the completion of her PhD, she was only able to validate two of these substrates AK2 and calreticulin. Since DP8 and DP9 are intracellular proteases and localized in the cytoplasm (Abbott *et al.*, 2000; Olsen and Wagtmann, 2002; Ajami *et al.*, 2004), interaction between these proteases and their potential substrates is a prerequisite in order to understand their biological functions. Thus the aim of this chapter was to investigate whether DP8 and DP9 proteases co-localize with the two *in vitro* validated substrates AK2 and calreticulin. In addition, an *in vitro* cleavage assay was used to further test DP8 and DP9 substrates identified using this proteomics approach.

3.2. Materials and methods

3.2.1. MALDI-TOF mass spectrometry analysis

Twelve DP8 and DP9 potential substrates were chosen and peptides corresponding to the first 15 to 20 amino acid residues in the N terminus were synthesized (GL Biochem, Shanghai, China). Two previously validated substrates (AK2 and calreticulin), were used as positive controls and obtained from Genscript (Piscataway, NJ). To assist in complete solubilization of these peptides, the final charge of each peptide was calculated using the manufacturers instructions: -1 for acidic residue and +1 for basic residue. If the overall charge was positive or negative, substrates then were dissolved in water to make 100 μ M stock solution whereas substrates with neutral charge were dissolved in a mixture of organic solvents such acetonitrile, methanol and isopropanol and water. The short isoform of recombinant human DP8_{882aa} and DP9_{863aa} proteins, which were generated by Dr. Melissa Pitman and Mrs Kym McNicholas, respectively were expressed in Sf9 insect cells (McNicholas, 2008; Pitman *et al.*, 2010). Recombinant human DP4 was

generated by Dr Melissa Pitman using a construct generously supplied by ProBiodrug for expression of DP4 in *Pichia pastoris* yeast (Bar *et al.*, 2003). Recombinant proteins were purified using nickel affinity chromatography and stored at -80°C, added with 10% (v/v) glycerol and 0.1% (v/v) Tween-20 (Ajami *et al.*, 2008; McNicholas, 2008; Pitman *et al.*, 2010). The day prior to the MALDI-TOF assay, the DP enzyme activity of stored purified recombinant DP4, DP8 and DP9 was confirmed using the method described in Chapter 2. Volumes of purified enzyme equating to 0.17 mU of DP activity for DP4 and 1.7 mU of DP activity for DP8 and DP9 proteases were incubated with 10 µM of each peptide substrates in Tris buffer solution, which contained 50 mM Tris-HCl pH 7.4 and 150 mM NaCl. Incubation of the reaction mix was performed in a heat block (Thermoline, Australia) at 37°C for up to 24 h. Proteolytic activity of DP4, DP8 and DP9 against each peptide was analyzed by collecting samples at 4 time points: 0, 3, 6 and 24 h. The reaction was stopped by adding an equal volume of stop solution, 0.1% (v/v) TFA (Sigma-Aldrich). Because purified recombinant DP8 was preserved with 0.1% Tween-20 detergent, some sample reactions were cleaned up using a C18 Zip Tip (Millipore Corporation, Billerica, MA, USA). The tip was firstly equilibrated with 0.1% (v/v) TFA and samples were eluted in buffer solution which contained 80% (v/v) acetonitrile and 0.1% TFA.

Each sample was mixed with matrix before application to the MALDI- plate. For matrix solution, 52.86 mM of alpha-cyano-4-hydroxycinnamid acid solution was prepared by dissolving in 0.495 % (v/v) acetonitrile, 0.495 % (v/v) ethanol and 0.001 % (v/v) TFA. Standard peptides (provided by Flinders Analytical Laboratory) and samples were mixed well with matrix solution at 1:1 ratio and loaded on to a

brushed metal plate (MTP 384, Bruker daltonics, Billerica, MA, USA). Spotted samples were allowed to dry at RT for 20 min and then analyzed using a Bruker Autoflex III, MALDI MS/MS (Bruker daltonics, Billerica, MA, USA). Before firing samples, the MALDI-TOF instrument was calibrated using the standard peptide mix which consisted of adrenocorticotrophic hormone fragment, rennin tetra-decapetide and human angiotensin I with molecular mass 2465, 1759 and 1296 Da respectively. Because molecular masses of all synthetic substrates were less than 4000 Da, positive reflectron mode was used to analyze cleavage products. The peptide standard provided data accuracy with less than 0.05% error.

3.2.2. Cell Culture

Stable SKOV3 ovarian cancer cell lines overexpressing wt and mt DP8 and DP9 proteins, vector only control and non-transfected wt SKOV3 cells were grown in complete RPMI 1640 medium. The detailed methods were described in chapter 2 in this thesis.

3.2.3. Flow cytometry analysis

To ensure that SKOV3 cell clones expressed high levels of EGFP, flow cytometry analysis was regularly carried out. When SKOV3 cell culture reached confluence, all cells were harvested as described in detail in Chapter 2 materials and methods (Section 2.5.3). 1×10^6 cells were resuspended in 200 μ l of fluorescence- activated cell sorting (FACs) solution, containing 2% (w/v) glucose, 1.04% (v/v) formaldehyde (Merck, KGaA, Darmstadt, Germany) and 0.05% (w/v) sodium azide in PBS pH 7.4. Samples were then analyzed using an Accuri[®] C6 flow cytometer (BD Biosciences, San Jose, California, USA). The flow cytometer instrument was

set up at the fluidic rate of 50,000 events per second and ungated samples were collected for 2 min. Collected data was presented as a histogram plot and non-transfected wt SKOV3 cells were used as negative control. To analyze EGFP expression, all data from SKOV3 cells with EGFP tag were gated with wt SKOV3 cells and the percentage of EGFP-positive cell population was determined.

3.2.4. Immunocytochemistry

After harvesting cells as described in Materials and Methods chapter 2, 2×10^3 cells of wt SKOV3, SKOV3 cells over-expressing wt and mt DP8/DP9 proteins and vector only cells were transferred on to a sterile glass cover slip in a 6 well plate. Cells were incubated at 37°C in a 5% CO₂ incubator for 1h in order to attach completely to the cover slip. Two ml complete RPMI-1640 medium with or without 500 µg/ml gentamycin was added carefully into each well plate and then the cells were further incubated o/n. The following day, the attached cells were washed twice with PBS and fixed with 1ml of 3.7% fresh formaldehyde. Incubation was performed at RT for 15 min and excess formaldehyde was washed with PBS for 5 min. The cells were then permeabilized in 1ml of 0.2% Triton X-100 in PBS for 5 min and washed with PBS. Cells were blocked with 1% BSA (w/v) in PBS for 30 min at RT and then incubated with 1:50 dilution of anti-AK2 and calreticulin antibodies (see Table 2.2 for details) in buffer solution containing 1% BSA and 0.2% Triton X-100 for 90 min at RT. The excess primary Ab was removed by washing twice with PBS and the cells were then incubated with 1:50 dilution of donkey anti rabbit-Dylight 594 IgG and donkey anti goat-Dylight 549 IgG, respectively (Abcam plc, Cambridge, UK) in PBS with 1% BSA and 0.2% Triton X-100 for 90 min at RT. Finally, covers slips were washed twice with PBS and mounted cells-down on a

glass slide with VectaShield (Vector laboratories, Burlingame, CA, USA) mounting medium containing 4'-6-diaminidino-2-phenylindole (DAPI). Each corner of the cover slip was sealed with clear nail polish and allowed to dry for 1-2 h. Slides were observed under a SP5 Leica confocal microscope (Leica microsystems, Wetzlar, Germany) equipped with an argon laser and conventional filter sets. Fluorescence emission and nucleic acid stained with DAPI were separately captured. Collected image data were analyzed using Image J (Rasband, 1997-2012; Abramoff *et al.*, 2004) and Photoshop software.

3.2.5. Western Blotting

25 µg total protein from the cytosol fraction derived from each SKOV3 cell sample was mixed with the sample buffer as described in detail in the Materials and Methods in Chapter 2. For detecting AK2 and calreticulin, blotted membranes were incubated with anti-AK2 or anti-calreticulin polyclonal antibodies at one in 5,000 and 10,000 dilution, respectively. To detect DP8 and DP9 proteins, anti-DP8 and anti-DP9 polyclonal antibodies were diluted in Tris buffer solution at ratio 1: 5,000. As a loading control, anti-human β-actin was diluted 1: 10,000 in Tris buffer solution. Anti-rabbit secondary antibody coupled with HRP was used to detect antigen-antibody binding complexes for AK2, DP8 and DP9. Calreticulin primary antibody binding complexes were detected using an anti-goat secondary antibody with HRP. Anti-mouse secondary antibody linked to HRP was used to detect the interaction between β-actin and its primary antibody (Section 2.5.7.4). The ChemiDoc™ imaging system was used to visualise band images with an exposure time of 20 sec for calreticulin and β-actin. Other immunoblotted membranes were exposed for 900 sec.

3.2.6. DP enzyme activity

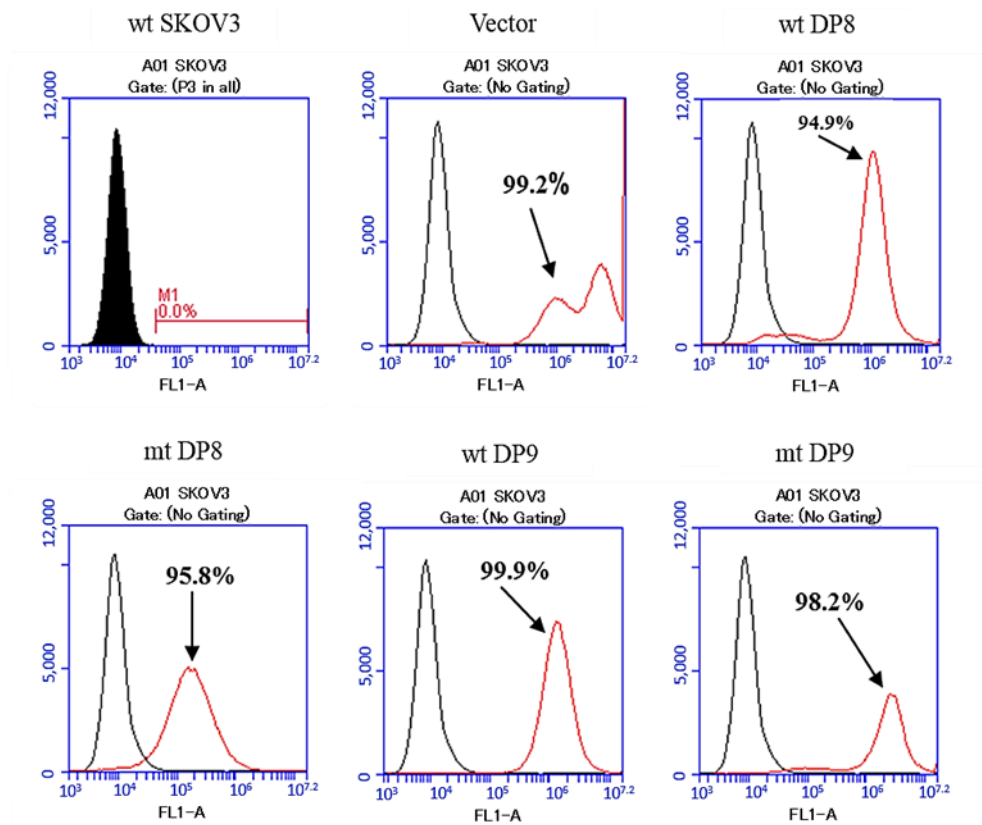
To ensure that SKOV3 cells overexpressed wt and mt DP8/DP9 and vector only, DP enzyme activity was measured in each batch of cells. The detailed method was described in Chapter 2.

3.3. Results

3.3.1. Characteristics of stable SKOV3 cell line

The stable DP8 and DP9 overexpressing cell lines were routinely monitored using flow cytometry to detect expression of EGFP fusion proteins and via DP enzyme assays. All stable SKOV3 cell lines expressed EGFP, 95% or more (Figure 3.1A). In addition, DP enzyme activity increased in SKOV3 cells with wt DP8 and DP9 overexpression while a lower DP enzyme activity was observed in SKOV3 cells with mt DP8 and mt DP9 overexpression, compared to that of SKOV3 cells with GFP expression vector (Figure 3.1B).

A. DP8 and DP9-EGFP expression



B. DP enzyme activity

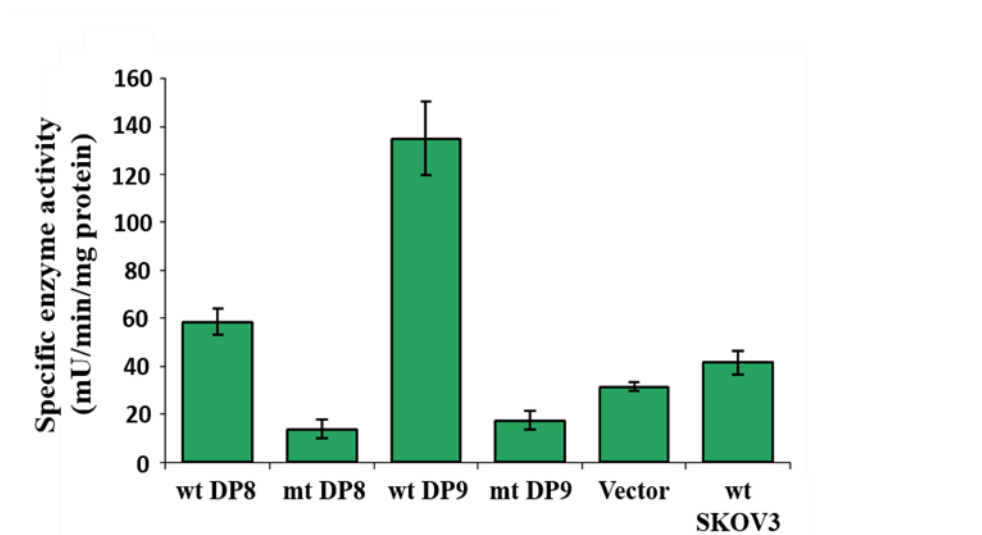


Figure 3.1. Characterization of SKOV3 cells overexpressing wt and mt DP8 and DP9 proteins. (A) Fluorescence intensity in SKOV3 cells overexpressing wt and mt DP8 or DP9, vector control (red open histogram) was analyzed using flow cytometry and gated with non-transfected cells (black histogram). (B) Specific enzyme activity of all SKOV3 cells was determined using 1 mM H-Ala-Pro pNA substrate. Data were presented in means \pm SEM in three independent experiments.

3.3.2. Co-localization of DP8/DP9 and AK2/calreticulin in SKOV3 cells

Endogenous DP8 and DP9 proteins appeared in all SKOV3 cell lines as a band of 99 kDa in mobility. The EGFP- fusion proteins ran as a band of 119 kDa in mobility (Figure 3.2). In the AK2 immunoblots a major band of 26 kDa in mobility appeared and in calreticulin immunoblots a major band of 55 kDa in mobility appeared. Neither AK2 or calreticulin were altered in their expression levels in the wt or mt DP8 and DP9 SKOV3 cell lines (Figure 3.2) indicating that DP8/DP9 proteolysis is unlikely to alter the stability of these two proteins. Co-localization of both wt and mt DP8- and DP9-EGFP with both AK2 and calreticulin was demonstrated by confocal microscopy (Figure 3.3 and Figure 3.4) suggesting that both proteases are not clearly localized in the mitochondria or endoplasmic reticulum. Unfortunately, immunostaining was not done with an endoplasmic reticulum or a mitochondrial marker in this study but these images were inserted as part of our recent publication (Wilson *et al.*, 2013). Application of these markers will be useful to determine localization of DP8/DP9-substrate complexes. No difference in the localization of either AK2 or calreticulin was detected between the wt DP8- and DP9-EGFP cell lines compared to the enzyme inactive mt DP8 and DP9-EGFP cell lines (Figure 3.3 and Figure 3.4).

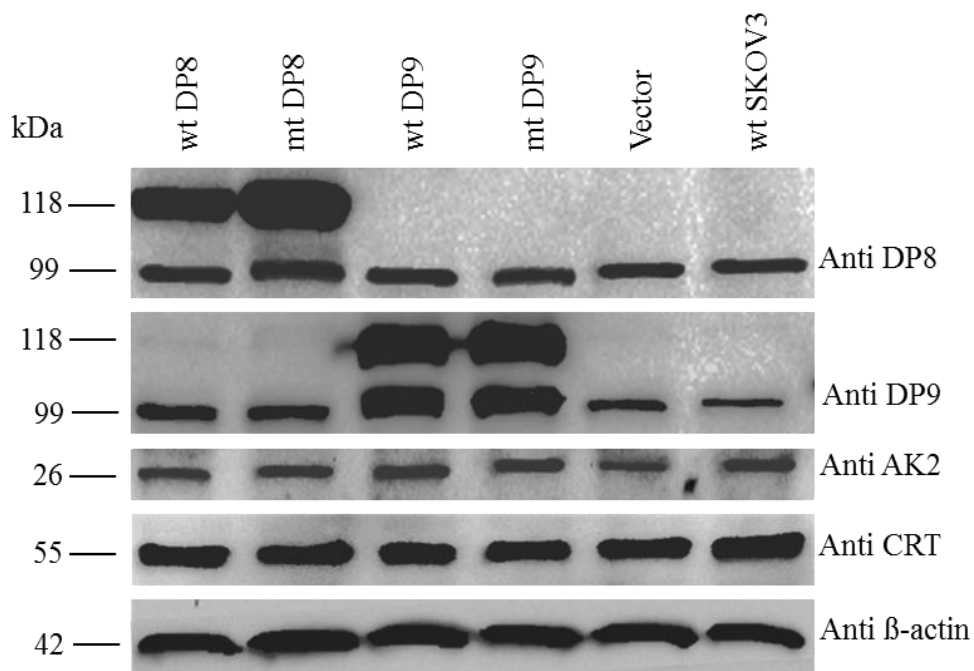


Figure 3.2. Protein expression in SKOV3 cells overexpressing wt and mt DP8 and DP9. Cell lysates (25 μ g) from DP8-EGFP, DP8(S739A)-EGFP, DP9-EGFP, DP9(S729A)-EGFP, vector-transfected and non-transfected SKOV3 cells were analyzed by 10% (w/v) SDS-PAGE and immunoblotting using DP8 (1:5000), anti DP9 (1: 5000), calreticulin (1:10,000), adenylate kinase 2(1:5000) and β -actin (1:10,000) as a loading control. The result is representative of three independent experiments.

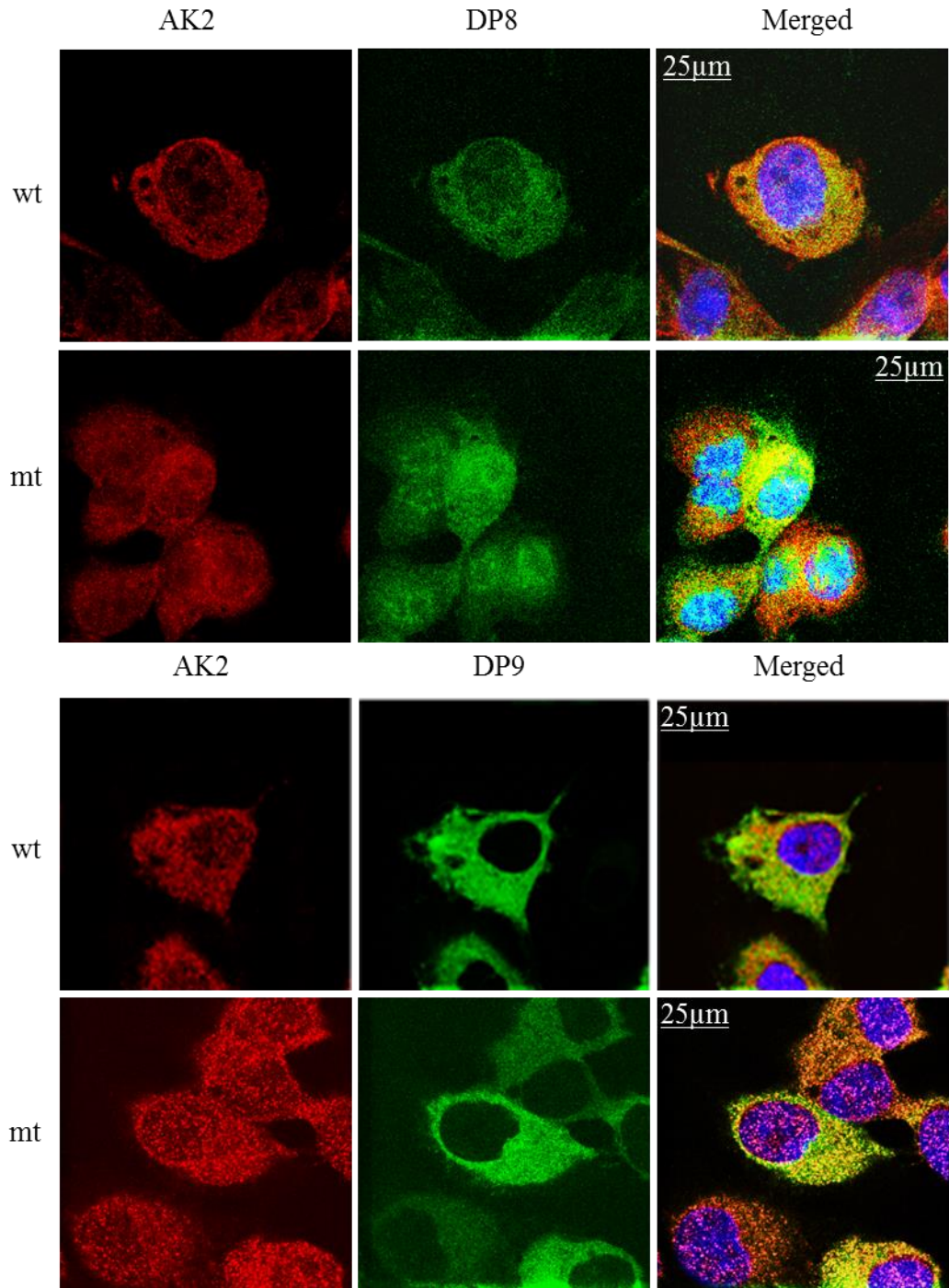


Figure 3.3. Co-localization of AK2 with DP8 and DP9 in stable SKOV3 cells. wt and mt DP8-EGFP and DP9-EGFP SKOV3 expressing cell lines were analysed by confocal microscopy and immunofluorescence using anti-AK2 (1:50) pAbs. As labelled, red panels display AK2 staining while green panels display wt and mt DP8-EGFP or DP9-EGFP expression. Merged images are shown in the far right hand panels. Blue is DAPI staining.

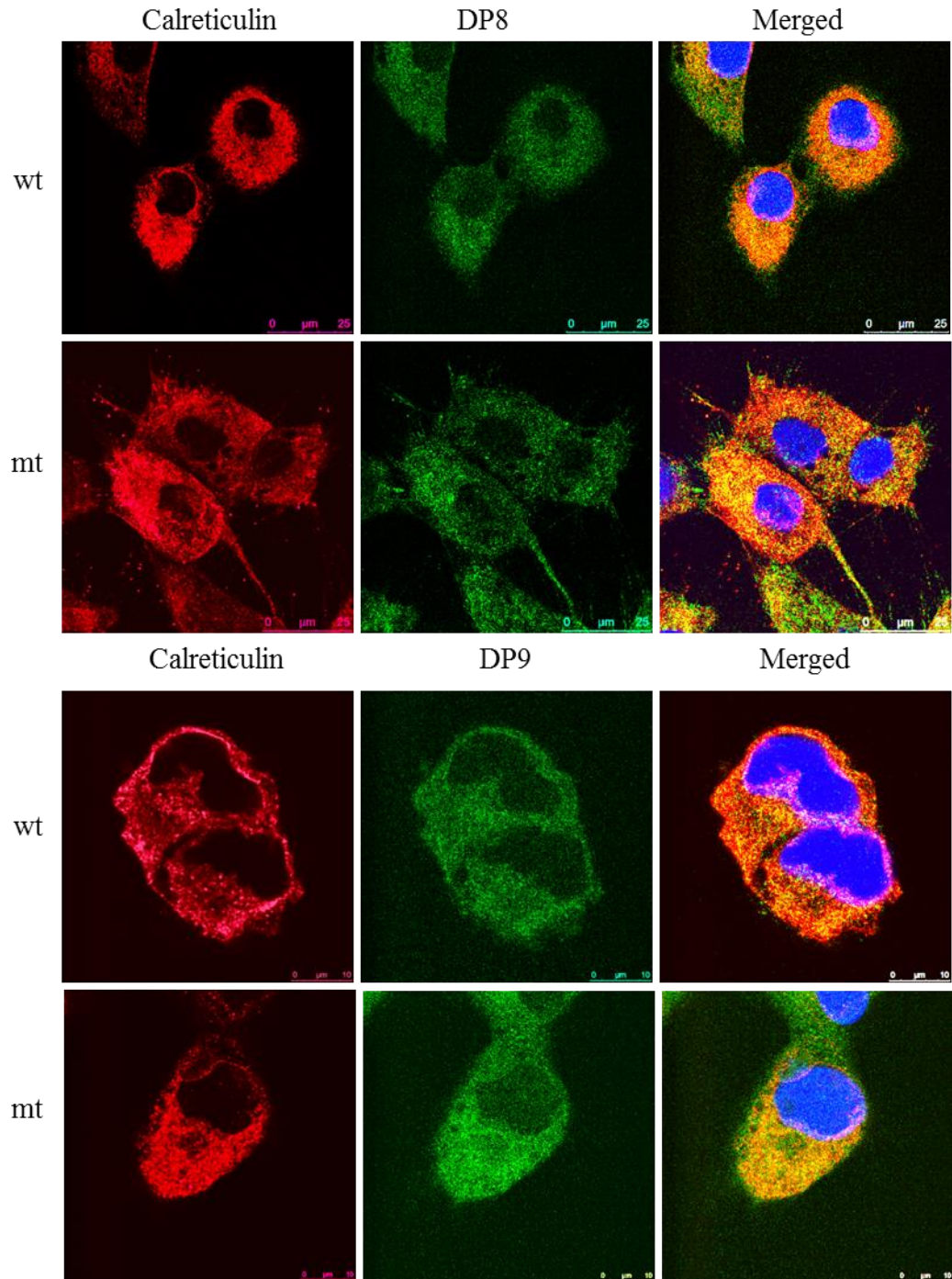


Figure 3.4. Co-localization of calreticulin with DP8 and DP9 in SKOV3 cells. wt and mt DP8-EGFP and DP9-EGFP SKOV3 expressing cell lines were analysed by confocal microscopy and immunofluorescence using anti-calreticulin (1:50) pAbs. As labelled, red panels display calreticulin staining while green panels display wt or mt DP8-EGFP or DP9-EGFP expression. Merged images are shown in the far right hand panels. Blue is DAPI staining.

3.3.3. Validation of potential DP8 and DP9 substrates

Although proteomic methods are able to identify potential protease substrates in a mixture of samples, it is necessary to validate whether these putative substrates are indeed substrates of the protease investigated or not. 12 potential substrates of DP8 and DP9 and two positive controls were tested using an *in vitro* cleavage assay and MALDI-TOF MS was used to detect cleavage products (Table 3.1). AK2 and calreticulin N-terminal oligopeptides were cleaved by DP8 and DP9 as previously demonstrated (see Appendix: Figure 8.2 and 8.3). In addition N terminal oligopeptides from bifunctional purine biosynthesis, cathepsin X/Z, C-1 tetrahydrofolate synthase, dihydropyrimidine dehydrogenase, mitochondrial import receptor subunit TOM34, obg-like ATPase 1 and serine/threonine protein phosphatase 6 which all have Pro residue in the P₁ position, were all cleaved by recombinant DP4, DP8 and DP9. Five of these substrates have an Ala residue at the P₂ position and either a Ser or Pro residue was observed at the P₂ position in N terminal cathepsin Z/X and obg-like ATPase 1, respectively. The molecular mass of observed cleavage products from DP8 and DP9 cleavage was similar to the expected cleavage products for the seven oligo substrates, which have full length of protein sequences ranging from 33.8 to 111.4 kDa. Five other potential substrates, acetyl-CoA acetyltransferase, mitochondrial, collagen-binding protein 2 (Serpine H-1), endoplasmic, enoyl-CoA hydratase, mitochondrial, and heat shock 70 kDa protein 1L were not cleaved by DP8 or DP9 proteases under the conditions tested (this data is presented in the Appendix, Figures 8.1, and 8.4 to 8.7). None of these N-terminal oligopeptides had a Ala or Pro in the P₁ position. However when these peptides were incubated with DP4, the N terminus of acetyl-CoA acetyltransferase was cleaved sequentially such that 4 amino acids were removed.

To investigate differences between DP8 and DP9 cleavage activity to each potential substrate, a time course experiment was performed where samples were collected at 0, 3, 6 and 24 h. In addition the ability of each substrate to be also cleaved by DP4 was also tested. As can be seen in Figure 3.5, the N terminus of bifunctional purine biosynthesis protein PURH was cleaved by DP8, DP9 and DP4 proteases. However, while a similar cleavage rate was observed for both DP8 and DP9, the cleavage rate was markedly lower than the DP4 cleavage rate. A 2040 Da cleavage product of bifunctional purine biosynthesis protein was first observed after 3h incubation. This cleavage is quite slow and after 24h incubation 50% of the full length peptide remained. In contrast, DP4 cleaved the peptide instantly and almost 100% of the peptide was cleaved after 3h incubation.

It can be seen in Figure 3.6 that the first cleaved peptide from N terminus of C-1-tetrahydrofolate synthase was observed after 24h incubation with DP8 but with DP9, the cleaved product was observed early, after 6h incubation. After 24h incubation, the peptide was completely cleaved by DP9. Meanwhile, DP4 cleaved this peptide instantly and it reached 100% after 6h incubation.

Table 3.1. Cleavage of DP8 and DP9 potential substrates. 12 potential substrates which have Pro, Ser, Glut, Asp and Thr residues in the P1 position of N terminus were selected and tested for cleavage by DP8 and DP9. AK2 and calreticulin N-terminal oligopeptides were used as positive controls. 10 μ M of peptide substrate was incubated with 1.7 mU of either purified recombinant DP8 or DP9. Samples were collected at 0 and 24 hours by adding stop solution, 0.1% (v/v) TFA. MALDI-TOF MS was used to analyze the cleavage products of DP8 or DP9 proteolytic activity. nc=no cleavage

Substrate	Biological pathway	Sequence length (aa)	Molecular mass (Da)	NH2 -terminal oligopeptide	Uniprot KB Accession	Molecular mass (Da)	Expected molecular Mass (Da) post cleavage	Observed molecular Mass (Da)		
								DP8	DP9	DP4
Acetyl-CoA acetyltransferase, mitochondrial	Fatty acid metabolism	427	45,200	VSKPTLKEVVIVSATR	P24752	1727.09	1540.87	nc	nc	nc
AK2	Purine metabolism, cellular energy homeostasis	239	26,478	APSVPAAEPEYPKGIR	P54819	1681.89	1512.79	1513.9	1514.0	1514.8
Bifunctional purine biosynthesis protein PURH	Purine metabolism	592	64,616	APGQLALFSVSDKTGLVEFAR	P31939	2206.55	2038.34	2039.4	2039.5	2039.4
C-1-tetrahydrofolate synthase, cytoplasmic	Glyoxylate and dicarboxylate metabolism, one carbon pool by folate	935	101,559	APAEILNGKEISAQIR	P11586	1709.98	1541.77	1542.8	1542.9	1542.9

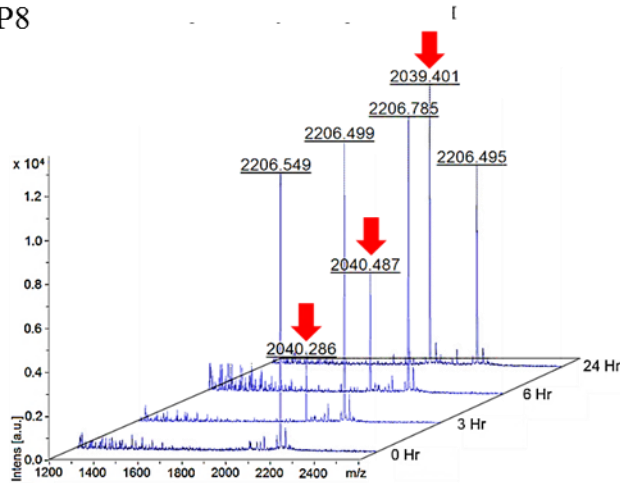
Calreticulin	Chaperone, antigen processing and presentation	417	48,142	EPAVYFKEQFLDGDGWTSR	P27797	2245.45	2017.95	2020.3	2019.2	2020.3
Cathepsin Z/X	Lysosome, proteolysis	303	33,868	SPADLPKSWDWRNVDG	Q9UBR2	1843	1658.8	1659.9	1659.9	1659.8
Collagen-binding protein 2 (Serpine H-1)	Response to unfolded protein, chaperone	418	46,441	AEVKKPAAAAAPGTAEKLSR	P50454	1907.21	1707	nc	nc	nc
Dihydropyrimidine dehydrogenase [NADPH ⁺]	Pyrimidine metabolism	1025	111,401	APVLSKDSADIESILALNPR	Q12882	2109.43	1941.22	1942.3	1942.4	1942.3
Endoplasmic reticulum chaperone	NOD-like receptor signaling pathway, chaperone	803	92,469	DDEVVDVGTVEEDLGKSR	P14625	1978.03	1749.81	nc	nc	nc
Enoyl-CoA hydratase, mitochondrial	Fatty acid	290	31,387	ASGANFEYIIAEKRGK	P30084	1753.99	1595.82	nc	nc	1596.8
Heat shock 70 kDa protein 1L	Response to unfolded protein, antigen processing	641	70,375	ATAKGIAIGIDLGTTYSCVG	P34931	1911.21	1739.01	nc	nc	nc
Mitochondrial import receptor subunit TOM34	Protein targeting and import, chaperone	309	34,559	APKFPDSVEELRAAG	Q15785	1586.78	1418.57	1419.6	1419.7	1419.6

Obg-like ATPase 1	ATP catabolism	396	44,744	PPKKGDDGIKPPPIGR	Q9NTK5	1727.1	1532.86	1533.9	1533.9	1533.9
Serine/threonine- protein phosphatase 6	Protein dephosphorylation, G1/S transition of mitotic cell cycle	305	35,144	APLDDKYVEIARLCK	O00743	1847.22	1679.01	1680.0	1679.6	1680.0

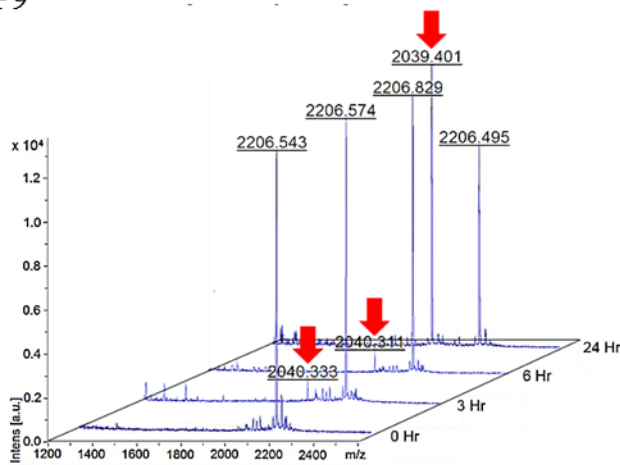
The N terminal peptide of cathepsin Z/X was cleaved by DP8 after 3h incubation and 50% of this peptide was still intact after 24h incubation (Figure 3.7). In contrast to DP8, DP9 cleaved this peptide more slowly, and cleavage was not observed till 6h incubation. Complete cleavage was observed by 24h. The cleavage activity of DP4 against this peptide was faster than that of DP8 and DP9 and the same pattern as the cleavage rate of bifunctional purine biosynthesis protein PURH.

The cleavage activity of DP8 and DP9 to N terminal peptide of dihydropyrimidine dehydrogenase [NADP⁺] seemed to have a similar pattern to cathepsinZ/X (Figure 3.8). The first cleaved peptide was observed after 3h incubation but it only reached around 50% cleavage after 24h incubation with DP8. In the DP9 incubation, this peptide was completely cleaved after 24h. Approximately 50% of this peptide was cleaved by DP4 instantly and no intact peptide was observed after 3h incubation.

A. DP8



B. DP9



C. DP4

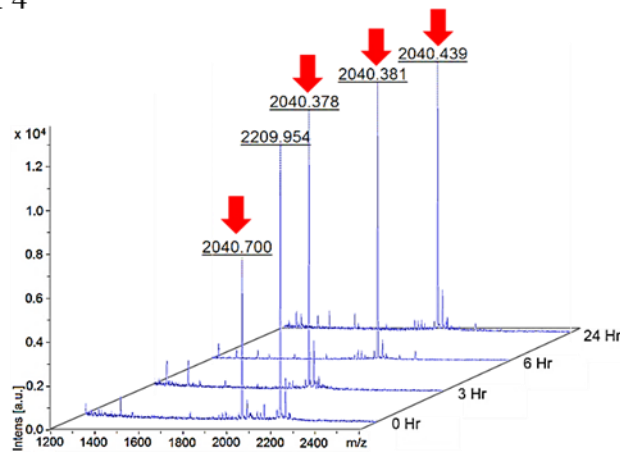
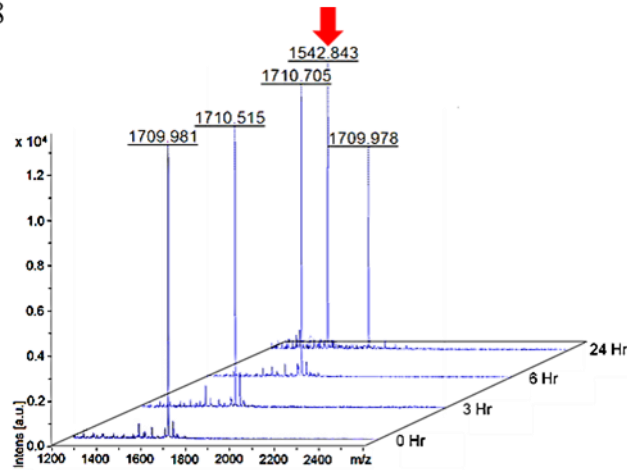
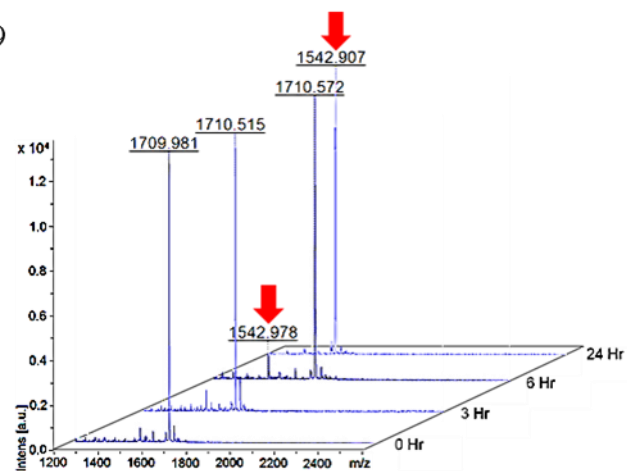


Figure 3.5. DP8, DP9 and DP4 cleavage activity toward the N- terminus bifunctional purine biosynthesis protein PURH. A cleaved peptide product (around 2040 Da) is indicated by red arrows and uncleaved peptide has expected molecular mass 2206.55 Da. Similar cleavage profiles were obtained for DP8 and DP9. The cleaved peptide was observed after 3h incubation and more than 50% peptide was cleaved after 24h incubation. In contrast, the peptide was directly cleaved by DP4 after 0 h incubation and this peptide was almost completely cleaved after 3h incubation. Data represents three independent experiments.

A. DP8



B. DP9



C. DP4

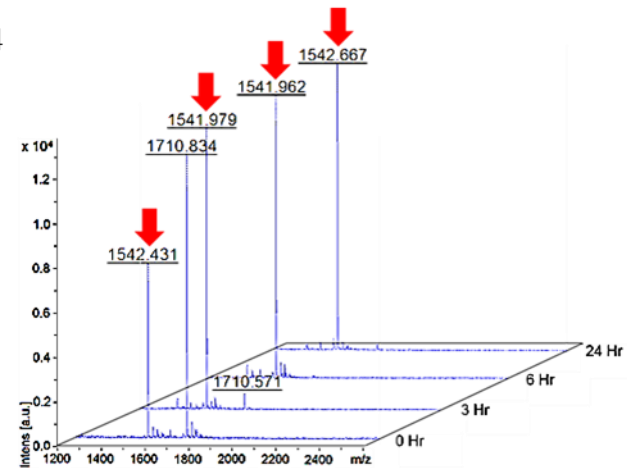
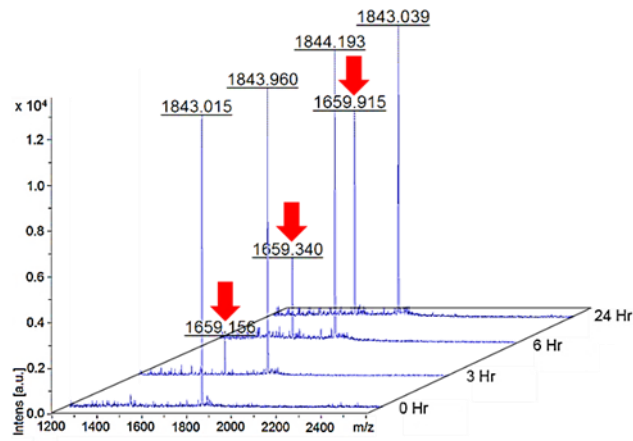
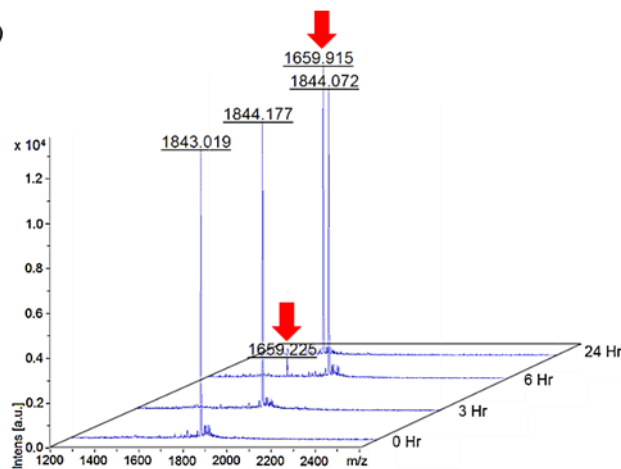


Figure 3.6. DP8, DP9 and DP4 cleavage activity toward the N- terminus of C-1-tetrahydrofolate synthase, cytoplasmic. A cleaved peptide product (around 1542 Da) is indicated by red arrows and uncleaved peptide has expected molecular mass 1709.98 Da. DP8 and DP9 had different cleavage profile for this peptide. The cleaved peptide was observed after 24h incubation with DP8 and 6h incubation with DP9. In contrast, the peptide was directly cleaved by DP4 after 0h incubation and this peptide was almost completely cleaved after 3h incubation. Data represents two independent experiments.

A. DP8



B. DP9



C. DP4

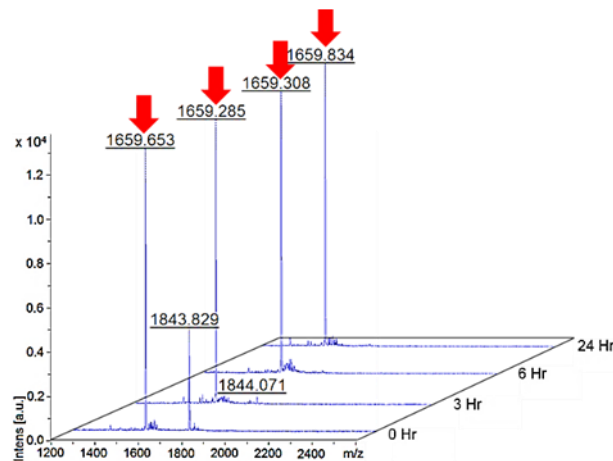
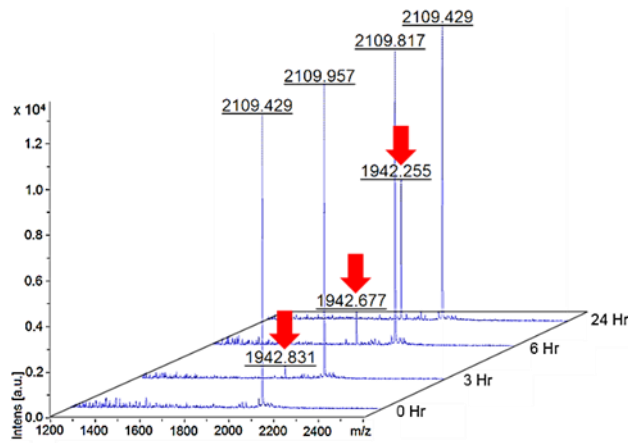
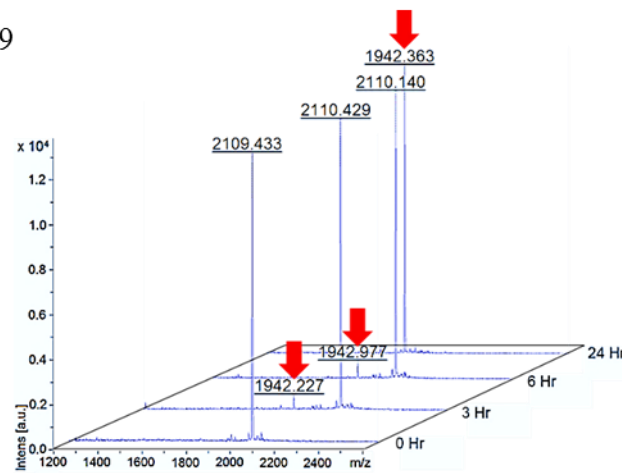


Figure 3.7. DP8, DP9 and DP4 cleavage activity toward the N – terminus of cathepsin Z/X. A cleaved peptide product (around 1659 Da) was indicated by red arrows and uncleaved peptide has molecular mass 1843 Da. DP8 and DP9 had different cleavage profiles for this peptide. The cleaved peptide was observed after 3h incubation with DP8 and 6h incubation with DP9. By contrast, the peptide was directly cleaved by DP4 after 0h incubation and this peptide was almost completely cleaved after 3h incubation. Data represents two independent experiments.

A. DP8



B. DP9



C. DP4

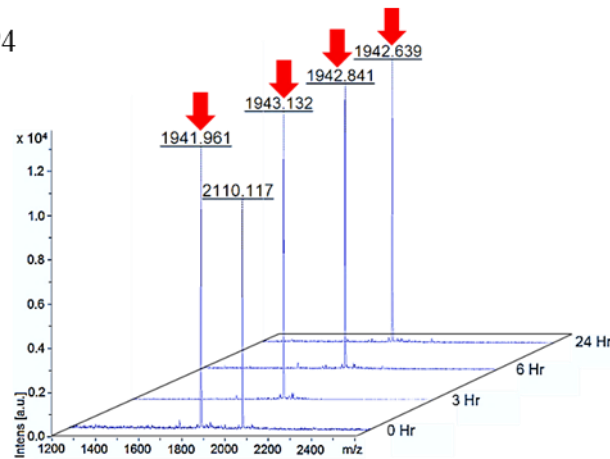


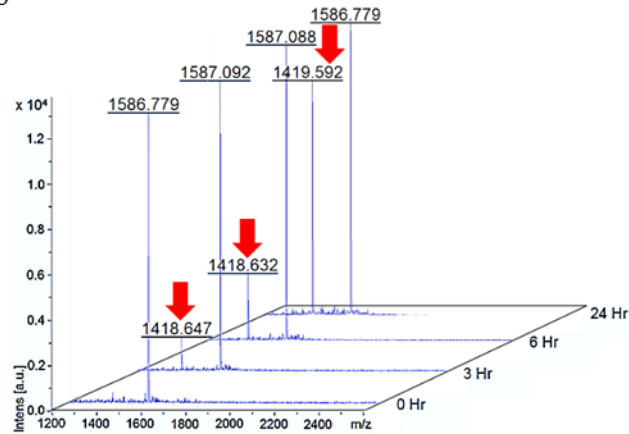
Figure 3.8. DP8, DP9 and DP4 cleavage activity toward the N- terminus of dihydropyrimidine dehydrogenase [NADP⁺]. A cleaved peptide product (around 1942 Da) is indicated by red arrows and uncleaved peptide has expected molecular mass 2109.43 Da. The first cleaved peptide was observed after 3h incubation with either DP8 or DP9. Around 50% of this peptide was cleaved by DP8 and this peptide was completely cleaved DP9 after 24h incubation. By contrast, the peptide was directly cleaved by DP4 after 0h incubation and this peptide was almost completely cleaved after 6h incubation.

In contrast to the N terminal peptide of dihydropyrimidine dehydrogenase [NADP⁺], a higher cleavage rate was observed for the N terminal peptide of mitochondrial import receptor subunit TOM34 incubated with DP8 than with DP9 (Figure 3.9). After 3h incubation, this peptide was cleaved by DP8 and DP9 with a similar rate but around 40% cleaved peptide was only observed after 24h incubation with DP8. Cleavage activity of DP4 to this peptide was similar to the cleavage activity to the peptide of dihydropyrimidine dehydrogenase.

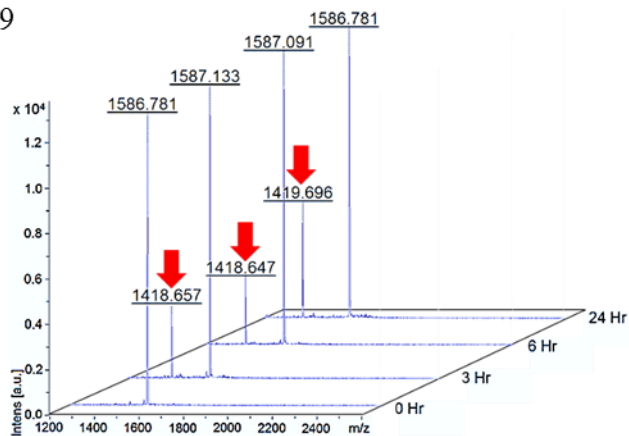
In Figure 3.10, DP8 and DP9 had different cleavage activity against the N terminal peptide of obg-like ATPase 1. The initial cleavage product was observed after 3h incubation with either DP8 or DP9. However, DP9 completely cleaved this peptide after 24h incubation while DP8 did not 100% cleave this peptide after this period of time. DP4 cleaved this peptide faster than DP8 and DP9. Most of this peptide was cleaved by DP4 after 6h incubation.

DP8 cleaved the N terminal peptide of serine/threonine-protein phosphatase 6 faster than DP9 (Figure 3.11). After 3h incubation, the initial cleavage product was obtained for both DP8 and DP9. The completely cleaved peptide was observed in DP8 after 24h incubation but only a half of the peptide was cleaved by DP9. The cleavage activity of DP4 to this peptide was the same as the previously validated peptides and was complete within 3h.

A. DP8



B. DP9



C. DP4

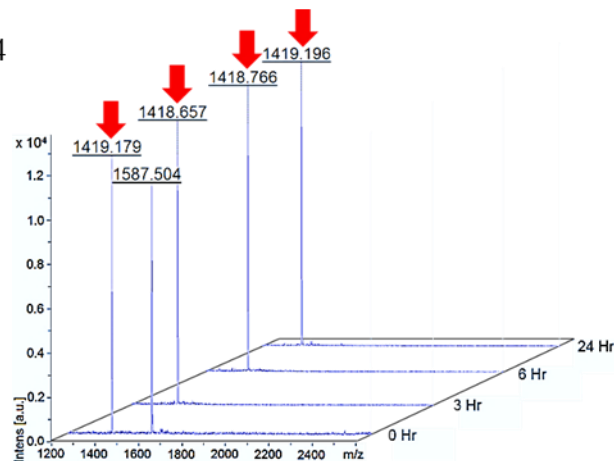
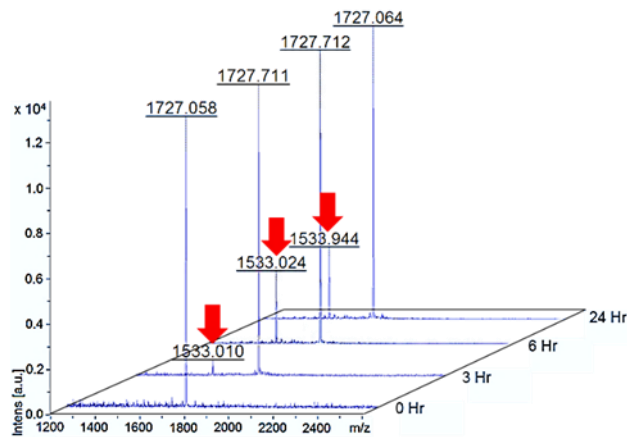
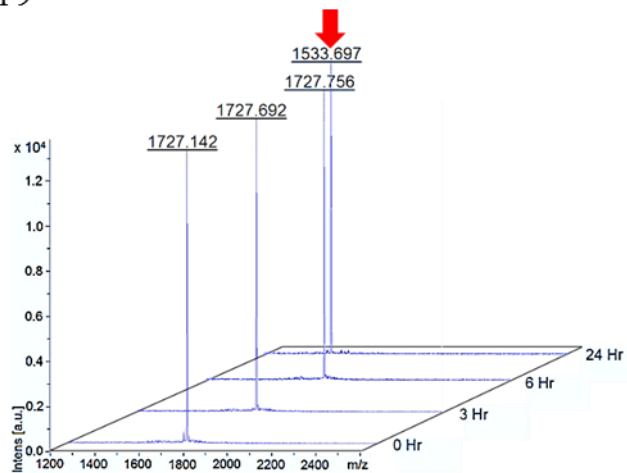


Figure 3.9. DP8, DP9 and DP4 cleavage activity towards the N-terminus of mitochondrial import receptor subunit TOM34. A cleaved peptide product (around 1419 Da) was indicated by red arrows and uncleaved peptide has expected molecular mass 1586.78 Da. The first cleaved peptide was observed after 3h incubation with either DP8 or DP9. 100% of this peptide was cleaved by DP8 and this peptide was partially cleaved DP9 after 24h incubation. By contrast, the peptide was directly cleaved by DP4 after 0h incubation and this peptide was completely cleaved after 3h incubation.

A. DP8



B. DP9



C. DP4

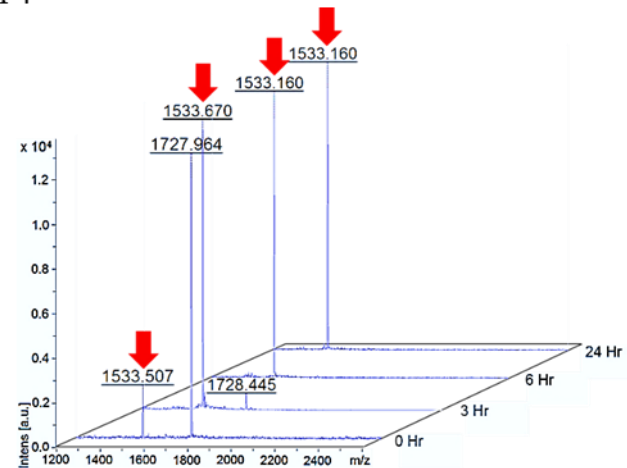
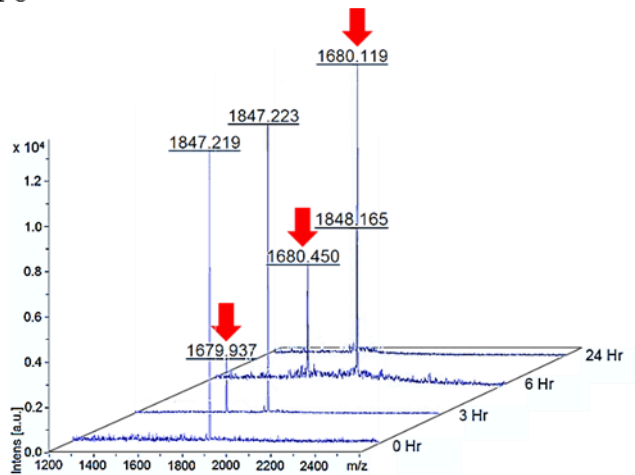
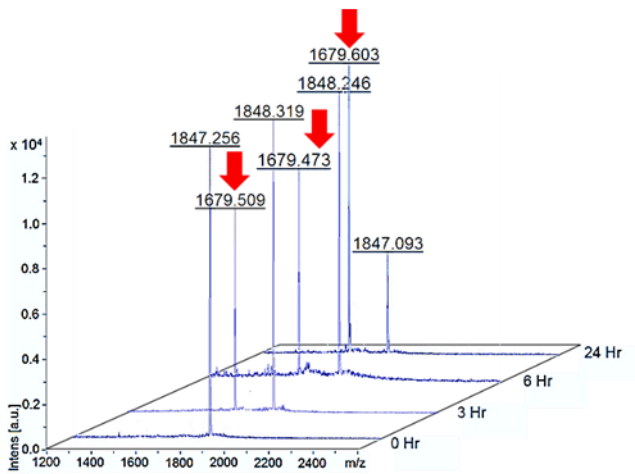


Figure 3.10. DP8, DP9 and DP4 cleavage activity toward the N- terminus of obg-like ATPase 1. A cleaved peptide product (around 1534 Da) is indicated by red arrows and uncleaved peptide has expected molecular mass 1727.1 Da. The first cleaved peptide was observed after 3h incubation with DP8 and 24h incubation with DP9. By contrast, the peptide was directly cleaved by DP4 after 0h incubation and this peptide was almost completely cleaved after 3h incubation.

A. DP8



B. DP9



C. DP4

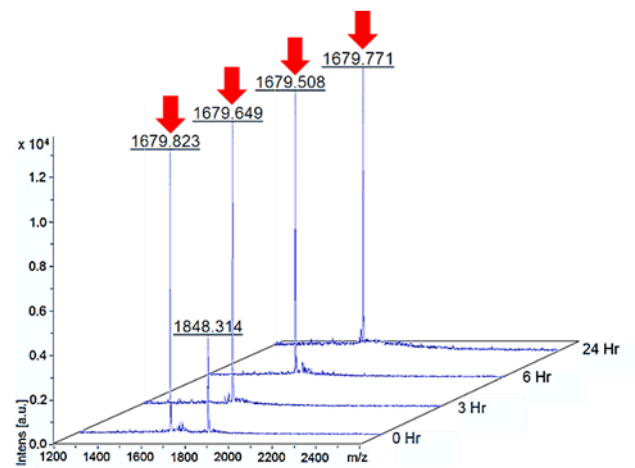


Figure 3.11. DP8, DP9 and DP4 cleavage activity towards the N- terminus of serine/threonine-protein phosphatase 6. A cleaved peptide product (around 1680 Da) is indicated by red arrows and uncleaved peptide has expected molecular mass 1847.22 Da. The first cleaved peptide was observed after 3h incubation with either DP8 or DP9. 100% of this peptide was cleaved by DP8 and this peptide was partially cleaved by DP9 after 24h incubation. By contrast, the peptide was completely cleaved by DP4 after 3h incubation.

3.4. Discussion

In this chapter it has been demonstrated that DP8 and DP9 protease expression can be co-localized with the expression of the newly identified substrates AK2 and calreticulin in the cytoplasm of SKOV cells. In addition during this study the cleavage of the N- terminus of a further seven potential DP8 and DP9 substrates was validated and the cleavage rates were monitored and compared to DP4. When DP8 and DP9 cleave AK2, calreticulin or any of these seven other substrates *in vivo*, there will be only two amino residues difference between the cleaved and uncleaved full-length proteins. In many other proteomic studies cleavage is confirmed using Western blotting as it results in two distinct bands in mobility in the immunoblot, in this instance cleavage of these substrates by the DPs will not be detected using Western Blotting, unless Abs were available for each neo –N – terminus of the cleaved N- terminus. Therefore, at present the only way to differentiate between the cleaved and uncleaved peptides is via MS.

3.4.1. AK2 and calreticulin are natural substrates for DP8 and DP9

The full sequence of AK2 protein has 239 aa residues, including Met-Ala-Pro residues at the amino terminus (Table 3.1). This protein is originally synthesized in the ribosome and undergoes transcriptional and translational modifications (Schlauderer and Schulz, 1996; Lee *et al.*, 1998). Some published studies have reported that AK2 has two isoforms, which encode 239 and 232 amino acids (Kishi *et al.*, 1987; Lee *et al.*, 1996; Lee *et al.*, 1998; Noma *et al.*, 1998). Both AK2 isoforms have the same N- terminus but the longer isoform has seven additional amino acid residues at the C terminus (Lee *et al.*, 1998). Therefore both of these isoforms are potential DP8 and DP9 substrates. Schlauderer and Schulz (1996)

isolated both these enzyme isoforms from bovine liver and both forms lack the Met and the Ala-Pro dipeptide. In addition, while the two isoforms are differentially expressed in some human tissues the AK enzyme activity of the long and short AK2 isoforms is not different (Lee *et al.*, 1998; Noma *et al.*, 1998). These results indicate that AK2 is regulated in a tissue-specific manner (Tanabe *et al.*, 1993).

Interestingly, cytosolic and mitochondrial AK2 protein has the same amino acid sequence (Kishi *et al.*, 1987; Lee *et al.*, 1996; Lee *et al.*, 1998). Naturally, the Met residue in AK2 seems to be removed by an unknown or known protease like methionine aminopeptidase (Ben-Bassat *et al.*, 1987). Our findings (Figure 3.3) suggest that DP8 and DP9 might have an important role in processing the N terminus of AK2 since the long and short isoforms of bovine AK2, which lack the Ala-Pro residues, have a two-fold increase in AK enzyme activity, compared to the enzyme activity of uncleaved AK2 isoforms (Schlauderer and Schulz, 1996). However, further studies are required for investigating whether Ala-Pro-cleaved AK2 exists in human tissues or not.

Lack of AK2 function in some living organisms leads to detrimental effects. For example, knock down of the AK2 gene in insect larvae can cause cessation of cell growth and development (Fujisawa *et al.*, 2009; Chen *et al.*, 2012). Interestingly, Lankas *et al.* (2005) found that administration of a DP8/DP9 selective inhibitor in animal models leads to serious effects in the lymphoid system like anemia, thrombocytopenia and spleen enlargement. The clinical signs of the toxicity of DP8/DP9 inhibitor resemble the clinical signs of human AK2 mutation, which is

characterized by failure of haematopoiesis (Lagresle-Peyrou *et al.*, 2009; Pannicke *et al.*, 2009).

Unlike AK2, calreticulin, which is not an enzymatic protein, is highly expressed in all living cells (Krause and Michalak, 1997; Michalak *et al.*, 2009). Looking at its structure, calreticulin has 417 aa residues with two endoplasmic reticulum-targeting signal sequences: a short signal sequence in the N terminus and KDEL sequence in the C terminus (Gelebart *et al.*, 2005; Michalak *et al.*, 2009). In the lumen of endoplasmic reticulum in human cells, the 17 aa signal sequence of calreticulin, which contains hydrophobic residues, is removed (Fliegel *et al.*, 1989; Denning *et al.*, 1997). Retrotranslocation of the active calreticulin to the cytoplasm was also observed in order for the protein to fulfil its function in modulation of cell adhesion, antigen presentation and complement activation (Gao *et al.*, 2002; Afshar *et al.*, 2005). Because the first two amino acids of active calreticulin are occupied by Glu-Pro residues, *in vivo* this N-terminus will be available to naturally become a DP8 and/or DP9 substrate. *In vitro* cleavage studies in this thesis and by Wilson *et al.* confirm that DP8 and DP9 cleave Glu-Pro from the N terminal peptide of calreticulin (Wilson *et al.*, 2013). However, other studies reported that under stress conditions, the cytosolic calreticulin undergoes arginylation, replacing Glu with the Arg residue, to associate with stress granules (Decca *et al.*, 2007; Carpio *et al.*, 2010). Therefore, DP8 and DP9 may not be able to cleave the arginylated calreticulin (Wilson *et al.*, 2013) or if DP8 or DP9 cleave calreticulin it is no longer able to be modified in order to associate with stress granules. Thus DP8 and DP9 may play an important role in the regulation of calreticulin.

3.4.2. Validation of potential substrates for DP8 and DP9

This study has validated that DP8 and DP9 are indeed processing some of the potential substrates identified during the TAILS proteomic study, which have numerous biological functions in processes such as metabolite degradation, immune responses, cell cycle regulation and cellular metabolism. However, compared to the proteolytic activity of DP4, their proteolytic activity is less efficient (Figure 3.5-3.11). Interestingly, all validated substrates in this study, including AK2 and calreticulin, are located in the cytoplasm, lysosomes and/or mitochondria. As reported by Abbott *et al.* (2000); Ajami *et al.* (2004) and Lee *et al.* (2006a), DP8 and DP9 are localized in cytoplasm, and will be able to interact with their substrates in this location. To date no evidence has been provided that suggests that DP8 and DP9 reside in the mitochondria. All of the mitochondrial substrates identified are translated in the cytoplasm and transported to the mitochondria so may be cleaved by either DP8 or DP9 before being transported.

All substrates that were validated in the *in vitro* cleavage activity had a Pro residue in the P₁ position and hydrophilic or hydrophobic residues in the P₂ position. Six substrates had Ala residues and the remaining substrates have Glu, Pro and Ser residues at the P₂ position (Table 3.1). This data confirms the preference data for DP8 and DP9 that has been determined by using substrate libraries and commercial substrates studies (Bjelke *et al.*, 2006; Ajami *et al.*, 2008) In addition, Bjelke and colleagues (2006) showed that DP8 and DP9 could cleave peptides that contain Arg and Lys or other residues in the P₂ position at the N terminus. None of the substrates that were identified using the TAILS proteomic approach contained these residues (Wilson *et al.*, 2013).

3.4.3. Proteins with a signal sequence:

Bifunctional purine biosynthesis protein PURH, for instance, is a cytoplasmic enzyme protein that has dual functions in catalysing the last two steps of purine synthesis. It has aminoimidazolecarboxamide ribonucleotide transformylase (AICAR Transformylase) activity in the carboxyl terminus and inosine monophosphate cyclohydrolase (IMPCH) activity in the amino terminus, respectively (An *et al.*, 2008). From the protein structure, this purine biosynthesis enzyme has 592 amino acid sequences. 1-198 aa residues, including the Met-Ala-Pro residues in the amino terminus belong to the IMPCH domain and 199-592 aa residues form the AICAR transformylase domain (Cheong *et al.*, 2004). Both domains can be expressed separately in active forms and are localised in the cytoplasm (Rayl *et al.*, 1996; Tibbetts and Appling, 2000). In the presence of Bas 1p and Bas 2p transcription factors, two metabolic intermediates (AICAR and succinyl-AICAR) and low concentrations of phosphate and purine bifunctional purine biosynthesis protein PURH gene expression is upregulated (Tibbetts and Appling, 2000; Pinson *et al.*, 2009). However, a proteolytic enzyme that degrades this enzyme has not been identified. Therefore, DP8 or DP9 might have a role in inactivation of this protein during purine metabolism. It is possible that when the Ala-Pro is removed from the N-terminus of the IMPCH domain it modifies this activity.

Cathepsin Z/X is another potential substrate of DP8 and DP9 proteins. As occurs in general enzyme biosynthesis, this cathepsin is synthesised as preproenzyme, which has 303 aa residues (Nägler and Menard, 1998). The 23 aa signal sequence is removed after translocation in the endoplasmic reticulum. The 38 aa transit sequence remains attached in the N terminus to stabilise the intact protein during migration to

the lysosomes (Nägler and Menard, 1998; Santamaria *et al.*, 1998; Deussing *et al.*, 2000). Our finding in a biochemical assay indicated that DP8 and DP9 proteins cleaved the N terminal peptide of cathepsin X but the N terminal peptide used in this study begin toward the end of pro peptide and is not present in the active Cathepsin X (Nägler and Menard, 1998; Deussing *et al.*, 2000). So, the proenzyme Cathepsin X is unlikely to become a proteolytic target by DP8 and DP9. Interestingly, activated Cathepsin X/Z has Leu-Pro residues in the N terminus that is secreted and found in some human tissues (Santamaria *et al.*, 1998; Krueger *et al.*, 2005; Staudt *et al.*, 2010). Therefore, DP4 may probably cleave this secreted cathepsin because from the results of *in vitro* cleavage assay, DP4 also cleaved the N terminal peptide of cathepsin X/Z, faster than the proteolytic activity of DP8 and DP9 (Figure 3.7).

3.4.4. Substrates which contain a Met that is removed

Seven of the substrates that were validated for DP8 and DP9 shared the common feature of having an initiator Met followed by Ala-Pro dipeptides (“MAP”) at their N termini. In nature there exists a class of aminopeptidases called methionine aminopeptidases whose function is to remove the initiator Met from the N- terminus (Ben-Bassat *et al.*, 1987). From examining Uniprot at present, there was evidence that only four of the seven proteins existed *in vivo* with the Met removed. So that they could be cleaved by either DP8 or DP9 but this does not mean *in vivo* that these modifications do not exist. All peptides that were validated in our study had this Met residue removed.

From our *in vitro* study, the N terminal peptide of cytoplasmic C-1-tetrahydrofolate (THF) synthase was cleaved by DP8 and DP9 proteases. Naturally, this enzyme has

three activities: a 10-formyl-THF synthetase, 5, a 10-methenyl-THF cyclohydrolase and 5, 10-methylene-THF dehydrogenase activity in a single protein (Hum *et al.*, 1988; Schmidt *et al.*, 2000). The TFH synthase has the function of transferring one monocarbon unit into tetrahydrofolate (active folic acid) during production and degradation of purine, pyrimidine, methionine, serine and glycine (Hum *et al.*, 1988; Schmidt *et al.*, 2000). From the primary structure, this enzyme has a 935 aa sequence, in which the dehydrogenase and the cyclohydrolase are located at the amino terminal domain and the synthase is localised at the carboxyl terminal domain (Hum *et al.*, 1988). In human cells, there are two types of this enzyme, one located in the cytoplasm and the other in the mitochondria. They share 61% amino acid identity (Prasanna *et al.*, 2003). However, the mitochondrial sequence contains a transit peptide sequence which is removed and the final chain does not have a sequence that could be cleaved by DP8 or DP9. Thus DP8 or DP9 proteins may work together to control the dehydrogenase and the cyclohydrolase activities of cytoplasmic THF in order to control intracellular biosynthesis of purine and pyrimidine. Once the two amino acids are removed it may affect the activity, binding or the stability of THF.

The next cytoplasmic substrate of DP8 and DP9 is dihydropyrimidine dehydrogenase (DPD) [NADPH⁺] enzyme, which degrades thymine and uracil to become β-amino-isobutyric acid and β-alanine respectively (Wasternack, 1980). This DPD enzyme is encoded by the DPD gene located on chromosome 1p22 which is approximately 150 kb in length. This active enzyme has 1025 aa sequence with Met-Ala-Pro residues in the amino terminus and 111.40 kDa molecular mass (Yokota *et al.*, 1994; Johnson *et al.*, 1997). This enzyme is also involved in metabolising a chemotherapeutic drug (5-Fluorouracil) by competing with the thymidilate synthase

activity (Wasternack, 1980; Heggie *et al.*, 1987; Yokota *et al.*, 1994; Johnson *et al.*, 1997). Some studies reported that up regulation of this enzyme are related to advanced stages of some human cancer cells (Ajiki *et al.*, 2006; Fukui *et al.*, 2008). So, DP8 and DP9 might play a role in keeping the balance between DPD and thymidilate enzymes in the cytosol compartments.

Another potential substrate for DP8 and DP9 proteins, which has Met-Ala-Pro residues at the amino terminus, is mitochondrial import receptor subunit TOM 34. From its name, this receptor contributes to importing mitochondrial proteins synthesized in the ribosome by interacting with the mature portion of mitochondrial precursor proteins (Chewawiwat *et al.*, 1999; Mukhopadhyay *et al.*, 2002). In contrast to TOM 34, TOM 20 which is another receptor component of TOM complex binds to mitochondrial precursor proteins. From the primary structure, TOM 20 possesses Met-Val-Gly residues in the amino terminus and also a mitochondrial targeted signal sequence. So, it would probably not be a DP8/DP9 substrate (Mukhopadhyay *et al.*, 2002). In the outer membrane of mitochondria, TOM protein complexes consist of TOM 40 as a core component and other TOM receptors such as TOM 20, 22, 34, 37 and 70 (Shimokawa *et al.*, 2006; Schmidt *et al.*, 2010). A 34 kDa protein is the active form of TOM 34 receptor and localised predominantly in the cytoplasm (Mukhopadhyay *et al.*, 2002). However, a proteolytic enzyme that degrades this enzyme has not been identified. Perhaps, once the Met is removed this transporter protein becomes a proteolytic target for DP8 or DP9 proteins.

Obg-like ATPase 1 or DNA damage-regulated overexpressed in cancer 45 is also a potential substrate of DP8 and DP9. This enzyme is newly identified and able to hydrolyse ATP but the biological function has not determined (Koller-Eichhorn *et al.*, 2007; Sun *et al.*, 2010). It is estimated that the 396 aa protein forms is the active form of Obg-like ATPase 1 with Met-Pro-Pro residues in the N terminus. This enzyme was immunologically detected in cytoplasm and nucleus but predominantly localised in the cytoplasm (Sun *et al.*, 2010). In some cancer cell lines derived from colon, rectum, ovary, lung and stomach, obg-like ATPase 1 expression is induced by DNA damage and PI3K/Ras cell signalling pathways (Sun *et al.*, 2010). However, a protease that modulates this enzyme has not been determined so far. Therefore, once the Met was removed the role of DP8 and DP9, which could cleave naturally this enzyme, needs further investigation.

The last cytoplasmic protein enzyme which has Met-Ala-Pro residues is Serine/threonine-protein phosphatase 6. The active form of this enzyme has 305 aa sequence and 35.144 kDa molecular mass (Bastians and Ponstingl, 1996). Functionally, this enzyme has a high homology to yeast Sit4p, which modulates cell cycle progression in biological and pathological conditions (Bastians and Ponstingl, 1996; Filali *et al.*, 1999; Stefansson and Brautigan, 2006; Stefansson and Brautigan, 2007). IL-2 up regulates this enzyme expression in human lymphocytes (Filali *et al.*, 1999) but down regulation of this enzyme has not been investigated. DP8 or DP9 might have a role in modulating the phosphatase activity of this enzyme as once the Met has been removed DP8 and DP would be able to cleave this protein.

3.4.5. Proteolytic activity rate of DP8 and DP9

From seven validated substrates, there are two substrates (mitochondrial TOM34 and serine/threonine-protein phosphatase 6) that DP8 cleaves faster than DP9. It suggests that both substrates are more likely DP8 substrates not DP9 substrates. In contrast, DP9 cleaves faster the remaining validated substrates compared to DP8, suggesting they may be more naturally DP9 substrates. These data demonstrate that while substrates with a lower molecular mass (approx. 30 kDa) are preferentially cleaved by DP4, DP8 and DP9 may cleave substrates with molecular mass ranging from 40 to 100 kDa. However, DP4 cleaves faster all of the DP8 and DP9 substrates, which indicate that DP4 family members share the same substrate specificity but as the enzyme activity of DP4 is localised extracellularly, it is unlikely that DP4 would come into contact with any of these cytoplasmically expressed substrates *in vivo*. In addition, DP8 and DP9 begin cleaving seven candidate substrates by 3 h and complete cleavage products were observed after 24 h. This implies that DP8 or DP9 may participate in cell signalling by interaction with their substrates. Binding of DP8 or DP9 to the substrates may be required to change the substrates conformation in order to activate other proteins. Therefore, DP8 and DP9 may be able to activate their substrates through enzymatic and non-enzymatic activities.

3.4.6. Limitation of these assays

SKOV3 cells with and without vector, DP8 or DP overexpression have comparable DP enzyme activity, their total activity may not come only from DP8 and DP9 but also other members of the DP4 gene family. According to a study performed by Wilson (2011) and Wilson and her colleagues (2013), SKOV3 cells also expresses DP4 and FAP. Therefore, endogenous activity of wt SKOV3 cells and SKOV3 cells

overexpressing pEGFPN1vector is coming from both membrane bound and cytoplasmic DP activities. In contrast to DP activity in wt DP9-overexpressing SKOV3 cells, wt DP8 cells seemed to lose exogenous DP activity (Figure 3.1B). This data is accordance to the data of recent flow cytometry analysis that SKOV3 cells with wt DP8 overexpression have lost some EGFP expression (data not shown). The plausible explanation is that prolonged storage of stably transfected SKOV3 cells might alter the cell behaviour or a large amount of DP8 in cytoplasm is toxic to the cells, so endogenous DP levels are downregulated in this cell line. Meanwhile, as we expected, a lower DP activity in mt DP8 and mt DP9 SKOV3 cells were observed (Figure 3.1B). The mt DP8 and DP9 overexpression might suppress the endogenous DP8 and DP9 expression in SKOV3 cells, leading to a decrease in their DP activity.

Many experimental methods are available to validate protease substrates. The methods are based on protein separation using gel electrophoresis, affinity chromatography and chemical or enzymatic digestion, which is followed by MS analysis. In general, all developed methods have advantages and disadvantages. The cleavage of a substrate by DP8 and DP9 will only change the substrate (protein) by two amino acids, and this will lead to a change in protein size that is difficult to detect using gel electrophoresis and immunoblots. One of the best ways of testing the cleavage would be to use full length protein in enzyme assays. However the potential substrates identified for DP8/DP9 range from 200 to 1000 amino acids, and many are processed at the N- terminus before they contain the available N-terminus for DP cleavage. This means that it would be hard to obtain recombinant protein with the appropriate N termini for each substrate, and due to the size it would also be

difficult to develop a technique to detect the proteins once cleaved. Thus at this present time synthesising N- terminal peptides for each potential substrate and using MALDI-TOF to detect the two amino acid cleavage is the best available method. As more and more proteomics data becomes available in databases it is hoped that further *in vivo* evidence for the cleavage of each substrate will be revealed.

During the validation of 12 potential substrates of DP8 and DP9, we found that rDP4 was able to cleave all DP8/DP9 substrates at the 0 hrs time point. Theoretically, no enzyme activity should be detected at this incubation time. rDP4 has a lower k_m and higher k_{cat} on a wide range of natural or artificial substrates at range of temperatures (20-37°C), compared with rDP8 and rDP9 and is also very stable at room temperature. Biochemical studies also show that rDP4 is able to hydrolyze any residues in P1 position of the N terminal peptide substrates while DP8 and DP9 prefer to hydrolyze basic residues in P1 position of the N terminal peptide (Abbott *et al.*, 2000; Ajami *et al.*, 2004; Bjelke *et al.*, 2006; Lee *et al.*, 2006a). One way of reducing cleavage observed at this time point would be to alter the work flow, or to lower the amount of rDP4 enzyme used in the assay.

In summary, DP8 and DP9 co-localized with AK2 and calreticulin in the cytoplasmic compartment. This result may indicate natural interaction between DP8 and DP9 and their substrates even though the levels of AK2 and calreticulin protein expression is not different in cell lines overexpressing wt and mt DP8 or DP9 proteases. These protease-substrate binding complexes should be investigated further by identifying AK2 and calreticulin cleaved products in biological microenvironments and comparing cleaved AK2 and calreticulin activities to

uncleaved AK2 and calreticulin activities. Seven potential substrates for DP8 and DP9 have been validated further indicating that DP8 or DP9 cleaves specifically at the prolyl bond. Further investigation is required to determine co-localization of DP 8 and DP9 and their substrates in a cellular context.

4. INVESTIGATION OF THE EFFECTS OF DP8 AND DP9 OVEREXPRESSION ON AK2 EXPRESSION AND ACTIVITY IN SKOV3 CELLS

4.1. Introduction

In chapter 3, many new potential *in vivo* natural substrates for DP8 and DP9 were identified but so far the role of DP8 and DP9 cleavage of these substrates in the physiological and pathological processes remains unclear. All living cells essentially require energy supply for various biological functions. Mitochondria have a central role in providing sufficient enough energy for the cells through interconverting ATP and ADP molecules (Hardie, 2007; Burkart *et al.*, 2011). AK2 is a key enzyme that is localised in intermembrane space of mitochondria. This enzyme regulates equilibrium between ATP and ADP levels and monitors the cellular energy state in conjunction with other AK isotypes and AMP signal transduction (Dzeja and Terzic, 2009; Panayiotou *et al.*, 2011; Amiri *et al.*, 2013).

From its primary structure, AK2 has Met-Ala-Pro residues in the N terminus but naturally, the active form AK2 is lacking the Met residue (Frank *et al.*, 1986). However, a truncated AK2 without Ala-Pro residues is found in bovine liver and has a specific enzyme activity twice as high as the specific enzyme activity of the intact AK2 (Schlauderer and Schulz, 1996), suggesting that DP8 or DP9 may naturally modify the N terminus of AK2. Some potential substrates for DP8 and DP9, which were validated in Chapter 3, are also involved in cellular metabolism. Therefore, in

this study we examined the role of DP8 and DP9 in cleavage of AK2 in context of cellular growth and proliferation. .

In recent years, high expression of DP4 family members has been implicated in several human cancers. Kajiyama et al. (2002) found that high expression of DP4 inhibits cancer migration and invasiveness of SKOV3 cancer cells. Moreover, injection of this cancer cell with DP4 overexpression into nude mice can cause inhibition of cancer metastasis in the peritoneum (Kajiyama *et al.*, 2002). It suggests that *in vivo* up regulation of DP4 has a tumour suppressor effect. The inhibition of cancer migration and invasiveness by DP4 overexpression is mediated by up regulation of E-caderin and tissue matrix metalloproteinases (Kajiyama *et al.*, 2003). In contrast, FAP up regulation may promote cancer progression. *In vitro* and *in vivo* studies show that FAP silencing reduced expression of type 1 collagen, which contributes in promotion of the invasive phenotype and metastatic potential of SB247 ovarian cancer cells (Kennedy *et al.*, 2009). Like DP4, DP8 and DP9 overexpression in HEK 293 cell lines reduced cell migration and wound healing and enhanced apoptosis but the observed effects of DP8 and DP9 in this cell were not related to their proteolytic activity (Yu *et al.*, 2006). In recent years, Yao and co-workers (2011) found that DP9 overexpression in liver cancer cell lines (HepG2 and Huh7) but not DP8 overexpression induced apoptosis, which is mediated by inhibition of Akt expression. The inhibited Akt expression leads to disruption of H-ras/PI3K cell signalling, which plays important roles in cell survival, growth, proliferation and differentiation (Yao *et al.*, 2011). Interestingly, the DP9-induced apoptosis in this cell is correlated to the DP9 proteolytic activity (Yao *et al.*, 2011), indicating that DP9 cleaves a substrate which plays important roles in H-ras/PI3K

cell signalling pathway. Based on these precedents, DP8 or DP9 overexpression may signify an important role in regulation of AK2 since DP8 and DP9 can cleave an N terminal peptide of AK2 (Chapter 3).

A crucial step toward understanding the effect of DP8 and DP9 proteolytic activity to their potential substrates is to study the effect of cleavage of substrates on their activity or function *in vivo*. Evidence in the literature (Schlauderer and Schulz, 1996) already suggests that when the Ala-Pro residues are removed from the N- terminus of AK2 it is more active. The aim of chapter 4 was to use the SKOV3 cell lines overexpressing DP8 and DP9 to study whether DP8 or DP9 have effects on AK2 activity in either the cytosol or mitochondria compartments of the cell. To address potential compensatory or redundant functions between DP8 and DP9 in these cells, we used SKOV3 cells overexpressing mt DP8 and DP9 as negative controls.

4.2. Materials and Methods

4.2.1. Cell culture

1×10^6 SKOV3 cells overexpressing wt and mt DP8 or DP9 and vector (Wilson, 2011; Wilson *et al.*, 2013) were maintained in RPMI supplemented with 10% heat-inactivated FBS, 100 U/ μ g Penicillin/Streptomycin and 500 μ g gentamycin (detailed in Chapter 2). All SKOV3 cells including wt SKOV3 were grown in T75 flasks and incubated in a 37°C humidified incubator with a 5% CO₂ atmosphere. Every three days, the cell medium was replaced and re-incubated until cells reached confluence (4-7 days).

4.2.2. Cell proliferation assay

Harvested wt SKOV3 and SKOV3 cells overexpressing wt and mt DP8 and DP9 were seeded in to a 96 well plate with different cell concentrations, starting from 4, 2, 1, 0.5 to 0.25×10^5 cells/well. Each cell concentration was repeated six times and medium only served as a negative control. Seeded cells were incubated at 37°C in a 5% CO₂ incubator and after 6, 12, 18, 24, 36 and 48 h time points cells were treated with 0.05% (w/v) pre-warmed 3-(4,5-dimethylthiazol-2-yl)-2,5-diphenyl tetrazolium bromide (MTT). Cells were then re-incubated at 37°C in a 5% CO₂ incubator for 1h. To solubilize formazan that was formed in living cells, 20% (w/v) SDS in 20 mM HCl was added. Finally, the plate was wrapped with aluminum foil and incubated at RT for 1h before reading it in a Fluorostar spectrophotometer with optical density 570 nm and 630 nm for background.

4.2.3. Adenylate energy charge (AEC) assay

Adenine nucleotide levels were measured using an established method with some modification (Li *et al.*, 2007). Harvested SKOV3 cells from a T75 flask were washed twice with PBS as described in detail in general materials and methods (Chapter 2). Washed cell pellets were re-suspended in 500µl of 0.6 M cold perchloric acid and incubated at 4°C for 10 min. The cell suspension was then centrifuged at 1,500 xg at 4°C for 10 min and the cleared supernatant was mixed with 500µl of 2 mM potassium phosphate buffer. The mixed solution was centrifuged again at 1,500xg for 10 min at 4°C. The cleared supernatant was transferred into HPLC vials (Agilent Technologies, USA). The sample analysis was performed at the Flinders Analytical Centre, by Dr. Daniel Jardine. Before running samples, a reverse-phase C18 column (25 x 4.6 mm in size) attached to a water 2695 HPLC instrument (Waters Milford,

MA, USA) was equilibrated with 50 mM potassium phosphate buffer pH 7.0. Each sample was then injected into the column and eluted with the elution buffer, containing 95% potassium phosphate buffer pH 7.0 and 5% methanol, with flow sample rate 1 ml/min. After a few minutes, the proportion of elution buffer was set up as 40% potassium phosphate buffer and 60% methanol and finally injected samples were eluted back to the first elution buffer. The retention time of adenine nucleotides was determined and the concentration of nucleotide samples was measured using a standard curve, generated from ATP, ADP and AMP standards. The AEC ratio was calculated using the formula $(ATP + 0.5 \times ADP) / (ATP + ADP + AMP)$ (Atkinson, 1968).

4.2.4. Mitochondria isolation

For conducting AK enzyme, DP enzyme, BCA protein and LDH assays, SKOV3 mitochondria were extracted from cells using a method as described in a published paper with some modifications (Rezaul *et al.*, 2005). Briefly, once SKOV3 cells, which were grown in T75 flask, reached confluence (see Chapter 2), cells were collected by centrifugation at 1,500 x g for 5 min at RT. The cell pellets were washed twice with pre-cold PBS pH 7.4 and centrifuged at 400 xg for 10 min at 4°C. The washed cell pellets were re-suspended in 1 ml of lysis buffer supplemented with 1x protease inhibitor cocktails and incubated at 4°C for 10 min. These protease inhibitors were used to inhibit the activity of serine, cysteine, acid and aminopeptidases, which potentially degrade isolated proteins during cell extraction. After incubation, the resuspended cells were lysed using a sonicator probe at 4°C for 5 sec. Trypan blue staining was carried out during cell extraction to ensure that approximately 75% of cells were lysed. To remove debris and live cells, cell lysates

were centrifuged twice at 650 xg for 10 min at 4°C. Some volume of cleared supernatants was retained as cell lysate and kept at -80°C for further analysis. The remaining supernatant was centrifuged at 12,500 x g for 25 min at 4°C and cell pellets were retained as the mitochondrial fraction, and re-suspended carefully in 500 µl of lysis buffer. Cleared supernatants were transferred into high speed centrifugation tubes and centrifuged at 100,000 x g for 60 min at 4°C in order to separate the cytosol and membrane fractions. To purify the mitochondrial fraction, re-suspended cell pellets were re-centrifuged at 12,500 xg for 25 min at 4°C and cell pellets were then dissolved in 500 µl of another buffer solution, which contained 250 mM sucrose, 1 mM EDTA, and 10 mM Tris-HCl pH 7.4. A sucrose gradient buffer was made by transferring 1 ml of 1 M sucrose first into a high speed centrifugation tube and adding 1 ml of 1.5 M sucrose carefully on top. The mitochondrial suspension was then transferred into the sucrose gradient. After that, crude mitochondria were centrifuged at 60,000 xg for 20 min at 4°C. The purified mitochondria were aspirated from the middle phase between the two sucrose concentrations and collected mitochondria were washed twice with lysis buffer, followed by centrifugation at 15,000 x g for 20 min at 4°C. Purified mitochondrial pellets were finally dissolved in 250 µl of mitochondrial buffer and incubated at 4°C for 60 min. To remove insoluble particles and debris from the mitochondrial fraction, the dissolved pellets were centrifuged 15,000 x g for 5 min and the cleared supernatant was kept at -80°C before use.

4.2.5. BCA protein assay

All fractionated cell suspensions prepared above had their total protein concentration estimated using the BCA protein assay. A detailed protocol was described in Chapter

2. Cell lysate and cytosol fractions were diluted with 1:10 volume ratio and the mitochondrial fraction was diluted in 1:5 volume ratio before the BCA assay was performed.

4.2.6. DP enzyme activity

DP enzyme activity was determined in all cell fractions collected to monitor whether DP8 and DP9 proteins were degraded or not during cell extraction and whether these proteins were located in the mitochondria. Fractionated cell suspensions were loaded into a 96 well plate and all experimental samples were tested in triplicate. The DP enzyme assay was then performed the same as described in materials and methods in Chapter 2.

4.2.7. LDH assay

This assay was intended to measure indirectly cell membrane integrity during mitochondrial purification. The protocol of this assay followed the manufacturer's instructions (Promega, Madison, WI, USA) with minor modifications. Forty μ l of either cell lysate, cytosol or mitochondrial fractions were transferred into a white opaque 96 wells plate (Corning Incorporated, Corning, NY, USA) and equilibrated at 22 °C for 20 min. Pre-warmed resazurin reagent suspension was equally added into each well and incubated at RT for 10 min. Twenty μ l of stop reaction solution which consists of 10% SDS was added into each well to stop the reaction. A short incubation at RT was required before measuring the fluorescence intensity. Formation of resorufin resulting from the complex reactions initiated by LDH released from broken cells was measured using a FLUOstar omega spectrophotometer with 560 nm laser excitation and 590 nm laser emission. The

fluorescence intensity was collected every min for 10 min and presented as relative fluorescence intensity (RFU).

4.2.8. AK assay

This assay was adopted and modified from (Bergmeyer, 1974). The cytosol fraction of all SKOV3 cells was diluted with the Rezaul's lysis buffer in 1: 10 dilution. Twenty μ l of diluted cytosol suspension and mitochondrial suspension were transferred into a 96 well plate. The AK assay was performed in triplicate. Before transferring the sample into the plate, a master mix of reagents for the AK assay was made in the ice box (Table 4.1). 151.22 μ l of mixed reagent was transferred into a 96 well plate and equilibrated at 25°C. Diluted cytosol, mitochondrial samples and buffer only was added into the plate up to 200 μ l. Decreased concentration of NADH substrate was measured in a FLUOstar omega spectrophotometer with absorbance 340 nm in length at 25°C every min for 20 min. AK activity was determined using the Beer-Lambert formula with 6.22×10^3 M extinction factor for NADH.

4.2.9. Western Blotting

25 μ g of total proteins in the cell lysate and the mitochondrial fractions from SKOV3 cells were mixed with 3x SDS-PAGE sample buffer before running in a 10% SDS-PAGE gel. This was described in detail in Chapter 2 materials and methods. For detecting DP8 and DP9 proteins, blotted membrane was incubated with anti DP8 and DP9 polyclonal antibodies with one in 5,000 dilution. Meanwhile, anti-human mitochondrial SOD2 at 1: 10,000 dilution was used as a positive control for purity of mitochondrial samples and anti AK2 polyclonal antibody was diluted in blocking buffer 1: 2,500 dilution. Exposure time for SOD2 antibody was a maximum of 20

sec and the other antibodies were exposed for 1200 sec unless band signals were detected earlier.

Table 4.1. AK assay mixture modified from Bergmeyer (1974). Master mix was made for 50 wells at any one time.

Substrate	Stock solution (mM)	Final concentration (mM)	Volume (μ l) per well
Triethanolamine pH 7.6	200	71.4	71.4
AMP	40	0.7	3.5
ATP	10	1.2	24
Phosphoenol pyruvate (PEP)	10.92	0.39	7.14
MgSO ₄	40	1.2	6
KCl	1000	142	28.4
Nicotinamide adenine dinucleotide (NADH)	13.48	0.4	5.93
Pyruvate kinase (PK)	1521.3	7.1	0.93
Lactate dehydrogenase (LDH)	1002.64	19.6	3.91
Sample in buffer			48.78
Total volume			200

4.2.10. Statistical analysis

Mean values of data from all experiments in this study were analyzed using IBM SPSS statistics software version 20. The significance value was set at $P < 0.05$. Collected data was expressed as mean \pm SEM. A one-way ANOVA was used to compare means between vector and DP8 or DP9 overexpression samples, followed by Tukey post-hoc test. If data of percentage of cell viability from SKOV3 cells was not homogenous, Games-Howell post-host test was used to compare the means.

4.3. Results

4.3.1. Characterization of SKOV3 cells overexpressing wt and mt DP8/DP9

In this study, SKOV3 cells overexpressing wt and mt DP8 and DP9 proteins were used to investigate whether overexpression of DP8 or DP9 proteases affected AK2 activity in either the cytosol or mitochondrial compartments. To ensure that SKOV3 cells retained DP8 and DP9 protein overexpression, SKOV3 cell overexpressing pEGFPN1 vector (detailed in section 2.5.1) were used as a functional control while wt SKOV3 cell provided a negative control. Morphologically all SKOV3 cells were single cells and spread throughout the flask surface. SKOV3 cells which overexpressed wt DP8 and DP9 were similar in shape and size to SKOV3 cell overexpressing vector control and they had a polyhedral shape and a large cell size (Figure 4.1). In contrast to wt DP8 overexpression, mt DP8-overexpressing SKOV3 cells looked different, these cells were larger in size and there were less cell numbers observed in some areas of the flask. These features were opposite to SKOV3 cell overexpressing mt DP9 which had a smaller spindle cell size and increased cell number in observed areas.

The effect of DP8 and DP9 overexpression on cell proliferation was measured using an MTT assay. In terms of proliferation rate, all DP-overexpressing SKOV3 cells displayed different proliferation rates compared to vector control-overexpressing SKOV3 cells (Figure 4.2A). After 6 h plating, SKOV3 cells overexpressing wt and mt DP8 proteins proliferated faster than non-transfected SKOV3 cells and SKOV3 cell overexpressing vector control. However by 48 h incubation, the cells proliferated equally. SKOV3 cells overexpressing wt and mt DP9 grew slower than

non-transfected SKOV3 and vector control-overexpressing SKOV3 cells. However, only wt DP9 cells achieved significantly lower cell growth ($p = 0.001$).

To further investigate whether DP8 and DP9 overexpression influenced cell viability or not, the percentage of viable cells was calculated by dividing the proliferation rate of overexpressing SKOV3 cells with the proliferation rate of non-transfected SKOV3 cells. The result of % cell viability is presented in figure 4.2B. DP8 overexpression has a very different pattern to DP9 overexpression. More viable cells were observed in SKOV3 cells overexpressing wt and mt DP8 compared to SKOV3 cell overexpressing vector control. The percentage of viable cells in wt and mt DP8 overexpressing cells was greater than the percentage of viable cells in wt and mt DP9 overexpression from 6h to 48h incubation. The viable cells decreased until the end of incubation and significant differences were found in wt overexpression after 24h incubation. While, DP9 overexpression had less viable cells than vector overexpression and the percentage of cell viability in wt DP9 overexpression remained unchanged after 48 h. incubation. For mt DP9 overexpression, the percentage of cell viability slightly increased after 24h incubation. In contrast to these results obtained in a 96 well plate when cells are routinely sub cultured in a T75 flask, the wt and mt DP8 cells take longer to reach confluence (6 or 7 days) versus the wt, vector control wt and mt DP9 cells (4 days) (data not shown).

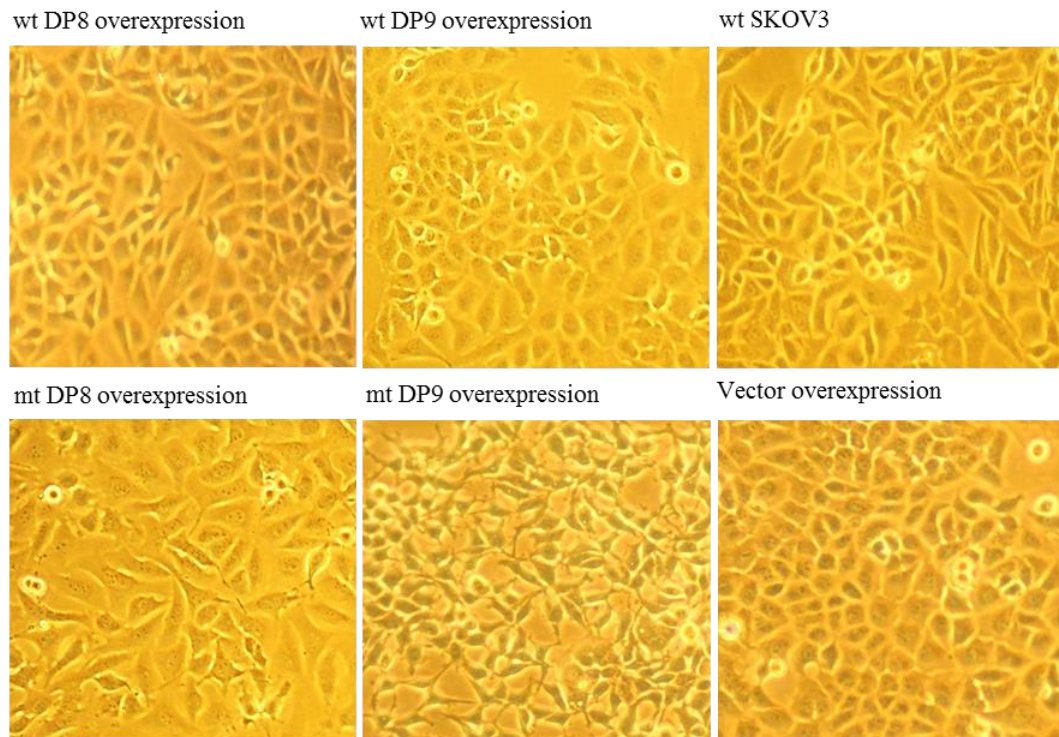


Figure 4.1. Characteristics of SKOV3 cells overexpressing wt and mt DP8/DP9 proteins. Morphology of all SKOV3 cells after 72h incubation. Cells were observed under an inverted microscope with x100 magnification.

4.3.2. Purity of mitochondria extracted from SKOV3 cells with DP8 and DP9 overexpression

To obtain high purity mitochondria during cell extraction, an established method was used, based on gradient centrifugation which resulted in three fractions, cell lysate, cytoplasmic and mitochondrial fractions. The purified mitochondria fractions were verified using DP and LDH assays and Western blotting. According to published studies (Abbott *et al.*, 2000; Olsen and Wagtmann, 2002; Ajami *et al.*, 2004), DP8 and DP9 are only expressed in the cytosolic compartment. Therefore, DP enzyme activity can be used to confirm the purity of the mitochondrial fraction.

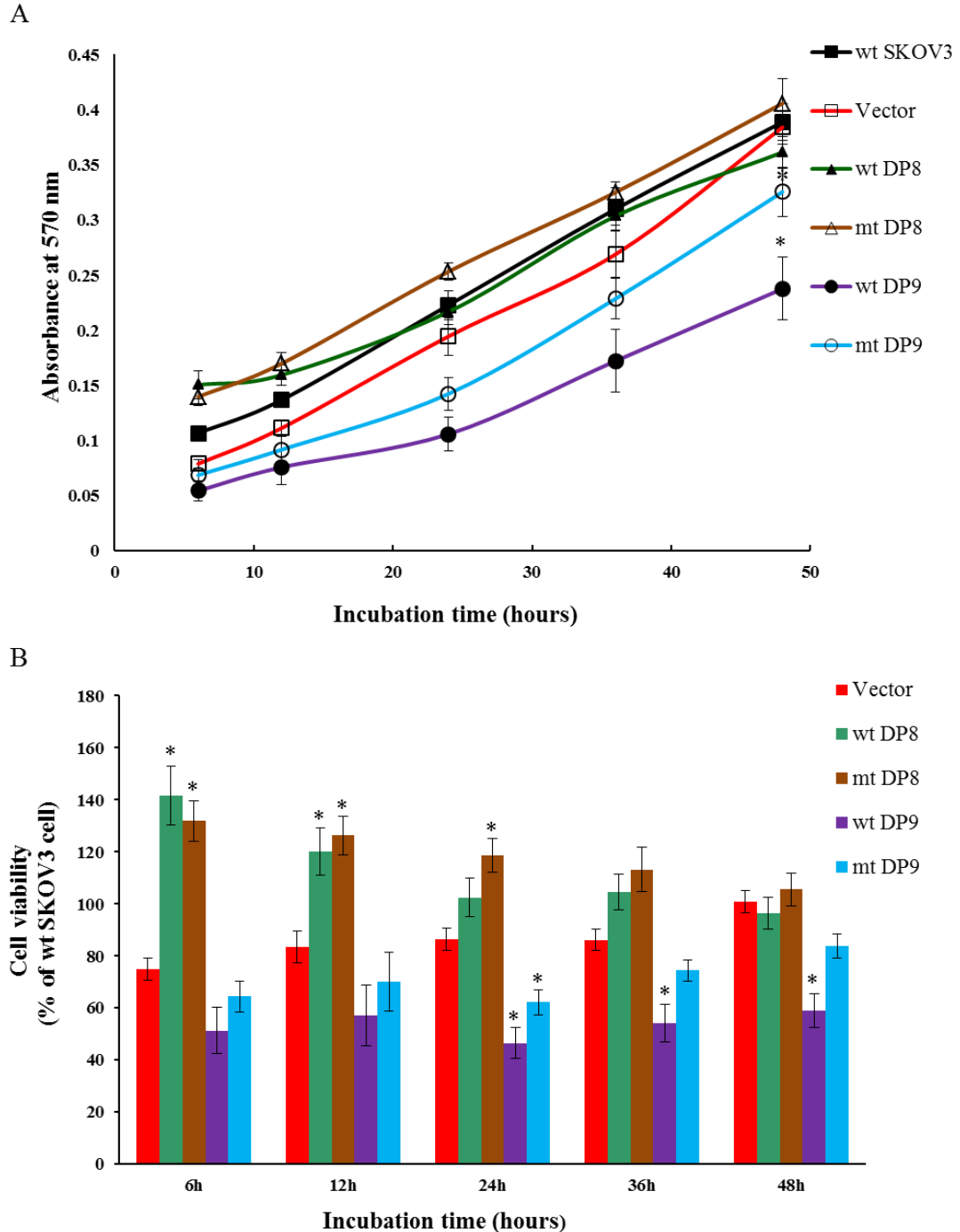


Figure 4.2. Cell viability of SKOV3 cells overexpressing wt and mt DP8/DP9 proteins. (A) Proliferation rate of all SKOV3 cells was measured using the MTT assay. 1×10^5 cells were plated and analysed at 6,12,24,36 and 48 h. (B) Cell viability of SKOV3 cells with DP8, DP9 and vector control overexpression was compared to that of non-transfected SKOV3 cells. All data were presented as mean \pm SEM (n = 3) and p value was set < 0.05. * denoted significant difference compared to SKOV3 cells with vector control overexpression.

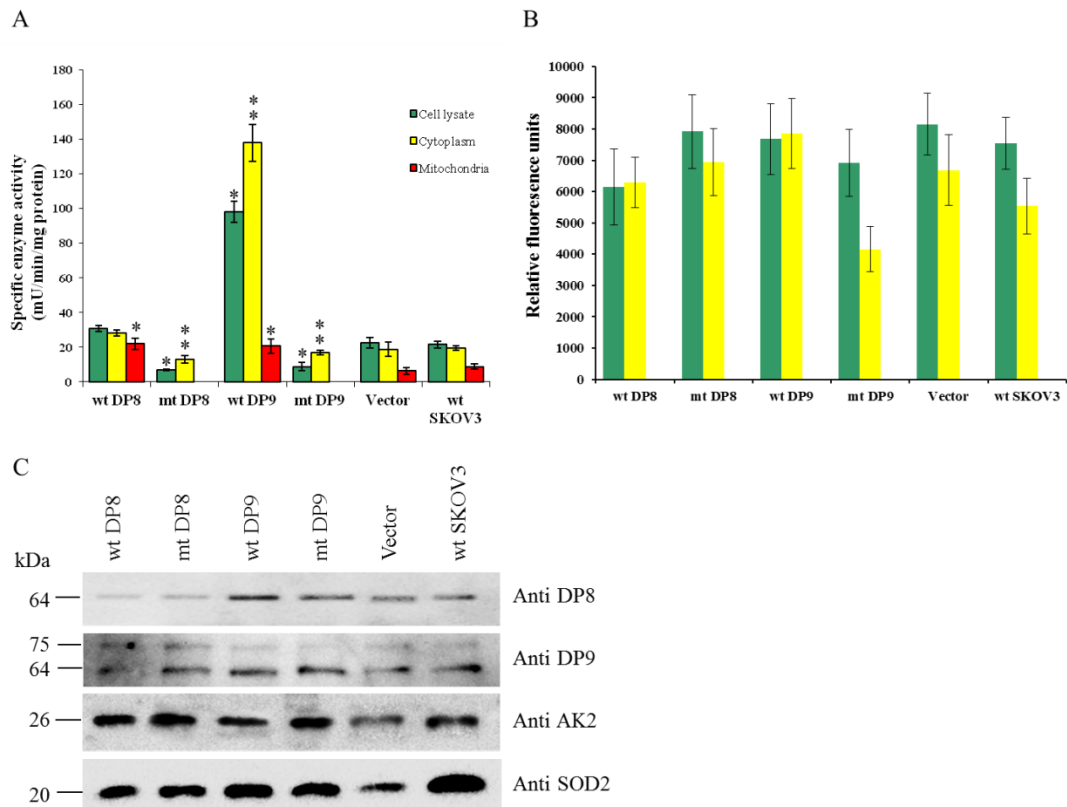


Figure 4.3. Characterization of purified mitochondria from wt and mt DP8/DP9 over-expressing SKOV3 cells. (A) All cell fractions were incubated with 1 mM of H-Ala-Pro-pNA substrate and absorbance values were measured at 405 nm in length. DP enzyme activity was determined using Beer-Lambert formula. (B) LDH activity was determined by incubation between all SKOV3 fractionated cell suspensions and rezasurin reagent. Fluorescence intensity resulting from resorufin formation was measured using 560 nm laser excitation and 590 nm laser emission. Each bar represented the mean of three separate experiments and asterisk denoted a significant difference. All data were presented as mean \pm SEM and p value was set < 0.05 . (C) 25 μ g of total proteins of purified mitochondria in all SKOV3 cells was loaded onto a 10% SDS-PAGE and analyzed by Western blotting. An antibody against SOD2 was used as a marker for mitochondrial purity.

Unexpectedly DP enzyme activity was detected in the mitochondrial fraction of all SKOV3 cells except those expressing mt DP8 and DP9 (Figure 4.3A). The DP enzyme activity in purified mitochondria fraction from wt DP8 and DP9 overexpression was 21.94 and 20.68 mU/min/mg protein respectively, which was higher than the enzyme activity in purified mitochondria fraction from vector control overexpression and it reached significant difference ($p = 0.005$ and 0.012

respectively). The increased enzyme activity was probably from wt DP8 and DP9 overexpression.

Regarding cell membrane integrity, there was no LDH activity observed in purified mitochondria fractions from all SKOV3 cells (Figure 2B), suggesting that there was no contamination from cell lysate and cytosolic fractions during cell extraction. In addition to this result, AK2 protein was seen at 26 kDa band in mobility in the purified mitochondria fraction of all SKOV3 cells (Figure 4.3C), which was expected. DP8 was also detected in the all cell mitochondria but the band was 64 kDa not 99 or 119 kDa as observed in cytoplasmic fraction of overexpressing SKOV3 cells. DP9 had dual band mobility (75 and 64 kDa) in all mitochondria fraction of all SKOV3 cells, which was different from the band mobility observed in cytoplasmic fraction of the cells (Chapter 3, Figure 3.2).

4.3.3. AK2 activity in SKOV3 cells with DP8 and DP9 overexpression

The *in vitro* study revealed that DP8 and DP9 cleave the N terminal peptide of AK2 protein, releasing Ala-Pro residues (Chapter 3, Table 3.1) however there is limited evidence that DP8 or DP9 cleaves AK2 *in vivo* in humans. AK2 lacking the N-terminal Ala- Pro residues has been isolated from bovine liver and found to be twice as active as the uncleaved form (Schlauderer and Schulz, 1996). Therefore, the effects of overexpressing DP8 and DP9 protein in SKOV3 cells, on AK2 enzyme activity were investigated. AK2 is a mitochondria enzyme that catalyses reversibly 2 ADP into ATP + AMP in the presence of Mg²⁺ (Dzeja *et al.*, 1998; Dzeja and Terzic, 2003). Cytoplasmic and mitochondrial fractions from all SKOV3 cells were incubated with different concentrations of AMP substrate in the presence of constant

ATP concentration. AK affinity and conversion rate of the AMP substrate in the cytoplasmic and mitochondrial fractions were measured using Michaelis-Menten enzyme kinetics. Figure 4.4 illustrates the Michaelis–Menten curves for AK activity in cytoplasmic and mitochondria extracts from the various cell lines. DP8 and DP9 overexpression had different effects on AK activity in the cytoplasmic and mitochondria fractions. A higher maximum conversion rate was observed in cytoplasmic fractions from wt and mt DP9 overexpressing cells and a lower maximum conversion was from cytoplasmic fraction from wt and mt DP8 overexpressing cells, compared to that of vector overexpression (Figure 4.4A and Table 1). However, a different pattern of maximum conversion rate was found in mitochondrial fractions from all DP overexpressing SKOV3 cells (Figure 4.4B and Table 1) but the maximum reaction rate decreased two fold compared to that of cytoplasmic fractions from all DP overexpressing lysates.

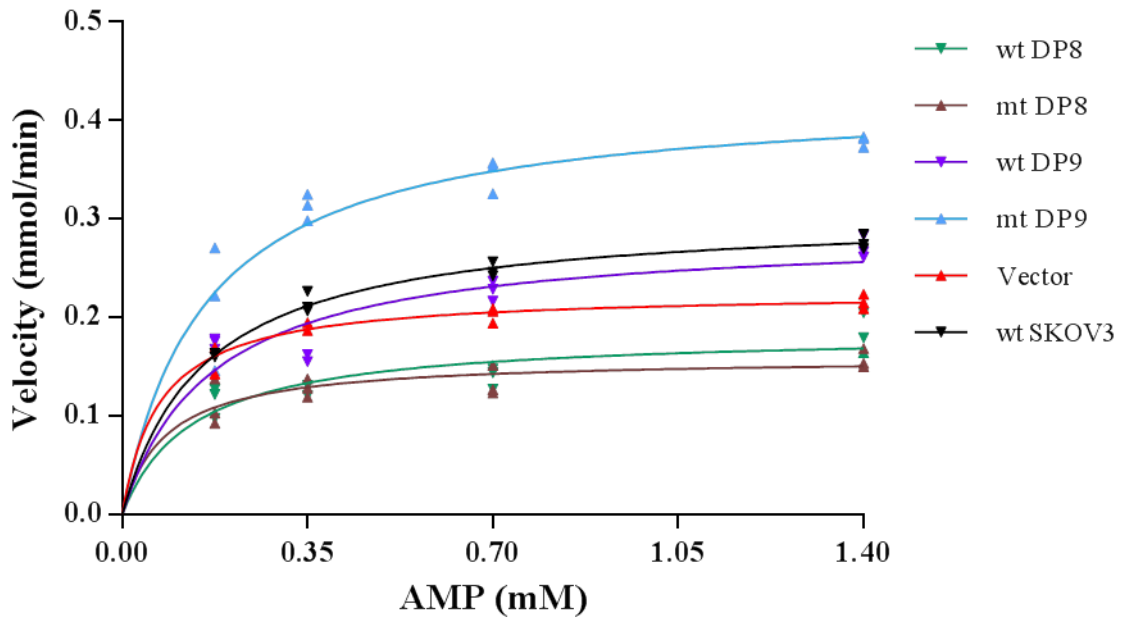
Table 4.1 demonstrates the binding affinity of AMP to AK in cytoplasmic and mitochondria fractions from SKOV3 cells with wt DP8 and DP9 overexpression. DP8 and DP9 overexpression influenced AK binding affinity to AMP in cytoplasmic and mitochondria fractions. When both DPs were overexpressed in cytoplasmic fractions, they had lower AK binding affinity than vector expressing fractions ($K_m = 134.1$ and 168 vs. $70 \mu\text{M}$). In the mitochondria fraction, a higher AK binding affinity ($60.6 \mu\text{M}$) was observed in fractions from SKOV3 cells overexpressing DP9, compared to the AK binding affinity of fractions from SKOV3 cells overexpressing DP8 and vector (119.5 and $117 \mu\text{M}$ respectively).

Table 4.2. AK binding affinity to AMP and maximum reaction rate of SKOV3 cells overexpressing wt and mt DP8/DP9.

SKOV3 cell overexpression	Cytoplasm		Mitochondria	
	Km (μM)	Vmax (μM)	Km (μM)	Vmax (μM)
wt DP8	134.1 \pm 43.9	184.7 \pm 13.9	119.5 \pm 72.7	143.9 \pm 18.82
mt DP8	81.26 \pm 29.21	159.2 \pm 9.74	186.6 \pm 79.04	244.5 \pm 28.14
wt DP9	168 \pm 48.4	287.1 \pm 21.3	60.6 \pm 17.8	139.9 \pm 8.1
mt DP9	156.2 \pm 37	426 \pm 25.07	107.7 \pm 79.26	211.2 \pm 31.46
Vector	70.7 \pm 10.8	225.9 \pm 5.3	117 \pm 76.3	194.3 \pm 72.95

DP8 and DP9 overexpression in SKOV3 cells have different AK specific activities in the cytoplasm and mitochondria (Figure 4.5). The cytoplasmic fractions from the SKOV3 cells overexpressing mt DP9 were significantly different to the specific AK enzyme activity of SKOV3 cells overexpressing vector cytoplasmic fractions (Figure 4.5A). In the mitochondria fractions AK specific activities were similar, however SKOV3 cells expressing both mt DP9 and mt DP8 had significant increased activity compared to the vector overexpressing SKOV3 cell fractions.

A. Cytoplasmic



B. Mitochondria

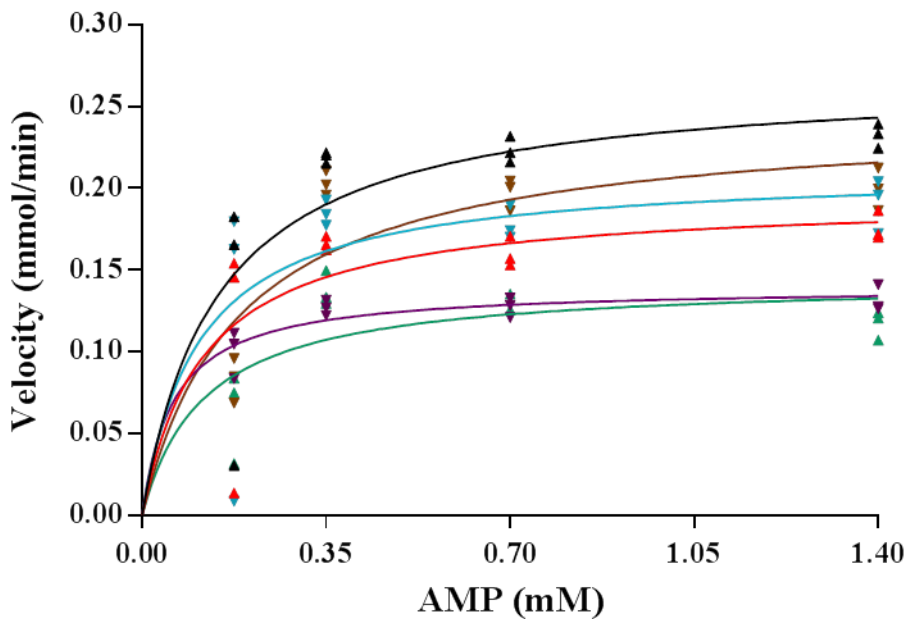
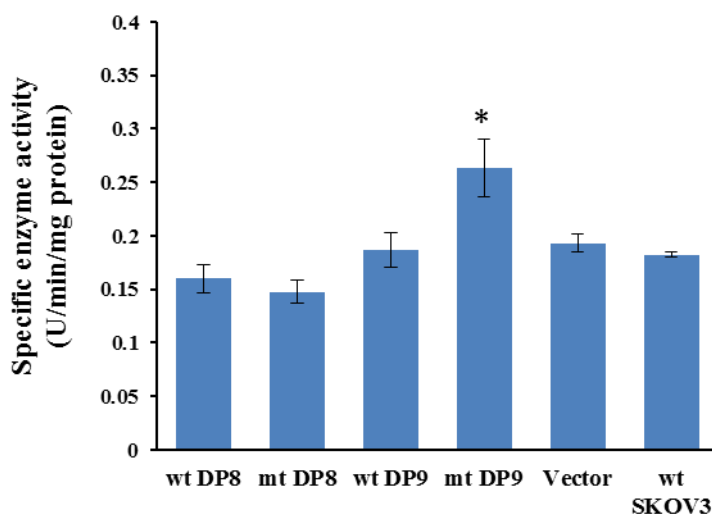


Figure 4.4. AK kinetic profiles in cytoplasmic and mitochondrial fractions from SKOV3 cells overexpressing wt and mt DP8/DP9. (A and B) SKOV3 cell fractions were incubated with different AMP concentrations (0.175, 0.35, 0.7 to 1.4 mM). Reduction of NADH substrate was spectrophotometrically measured. Michaelis-Menten graphs were generated from collected data using GraphPad Prism software.

A. Cytoplasm



B. Mitochondria

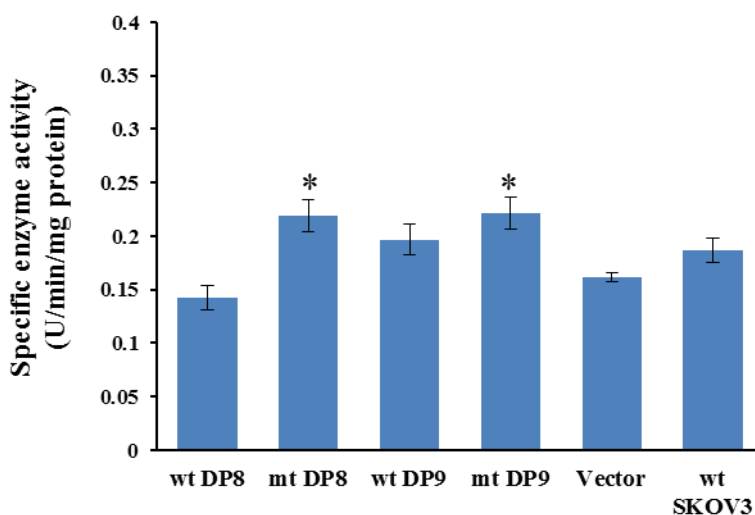
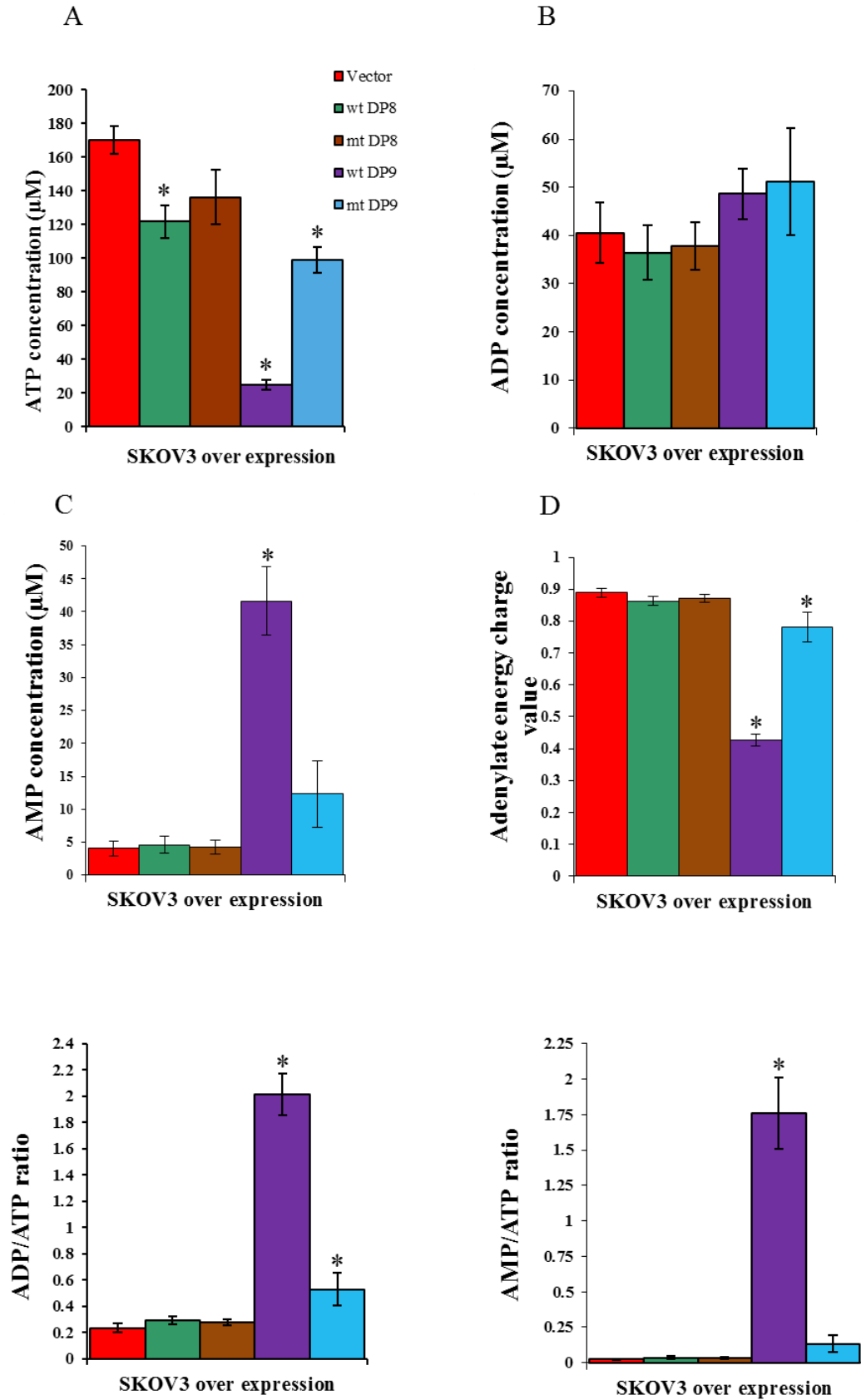


Figure 4.5. Specific AK enzyme activity in cytoplasmic and mitochondrial fractions from SKOV3 cells overexpressing wt and mt DP8/DP9. Cell fractions were incubated with 0.7 mM AMP. 20 μ g of cell lysate was incubated with 0.7 mM AMP. The AK enzymatic reaction was performed at RT and spectrophotometrically measured at 340 nm absorbance every min for 20 min. Each bar represented the mean of three separate experiments and asterisk denoted a significant difference, compared to vector and p value < 0.05.

4.3.4. Adenine nucleotide levels in DP8 and DP9-overexpressing SKOV3 cells

Given the role of AK2 in regulating adenine homeostasis in order to further investigate the effect of DP8 and DP9 overexpression on AK2, adenine nucleotide

levels were measured using HPLC. Adenine nucleotide levels were different between DP8 and DP9-overexpressing SKOV3 cells (Figure 4.6). ATP levels decreased significantly in all SKOV3 cells overexpressing DPs, excluding mt DP8 overexpression, compared to ATP levels in vector expressing SKOV3 cells (Figure 4.6A). The decrease in ATP levels in wt DP9 overexpressing cells was accompanied with an increase in AMP levels. The AMP levels in wt DP9 overexpressing cells were statistically increased around eight times, compared to that of vector overexpression (Figure 4.6C). In contrast to DP9 overexpression, ATP and ADP levels in DP8 overexpression were lower than that of vector overexpression (Figure 4.6A-B). Significant reductions were also observed in AEC values of wt and mt DP9 overexpression (approximately 50 and 10%, respectively), indicating a low energy pool (Figure 4.6D). The ADP/ATP ratio was markedly elevated in DP9 overexpression compared with ADP/ATP ratio in vector overexpression (Figure 4.6E). Next, the AMP/ATP ratio was evaluated since the elevated ADP/ATP ratio was seen in DP9 overexpression. In wt and mt DP9 overexpression, AMP/ATP ratio was increased but the significant increase was only observed in wt DP9 overexpression.



$(\text{ATP}+0.5\text{ADP})/(\text{ATP}+\text{ADP}+\text{AMP})$. (E and F) indicated ADP/ATP and AMP/ATP ratio respectively that were used as an indicator of energy demand in viable cells. One way ANOVA test was used to compare the mean of adenine and adenylate energy levels of individual cell line to the vector. Each bar represented the mean of three separate experiments and asterisk denoted a significant difference. All data were presented as mean \pm SEM and p value was set < 0.05 .

4.4. Discussion

This chapter investigated the effects of DP8 and DP9 overexpression on AK2 protein expression and AK enzyme activity in SKOV3 cell lines. DP8 and DP9 overexpression changed SKOV3 cell morphology. However, proliferation rate of SKOV3 cells with DP8 and DP9 were negatively correlated with the morphological changes. Moreover, initially the proportion of viable cells in wt and mt DP8 overexpression was greater than proportion of viable cells in wt and mt DP9 overexpression from 6h to 48h incubation. In contrast to the changes in morphology and proliferation rate, in the mitochondria mt DP8 and mt DP9 overexpression decreased specific AK enzyme activity and in the cytoplasm mt DP9 overexpression increased the AK enzyme activity. In DP9 overexpressing cell lines, ATP levels decreased and ADP and AMP levels increased. This work shows that following stable transfection with wt and mt DP8 or DP9, SKOV3 cell behaviour changed as measured visually, by proliferation rates, AK activity and AEC values. Cells overexpressing wt and mt DP8 and DP9 proteins behaved differently suggesting these proteins may play different biological roles.

Changing cell morphology in ovarian cancer cells frequently occurs. In primary cell culture of normal ovarian epithelial cells, the cells undergo phenotypic changes, which are characterised by losing some epithelial markers such as keratin and

cytovillin and becoming mesenchymal-like cells. The cell differentiation apparently occurs after a few cell culture passages (Auersperg *et al.*, 2001). During reproductive age, this phenotypic change is associated with degenerative response during ovulation cycles (Auersperg *et al.*, 2001). However, the morphology of ovarian cancer cells remains unchanged during cell culture but cell differentiation strongly correlates with low cancer progression (Auersperg *et al.*, 2001). SKOV3 cells with DP8 and DP9 overexpression have the morphology of a differentiated cell type. The phenotype change may be in response to external stimuli in cell culture (Auersperg *et al.*, 2001; Ahmed *et al.*, 2007). This phenotypic change is also found in SKOV3 cells with DP4 overexpression (Kajiyama *et al.*, 2002; Kajiyama *et al.*, 2003), indicating that DP8 and DP9 overexpression has a similar effect on SKOV3 cells. In order to verify whether the morphological changes in SKOV3 cells is caused by DP8/DP9 enzyme activity or not, identification of DP8 and DP9 substrates involved in cell proliferation is necessary. So far, there has been no data identifying potential substrates for DP8 and DP9 that may promote ovarian cancer cell progression. In addition, wt DP9 overexpression in human hepatoma and embryonic kidney cells reduced cell survival and proliferation via inhibition of protein kinase B signaling cascade (Yao *et al.*, 2011). Therefore, this data suggests that DP8 and DP9 may play an important role in cell differentiation that is independent of their enzyme activity.

In terms of cell proliferation, SKOV3 cells with wt and mt DP9 overexpression in this study had lower proliferation rates than their counterparts with wt and mt DP8 overexpression (Figure 4.2A). These findings result from lower cell viability in cells overexpressing DP9, approximately half the cell viability in cells overexpressing DP8 (Figure 4.2B). DP9 overexpression led to a drop in ATP levels and an increase

in the ADP/ATP ratio (Figure 4.6A&E), clearly indicating that DP9 overexpression influences ATP production, leading to decrease in cell viability. The induction of cell death by DP9 overexpression may be related to apoptosis due to lack of essential nutrients in the cell culture. More active AK2 in wt and mt DP9 overexpressing cells in response to metabolic stress in these cells, should result in inhibition of AMPK. As a consequence, ATP demand and consumption are higher than ATP production in DP9 overexpressing cells (Hardie, 2007; Hardie 2011b; Hardie, 2011a). Recent data obtained by another PhD student, shows that SKOV3 cells with mt DP9 overexpression have high CO₂ production, when carbon labelled glucose or acetate are provided as energy sources (Appendix, Figure 8.8). Therefore, SKOV3 cells with overexpressing mt DP9 may use an alternative energy source to survive.

Mitochondrial fractionation is required for studying DP8 and DP9 proteolytic activity to AK2. Disruption of intact cells and purification of mitochondria are two crucial steps in this procedure. There are several techniques that can be used to disrupt cell membrane, chemical, physical and mechanical protocols but the mechanical protocol using a sonicator provides the best choice for mitochondrial isolation (Chaiyarit and Thongboonkerd, 2009). The next step is to isolate and to purify mitochondria which can use gradient centrifugation, affinity chromatography or free flow electrophoresis. The gradient centrifugation is the most common technique applied in mitochondrial purification (Chaiyarit and Thongboonkerd, 2009). In our study, we used a combination technique of sonicator cell disruption and gradient centrifugation. However, both techniques are laborious and time consuming. So, we always add protease inhibitor cocktail in SKOV3 cell samples. From biochemical assays and Western blotting, the mitochondria fraction of wt

SKOV3 and SKOV3 overexpressing DP8 and DP9 proteins have high purity (Figure 4.3). Low and high DP enzyme activity in cell lysate and cytoplasmic fractions of SKOV3 cell overexpressing wt DP8 and wt DP9 respectively may not relate to addition of protease inhibitor cocktail because the similar enzyme activity was also observed in cell lysate of the same cell in Chapter 3 (Figure 3.1). In Western blotting analysis, protein expression of wt DP8 and wt DP9 expression in cell lysate and cytoplasmic fractions did not differ (data not shown). Therefore, SKOV3 cells might lose wt DP8 overexpression, resulting from prolonged cell storage or DP8 toxicity.

It is worth noting that DP8 and DP9 might also cleave AK2 in the mitochondria. The DP activity and immunoblot analysis (Figure 4.3A&C) suggests that DP8 and DP9 proteins are present in the mitochondria. However, the expression of protein indicative of active DP8 and DP9 proteins (99 kDa) was not observed. In the mitochondria, DP9 was seen as a band 75 and 64 kDa in mobility and DP8 has a band 64 kDa in mobility but these truncated proteins appeared to demonstrate DP enzyme activity. A similar truncated DP4 (60 kDa) was also found in rat kidney (Iwaki-Egawa *et al.*, 1993). This suggests that DP8 or DP9 may activate AK2 in the cytoplasm and the mitochondria.

It is more difficult to perform a kinetic study of AK2 using cytoplasmic fractions of SKOV3 cells because so far nine AK isotypes have been identified (Amiri *et al.*, 2013). AK1, AK6, AK7 and AK8 isotypes are localised in the cytoplasm and are widely expressed in all human tissues (Khoo and Russell, 1972; Ren *et al.*, 2005; Panayiotou *et al.*, 2011). Our immunoblot data suggest that the AK2 isotype is present in the cytoplasm as well as the mitochondria (Appendix, Figure 8.9).

Moreover, these all AK isotypes have strong affinity for the AMP substrate in the presence of ATP instead of GTP (Panayiotou *et al.*, 2011). In contrast to the expression of the AK family in the cytoplasm, expression of AK2, AK3 and AK4 is limited to the mitochondria compartment and only AK2 binds to the AMP substrate with high affinity in the presence of ATP (Khoo and Russell, 1972; Noma *et al.*, 2001; Dzeja and Terzic, 2009; Chen *et al.*, 2012). Therefore, our data suggest that AK binding affinity to AMP substrate in mitochondria (Figure 4.4 and Table 4.2) comes from AK2 but AK binding affinity to AMP substrate in the cytoplasm may not reflect AK2 activity, and may in fact be coming from other cytoplasmic AK family members. In addition, the kinetic study showed that mitochondrial fractions from wt DP9 overexpressing SKOV3 cell lines have lower binding affinity to AMP than that of the other cell lines (Figure 4.4), suggesting that only AK2 binds to AMP. However, the increased binding affinity in mitochondrial fractions from wt DP9 overexpression was not followed by increases in AK enzyme activity (Figure 4.4). These binding affinities and AK activity patterns were reversed in the mitochondrial fractions from mt DP9 overexpressing SKOV3 cells. Therefore, we speculate that DP9-activated AK2 is due, at least in part, to another mechanism independent of DP9 enzyme activity.

In summary, DP9 and DP8 overexpression change cell phenotype, proliferation rate and cell viability. Mutant DP9 overexpression enhances AK enzyme activity and decreases slightly binding affinity of AMP in the mitochondria. Meanwhile, wt DP9 overexpression increases AK enzyme activity and binding affinity of AMP in the mitochondria. The increased AK activity in this cell is followed by decrease in ATP and energy charge values. Silencing DP8 and DP9 genes in SKOV3 cells will

provide important data to whether these proteases cleave AK2 or not in vivo. Because AMPK plays a central role in controlling cellular energy through interacting with ADP and AMP, measurement of AMPK phosphorylation in DP8 and DP9 silencing is required for identification of the downstream effects of AK activity.

5. INVESTIGATION OF THE EFFECT OF DP8 AND DP9 SILENCING ON AK2 PROTEIN EXPRESSION AND ENZYME ACTIVITY IN OVARIAN CANCER CELL LINES

5.1. Introduction

The majority of ovarian cancer cases are derived from the surface epithelium but the cancer origin comes from celomic epithelium in the Müllerian duct, which also develops to the lining of the fallopian tubes, uterus, and endocervix (Auersperg *et al.*, 2001; Dubeau, 2008; Vaughan *et al.*, 2011). So far, ovarian cancer has a low survival rate because it is difficult to diagnose at an early cancer stage, leading to widespread metastasis especially in the peritoneum and there are limited therapeutical options (Jemal *et al.*, 2008). There are only two chemotherapeutic agents to date that effectively kill ovarian cancer cells (carboplatin and doxorubicin) (Vaughan *et al.*, 2011). Unfortunately, some ovarian cancers have become resistant to the available drugs (Bast *et al.*, 2009). In addition, the main characteristic of ovarian cancer is its differentiation into an epithelial phenotype during early cancer progression, which is different from most human cancers which maintain an undifferentiated phenotype (Yoshioka *et al.*, 2012). Thus, a better understanding of the cellular and molecular mechanisms of ovarian cancer is required to identify targets for future cancer therapy (Cheung *et al.*, 2010).

To achieve this goal, reproducible material sources are certainly required (Langdon *et al.*, 1988). For example, ovarian cancer cell lines (OVCA 429 and 432) derived

from ascites fluid of patients with ovarian cancer were developed by the laboratory of Gynecological Oncology, Brigham and Women's Hospital, Boston, USA, (Kim *et al.*, 2002). The SKOV3 cell line is also derived from the same tissue source and was established by the American type tissue collection (ATTC, Rockville, MD). In addition, these cancer lines have the same pathological cancer type, serous cystadenocarcinoma (Kim *et al.*, 2002). All these cell lines are also suitable as a host for transfection in order to study oncogene expression with comparable results (Kajiyama *et al.*, 2003; Zhang *et al.*, 2004; Meng *et al.*, 2009; Wilson, 2011).

Even though ovarian cancer cell lines originated from the same disease, heterogeneity of gene expression has been reported. Tumor suppressor gene (p53), for instance, is differentially expressed in the OVCA cell lines. OVCA 429 cells have the wt p53 gene and mt p53 was detected in OVCA 432 cell lines (Elbendary *et al.*, 1994) whilst SKOV3 cells express a null p53 gene (Yaginuma and Westphal, 1992). Using semi quantitative RT-PCR, higher expression of sex steroid receptors (the follicle stimulating and luteinizing hormone receptors) were observed in OVCA 429 cells, compared to that of OVCA 432 cells (Syed *et al.*, 2001). Both sex receptors are not expressed in the SKOV3 cells, when using either a Northern blot or RT-PCR (Parrott *et al.*, 2001; Mandai *et al.*, 2007). At present, the role of sex steroid hormones in OVCA pathogenesis is still controversial (Choi *et al.*, 2007; Sanner *et al.*, 2009). The OVCA cell lines express DP8 and DP9 differently at the mRNA and protein levels (Wilson, 2011). The highest mRNA expression of DP8 was found in SKOV3, followed by OVCA 432 and OVCA 429, respectively. By contrast, OVCA 429 and SKOV3 cells express similar DP9 mRNA level and low mRNA expression was found in OVCA 432 cells (Wilson, 2011; Wilson *et al.*, 2013). From

immunoblot analysis, OVCA 429 and SKOV3 cells have similar DP8 expression and a higher DP8 expression was observed in OVCA 432 cells. Meanwhile, similar DP9 protein expression was found in OVCA 429 and OVCA 432 cells, whilst SKOV3 cells have lower DP9 protein expression (Wilson, 2011). Interestingly, mRNA and protein levels of DP4 were only detected in SKOV3 cells (Wilson, 2011; Wilson *et al.*, 2013). However, to our knowledge AK2 expression in these cancer cells has not been examined.

AK2 is a mitochondrial enzyme that maintains the fixed ratio of adenine nucleotide levels by catalysing reversibly the exchange of phosphate bond from ATP to AMP, which generates 2 molecules of ADP (Dzeja and Terzic, 2003; Noma, 2005). This AK function becomes a critical sensor in all living cells that regulates small changes in the ADP/ATP and AMP/ATP balances (Dzeja and Terzic, 2009). AK2 interacts with other metabolic sensors such as AMPK and creatine kinase to monitor energy consumption and energy utilization in cells (Dzeja and Terzic, 2009). Hypoxia and glucose deprivation decrease ATP production whilst exercise or muscle contraction increases ATP consumption. Such conditions will stimulate AMPK phosphorylation (Hardie, 2007; Dzeja and Terzic, 2009; Carling *et al.*, 2011; Hardie, 2011b; Hardie, 2011a; Oakhill *et al.*, 2012). Once AMPK has been activated, catabolic pathways are turned on to generate ATP and anabolic pathways are turned off to promote energy efficiency, which results in inhibition of cell growth and proliferation (Hardie, 2011a). Chapter 3 and 4 demonstrate that AK2 is a potential natural substrate of DP8 and DP9 proteases and mt DP9 overexpression in SKOV3 cell increased AK enzyme activity. Thus, we postulated that DP8 or DP9 silencing would decrease AK activity, resulting in phosphorylation of AMPK (more activation).

Therefore, the aim of this chapter was to examine AK2 expression in three different ovarian cancer cell lines and the effect of DP8 or DP9 silencing on AK enzyme activity. Because animal models lacking DP8 and DP9 genes have not been established, DP8 and DP9 genes were silenced using siRNA.

5.2. Material and Methods

5.2.1. Cell culture of ovarian cancer cell lines

OVCA 432 and SKOV3 cell lines were grown in RPMI supplemented with 10% heat-inactivated FBS, 100 U/ml penicillin and 100 µg/ml streptomycin whilst OVCA 429 cell line was grown in DMEM with the same supplementation. All cancer cells were maintained at 37°C in a humidified incubator with 5% CO₂ atmosphere.

5.2.2. siRNA transfection

One day before transfection, 2×10^5 cells from OVCA 432, SKOV3 and OVCA 429 cell lines were propagated into a 6 well plate with two ml of complete RPMI or DMEM without antibiotics. Cells were cultured at 37°C for 24h in a 5% CO₂ incubator in order to attach to the vessel surface. AK2 siRNA (5'-GCUUGAUUCUGUGAUUGAA-3', Cat#4390824-s1209), DP8 siRNA (5'-CAACGAUAAUUUGGAUAUCU-3', Cat#4390824-s29657), DP9 siRNA (5'-CCGCCGUUUUAAAUAUCCCA-3', Cat#4392420-s40557) Silencer Select and Silencer Select negative control no 2 siRNA (Cat#4390846) were obtained from Ambion[®] Life Technologies, Carlsbad, CA USA. After cells reached 50-70% confluence, the cells were carefully washed with RPMI or DMEM without supplementation in order to remove excess FBS. Washed cells were then resuspended in two ml fresh RPMI or DMEM with 10% inactivated serum.

Meanwhile, 100 μ M siRNA suspensions and 15 μ l Lipofectamine®RNAiMAX reagent (Ambion) were diluted in 250 μ l RPMI or DMEM without supplementation and incubated them at RT for 5 min. Both solutions were then mixed thoroughly and incubated at RT for 30 min. At the end of the incubation, 500 μ l of siRNA-liposome complexes were dropped carefully into the cells in a 6 well plate and incubated at 37° C for 24 h in a 5% CO₂ incubator. The following day, media were removed and replaced with RPMI or DMEM supplemented with 10% FBS, 100 U/ml penicillin and 100 μ g/ml streptomycin and re-incubated to reach confluence for 48h.

5.2.3. Cell extraction and protein quantification

Post transfection (48h) cells were washed with PBS pH 7.4 twice and cells were then detached using 200 μ l of pre-warmed trypsin-EDTA for 5 min. In order to inactivate trypsin, detached cells were resuspended in 1 ml of complete media and centrifuged at 1,500 xg at RT for 5 min. After that, cells were washed again with cold PBS pH 7.4 twice and washed cells were resuspended in 200 μ l of cold lysis buffer. For breaking up cells, cell suspensions were sonicated on an ice box for 10 sec (detailed description in Materials and Methods section 2.5.6.1). To collect cell lysates, sonicated cells were centrifuged twice at 650 xg for 10 min at 4°C and cleared supernatant was then kept at -80°C before use. Protein concentration of individual samples was measured using the BCA method (see in materials and methods in Chapter 2). Samples were diluted one in five in lysis buffer and mixed with 200 μ l of BCA reagent.

5.2.4. Measuring adenine levels and AEC values

To do AEC assay in siRNA transfected cells in a 6 well plate, the existing method was modified (Matsui *et al.*, 1994). After 48h incubation, cell culture medium was removed by pipetting and the plate was placed in an icebox. 500 μ l of 0.6 M cold perchloric acid was directly added into cells and cell were scraped off with a sterile cell scraper. Lysed cells were transferred into 1.5 ml sterile tubes and neutralized with 480 μ l of water and 20 μ l of 50 mM potassium phosphate buffer pH 7.0. Cell suspensions were then vortexed briefly and centrifuged at 10,000 xg for 10 minutes at 4°C. Cleared supernatants were transferred into three HPLC vials and each vial contained 300 μ l cell lysate. The next step was exactly the same procedure as described in Chapter 4.

5.2.5. DP enzyme activity assay

The DP enzyme activity of all cell lysates was measured spectrophotometrically using H-Ala-Pro-pNA synthetic substrate. 10 μ g of each protein sample was diluted with 40 μ l of lysis buffer in a 96 well plate. Diluted samples were then added with 50 μ l of 1 mM H-Ala-Pro-pNA substrate in lysis buffer. The absorbance values were directly measured using a micro plate reader with optical density 405 nm at 37°C every five min for 60 min.

5.2.6. AK activity assay

AK activity in cell lysates was assayed by adding different concentrations of AMP as the AK substrate as described in Chapter 4.

5.2.7. Western Blotting

15 µg protein samples were diluted in 3x SDS-PAGE sample buffer and boiled at 100°C for 5 min in a dry block heater (detailed in Chapter 2 materials and methods). Blotted membranes were incubated with diluted primary antibodies at 4°C o/n with shaking. Unbound antibody was washed with washing buffer 3 times for 10 min at RT and membranes were then incubated with anti rabbit secondary antibodies conjugated with HRP (1: 5,000 dilution in blocking buffer for AMPK, phospho-AMPK, AK2 and DP8 and 1: 10,000 dilution for DP9) and an anti mouse antibody conjugated with HRP (1:20,000 dilution for β-actin) at RT for 60 min. The ChemiDoc™ imaging system was used to develop signals from 1 sec to 900 sec. The resulting images of protein bands were quantified using Image lab™ software package program and presented in mean volume pixel intensity per mm² area. Bands were normalized with background and band intensity of wt OVCA 429, OVCA 432 and SKOV3 cells between each immunoblot.

5.2.8. Statistical analysis

Each experiment was repeated three times and presented as mean ± SEM. However AK activity data were collected from only two independent assays. Statistical analysis was performed using the student's *t*- test for comparing mean of DPP and AK enzyme activities among siRNA transfected OVCA 429, OVCA 432 and SKOV3 cell lines. Because distribution of collected data was not homogenous, we also used non parametric statistical analysis, *Kruskal-Wallis and Mann-Whitney U* tests to compare mean of adenine nucleotide levels. A significant difference value was set at $p < 0.05$.

5.3. Results

5.3.1. Characteristics of the three ovarian cancer lines

Before examining the effects of DP8 and DP9 silencing, the OVCA 429, OVCA 432 and SKOV3 cell lines were first characterized. Figure 5.1 demonstrates that the three ovarian cancer cells had different characteristics. OVCA 432 and SKOV3 were morphologically similar and formed single cell colonies with fibroblast-like cells. While fibroblast-like cells were observed in OVCA 429 cell lines, which formed clumped colonies. In addition, OVCA 432 and SKOV3 cells had similar AK enzyme activity while OVCA 429 cell had a two-fold increase in AK enzyme activity (Figure 5.1B). However, a similar DP enzyme activity was observed in OVCA 429 and OVCA 432 cells. DP enzyme activity doubled in SKOV3 cells, compared to DP activity in other cells (Figure 5.1C). From immunoblot analysis, AK2 protein was observed in all three cancer cells (Figure 5.1D&E). Higher AK2 protein levels were detected in OVCA 429 cell followed by OVCA 432 and SKOV3 cells. DP8 and DP9 proteins were also detected in all

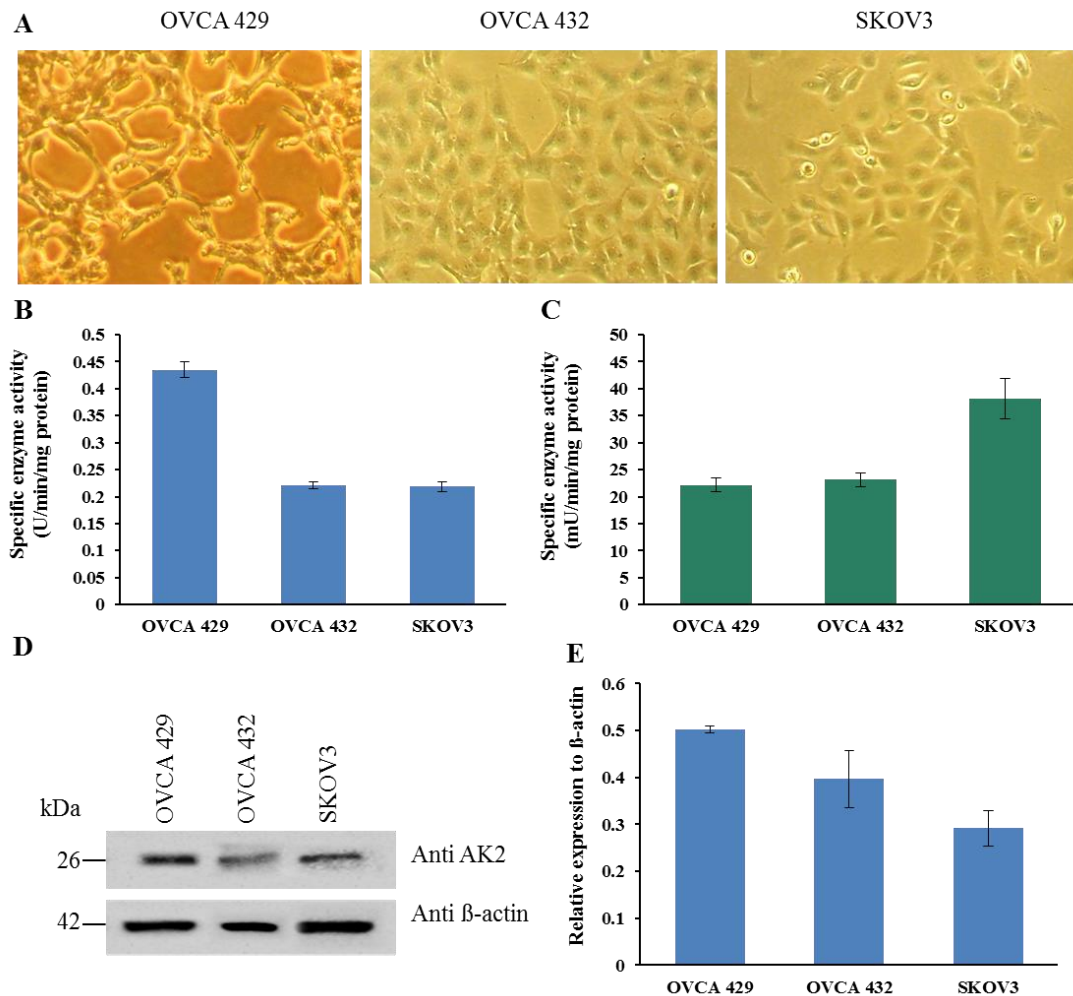


Figure 5.1. Characteristics of the three ovarian cancer cell lines. (A) Morphology: OVCA429 cells were grown in DMEM and OVCA 432 and SKOV3 cells were grown in RPMI. Images were taken under an inverted microscope with x100 magnification after 48h incubation. (B) AK enzyme activity of the cell lines against 0.7 mM AMP substrate. The AK enzymatic reaction was performed at RT and spectrophotometrically measured at 340 nm absorbance every min for 20 min. (C) 10 μ g of extract cells were incubated with 1 mM of H-Ala-Pro-pNA substrate and absorbance values were measured at 405 nm in length. (D) 15 μ g of protein samples were analysed by Western blotting using anti AK2 and β -actin antibodies. (E) AK2 band intensity in cancer cells was quantified with Bio-Rad Image lab™ software and normalised with band intensity of β -actin. The DP assay was performed three times on lysates from the three ovarian cancer cells and the AK2 assay was performed twice. Data were presented as mean \pm SEM.

cancer cell lines. DP9 protein levels were higher in OVCA 429 and SKOV3 cells compared to DP8 protein level in the same cancer cells while DP8 and DP9 levels in OVCA 432 cells was the opposite to those in OVCA 429 and SKOV3 cells (Figure

5.2D). A higher DP8 protein level was observed in OVCA 432 cells than that of OVCA 429 and SKOV3 cells, which had half the DP8 protein level (Figure 5.2D). The highest DP9 protein level was detected in SKOV3 cells followed by OVCA 429 and OVCA 432 cells, respectively.

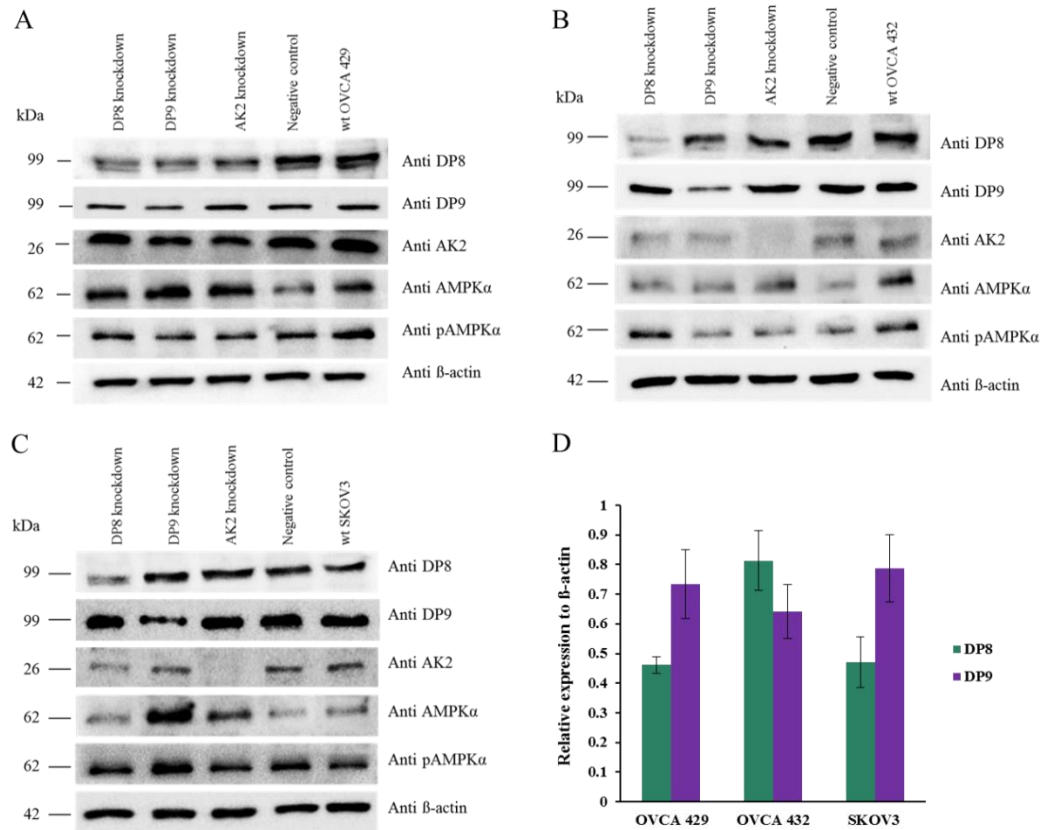


Figure 5.2. Immunoblot analysis of ovarian cancer lines transfected with DP8, DP9 and AK2 siRNAs. (A-C) Protein expression of DP8, DP9, AK2, AMPK and pAMPK in OVCA 429, OVCA 432 and SKOV3 cells transfected with DP8, DP9 and AK2 siRNAs. 15 μ g protein samples were separated using 10% SDS-PAGE and electro-transferred on to PVDF membrane. Blotted membranes were then analysed in immunoblots using anti DP8, DP9, AK2, AMPK and phosphorylated AMPK antibodies and anti β -actin antibody was used as a control. (D) DP8 and DP9 band intensities in wt cancer cells were quantified using Bio-Rad Image lab™ software and normalised with band intensity of β -actin. Images were representative of three immunoblots.

5.3.2. Validation of DP8, DP9 and AK2 siRNAs in ovarian cancer cell lines

To verify that DP8, DP9 and AK2 siRNA silencing actually reduced DP8, DP9 and AK2 respectively, DP and AK enzyme activity and protein levels were evaluated in

all ovarian cancer cell lines after transfection with 50 nM siRNAs. The same gels were used to do immunoblot and densitometry analysis in Figure 5.2 and 5.4. In Figure 5.2D, only the band intensity of DP8 and DP9 in wt SKOV3 cell was analyzed and normalized with band intensity of β -actin while in Figure 5.4, the band intensity of DP8 and DP9 in SKOV3 cells with all siRNA silencing was analyzed and normalized with band intensity of wt SKOV3 cell. Interestingly, DP8 and DP9 siRNA silencing decreased the DP8 and DP9 activities and protein levels in all cancer cells even though the decreased activity and protein level were variable among the cells (Figure 5.2 – 5.4). DP8 and DP9 silencing reduced DP enzyme activity in all cancer cells but a greater reduction was observed in cancer cells with DP9 silencing. Similar results were also found in DP8 and DP9 protein expression. Around 20-60% reduction of DP8 protein levels were found in all cancer cells with DP8 silencing and the DP8 silencing also reduced 20% DP9 protein level in OVCA 429 and OVCA 432 cells (Figure 5.4). A similar reduction was also observed in cancer cells with DP9 silencing. Similar results were also found in DP8 and DP9 protein expression. Around 20-60% reduction of DP8 protein levels were found in all cancer cells with DP8 silencing and the DP8 silencing also reduced 20% DP9 protein level in OVCA 429 and OVCA 432 cells (Figure 5.3). The similar reduction was also observed in cancer cells with DP9 silencing. Surprisingly, DP8 silencing in SKOV3 cells does not affect DP9 protein levels and vice versa. Further investigation is required in order to understand the different effects of DP8 and DP9 silencing in the ovarian cancer cells. However, overall the data demonstrated that all three cancer cells are suitable for examining whether DP8 and DP9 silencing influences AK2 activity and protein level or not.

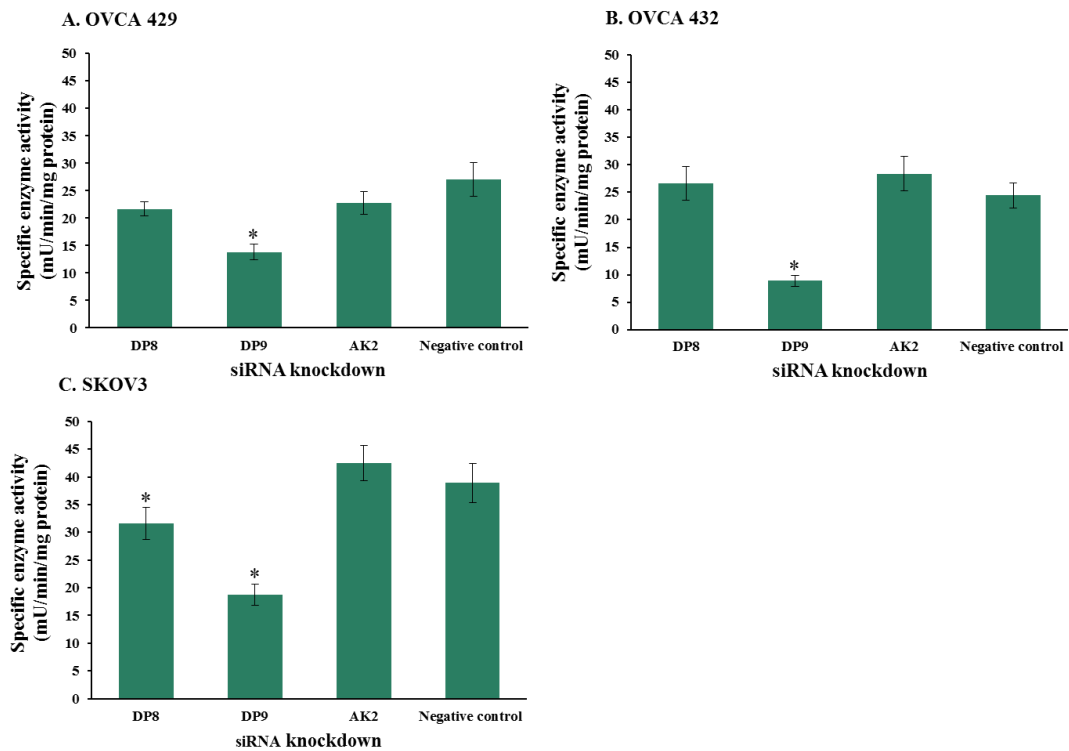


Figure 5.3. DP enzyme activity in ovarian cancer cell lines transfected with 50 nM DP8, DP9 and AK2 siRNA. 10 μ g of cell lysate were added to 1 mM H-Ala-Pro-pNA synthetic substrate. Enzymatic assay was measured in a microplate reader at 405 nm for 60 min at 37°C. Specific enzyme activity was determined using Beer-Lambert formula with extinction factor 9.45 M for pNA. The DP assay was performed three times from different transfections and data were presented as mean \pm SEM with * $P < 0.05$.

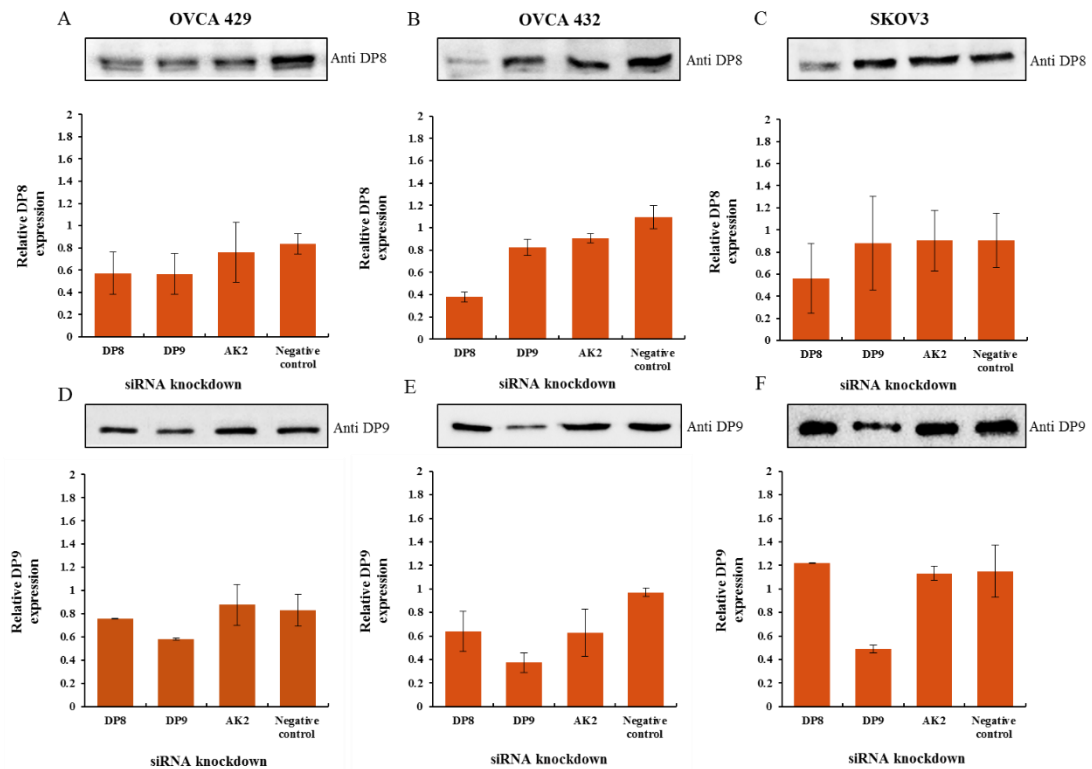


Figure 5.4. Relative protein expression of DP8 and DP9 in ovarian cancer lines transfected with DP8, DP9 and AK2 siRNAs. (A-F) 15µg of protein samples were analysed by Western blotting using anti DP8 and DP9 antibodies. Band intensity was quantified with Bio-Rad Image lab™ software and normalised with band intensity of wt ovarian cancer lines. Results were mean ± SEM of relative protein expression of duplicate blotted membranes. Immunoblot images were representative images using anti DP8 and DP9 antibodies (the experiment was performed three times). A and D were OVCA 429 cells with DP8 and DP9 protein levels respectively. B and E were OVCA 432 cells with DP8 and DP9 protein levels and C and F were SKOV3 cells with DP8 and DP9 protein levels respectively.

5.3.3. Effects of DP8 and DP9 siRNA silencing on AK2, AMPK and AEC levels

AK2, AMPK and AEC levels were examined in the three ovarian cancer cells after silencing. DP8 and DP9 siRNA silencing had different effects on AK and AMPK activities (5.5 – 5.6). AEC levels were also different in SKOV3 cells with DP8 and DP9 silencing (Figure 5.7). DP8 and AK2 silencing decreased AK enzyme activity in OVCA 432 and SKOV3 cells (Figure 5.5B & C). Meanwhile, DP9 silencing had no effect on AK enzyme activity in these cells. In contrast, in OVCA 429 cells a different effect was observed. DP9 silencing and not AK2 nor DP8 silencing resulted

in lower AK enzyme activity (Figure 5.5A). In contrast to AK enzyme activity, DP8 and DP9 siRNA silencing decreased AK2 protein levels in all cancer cells (Figure 5.5 A-C).

To evaluate the effects of DP8 and DP9 silencing on AK2, total AMPK and phosphorylated AMPK protein levels, Western blotting was performed. The same immunoblots were used to analyse band intensities of AK2, total AMPK and phosphorylated AMPK proteins using Bio-Rad software (Figure 5.2 and 5.6). Greater reduction of AK2 protein levels was detected in OVCA 429 and SKOV3 cells with DP8 siRNA silencing than in OVCA 429 and SKOV3 cells with DP9 and negative siRNAs silencing. In OVCA 432 cells, reduction of AK2 protein levels was similar between DP8 and DP9 siRNA (Figure 5.6B). Total AMPK protein levels were decreased in OVCA 429 cells by AK silencing (Figure 5.6D), and in OVC 432 cells by DP9 silencing (Figure 5.6E), but no effects on AMPK phosphorylation were observed (Figure 5.6G and H). In contrast in SKOV3 cells both AK2 and DP9 silencing lead to an increase in total AMPK levels, but again no differences in AMPK phosphorylation were observed (Figure 5.6F & I).

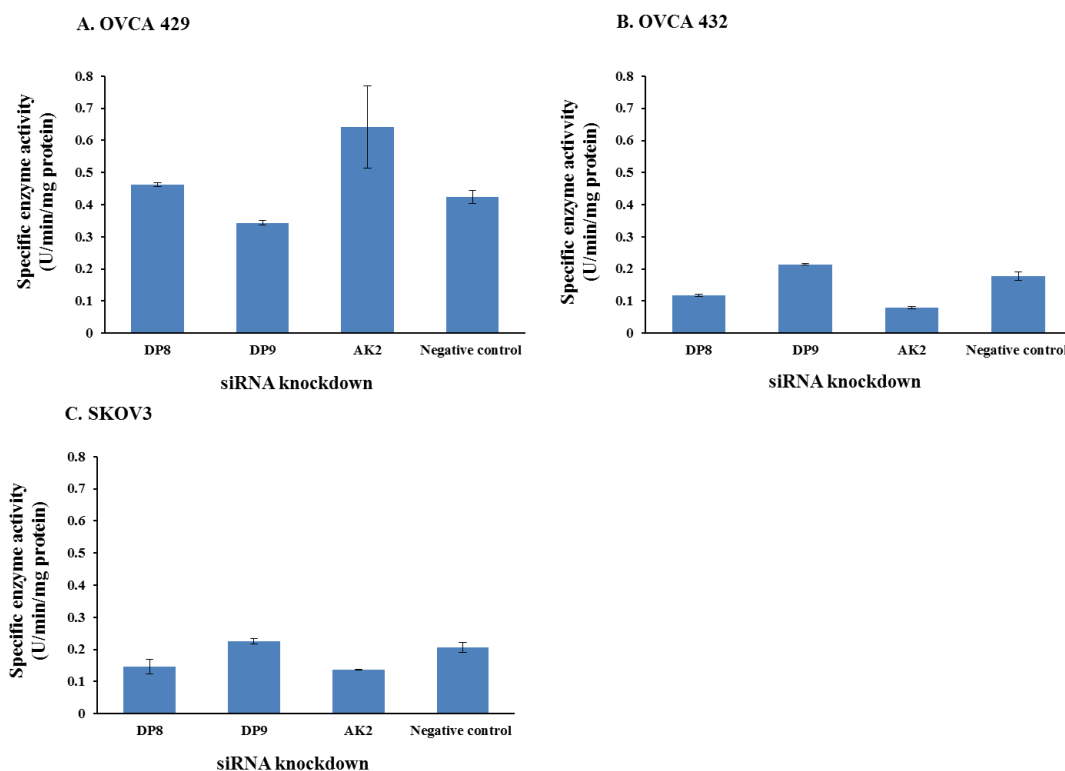


Figure 5.5. AK specific enzyme activity in ovarian cancer cell lines transfected with 50 nM DP8, DP9 and AK2 siRNA. 20 μ g of cell lysate of OVCA 429 (A), OVCA 432(B) and SKOV3 cells (C) was incubated with 0.7 mM AMP. The AK enzymatic reaction was performed at RT and spectrophotometrically measured at 340 nm absorbance every min for 20 min. Each bar represented the mean of two separate experiments.

Only SKOV3 cells transfected with DP8 and DP9 siRNAs were used to examine adenine nucleotide levels. Silencing with AK2, DP8 and DP9 had no significant effect on ATP or AMP levels, AEC values or ADP/ATP ratio (Figure 5.7A-E). However silencing with DP8 and DP9 did lower ADP levels, compared to the control, but only DP8 silencing reach significance (Figure 5.7B). Following from this, DP8 silencing reduced the ADP/ATP ratio but this did not reach significance (Figure 5.7E).

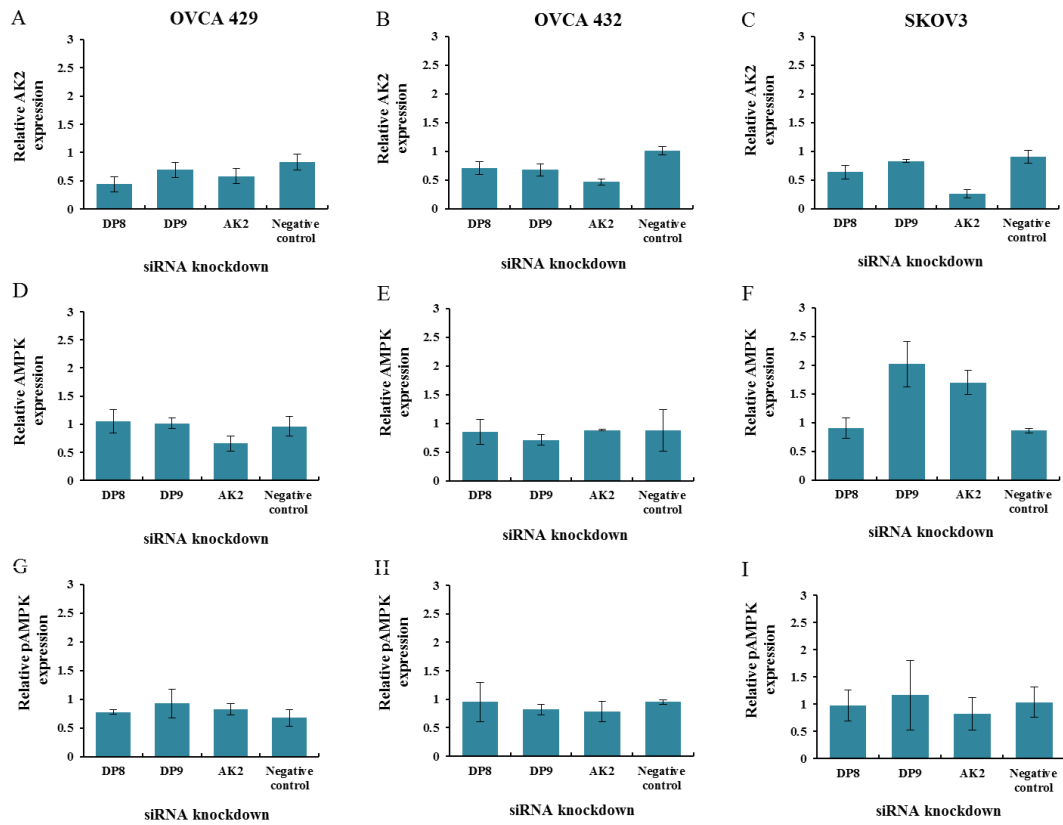


Figure 5.6. Relative protein expression of AK2, total AMPK and phosphorylated AMPK in ovarian cancer lines transfected with 50 nM DP8, DP9 and AK2 siRNA. A, D and G are OVCA-429, B, E and H are OVCA 432 and C, F and I are SKOV3 cells 15µg protein samples were analysed via Western blot using anti AK2, AMPK and pAMPK antibodies. Band intensity was quantified with Bio-Rad Image lab™ software and normalised to band intensity of wt ovarian cancer lines.

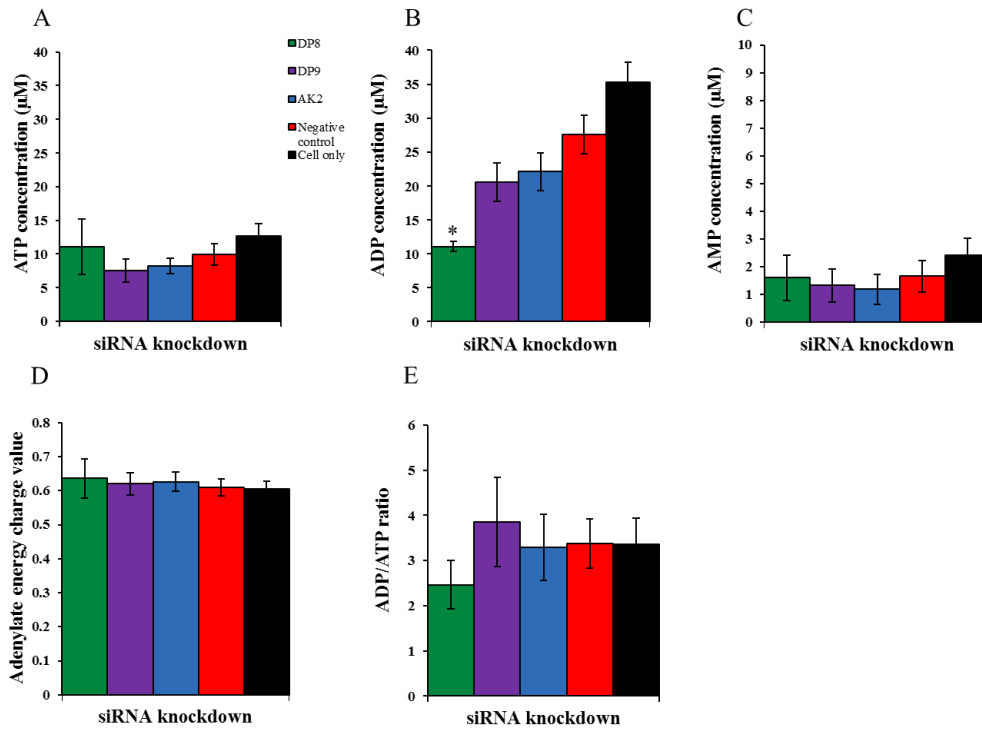


Figure 5.7. Adenylate energy charge of SKOV3 cells 72h after transfection with 50 nM DP8, DP9 and AK2 siRNAs. 1×10^6 cells were lysed with 0.6 M cold perchloric acid and neutralised with potassium phosphate buffer. (A-C) Adenine nucleotide levels were determined using HPLC and (D) the adenylate energy charge was calculated using Atkinson's formula, $AEC = (ATP + 0.5ADP) / (ATP + ADP + AMP)$. (E) ADP/ATP ratio was used as an indicator of cell viability. Data were presented in means \pm SEM in three independent experiments. * $P < 0.05$, difference with negative control.

5.4. Discussion

Although AK2 structure and function have been extensively studied, AK2 protein expression and activity are not established yet in ovarian cancer cells. In this chapter, it was demonstrated that OVCA 432 and SKOV3 cells expressed the same levels of AK2 protein and similar AK enzyme activity. However, AK enzyme activity in OVCA 429 cells was twice that in the other ovarian cancer cells. All of the three ovarian cancer cells were fit to be used as a cell model to investigate the effect of DP8 and DP9 silencing on AK2, AMPK and AEC levels. Activation of AK2 seemed to require DP8 proteolytic activity in OVCA 432 and SKOV3 cells. DP8 silencing

decreased AK2 expression in all three ovarian cancer cells and increased AMPK phosphorylation in OVCA 429 cells. However, down regulation AK2 protein in SKOV3 cells did not lead to decreases in phosphorylation of AMPK.

Although the ovarian cancer cell lines used in this study are derived from the same disease (Kim *et al.*, 2002), they demonstrated different characteristics. OVCA 432 cells showed similar morphology to SKOV3 cells but OVCA 429 cell morphology was different. The discrepancies in cell morphology are more likely related to repeated *in vitro* culture. These cells were originally obtained from the Peter Macallum Cancer Research Institute in Melbourne and may no longer have the same phenotype as the original cells. From a previous study performed by Wilson (2013), mRNA and protein expression of DP8 in SKOV3 cells were higher than mRNA and protein expression of DP8 in OVCA 429 and OVCA 432 cells and a similar pattern of expression was also seen in mRNA and protein expression of DP9 in these cancer cells. However, DP9 expression was lower than DP8 expression in all cancer cells. It is not surprising that SKOV3 cells have higher DP enzyme activity because the SKOV3 cell lysates used to measure the DP enzyme activity, also express DP4 on their cell membrane (Abbott *et al.*, 2000; Wilson *et al.*, 2013). Wilson (2011) has demonstrated that neither OVCA 429 nor OVCA 432 cells express DP4 mRNA or DP4 protein.. Thus, DP enzyme activity in these cancer cells would be more similar if the cytoplasmic fraction was used. Therefore, it is hard to evaluate alteration of the DP enzyme activity in OVCA 429 cells after transfection with DP8 and DP9 siRNAs.

Silencing DP8 and DP9 expression modulates AK2 protein expression and AK enzyme activity in the three cancer cells. However, down regulation of AK2 protein is not followed by reduction of AK enzyme activity in OVCA 429 cells with DP8 silencing and in OVCA 432 and SKOV3 cells with DP9 silencing. The reduction of AK2 protein expression might be compensated by increasing cytoplasmic AK1 protein expression because these AK proteins have the same role in catalyzing 2ADP into ATP and AMP, just different cellular location (Dzeja and Terzic, 2009). Therefore, AK enzyme activity in this study should be taken from the mitochondrial fraction of these cells in order to provide more accurate AK2 enzyme activity. However it is difficult to prepare such fractions when the silencing experiments are conducted in small scale. Because OVCA 432 and SKOV3 cells have the same morphology, reduction of AK activity and protein level are comparable in these cells with DP8 silencing whilst DP8 silencing did not affect AK activity and protein level in OVCA 429 cells, which has a slightly different morphology. In addition these cells were cultured in different media and it is possible that if OVCA 429 cells were adapted to the RPMI media that silencing effects might be more similar. Thus, DP8 may be required for AK2 activation but the mechanism underlying AK2 activation by DP8 needs further investigation.

Based on the quantitation of the immunoblots, down regulation of AK2 protein expression in three cancer cells does not affect total AMPK expression level or phosphorylation of AMPK. However a visual inspection of the blot in Figure 5.4 shows that in this experiment pAMPK signal was increased by DP8 siRNA silencing. To give additional evidence, adenine nucleotide levels were measured in SKOV3 cells with DP8, DP9 and AK2 silencing. DP8 silencing led to a significant

decrease in ADP thus suggesting less AK2 activation and more phosphorylation of AMPK as observed. As described in several studies, AMPK expression is stimulated by increasing cellular levels of AMP and ADP or decreasing ATP level through interacting with γ subunit of AMPK, which results in more sensitivity to phosphorylation by the tumor suppressor protein LKB1 and Ca^{2+} -activated, calmodulin-dependent kinase kinases (Hardie, 2007; Carling *et al.*, 2011; Hardie, 2011b; Oakhill *et al.*, 2011; Oakhill *et al.*, 2012). Our findings confirmed that DP8 silencing activates AMPK in order to keep energy balance, which inhibits ATP consumption and accelerate ATP production (Hardie, 2007; Hardie, 2011b). The changed energy balance will then suppress cell growth and proliferation in order to increase survival (Hardie, 2011a). As a result, ATP level increases and ADP and AMP levels decrease as observed in SKOV3 cells with DP8 silencing.

In summary, AK2 expression was investigated in three different ovarian cancer cell lines. Additionally, the effects of DP8 and DP9 silencing on AK enzyme activity and expression in the three ovarian cancer cells were also investigated. All cancer cells express AK2 protein and two fold AK2 protein expression was found in OVCA 429 cells, which correlates with its increased AK enzyme activity. DP8 silencing down regulates AK2 expression and AK enzyme activity in SKOV3 cells. Reduced AK2 activation stimulates phosphorylation of AMPK to maintain cellular energy homeostasis in these cells. Therefore, DP8 plays a central role in activation of AK2 and the enzyme activity of DP8 may contribute to the pathogenesis of ovarian cancer.

6. GENERAL DISCUSSION AND CONCLUSION

Determining the full substrate repertoire for DP8 and DP9 is essential for determining their physiological and pathological roles. At the beginning of this work although many potential substrates for DP8 and DP9 had been identified only AK2 and calreticulin had been validated (Wilson, 2011). Many of the candidate substrates identified for DP8 and DP9 play crucial roles in metabolism and maintaining cellular homeostasis. AK2 which has been validated as a DP substrate plays a key role in energy metabolism and energy transfer. In this thesis, the substrates AK2 and calreticulin were shown to be in close proximity to DP8 and DP9 proteases, and a further seven substrates that play roles in regulating metabolism were confirmed. In addition by studying the effects of over expression and silencing of these proteases, further functional evidence has been provided to support the role of these proteases in regulating cell growth, adenine nucleotide levels, and AK2 activity. In particular overexpression of wt and mt DP9 decreased AK enzyme activity, ATP levels and adenylate energy charge while ADP, AMP, ADP/ATP ratio and AMP/ATP ratio were increased. DP8 and AK2 silencing in SKOV3 cells decreased AK enzyme activity and phosphorylation of AMPK and suggests *in vivo* that AK2 is a substrate for DP8 and not DP9. However these results need further validation. In addition preliminary evidence was found suggesting that a shorter form of both DP8 and DP9 which may or may not be active is present in the mitochondria of cells.

6.1. Potential natural substrates for DP8 and DP9

In this study, DP8 and DP9 proteases were able to modify the N terminus of seven oligopeptides (Chapter 3). Six of these seven potential substrates were localized in the cytoplasm together with DP8 and DP9, suggesting that DP8 and DP9 would

come into close contact with these substrates *in vivo*. In physiological conditions, three potential substrates (bifunctional purine biosynthesis, C-1-tetrahydrofolate synthase and dihydropyrimidine dehydrogenase) have important roles in base and amino acid metabolism. Thus DP8 and DP9 may play important roles in the maintenance of cellular energy metabolism *in vivo*. From the available data, the full length of seven potential substrates except cathepsin Z/X still have a Met residue in the N terminus. To examine DP8 and DP9 proteolytic activity to these substrates, it should be done using the full aa sequences. Unfortunately, there is no available cleavage assay that will do this. Most recombinant protein that is available either contains a His tag at the N- terminus or the incorrect pre-processing, for it to be recognised as substrate for DP8 or DP9. More importantly in the literature, pre molecular biology, when some of these enzymes were isolated and purified from heart and liver tissues and sequenced using Edman sequencing, they have been found to exist mostly in the form that is missing the two aa residues that DP8 and DP9 cleave (Frank *et al.*, 1986; Hum *et al.*, 1988; Schlauderer and Schulz, 1996; Schmidt *et al.*, 2000). DP8 and DP9 are one of very few cytoplasmic enzymes that have the unique prolyl bond. Thus this is strong *in vivo* evidence that DP8 and/or DP9 cleave these substrates.

Although DP8 and DP9 modified slowly (still not 100% after 24h) the seven potential substrates *in vitro*, the proteolytic activity of DP8 and DP9 *in vivo* may be faster. Studies in healthy and diabetic people, for instance, confirmed that GLP-1 inactivation *in vivo* required a shorter time than that observed *in vitro* (Deacon *et al.*, 1995; Kieffer *et al.*, 1995; Deacon *et al.*, 2000). An *in vitro* study reported that recombinant human DP4 inactivated -GLP-1 with half-life from 0.2 to 1.2h whereas

elimination of GLP-1 required just two min after intravenous administration of GLP-1 in healthy and diabetic subjects (Vilsboll *et al.*, 2003; Bjelke *et al.*, 2006). Therefore, those studies clearly indicate that natural microenvironments greatly influence proteolysis. Another possibility is that while substrates are bound in the active pocket of DP8 or DP9 that this has effects on the substrate activity, and this is a more important part of the regulatory process than cleavage. Thus it is an advantage for cleavage to be very slow, as once cleaved the substrate would no longer bind to the protease.

Further work over many years will be needed in order to further establish whether the seven other substrates identified in this work and calreticulin are actually true DP8 and DP9 substrates *in vivo* using many different cell-based assays as was performed for AK2 in this thesis. Each substrate plays differing roles in regulating cellular metabolism, different assays will need to be developed in order to assess the role that DP8 and DP9 cleavage plays in the function of each substrate. To date mice deficient in either DP8 or DP9 have not been made, these mice will be invaluable tools to help validate what effects that lack of protease cleavage will have on the functions of each of these substrates. Until these tools are available, this work needs to be continued using cell models where DP8/DP9 is overexpressed or silenced.

In general, the majority of mitochondrial proteins are synthesised by the ribosomes in the cytoplasm as precursor proteins and transported into the mitochondria using protein transporter networks such TOM and TIM (Endo and Kohda, 2002; Schmidt *et al.*, 2010). Most mitochondrial proteins have amino signal sequences that are cleaved by membrane-bound proteases and bind to TOM and TIM protein

complexes during importing process into the inner membrane and matrix of the mitochondria (Endo and Kohda, 2002; Schmidt *et al.*, 2010). For nuclear-encoded mitochondrial proteins translocated into the intermembrane space of mitochondria, these proteins do not have external targeting signal and are directly imported by the TOM complex (Schmidt *et al.*, 2010). For example, yeast Mic14, Mic 17 and Mdm 35 proteins and human Cox 17 and ATP/ADP translocator proteins possess internal targeting sequences in their mature proteins (Cys motif) (Gabriel *et al.*, 2007; Sideris *et al.*, 2009; Schmidt *et al.*, 2010). These proteins interact with the mitochondrial intermembrane space assembly protein complex to become mature proteins with disulphide bonds (Schmidt *et al.*, 2010).

Unfortunately, translocation of AK2 protein into the intermembrane space of mitochondria does not follow the above pathway. Some studies have demonstrated that translated AK2 proteins are directly imported into the intermembrane space of mitochondria via interactions with the cognate receptor in the outer membrane of the mitochondria (Nobumoto *et al.*, 1998; Angermayr *et al.*, 2001; Schricker *et al.*, 2002; Strobel *et al.*, 2002). This AK2 import mechanism is based on observations in wt and mt yeast adenylate kinase. The majority of mature AK2 protein is localised in the cytoplasm and around 6-8% mature AK2 proteins are translocated into intermembrane space of the mitochondria (Angermayr *et al.*, 2001; Schricker *et al.*, 2002; Strobel *et al.*, 2002). However, in higher vertebrates the proportion of AK2 localization in the cytoplasm shifts to 30-70% (Watanabe and Kubo, 1982; Nobumoto *et al.*, 1998). Our findings are in agreement to Nobumoto *et al.*, where AK enzyme activity in the cytoplasmic fraction was approximately two fold higher than AK enzyme activity in the mitochondria fraction. Because translated AK2

protein is susceptible to protein degradation, it is not surprising that only small amounts of AK2 protein reach the intermembrane space of the mitochondria (Angermayr *et al.*, 2001; Strobel *et al.*, 2002).

6.2. AK2 processing by DP8

In Chapter 5, DP8 silencing in OVCA 432 and SKOV3 cells resulted in reduction of AK2 protein together with a decrease in AK enzyme activity. From these findings, it suggests that DP8 cleaves AK2 protein in order to make it more active in these cancer cells. However, further evidence is required to support this. To confirm the reduction of AK2 protein expression, semi quantitative RT-PCR to measure mRNA level of AK2 in the cancer cells should be performed. AK2 kinetic profiles in cytoplasmic and mitochondria fractions of ovarian cancers with DP8 silencing will also provide data on the activated AK2, which may have higher binding affinity and maximum reaction rate for AMP. Purification and amino acid sequencing of cleaved and uncleaved AK2 protein from cell extracts would also provide further evidence for the role of DP8 in processing AK2 *in vivo*. Schlauderer and Schulz (1996) have demonstrated that cleaved AK2 was more active than uncleaved AK2 in bovine liver. In the natural microenvironment there is evidence that the Met-Ala-Pro residues at the N-terminus of AK2 are removed and data obtained in this thesis implies that DP8 is involved in this AK2 processing.

6.3. DP8 protein is a potential target for inhibition of ovarian cancer cells

In this study, wt DP8 overexpression in SKOV3 cells caused a morphological change in the cells from a fibroblast-like appearance to a polyhedral shape.

Furthermore, AK enzyme activity also was reduced by the overexpression of wt DP8. However, mitochondria AK enzyme activity was negatively correlated to adenine nucleotide and AEC values (Chapter 4). Overall these data suggest that wt DP8 overexpression inhibits AK enzyme activity. Several studies have demonstrated that mitochondria dysfunction has an essential role in activating apoptosis (Richter *et al.*, 1996; de Graaf *et al.*, 2002; Comelli *et al.*, 2003; Wang and Youle, 2009; Otera and Mihara, 2012). Depending on stimuli, the apoptotic process can be initiated through intrinsic (mitochondrial) and extrinsic pathways (Wang and Youle, 2009). In response to stress stimuli, cytochrome c is released from the mitochondria into the cytoplasm to form the apoptosome by associating with Apaf-1 and pro-caspase-9, which leads to caspase-3 activation (Li *et al.*, 1997; Zou *et al.*, 1997). However, inhibition of ATP production and ATP/ADP exchange transport is detected earlier in the apoptotic process than releasing cytochrome c and opening of permeability transition pore (Richter *et al.*, 1996; Vander Heiden *et al.*, 1999; Bradbury *et al.*, 2000). Impairment of mitochondrial energy metabolism has been used as an apoptotic marker in B cell and leukaemia cell lines treated with various stimuli (Vander Heiden *et al.*, 1999; Bradbury *et al.*, 2000; de Graaf *et al.*, 2002; Comelli *et al.*, 2003). Therefore, further studies are required in order to see whether wt DP8 overexpression induces apoptosis or not. Because DP8 silencing leads to a decrease in AK2 expression and AK enzyme activity, imbalance of adenylate nucleotide levels will activate phosphorylation of AMPK. Catabolic pathways should then be switched on to increase ATP production via increasing glucose uptake and fatty acid metabolism (Carling *et al.*, 2011; Hardie, 2011a; Oakhill *et al.*, 2011; Oakhill *et al.*, 2012). On the other hand, anabolic pathways are switched off to reduce ATP consumption, resulting in inhibition of cell growth and proliferation (Hardie, 2007;

Hardie, 2011b; Hardie, 2011a). In the silencing study glucose uptake, aerobic glycolysis and fatty acid oxidation have not yet been examined, but this work should be done in future.

A possible mechanism for targeted inhibition of DP8 in ovarian cancer cell is related to DP8 proteolytic activity on AK2 (Figure 6.1). DP8 silencing will reduce activation of AK2 protein, which results in changing cellular adenine nucleotide levels. We assume that a reduction of ATP levels and increase of ADP and AMP levels will stimulate AMPK expression, followed by inhibition of mTOR protein. This protein has an important role in PIK3/Akt cell signalling and is a direct downstream target of AMPK (Guertin and Sabatini, 2007; Luo *et al.*, 2010). Therefore, mTOR inactivation will lead to inhibition of cell growth (Luo *et al.*, 2010). Overall, DP8 silencing may inhibit mTOR expression, leading to inhibition of cell growth and promotion of autophagy (Luo *et al.*, 2010; Mihaylova and Shaw, 2011). However, further investigation is required to support this hypothesis.

If DP8 silencing leads to inhibition of ovarian cancer cell growth we would expect overexpression of DP8 to increase the activity of AK2 decrease the ratio of AMP/ATP and lead to a reduction in AMPK activation and increased proliferation of SKOV3 cells. Both wt and mt DP8 overexpressing cells had increased cell viability and decreased AMP and ATP levels compared to vector transfected cells. Therefore, this change of nucleotide levels should inhibit AMPK activation, leading to cell growth and proliferation that are mediated by the mTOR signaling cascade. However, as similar results were observed for mt and wt DP9 the molecular action of DP8 in increasing cancer progression may not be associated with its enzyme activity.

A lot of extra studies are required to tease out the enzyme dependent and enzyme independent roles of DP8 in cell growth and the AMPK/mTOR pathway.

6.4. DP9 promotes cancer progression

Preliminary evidence that mt DP9 overexpression in SKOV3 cells increased glycolysis and fatty acid oxidation was obtained (Figure 8.8 in Appendix). Thus, our data suggest that mt DP9 overexpression resembles cancer progression, which uses aerobic glycolysis to fulfil the higher energy demand (the Warburg effect) (Vander Heiden *et al.*, 2009). SKOV3 cells overexpressing mt DP9 had increased proliferation rates and AK enzyme activity. Greater reduction of ATP levels and AEC values was also observed. As a consequence, ADP and AMP would accumulate in the cytoplasm (Figure 4.1 in Chapter 4). Faubert and colleagues (2013) demonstrated that a AMPK mutation promotes tumorigenesis in E μ -Myc transgenic mice. Loss of AMPK activity also increased glucose consumption and fatty acid oxidation either in the transgenic mice, lung cancer or colon cancer cells with AMPK silencing (Faubert *et al.*, 2013). This study suggests that highly proliferating cells like cancer shift the energy supply from oxidative phosphorylation to aerobic glycolysis, which is in accordance to the Warburg effect (Vander Heiden *et al.*, 2009). Figure 4.5 and Table 4.1, clearly show that mt DP9 overexpression in SKOV3 cells up regulates AK activity, which may cause inhibition of AMPK activity. However, some additional work needs to be performed to measure the total and phosphorylated AMPK in these overexpressing cells.

Cellular Stress
Nutrient Deprivation

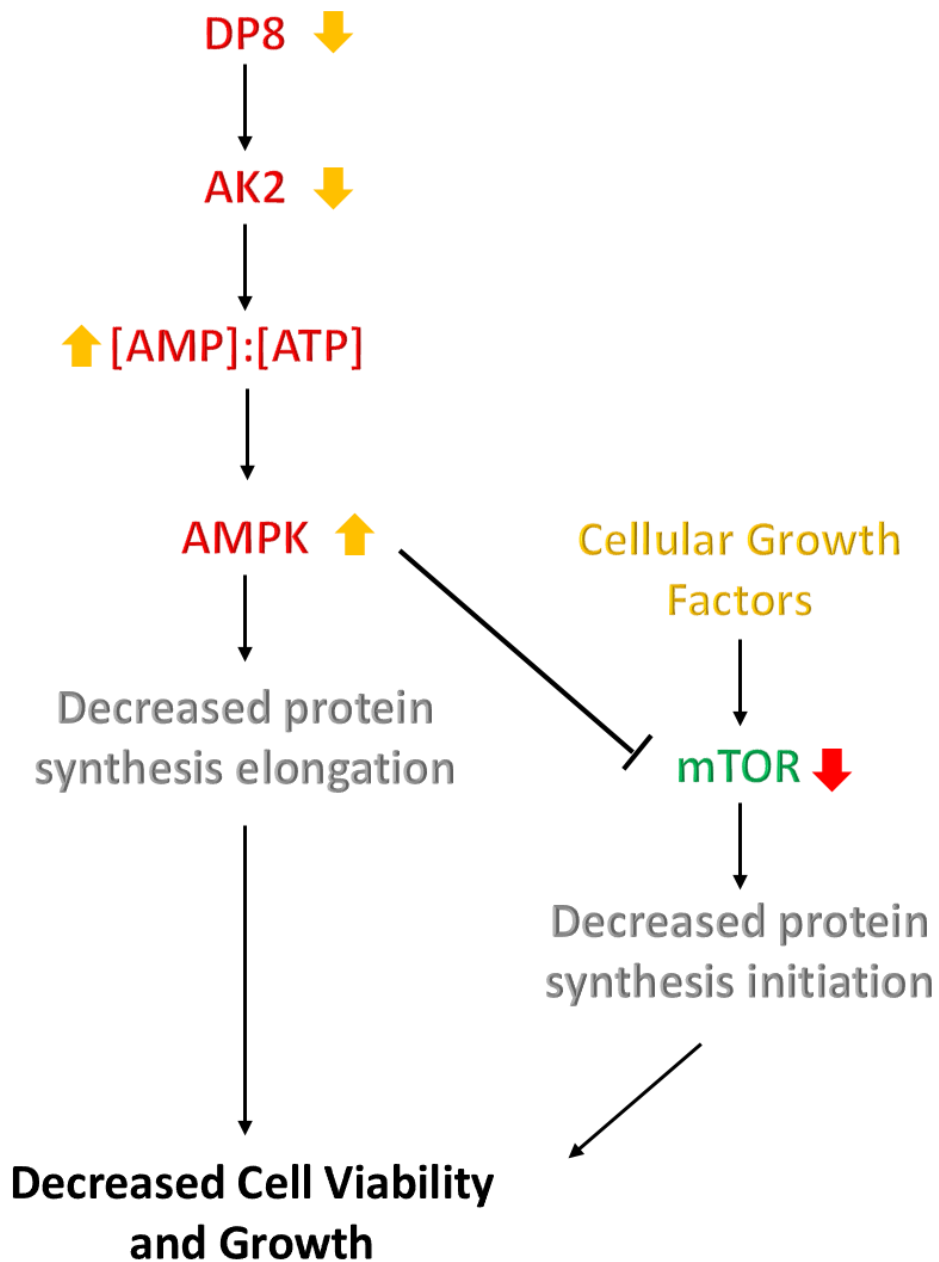


Figure 6.1. A model for the regulation of AK2 activity by DP8. Modified from (Luo et al., 2010; Hardie, 2011a).

mt DP9 overexpression may also abrogate AMPK activity through a mechanism independent of its proteolytic activity. With the advent of molecular and proteomics technologies, our concept of carcinogenesis has changed (Hanahan and Weinberg,

2011). A decade ago, cancer formation was characterised by six hallmarks: immortalised cell growth, increase in angiogenesis, decrease in programmed cell death, inhibition of tumour suppressors, activation of invasion and metastasis and auto activation of cell signalling (Hanahan and Weinberg, 2000). However, applying these concepts to investigate a new potential target for diagnostic and therapeutic biomarkers is very often not successful. The majority of ovarian cancer cells have mutations in the TRP53 gene and some efforts have been performed to increase this suppressor protein (Buller *et al.*, 2002; Vasey *et al.*, 2002; Ahmed *et al.*, 2010; Cancer Genome Atlas Research, 2011). Nevertheless, administration of wt TRP 53 failed to inhibit proliferation of ovarian cancer cells during a preclinical trial (Zeimet and Marth, 2003). Around 50% cases of ovarian cancers have mutations in either PI3K or RAS cell signalling (Cancer Genome Atlas Research, 2011). Hyperactivity in these cell signalling pathways leads to constitutive cell proliferation and mutations in upstream pathways (growth factor receptors) such as EGFR or downstream pathways for PI3K or RAS proteins have similarity effects in cell proliferation responses (Hernandez-Aya and Gonzalez-Angulo, 2011; Janku *et al.*, 2011). Some research centres have tried to develop potential inhibitors that down-regulate the PI3K or RAS cell signalling but the clinical trials are still in progress (Baines *et al.*, 2011; Kalachand *et al.*, 2011). Therefore, mt DP9 overexpression may activate Akt B protein that is involved in PI3K or RAS cell signalling, resulting in inhibition of AMPK activity and activation of mTOR expression (Luo *et al.*, 2010). In contrast, Yao *et al.* (2011) reported that wt DP9 overexpression in liver cancer cell lines induced apoptosis by inhibiting Akt B protein. Therefore, to confirm the effect of mt DP9 overexpression in cancer progression, migration and invasion assays and injection of these cancer cell lines into nude mice needs to be performed as Kajiyama

et al. (2002). Kajiyama *et al.* were able to show that DP4 overexpression has a tumour suppressor effect using animal models (2002). Thus, DP9 overexpression may play a differing tissue specific role to that observed for DP4.

There are four additional factors that are identified to date to be involved in cancer cell progression that are probably also found in ovarian cancer cells. These factors are genome instability and mutation, tumour-promoting inflammation, escape of immune destruction and reprogramming energy metabolism (Hanahan and Weinberg, 2011; Hanahan and Coussens, 2012). From our collected data, mt DP9 overexpression in SKOV3 cells shifted energy metabolism in the cells toward aerobic glycolysis and fatty acid oxidation. To support this finding, the activity of glucose transporter 4 (GLUT4) in this cell needs to be measured because intracellular glucose uptake requires GLUT4 (Calvo *et al.*, 2010; Nagendran *et al.*, 2013). Thus, DP9 might contribute to cancer cell progression and may be a potential drug target for ovarian cancer therapy.

6.5. Limitation of this study

Although our developed assays have some benefits, some disadvantages were also identified. The expression of DP8 and DP9 proteins are different between various cancer cell lines. It has been demonstrated that human leukaemia, ovarian cancer, colon cancer and breast cancer cell lines differently express DP8 and DP9 proteins. (Sulda, 2009; Wilson, 2011). The ovarian cancer cells used in this study have different expression of DP8, DP9 and AK2 expression. These cancer cell lines are immortalised and as such some important genes may no longer be expressed in these cells. Therefore, the cells may no longer behave like they would in the natural

environment and mutated genes might influence the experimental outcome (Zang *et al.*, 2012). Since the SKOV3 cells were stably transfected, prolonged DP8 and DP9 exposure might change the SKOV3 phenotype so that it is different from the original cancer cell line. So, the result of this study may not represent normal ovarian tumor cells but at least, this result provides valuable data for further studies. Transient transfection of DP8 and DP9 into low passage SKOV3 cells may minimize these unexpected effects.

The variability between immunoblots throughout this study was high, in future experiments all aspects that influence Western blotting experiment need to be more tightly controlled. Antibodies that can recognise aa sequences not only in the N terminus of DPs need to be utilised. From recent flow cytometry analysis, SKOV3 cells stably overexpressing wt DP8 had lost some EGFP expression toward the end of this project. When glucose was used as energy sources, CO₂ production in wt DP8 overexpressing SKOV3 cells was also lower than that in wt DP9 overexpressing SKOV3 cells (Figure 8.8 in Appendices). These cell lines need to be recloned in order to get reliable and reproducible data. The plausible mechanism for EGFP loss may be due to toxicity of DP8 to the cell host and inappropriate insertion of gene of interest in host genome (Taghizadeh and Sherley, 2008). As explained previously overexpression of DP8 may also lead to inhibition of cell proliferation, so there might be adaptive pressure on the transfected cells to discard the DP8 gene.

The AK2 enzyme activity results are not consistent in the SKOV3 cells between overexpression and silencing, alternative techniques need to be considered. During the study, the K_m value of human AK2 proteins in cancer cell lines was measured

using four different concentrations of AMP, higher than the AMP concentration used in an existing method in a parasite *Leishmania donovani* (Bergmeyer, 1974; Villa *et al.*, 2003). The AK assays in this thesis were performed in a 96 microplate reader instead of in a 1ml cuvette. Our AK enzyme activity data was compared to that from parasite recombinant AK2 (Villa *et al.*, 2003). The AMP concentrations used in this thesis were higher than the K_m value of parasite AK2 (Dzeja and Terzic, 2009). Therefore, in future AMP concentrations less than 0.07 mM should be used in order to gain better AK2 kinetic results. In the next study, different concentrations of ATP substrate should also be used to confirm that AK enzyme activity is specific to AK2, not overlapping with other AK family members such as AK1.

For improving the indirect measurement of AK enzyme activity, a more sensitive method is required to measure adenine nucleotide levels in subcellular compartments. For higher cell numbers, our modified HPLC method worked well but for smaller cell numbers, AMP concentrations were very low even undetectable in some cases. ATP and ADP concentrations in these samples also had high variability. So, it is essential to use a more sensitive and reliable assays to measure adenine nucleotide levels in SKOV3 cells. For example, bioluminescence detection may be used to measure ATP levels in cell culture (Taylor *et al.*, 1998). This technique is based on releasing ATP concentration from cell culture and then incubating with D-luciferin-H₂ and O₂ in the presence of the luciferase enzyme. This reaction will produce oxy-luciferin, AMP, CO₂, Ppi-Mg²⁺ and light. The light intensity released is correlated with the released ATP level from the cells (Taylor *et al.*, 1998). This basic technique is currently used to evaluate ATP levels and

ADP/ATP ratio in culture cells with many different drug treatments (Schafer *et al.*, 2009; Chandak *et al.*, 2010).

Regarding AMPK signalling, changes in total and phosphorylated AMPK expression were not consistently observed in response to reduced activity of AK2 in SKOV3 cells with DP8 siRNA silencing. It is very hard to interpret the data if just using results of immunoblot analysis. Verification of these results via silencing with a different siRNA for each gene and using more than one siRNAs for each gene at any one time may overcome the variability but these experiment will require much more time and funding. However when higher concentrations of siRNAs (100uM) were used in these experiments, silencing even using the negative control siRNA seemed to have impact on AK activity, suggesting cells were undergoing some stress that also affected adenine concentrations just from transfection independent of silencing the DP8, DP9 or AK2 genes. Some studies have demonstrated that phosphorylation of AMPK can be assessed by using a combination of Western blotting and AMPK enzyme activity. These assays might provide more accurate data (Zou *et al.*, 2004; Oakhill *et al.*, 2011; Wu *et al.*, 2012). However, they measured AMPK enzyme activity using a radioisotope method and it is not suitable to be performed in laboratory centres without radioisotope facilities. Recently, one study has developed a simple technique that uses a fluorescently labelled peptide (Reichling *et al.*, 2008) but this technique also require radiation to excite the europium chelate dye to induce 665 nm emission. Some studies have reported that AMP, LKBI (calcium-calmodulin dependent protein kinase kinase β) and Ca directly modulate the AMPK expression (Hardie, 2007; Oakhill *et al.*, 2010; Oakhill *et al.*, 2011) and metformin, an anti-diabetic drug, up regulates AMPK expression by inhibition of AMP deaminase,

which degrades AMP to become IMP (Ouyang *et al.*, 2011). To provide strong evidence whether AK2 regulates AMPK or not, more sensitive and reliable cell-based assays that cover measurement of AK2 and AMPK activities at the same time are required.

6.6. Conclusions and future directions

This study demonstrated that AK2 and calreticulin co-localized with DP8 and DP9 in the cytoplasm, which confirmed the *in vitro* cleavage study. Seven potential substrates of DP8 and DP9 were biochemically validated and most of these substrates are involved in regulating cellular metabolism and energy homeostasis. DP9 overexpression in SKOV3 cells may promote cancer progression through enzymatic and non-enzymatic activities. Meanwhile, DP8 silencing in ovarian cancer cells down regulates AK2 protein expression and AK enzyme activity.

In future, further research is required for unravelling the mechanism of cancer progression in DP9 overexpression. DP8 silencing may become a biological model to investigate the role of these proteins in cellular energy metabolism in normal and pathological conditions. DP8 protein may also become a molecular target for drug development in ovarian cancer.

7. REFERENCES

- Abbott, C.A., Baker, E., Sutherland, G.R. and McCaughan, G.W. (1994) Genomic Organization, Exact Localization, and Tissue Expression of the Human Cd26 (Dipeptidyl Peptidase-Iv) Gene. *Immunogenetics* **40**: 331-338.
- Abbott, C.A., McCaughan, G.W. and Gorrell, M.D. (1999) Two highly conserved glutamic acid residues in the predicted beta propeller domain of dipeptidyl peptidase IV are required for its enzyme activity. *FEBS Letters* **458**: 278-284.
- Abbott, C.A., Yu, D.M., Woollatt, E., Sutherland, G.R., McCaughan, G.W. and Gorrell, M.D. (2000) Cloning, expression and chromosomal localization of a novel human dipeptidyl peptidase (DPP) IV homolog, DPP8. *Eur J Biochem* **267**: 6140-6150.
- Abramoff, M.D., Magalhães, P.J. and Ram, S.J. (2004) Image processing with image J. *Biophotonics International* **11**: 36-42.
- Aertgeerts, K., Levin, I., Shi, L., Snell, G.P., Jennings, A., Prasad, G.S., Zhang, Y., Kraus, M.L., Salakian, S., Sridhar, V., Wijnands, R. and Tennant, M.G. (2005) Structural and kinetic analysis of the substrate specificity of human fibroblast activation protein alpha. *J Biol Chem* **280**: 19441-19444.
- Afshar, N., Black, B.E. and Paschal, B.M. (2005) Retrotranslocation of the chaperone calreticulin from the endoplasmic reticulum lumen to the cytosol. *Mol Cell Biol* **25**: 8844-8853.
- Agard, N.J. and Wells, J.A. (2009) Methods for the proteomic identification of protease substrates. *Curr Opin Chem Biol* **13**: 503-509.
- Ahmed, A.A., Etemadmoghadam, D., Temple, J., Lynch, A.G., Riad, M., Sharma, R., Stewart, C., Fereday, S., Caldas, C., Defazio, A., Bowtell, D. and Brenton, J.D. (2010) Driver mutations in TP53 are ubiquitous in high grade serous carcinoma of the ovary. *J Pathol* **221**: 49-56.
- Ahmed, N., Thompson, E.W. and Quinn, M.A. (2007) Epithelial-mesenchymal interconversions in normal ovarian surface epithelium and ovarian carcinomas: an exception to the norm. *J Cell Physiol* **213**: 581-588.
- Ahn, H.J., Kim, Y.S., Kim, J.U., Han, S.M., Shin, J.W. and Yang, H.O. (2004) Mechanism of taxol-induced apoptosis in human SKOV3 ovarian carcinoma cells. *J Cell Biochem* **91**: 1043-1052.
- Ajami, K., Abbott, C.A., McCaughan, G.W. and Gorrell, M.D. (2004) Dipeptidyl peptidase 9 has two forms, a broad tissue distribution, cytoplasmic localization and DPIV-like peptidase activity. *Biochim Biophys Acta* **1679**: 18-28.

Ajami, K., Abbott, C.A., Obradovic, M., Gysbers, V., Kahne, T., McCaughan, G.W. and Gorrell, M.D. (2003) Structural requirements for catalysis, expression, and dimerization in the CD26/DPIV gene family. *Biochemistry* **42**: 694-701.

Ajami, K., Pitman, M.R., Wilson, C.H., Park, J., Menz, R.I., Starr, A.E., Cox, J.H., Abbott, C.A., Overall, C.M. and Gorrell, M.D. (2008) Stromal cell-derived factors 1 alpha and 1 beta, inflammatory protein-10 and interferon-inducible T cell chemo-attractant are novel substrates of dipeptidyl peptidase 8. *FEBS Lett* **582**: 819-825.

Ajiki, T., Hirata, K., Okazaki, T., Horiuchi, H., Fujita, T., Habara, K., Kamigaki, T., Suzuki, Y. and Kuroda, Y. (2006) Thymidylate synthase and dihydropyrimidine dehydrogenase expressions in gallbladder cancer. *Anticancer Res* **26**: 1391-1396.

Amiri, M., Conserva, F., Panayiotou, C., Karlsson, A. and Solaroli, N. (2013) The human adenylate kinase 9 is a nucleoside mono- and diphosphate kinase. *Int J Biochem Cell Biol* **45**: 925-931.

Amori, R.E., Lau, J. and Pittas, A.G. (2007) Efficacy and safety of incretin therapy in type 2 diabetes - Systematic review and meta-analysis. *JAMA* **298**: 194-206.

An, S.G., Kumar, R., Sheets, E.D. and Benkovic, S.J. (2008) Reversible compartmentalization of de novo purine biosynthetic complexes in living cells. *Science* **320**: 103-106.

Angermayr, M., Strobel, G., Zollner, A., Korber, D. and Bandlow, W. (2001) Two parameters improve efficiency of mitochondrial uptake of adenylate kinase: decreased folding velocity and increased propensity of N-terminal alpha-helix formation. *FEBS Lett* **508**: 427-432.

Ansorge, S., Bank, U., Heimburg, A., Helmuth, M., Koch, G., Tadge, J., Lendeckel, U., Wolke, C., Neubert, K., Faust, J., Fuchs, P., Reinhold, D., Thielitz, A. and Tager, M. (2009) Recent insights into the role of dipeptidyl aminopeptidase IV (DPIV) and aminopeptidase N (APN) families in immune functions. *Clin Chem Lab Med* **47**: 253-261.

Atkinson, D.E. (1968) The energy charge of the adenylate pool as a regulatory parameter. Interaction with feedback modifiers. *Biochemistry* **7**: 4030-4034.

Auersperg, N., Wong, A.S., Choi, K.C., Kang, S.K. and Leung, P.C. (2001) Ovarian surface epithelium: biology, endocrinology, and pathology. *Endocr Rev* **22**: 255-288.

auf dem Keller, U. and Schilling, O. (2010) Proteomic techniques and activity-based probes for the system-wide study of proteolysis. *Biochimie* **92**: 1705-1714.

Baines, A.T., Xu, D. and Der, C.J. (2011) Inhibition of Ras for cancer treatment: the search continues. *Future Med Chem* **3**: 1787-808.

Bar, J., Weber, A., Hoffmann, T., Stork, J., Wermann, M., Wagner, L., Aust, S., Gerhartz, B. and Demuth, H.U. (2003) Characterisation of human dipeptidyl peptidase IV expressed in *Pichia pastoris*. A structural and mechanistic comparison

between the recombinant human and the purified porcine enzyme. *Biol Chem* **384**: 1553-1563.

Bast, R.C., Jr., Hennessy, B. and Mills, G.B. (2009) The biology of ovarian cancer: new opportunities for translation. *Nat Rev Cancer* **9**: 415-28.

Bastians, H. and Ponstingl, H. (1996) The novel human protein serine/threonine phosphatase 6 is a functional homologue of budding yeast Sit4p and fission yeast ppe1, which are involved in cell cycle regulation. *J Cell Sci* **109**: 2865-2874.

Baum, P., Muller, D., Ruger, R. and Kontermann, R.E. (2007) Single-chain Fv immunoliposomes for the targeting of fibroblast activation protein-expressing tumor stromal cells. *J Drug Target* **15**: 399-406.

Ben-Bassat, A., Bauer, K., Chang, S.Y., Myambo, K., Boosman, A. and Chang, S. (1987) Processing of the initiation methionine from proteins: properties of the Escherichia coli methionine aminopeptidase and its gene structure. *J Bacteriol* **169**: 751-757.

Bergmeyer, H.U. (1974) *Methods of enzymatic analysis*, Verlag Chemie Weinheim Academic Press, Inc., New York.

Bhowmick, N.A., Neilson, E.G. and Moses, H.L. (2004) Stromal fibroblasts in cancer initiation and progression. *Nature* **432**: 332-337.

Bjelke, J.R., Christensen, J., Nielsen, P.F., Branner, S., Kanstrup, A.B., Wagtmann, N. and Rasmussen, H.B. (2006) Dipeptidyl peptidases 8 and 9: specificity and molecular characterization compared with dipeptidyl peptidase IV. *Biochem J* **396**: 391-399.

Bradbury, D.A., Simmons, T.D., Slater, K.J. and Crouch, S.P.M. (2000) Measurement of the ADP:ATP ratio in human leukaemic cell lines can be used as an indicator of cell viability, necrosis and apoptosis. *J Immunol Methods* **240**: 79-92.

Bühling, F., Junker, U., Reinhold, D., Neubert, K., Jager, L. and Ansorge, S. (1995) Functional-Role of CD26 on Human B-Lymphocytes. *Immunol Lett* **45**: 47-51.

Bühling, F., Kunz, D., Reinhold, D., Ulmer, A.J., Ernst, M., Flad, H.D. and Ansorge, S. (1994) Expression and Functional-Role of Dipeptidyl Peptidase-Iv (Cd26) on Human Natural-Killer-Cells. *Nat Immun* **13**: 270-279.

Buller, R.E., Shahin, M.S., Horowitz, J.A., Runnebaum, I.B., Mahavni, V., Petrauskas, S., Kreienberg, R., Karlan, B., Slamon, D. and Pegram, M. (2002) Long term follow-up of patients with recurrent ovarian cancer after Ad p53 gene replacement with SCH 58500. *Cancer Gene Ther* **9**: 567-572.

Burkart, A., Shi, X., Chouinard, M. and Corvera, S. (2011) Adenylate kinase 2 links mitochondrial energy metabolism to the induction of the unfolded protein response. *J Biol Chem* **286**: 4081-4089.

Busso, N., Wagtmann, N., Herling, C., Chobaz-Peclat, V., Bischof-Delaloye, A., So, A. and Grouzmann, E. (2005) Circulating CD26 is negatively associated with inflammation in human and experimental arthritis. *Am J Pathol* **166**: 433-442.

Calvo, M.B., Figueroa, A., Pulido, E.G., Campelo, R.G. and Aparicio, L.A. (2010) Potential Role of Sugar Transporters in Cancer and Their Relationship with Anticancer Therapy. *Int J Endocrinol*.

Cancer Genome Atlas Research, N. (2011) Integrated genomic analyses of ovarian carcinoma. *Nature* **474**: 609-615.

Carling, D., Mayer, F.V., Sanders, M.J. and Gamblin, S.J. (2011) AMP-activated protein kinase: nature's energy sensor. *Nat Chem Biol* **7**: 512-518.

Carpio, M.A., Lopez Sambrooks, C., Durand, E.S. and Hallak, M.E. (2010) The arginylation-dependent association of calreticulin with stress granules is regulated by calcium. *Biochem J* **429**: 63-72.

Chaiyarit, S. and Thongboonkerd, V. (2009) Comparative analyses of cell disruption methods for mitochondrial isolation in high-throughput proteomics study. *Anal Biochem* **394**: 249-258.

Chandak, P.G., Radovic, B., Aflaki, E., Kolb, D., Buchebner, M., Frohlich, E., Magnes, C., Sinner, F., Haemmerle, G., Zechner, R., Tabas, I., Levak-Frank, S. and Kratky, D. (2010) Efficient phagocytosis requires triacylglycerol hydrolysis by adipose triglyceride lipase. *J Biol Chem* **285**: 20192-20201.

Chen, R.P., Liu, C.Y., Shao, H.L., Zheng, W.W., Wang, J.X. and Zhao, X.F. (2012) Adenylate kinase 2 (AK2) promotes cell proliferation in insect development. *BMC Mol Biol* **13**: 31.

Cheng, J.D., Valianou, M., Canutescu, A.A., Jaffe, E.K., Lee, H.O., Wang, H., Lai, J.H., Bachovchin, W.W. and Weiner, L.M. (2005) Abrogation of fibroblast activation protein enzymatic activity attenuates tumor growth. *Mol Cancer Ther* **4**: 351-360.

Cheong, C.G., Wolan, D.W., Greasley, S.E., Horton, P.A., Beardsley, G.P. and Wilson, I.A. (2004) Crystal structures of human bifunctional enzyme aminoimidazole-4-carboxamide ribonucleotide transformylase/IMP cyclohydrolase in complex with potent sulfonyl-containing antifolates. *J Biol Chem* **279**: 18034-18045.

Cheung, L.W., Leung, P.C. and Wong, A.S. (2010) Cadherin switching and activation of p120 catenin signaling are mediators of gonadotropin-releasing hormone to promote tumor cell migration and invasion in ovarian cancer. *Oncogene* **29**: 2427-2440.

Chewawiwat, N., Yano, M., Terada, K., Hoogenraad, N.J. and Mori, M. (1999) Characterization of the novel mitochondrial protein import component, Tom34, in mammalian cells. *J Biochem* **125**: 721-727.

Choi, J.H., Wong, A.S., Huang, H.F. and Leung, P.C. (2007) Gonadotropins and ovarian cancer. *Endocr Rev* **28**: 440-461.

Chowdhury, S., Chen, Y.Q., Yao, T.W., Ajami, K., Wang, X.M., Popov, Y., Schuppan, D., Bertolino, P., McCaughan, G.W., Yu, D.M.T. and Gorrell, M.D. (2013) Regulation of dipeptidyl peptidase 8 and 9 expression in activated lymphocytes and injured liver. *World J Gastroenterol* **19**: 2883-2893.

Comelli, M., Di Pancrazio, F. and Mavelli, I. (2003) Apoptosis is induced by decline of mitochondrial ATP synthesis in erythroleukemia cells. *Free Radic Biol Med* **34**: 1190-1199.

David, F., Bernard, A.M., Pierres, M. and Marguet, D. (1993) Identification of serine 624, aspartic acid 702, and histidine 734 as the catalytic triad residues of mouse dipeptidyl-peptidase IV (CD26). A member of a novel family of nonclassical serine hydrolases. *J Biol Chem* **268**: 17247-17252.

de Graaf, A.O., Meijerink, J.P.P., van den Heuvel, L.P., DeAbreu, R.A., de Witte, T., Jansen, J.H. and Smeitink, J.A.M. (2002) Bcl-2 protects against apoptosis induced by antimycin A and bongkreikic acid without restoring cellular ATP levels. *Biochim Biophys Acta* **1554**: 57-65.

De Meester, I., Korom, S., Van Damme, J. and Scharpe, S. (1999) CD26, let it cut or cut it down. *Immunol Today* **20**: 367-375.

Deacon, C.F., Nauck, M.A., Meier, J., Hucking, K. and Holst, J.J. (2000) Degradation of endogenous and exogenous gastric inhibitory polypeptide in healthy and in type 2 diabetic subjects as revealed using a new assay for the intact peptide. *J Clin Endocrinol Metab* **85**: 3575-3581.

Deacon, C.F., Nauck, M.A., Toft-Nielsen, M., Pridal, L., Willms, B. and Holst, J.J. (1995) Both subcutaneously and intravenously administered glucagon-like peptide I are rapidly degraded from the NH₂-terminus in type II diabetic patients and in healthy subjects. *Diabetes* **44**: 1126-1131.

Decca, M.B., Carpio, M.A., Bosc, C., Galiano, M.R., Job, D., Andrieux, A. and Hallak, M.E. (2007) Post-translational arginylation of calreticulin: a new isospecies of calreticulin component of stress granules. *J Biol Chem* **282**: 8237-8245.

DeFuria, J., Belkina, A.C., Jagannathan-Bogdan, M., Snyder-Cappione, J., Carr, J.D., Nersesova, Y.R., Markham, D., Strissel, K.J., Watkins, A.A., Zhu, M., Allen, J., Bouchard, J., Toraldo, G., Jasuja, R., Obin, M.S., McDonnell, M.E., Apovian, C., Denis, G.V. and Nikolajczyk, B.S. (2013) B cells promote inflammation in obesity and type 2 diabetes through regulation of T-cell function and an inflammatory cytokine profile. *Proc Natl Acad Sci U S A* **110**: 5133-5138.

Denning, G.M., Leidal, K.G., Holst, V.A., Iyer, S.S., Pearson, D.W., Clark, J.R., Nauseef, W.M. and Clark, R.A. (1997) Calreticulin biosynthesis and processing in

human myeloid cells: demonstration of signal peptide cleavage and N-glycosylation. *Blood* **90**: 372-381.

Deussing, J., von Olshausen, I. and Peters, C. (2000) Murine and human cathepsin Z: cDNA-cloning, characterization of the genes and chromosomal localization. *Biochim Biophys Acta* **1491**: 93-106.

Dohi, O., Ohtani, H., Hatori, M., Sato, E., Hosaka, M., Nagura, H., Itoi, E. and Kokubun, S. (2009) Histogenesis-specific expression of fibroblast activation protein and dipeptidylpeptidase-IV in human bone and soft tissue tumours. *Histopathology* **55**: 432-440.

Donath, M.Y. and Shoelson, S.E. (2011) Type 2 diabetes as an inflammatory disease. *Nat Rev Immunol* **11**: 98-107.

Doucet, A. and Overall, C.M. (2008) Protease proteomics: revealing protease in vivo functions using systems biology approaches. *Mol Aspects Med* **29**: 339-358.

Drucker, D.J. and Nauck, M.A. (2006) The incretin system: glucagon-like peptide-1 receptor agonists and dipeptidyl peptidase-4 inhibitors in type 2 diabetes. *Lancet* **368**: 1696-1705.

Dubeau, L. (2008) The cell of origin of ovarian epithelial tumours. *Lancet Oncol* **9**: 1191-1197.

Dubois, V., Lambeir, A.M., Van der Veken, P., Augustyns, K., Creemers, J., Chen, X., Scharpe, S. and De Meester, I. (2008) Purification and characterization of dipeptidyl peptidase IV-like enzymes from bovine testes. *Front Biosci* **13**: 3558-3568.

Dubois, V., Lambeir, A.M., Vandamme, S., Matheeussen, V., Guisez, Y., Scharpe, S. and De Meester, I. (2010) Dipeptidyl peptidase 9 (DPP9) from bovine testes: Identification and characterization as the short form by mass spectrometry. *Biochim Biophys Acta* **1804**: 781-788.

Dubois, V., Van Ginneken, C., De Cock, H., Lambeir, A.M., Van der Veken, P., Augustyns, K., Chen, X., Scharpe, S. and De Meester, I. (2009) Enzyme activity and immunohistochemical localization of dipeptidyl peptidase 8 and 9 in male reproductive tissues. *J Histochem Cytochem* **57**: 531-541.

Durinx, C., Lambeir, A.M., Bosmans, E., Falmagne, J.B., Berghmans, R., Haemers, A., Scharpe, S. and De Meester, I. (2000) Molecular characterization of dipeptidyl peptidase activity in serum - Soluble CD26/dipeptidyl peptidase IV is responsible for the release of X-Pro dipeptides. *Eur J Biochem* **267**: 5608-5613.

Dzeja, P. and Terzic, A. (2009) Adenylate kinase and AMP signaling networks: Metabolic monitoring, signal communication and body energy sensing. *Int J Mol Sci* **10**: 1729-1772.

Dzeja, P.P. and Terzic, A. (2003) Phosphotransfer networks and cellular energetics. *J Exp Biol* **206**: 2039-2047.

Elbendary, A., Berchuck, A., Davis, P., Havrilesky, L., Bast, R.C., Iglehart, J.D. and Marks, J.R. (1994) Transforming Growth-Factor-Beta-1 Can Induce Cip1/Waf1 Expression Independent of the P53 Pathway in Ovarian-Cancer Cells. *Cell Growth Differ* **5**: 1301-1307.

Endo, T. and Kohda, D. (2002) Functions of outer membrane receptors in mitochondrial protein import. *Biochim Biophys Acta* **1592**: 3-14.

Engel, M., Hoffmann, T., Wagner, L., Wermann, M., Heiser, U., Kiefersauer, R., Huber, R., Bode, W., Demuth, H.U. and Brandstetter, H. (2003) The crystal structure of dipeptidyl peptidase IV(CD26) reveals its functional regulation and enzymatic mechanism. *Proc Natl Acad Sci U S A* **100**: 5063-5068.

Faubert, B., Boily, G., Izreig, S., Griss, T., Samborska, B., Dong, Z.F., Dupuy, F., Chambers, C., Fuerth, B.J., Viollet, B., Mamer, O.A., Avizonis, D., DeBerardinis, R.J., Siegel, P.M. and Jones, R.G. (2013) AMPK Is a Negative Regulator of the Warburg Effect and Suppresses Tumor Growth In Vivo. *Cell Metab* **17**: 113-124.

Filali, M., Li, S., Kim, H.W., Wadzinski, B. and Kamoun, M. (1999) Identification of a type 6 protein ser/thr phosphatase regulated by interleukin-2 stimulation. *J Cell Biochem* **73**: 153-163.

Firestein, G.S. (2003) Evolving concepts of rheumatoid arthritis. *Nature* **423**: 356-361.

Fleischer, B. (1987) A novel pathway of human T cell activation via a 103 kD T cell activation antigen. *J Immunol* **138**: 1346-1350.

Fliegel, L., Burns, K., MacLennan, D.H., Reithmeier, R.A. and Michalak, M. (1989) Molecular cloning of the high affinity calcium-binding protein (calreticulin) of skeletal muscle sarcoplasmic reticulum. *J Biol Chem* **264**: 21522-21528.

Fox, D.A., Hussey, R.E., Fitzgerald, K.A., Acuto, O., Poole, C., Palley, L., Daley, J.F., Schlossman, S.F. and Reinherz, E.L. (1984) Ta1, a Novel 105-Kd Human T-Cell Activation Antigen Defined by a Monoclonal-Antibody. *J Immunol* **133**: 1250-1256.

Frank, R., Trosin, M., Tomasselli, A.G., Noda, L., Krauth-Siegel, R.L. and Schirmer, R.H. (1986) Mitochondrial adenylate kinase (AK2) from bovine heart. The complete primary structure. *Eur J Biochem* **154**: 205-211.

Fujisawa, K., Murakami, R., Horiguchi, T. and Noma, T. (2009) Adenylate kinase isozyme 2 is essential for growth and development of *Drosophila melanogaster*. *Comp Biochem Phys B* **153**: 29-38.

Fukui, Y., Oka, T., Nagayama, S., Danenberg, P.V., Danenberg, K.D. and Fukushima, M. (2008) Thymidylate synthase, dihydropyrimidine dehydrogenase,

orotate phosphoribosyltransferase mRNA and protein expression levels in solid tumors in large scale population analysis. *Int J Mol Med* **22**: 709-716.

Gabriel, K., Milenkovic, D., Chacinska, A., Muller, J., Guiard, B., Pfanner, N. and Meisinger, C. (2007) Novel mitochondrial intermembrane space proteins as substrates of the MIA import pathway. *J Mol Biol* **365**: 612-620.

Gao, B., Adhikari, R., Howarth, M., Nakamura, K., Gold, M.C., Hill, A.B., Knee, R., Michalak, M. and Elliott, T. (2002) Assembly and antigen-presenting function of MHC class I molecules in cells lacking the ER chaperone calreticulin. *Immunity* **16**: 99-109.

Garin-Chesa, P., Old, L.J. and Rettig, W.J. (1990) Cell surface glycoprotein of reactive stromal fibroblasts as a potential antibody target in human epithelial cancers. *Proc Natl Acad Sci U S A* **87**: 7235-7239.

Ge, Y., Zhan, F.G., Barlogie, B., Epstein, J., Shaughnessy, J. and Yaccoby, S. (2006) Fibroblast activation protein (FAP) is upregulated in myelomatous bone and supports myeloma cell survival. *Brit J Haematol* **133**: 83-92.

Geiss-Friedlander, R., Parmentier, N., Moller, U., Urlaub, H., Van den Eynde, B.J. and Melchior, F. (2009) The cytoplasmic peptidase DPP9 is rate-limiting for degradation of proline-containing peptides. *J Biol Chem* **284**: 27211-27219.

Gelebart, P., Opas, M. and Michalak, M. (2005) Calreticulin, a Ca²⁺-binding chaperone of the endoplasmic reticulum. *Int J Biochem Cell Biol* **37**: 260-266.

Gerli, R., Muscat, C., Bertotto, A., Bistoni, O., Agea, E., Tognellini, R., Fiorucci, G., Cesarotti, M. and Bombardieri, S. (1996) CD26 surface molecule involvement in T cell activation and lymphokine synthesis in rheumatoid and other inflammatory synovitis. *Clin Immunol Immunopathol* **80**: 31-37.

Gevaert, K., Goethals, M., Martens, L., Van Damme, J., Staes, A., Thomas, G.R. and Vandekerckhove, J. (2003) Exploring proteomes and analyzing protein processing by mass spectrometric identification of sorted N-terminal peptides. *Nat Biotechnol* **21**: 566-569.

Gherzi, G., Dong, H., Goldstein, L.A., Yeh, Y., Hakkinen, L., Larjava, H.S. and Chen, W.T. (2002) Regulation of fibroblast migration on collagenous matrix by a cell surface peptidase complex. *J Biol Chem* **277**: 29231-29241.

Gliddon, D.R. and Howard, C.J. (2002) CD26 is expressed on a restricted subpopulation of dendritic cells in vivo. *Eur J Immunol* **32**: 1472-1481.

Gorrell, M.D. (2005) Dipeptidyl peptidase IV and related enzymes in cell biology and liver disorders. *Clin Sci (Lond)* **108**: 277-292.

Gorrell, M.D., Wickson, J. and McCaughan, G.W. (1991) Expression of the rat CD26 antigen (dipeptidyl peptidase IV) on subpopulations of rat lymphocytes. *Cell Immunol* **134**: 205-215.

- Guertin, D.A. and Sabatini, D.M. (2007) Defining the role of mTOR in cancer. *Cancer Cell* **12**: 9-22.
- Hanahan, D. and Coussens, L.M. (2012) Accessories to the Crime: Functions of Cells Recruited to the Tumor Microenvironment. *Cancer Cell* **21**: 309-322.
- Hanahan, D. and Weinberg, R.A. (2000) The hallmarks of cancer. *Cell* **100**: 57-70.
- Hanahan, D. and Weinberg, R.A. (2011) Hallmarks of cancer: the next generation. *Cell* **144**: 646-674.
- Hardie, D.G. (2007) AMP-activated/SNF1 protein kinases: conserved guardians of cellular energy. *Nat Rev Mol Cell Biol* **8**: 774-785.
- Hardie, D.G. (2011a) Adenosine Monophosphate-Activated Protein Kinase: A Central Regulator of Metabolism with Roles in Diabetes, Cancer, and Viral Infection. *Cold Spring Harb Symp Quant Biol* **76**: 155-164.
- Hardie, D.G. (2011b) AMP-activated protein kinase: an energy sensor that regulates all aspects of cell function. *Genes Dev* **25**: 1895-1908.
- Heggie, G.D., Sommadossi, J.P., Cross, D.S., Huster, W.J. and Diasio, R.B. (1987) Clinical pharmacokinetics of 5-fluorouracil and its metabolites in plasma, urine, and bile. *Cancer Res* **47**: 2203-2206.
- Henry, L.R., Lee, H.O., Lee, J.S., Klein-Szanto, A., Watts, P., Ross, E.A., Chen, W.T. and Cheng, J.D. (2007) Clinical implications of fibroblast activation protein in patients with colon cancer. *Clin Cancer Res* **13**: 1736-1741.
- Hernandez-Aya, L.F. and Gonzalez-Angulo, A.M. (2011) Targeting the phosphatidylinositol 3-kinase signaling pathway in breast cancer. *Oncologist* **16**: 404-414.
- Hiramatsu, H., Kyono, K., Higashiyama, Y., Fukushima, C., Shima, H., Sugiyama, S., Inaka, K., Yamamoto, A. and Shimizu, R. (2003) The structure and function of human dipeptidyl peptidase IV, possessing a unique eight-bladed beta-propeller fold. *Biochem Biophys Res Commun* **302**: 849-854.
- Holst, J.J. and Gromada, J. (2004) Role of incretin hormones in the regulation of insulin secretion in diabetic and nondiabetic humans. *Am J Physiol Endocrinol Metab* **287**: E199-206.
- Hopsu-Havu, V.K. and Glenner, G.G. (1966) A new dipeptide naphthylamidase hydrolyzing glycyl-prolyl-beta-naphthylamide. *Histochemie* **7**: 197-201.
- Huang, Y., Wang, S. and Kelly, T. (2004) Seprase promotes rapid tumor growth and increased microvessel density in a mouse model of human breast cancer. *Cancer Res* **64**: 2712-2716.

Huber, M.A., Kraut, N., Park, J.E., Schubert, R.D., Rettig, W.J., Peter, R.U. and Garin-Chesa, P. (2003) Fibroblast activation protein: Differential expression and serine protease activity in reactive stromal fibroblasts of melanocytic skin tumors. *J Invest Dermatol* **120**: 182-188.

Huesgen, P.F. and Overall, C.M. (2012) N- and C-terminal degradomics: new approaches to reveal biological roles for plant proteases from substrate identification. *Physiol Plant* **145**: 5-17.

Hum, D.W., Bell, A.W., Rozen, R. and MacKenzie, R.E. (1988) Primary structure of a human trifunctional enzyme. Isolation of a cDNA encoding methylenetetrahydrofolate dehydrogenase-methenyltetrahydrofolate cyclohydrolase-formyltetrahydrofolate synthetase. *J Biol Chem* **263**: 15946-15950.

Iwaki-Egawa, S., Watanabe, Y. and Fujimoto, Y. (1993) N-terminal amino acid sequence of the 60-kDa protein of rat kidney dipeptidyl peptidase IV. *Biol Chem Hoppe Seyler* **374**: 973-975.

Janku, F., Lee, J.J., Tsimberidou, A.M., Hong, D.S., Naing, A., Falchook, G.S., Fu, S., Luthra, R., Garrido-Laguna, I. and Kurzrock, R. (2011) PIK3CA mutations frequently coexist with RAS and BRAF mutations in patients with advanced cancers. *PLoS One* **6**: e22769.

Jemal, A., Siegel, R., Ward, E., Hao, Y., Xu, J., Murray, T. and Thun, M.J. (2008) Cancer statistics, 2008. *CA Cancer J Clin* **58**: 71-96.

Johnson, M.R., Wang, K., Tillmanns, S., Albin, N. and Diasio, R.B. (1997) Structural organization of the human dihydropyrimidine dehydrogenase gene. *Cancer Res* **57**: 1660-1663.

Johnson, S., Michalak, M., Opas, M. and Eggleton, P. (2001) The ins and outs of calreticulin: from the ER lumen to the extracellular space. *Trends Cell Biol* **11**: 122-129.

Kajiyama, H., Kikkawa, F., Khin, E., Shibata, K., Ino, K. and Mizutani, S. (2003) Dipeptidyl peptidase IV overexpression induces up-regulation of E-cadherin and tissue inhibitors of matrix metalloproteinases, resulting in decreased invasive potential in ovarian carcinoma cells. *Cancer Res* **63**: 2278-2283.

Kajiyama, H., Kikkawa, F., Suzuki, T., Shibata, K., Ino, K. and Mizutani, S. (2002) Prolonged survival and decreased invasive activity attributable to dipeptidyl peptidase IV overexpression in ovarian carcinoma. *Cancer Res* **62**: 2753-2757.

Kalachand, R., Hennessy, B.T. and Markman, M. (2011) Molecular targeted therapy in ovarian cancer: what is on the horizon? *Drugs* **71**: 947-967.

Kelly, T. (2005) Fibroblast activation protein-alpha and dipeptidyl peptidase IV (CD26): cell-surface proteases that activate cell signaling and are potential targets for cancer therapy. *Drug Resist Update* **8**: 51-58.

Kennedy, A., Dong, H., Chen, D.H. and Chen, W.T. (2009) Elevation of seprase expression and promotion of an invasive phenotype by collagenous matrices in ovarian tumor cells. *Int J Cancer* **124**: 27-35.

Khoo, J.C. and Russell, P.J. (1972) Isoenzymes of Adenylate Kinase in Human Tissue. *Biochim Biophys Acta* **268**: 98-101.

Kieffer, T.J., McIntosh, C.H. and Pederson, R.A. (1995) Degradation of glucose-dependent insulinotropic polypeptide and truncated glucagon-like peptide 1 in vitro and in vivo by dipeptidyl peptidase IV. *Endocrinology* **136**: 3585-3596.

Kim, J.-H., Skates, S.J., Uede, T., Wong, K.-K., Schorge, J.O., Feltmate, C.M., Berkowitz, R.S., Cramer, D.W. and Mok, S.C. (2002) Osteopontin as a potential diagnostic biomarker for ovarian cancer. *JAMA* **287**: 1671-1679.

Kim, S.-J., Nian, C., Doudet, D.J. and McIntosh, C.H. (2009) Dipeptidyl peptidase IV inhibition with MK0431 improves islet graft survival in diabetic NOD mice partially via T-cell modulation. *Diabetes* **58**: 641-651.

Kishi, F., Tanizawa, Y. and Nakazawa, A. (1987) Isolation and characterization of two types of cDNA for mitochondrial adenylate kinase and their expression in *Escherichia coli*. *J Biol Chem* **262**: 11785-11789.

Kleifeld, O., Doucet, A., auf dem Keller, U., Prudova, A., Schilling, O., Kainthan, R.K., Starr, A.E., Foster, L.J., Kizhakkedathu, J.N. and Overall, C.M. (2010) Isotopic labeling of terminal amines in complex samples identifies protein N-termini and protease cleavage products. *Nat Biotechnol* **28**: 281-288.

Kleifeld, O., Doucet, A., Prudova, A., Keller, U.A.D., Gioia, M., Kizhakkedathu, J.N. and Overall, C.M. (2011) Identifying and quantifying proteolytic events and the natural N terminome by terminal amine isotopic labeling of substrates. *Nat Protoc* **6**: 1578-1611.

Klemann, C., Schade, J., Pabst, R., Leitner, S., Stiller, J., von Horsten, S. and Stephan, M. (2009) CD26/dipeptidyl peptidase 4-deficiency alters thymic emigration patterns and leukocyte subsets in F344-rats age-dependently. *Clin Exp Immunol* **155**: 357-365.

Klingler, D. and Hardt, M. (2012) Profiling protease activities by dynamic proteomics workflows. *Proteomics* **12**: 587-596.

Kloft, C., Graefe, E.U., Tanswell, P., Scott, A.M., Hofheinz, R., Amelsberg, A. and Karlsson, M.O. (2004) Population pharmacokinetics of sibrotuzumab, a novel therapeutic monoclonal antibody, in cancer patients. *Invest New Drugs* **22**: 39-52.

Koller-Eichhorn, R., Marquardt, T., Gail, R., Wittinghofer, A., Kostrewa, D., Kutay, U. and Kambach, C. (2007) Human OLA1 defines an ATPase subfamily in the Obg family of GTP-binding proteins. *J Biol Chem* **282**: 19928-19937.

Krause, K.H. and Michalak, M. (1997) Calreticulin. *Cell* **88**: 439-443.

Krueger, S., Kalinski, T., Hundertmark, T., Wex, T., Küster, D., Peitz, U., Ebert, M., Nögler, D.K., Kellner, U., Malfertheiner, P., Naumann, M., Röcken, C. and Roessner, A. (2005) Up-regulation of cathepsin X in *Helicobacter pylori* gastritis and gastric cancer. *J Pathol* **207**: 32-42.

Lagresle-Peyrou, C., Six, E.M., Picard, C., Rieux-Laucat, F., Michel, V., Ditadi, A., Demerens-de Chappedelaine, C., Morillon, E., Valensi, F., Simon-Stoos, K.L., Mullikin, J.C., Noroski, L.M., Besse, C., Wulffraat, N.M., Ferster, A., Abecasis, M.M., Calvo, F., Petit, C., Candotti, F., Abel, L., Fischer, A. and Cavazzana-Calvo, M. (2009) Human adenylate kinase 2 deficiency causes a profound haematopoietic defect associated with sensorineural deafness. *Nat Genet* **41**: 106-111.

Lambeir, A.-M., Durinx, C., Scharpe, S. and De Meester, I. (2003a) Dipeptidyl-peptidase IV from bench to bedside: an update on structural properties, functions, and clinical aspects of the enzyme DPP IV. *Crit Rev Clin Lab Sci* **40**: 209-294.

Lambeir, A.M., Rea, D., Fulop, V., Kumagai, Y., Augustyns, K., De Meester, I., Haemers, A. and Scharpe, S. (2003b) Exploration of the active site of dipeptidyl peptidase IV from *Porphyromonas gingivalis* - Comparison with the human enzyme. *Dipeptidyl Aminopeptidases in Health and Disease* **524**: 29-35.

Langdon, S.P., Lawrie, S.S., Hay, F.G., Hawkes, M.M., McDonald, A., Hayward, I.P., Schol, D.J., Hilgers, J., Leonard, R.C. and Smyth, J.F. (1988) Characterization and properties of nine human ovarian adenocarcinoma cell lines. *Cancer Res* **48**: 6166-6172.

Lange, P.F. and Overall, C.M. (2013) Protein TAILS: when termini tell tales of proteolysis and function. *Curr Opin Chem Biol* **17**: 73-82.

Lankas, G.R., Leiting, B., Roy, R.S., Eiermann, G.J., Beconi, M.G., Biftu, T., Chan, C.C., Edmondson, S., Feeney, W.P., He, H., Ippolito, D.E., Kim, D., Lyons, K.A., Ok, H.O., Patel, R.A., Petrov, A.N., Pryor, K.A., Qian, X., Reigle, L., Woods, A., Wu, J.K., Zaller, D., Zhang, X., Zhu, L., Weber, A.E. and Thornberry, N.A. (2005) Dipeptidyl peptidase IV inhibition for the treatment of type 2 diabetes: potential importance of selectivity over dipeptidyl peptidases 8 and 9. *Diabetes* **54**: 2988-2994.

LeBeau, A.M., Brennen, W.N., Aggarwal, S. and Denmeade, S.R. (2009) Targeting the cancer stroma with a fibroblast activation protein-activated promelittin protoxin. *Mol Cancer Ther* **8**: 1378-1386.

Lee, H.J., Chen, Y.S., Chou, C.Y., Chien, C.H., Lin, C.H., Chang, G.G. and Chen, X. (2006a) Investigation of the dimer interface and substrate specificity of prolyl dipeptidase DPP8. *J Biol Chem* **281**: 38653-38662.

Lee, K.N., Jackson, K.W., Christiansen, V.J., Chung, K.H. and McKee, P.A. (2004) A novel plasma proteinase potentiates alpha2-antiplasmin inhibition of fibrin digestion. *Blood* **103**: 3783-3788.

- Lee, K.N., Jackson, K.W., Christiansen, V.J., Lee, C.S., Chun, J.G. and McKee, P.A. (2006b) Antiplasmin-cleaving enzyme is a soluble form of fibroblast activation protein. *Blood* **107**: 1397-1404.
- Lee, Y., Kim, J.W., Lee, I.A., Kang, H.B., Choe, Y.K., Lee, H.G., Lim, J.S., Kim, H.J., Park, C. and Choe, I.S. (1996) Cloning and characterization of cDNA for human adenylate kinase 2A. *Biochem Mol Biol Int* **39**: 833-842.
- Lee, Y., Kim, J.W., Lee, S.M., Kim, H.J., Lee, K.S., Park, C. and Choe, I.S. (1998) Cloning and expression of human adenylate kinase 2 isozymes: differential expression of adenylate kinase 1 and 2 in human muscle tissues. *J Biochem* **123**: 47-54.
- Levy, M.T., McCaughan, G.W., Abbott, C.A., Park, J.E., Cunningham, A.M., Muller, E., Rettig, W.J. and Gorrell, M.D. (1999) Fibroblast activation protein: a cell surface dipeptidyl peptidase and gelatinase expressed by stellate cells at the tissue remodelling interface in human cirrhosis. *Hepatology* **29**: 1768-1778.
- Li, P., Nijhawan, D., Budihardjo, I., Srinivasula, S.M., Ahmad, M., Alnemri, E.S. and Wang, X. (1997) Cytochrome c and dATP-Dependent Formation of Apaf-1/Caspase-9 Complex Initiates an Apoptotic Protease Cascade. *Cell* **91**: 479-489.
- Li, Y., Qin, J.G., Abbott, C.A., Li, X. and Benkendorff, K. (2007) Synergistic impacts of heat shock and spawning on the physiology and immune health of *Crassostrea gigas*: an explanation for summer mortality in Pacific oysters. *Am J Physiol Regul Integr Comp Physiol* **293**: R2353-2362.
- Liu, Z., Christensson, M., Forslow, A., De Meester, I. and Sundqvist, K.G. (2009) A CD26-controlled cell surface cascade for regulation of T cell motility and chemokine signals. *J Immunol* **183**: 3616-3624.
- Lo, P.C., Chen, J., Stefflova, K., Warren, M.S., Navab, R., Bandarchi, B., Mullins, S., Tsao, M., Cheng, J.D. and Zheng, G. (2009) Photodynamic molecular beacon triggered by fibroblast activation protein on cancer-associated fibroblasts for diagnosis and treatment of epithelial cancers. *J Med Chem* **52**: 358-368.
- Lopez-Otin, C. and Bond, J.S. (2008) Proteases: multifunctional enzymes in life and disease. *J Biol Chem* **283**: 30433-30437.
- Luo, Z.J., Zang, M.W. and Guo, W. (2010) AMPK as a metabolic tumor suppressor: control of metabolism and cell growth. *Future Oncol* **6**: 457-470.
- Maes, M.-B., Dubois, V., Brandt, I., Lambeir, A.-M., Van der Veken, P., Augustyns, K., Cheng, J.D., Chen, X., Scharpe, S. and De Meester, I. (2007) Dipeptidyl peptidase 8/9-like activity in human leukocytes. *J Leukocyte Biol* **81**: 1252-1257.
- Mandai, M., Konishi, I., Kuroda, H. and Fujii, S. (2007) LH/hCG action and development of ovarian cancer--a short review on biological and clinical/epidemiological aspects. *Mol Cell Endocrinol* **269**: 61-64.

Marguet, D., Bernard, A.M., Vivier, I., Darmoul, D., Naquet, P. and Pierres, M. (1992) cDNA cloning for mouse thymocyte-activating molecule. A multifunctional ecto-dipeptidyl peptidase IV (CD26) included in a subgroup of serine proteases. *J Biol Chem* **267**: 2200-2208.

Matsui, Y., Kitade, H., Kamiya, T., Kanemaki, T., Hiramatsu, Y., Okumura, T. and Kamiyama, Y. (1994) Adenylate energy charge of rat and human cultured hepatocytes. *In Vitro Cell Dev Biol Anim* **30A**: 609-614.

McCauliffe, D.P., Yang, Y.S., Wilson, J., Sontheimer, R.D. and Capra, J.D. (1992) The 5'-flanking region of the human calreticulin gene shares homology with the human GRP78, GRP94, and protein disulfide isomerase promoters. *J Biol Chem* **267**: 2557-2562.

McNicholas, K. (2008) *Expression and purification of dipeptidyl peptidase 9*, School of Biological Sciences, Flinders University.

Meng, Y., Gu, C., Wu, Z., Zhao, Y., Si, Y., Fu, X. and Han, W. (2009) Id2 promotes the invasive growth of MCF-7 and SKOV-3 cells by a novel mechanism independent of dimerization to basic helix-loop-helix factors. *BMC Cancer* **9**: 75.

Mentlein, R. (1999) Dipeptidyl-peptidase IV (CD26)--role in the inactivation of regulatory peptides. *Regul Pept* **85**: 9-24.

Michalak, M., Groenendyk, J., Szabo, E., Gold, L.I. and Opas, M. (2009) Calreticulin, a multi-process calcium-buffering chaperone of the endoplasmic reticulum. *Biochem J* **417**: 651-666.

Mihaylova, M.M. and Shaw, R.J. (2011) The AMPK signalling pathway coordinates cell growth, autophagy and metabolism. *Nat Cell Biol* **13**: 1016-1023.

Mu, J., Petrov, A., Eiermann, G.J., Woods, J., Zhou, Y.P., Li, Z.H., Zychband, E., Feng, Y., Zhu, L., Roy, R.S., Howard, A.D., Li, C., Thornberry, N.A. and Zhang, B.B. (2009) Inhibition of DPP-4 with sitagliptin improves glycemic control and restores islet cell mass and function in a rodent model of type 2 diabetes. *Eur J Pharmacol* **623**: 148-154.

Mukhopadhyay, A., Avramova, L.V. and Weiner, H. (2002) Tom34 unlike Tom20 does not interact with the leader sequences of mitochondrial precursor proteins. *Arch Biochem Biophys* **400**: 97-104.

Muscat, C., Bertotto, A., Agea, E., Bistoni, O., Ercolani, R., Tognellini, R., Spinozzi, F., Cesarotti, M. and Gerli, R. (1994) Expression and functional role of 1F7 (CD26) antigen on peripheral blood and synovial fluid T cells in rheumatoid arthritis patients. *Clin Exp Immunol* **98**: 252-256.

Nagendran, J., Waller, T.J. and Dyck, J.R.B. (2013) AMPK signalling and the control of substrate use in the heart. *Mol Cell Endocrinol* **366**: 180-193.

Nägler, D.K. and Menard, R. (1998) Human cathepsin X: A novel cysteine protease of the papain family with a very short proregion and unique insertions. *FEBS Lett* **434**: 135-139.

Narra, K., Mullins, S.R., Lee, H.O., Strzemkowski-Brun, B., Magalong, K., Christiansen, V.J., McKee, P.A., Egleston, B., Cohen, S.J., Weiner, L.M., Meropol, N.J. and Cheng, J.D. (2007) Phase II trial of single agent Val-boroPro (Talabostat) inhibiting Fibroblast Activation Protein in patients with metastatic colorectal cancer. *Cancer Biol Ther* **6**: 1691-1699.

Nauck, M.A., Homberger, E., Siegel, E.G., Allen, R.C., Eaton, R.P., Ebert, R. and Creutzfeldt, W. (1986) Incretin effects of increasing glucose loads in man calculated from venous insulin and C-peptide responses. *J Clin Endocrinol Metab* **63**: 492-8.

Neurath, H. (1984) Evolution of Proteolytic-Enzymes. *Science* **224**: 350-357.

Niedermeyer, J., Enenkel, B., Park, J.E., Lenter, M., Rettig, W.J., Damm, K. and Schnapp, A. (1998) Mouse fibroblast-activation protein--conserved Fap gene organization and biochemical function as a serine protease. *Eur J Biochem* **254**: 650-654.

Niedermeyer, J., Kriz, M., Hilberg, F., Garin-Chesa, P., Bamberger, U., Lenter, M.C., Park, J., Viertel, B., Puschner, H., Mauz, M., Rettig, W.J. and Schnapp, A. (2000) Targeted disruption of mouse fibroblast activation protein. *Mol Cell Biol* **20**: 1089-1094.

Nikolajczyk, B.S., Jagannathan-Bogdan, M., Shin, H. and Gyurko, R. (2011) State of the union between metabolism and the immune system in type 2 diabetes. *Genes Immun* **12**: 239-250.

Nobumoto, M., Yamada, M., Song, S., Inouye, S. and Nakazawa, A. (1998) Mechanism of mitochondrial import of adenylate kinase isozymes. *J Biochem* **123**: 128-135.

Noma, T. (2005) Dynamics of nucleotide metabolism as a supporter of life phenomena. *J Med Invest* **52**: 127-136.

Noma, T., Fujisawa, K., Yamashiro, Y., Shinohara, M., Nakazawa, A., Gondo, T., Ishihara, T. and Yoshinobu, K. (2001) Structure and expression of human mitochondrial adenylate kinase targeted to the mitochondrial matrix. *Biochem J* **358**: 225-232.

Noma, T., Song, S., Yoon, Y.S., Tanaka, S. and Nakazawa, A. (1998) cDNA cloning and tissue-specific expression of the gene encoding human adenylate kinase isozyme 2. *Biochim Biophys Acta* **1395**: 34-39.

Oakhill, J.S., Chen, Z.P., Scott, J.W., Steel, R., Castelli, L.A., Ling, N., Macaulay, S.L. and Kemp, B.E. (2010) beta-Subunit myristoylation is the gatekeeper for initiating metabolic stress sensing by AMP-activated protein kinase (AMPK). *Proc Natl Acad Sci U S A* **107**: 19237-19241.

- Oakhill, J.S., Scott, J.W. and Kemp, B.E. (2012) AMPK functions as an adenylate charge-regulated protein kinase. *Trends Endocrinol Metab* **23**: 125-132.
- Oakhill, J.S., Steel, R., Chen, Z.P., Scott, J.W., Ling, N., Tam, S. and Kemp, B.E. (2011) AMPK Is a Direct Adenylate Charge-Regulated Protein Kinase. *Science* **332**: 1433-1435.
- Oefner, C., D'Arcy, A., Mac Sweeney, A., Pierau, S., Gardiner, R. and Dale, G.E. (2003) High-resolution structure of human apo dipeptidyl peptidase IV/CD26 and its complex with 1-[(2-[(5-iodopyridin-2-yl)amino]-ethyl)amino]-acetyl]-2-cyano-(S)-pyrrolidine. *Acta Crystallogr D Biol Crystallogr* **59**: 1206-1212.
- Ogata, S., Misumi, Y. and Ikehara, Y. (1989) Primary structure of rat liver dipeptidyl peptidase IV deduced from its cDNA and identification of the NH₂-terminal signal sequence as the membrane-anchoring domain. *J Biol Chem* **264**: 3596-3601.
- Ohnuma, K., Dang, N.H. and Morimoto, C. (2008) Revisiting an old acquaintance: CD26 and its molecular mechanisms in T cell function. *Trends Immunol* **29**: 295-301.
- Ohnuma, K., Inoue, H., Uchiyama, M., Yamochi, T., Hosono, O., Dang, N.H. and Morimoto, C. (2006) T-cell activation via CD26 and caveolin-1 in rheumatoid synovium. *Mod Rheumatol* **16**: 3-13.
- Olsen, C. and Wagtmann, N. (2002) Identification and characterization of human DPP9, a novel homologue of dipeptidyl peptidase IV. *Gene* **299**: 185-193.
- Ostermann, E., Garin-Chesa, P., Heider, K.H., Kalat, M., Lamche, H., Puri, C., Kerjaschki, D., Rettig, W.J. and Adolf, G.R. (2008) Effective immunoconjugate therapy in cancer models targeting a serine protease of tumor fibroblasts. *Clin Cancer Res* **14**: 4584-4592.
- Otera, H. and Mihara, K. (2012) Mitochondrial dynamics: functional link with apoptosis. *Int J Cell Biol* **2012**: 821676.
- Ouyang, J., Parakhia, R.A. and Ochs, R.S. (2011) Metformin activates AMP kinase through inhibition of AMP deaminase. *J Biol Chem* **286**: 1-11.
- Panayiotou, C., Solaroli, N., Xu, Y.J., Johansson, M. and Karlsson, A. (2011) The characterization of human adenylate kinases 7 and 8 demonstrates differences in kinetic parameters and structural organization among the family of adenylate kinase isoenzymes. *Biochem J* **433**: 527-534.
- Pannicke, U., Hönig, M., Hess, I., Friesen, C., Holzmann, K., Rump, E.M., Barth, T.F., Rojewski, M.T., Schulz, A., Boehm, T., Friedrich, W. and Schwarz, K. (2009) Reticular dysgenesis (aleukocytosis) is caused by mutations in the gene encoding mitochondrial adenylate kinase 2. *Nat Genet* **41**: 101-105.

Park, J.E., Lenter, M.C., Zimmermann, R.N., Garin-Chesa, P., Old, L.J. and Rettig, W.J. (1999) Fibroblast activation protein, a dual specificity serine protease expressed in reactive human tumor stromal fibroblasts. *J Biol Chem* **274**: 36505-36512.

Parrott, J.A., Doraiswamy, V., Kim, G., Mosher, R. and Skinner, M.K. (2001) Expression and actions of both the follicle stimulating hormone receptor and the luteinizing hormone receptor in normal ovarian surface epithelium and ovarian cancer. *Mol Cell Endocrinol* **172**: 213-222.

Pedicino, D., Liuzzo, G., Trotta, F., Giglio, A.F., Giubilato, S., Martini, F., Zaccardi, F., Scavone, G., Previtiero, M., Massaro, G., Cialdella, P., Cardillo, M.T., Pitocco, D., Ghirlanda, G. and Crea, F. (2013) Adaptive Immunity, Inflammation, and Cardiovascular Complications in Type 1 and Type 2 Diabetes Mellitus. *J Diabetes Res* **2013**: 184258.

Pinson, B., Vaur, S., Sagot, I., Couplier, F., Lemoine, S. and Daignan-Fornier, B. (2009) Metabolic intermediates selectively stimulate transcription factor interaction and modulate phosphate and purine pathways. *Genes Dev* **23**: 1399-1407.

Pitman, M.R., Menz, R.I. and Abbott, C.A. (2010) Hydrophilic residues surrounding the S1 and S2 pockets contribute to dimerisation and catalysis in human dipeptidyl peptidase 8 (DP8). *Biol Chem* **391**: 959-972.

Pitman, M.R., Sulda, M.L., Kuss, B. and Abbott, C.A. (2009) Dipeptidyl peptidase 8 and 9--guilty by association? *Front Biosci* **14**: 3619-3633.

Prasanna, P., Pike, S., Peng, K., Shane, B. and Appling, D.R. (2003) Human mitochondrial C1-tetrahydrofolate synthase: gene structure, tissue distribution of the mRNA, and immunolocalization in Chinese hamster ovary cells. *J Biol Chem* **278**: 43178-43187.

Puente, X.S., Sanchez, L.M., Overall, C.M. and Lopez-Otin, C. (2003) Human and mouse proteases: a comparative genomic approach. *Nat Rev Genet* **4**: 544-558.

Qi, S.Y., Riviere, P.J., Trojnar, J., Junien, J.L. and Akinsanya, K.O. (2003) Cloning and characterization of dipeptidyl peptidase 10, a new member of an emerging subgroup of serine proteases. *Biochem J* **373**: 179-189.

Rasband, W.S. (1997-2012) Image J, <http://imagej.nih.gov/ij/>, 15 July 2013.

Rasmussen, H.B., Branner, S., Wiberg, F.C. and Wagtmann, N. (2003) Crystal structure of human dipeptidyl peptidase IV/CD26 in complex with a substrate analog. *Nat Struct Biol* **10**: 19-25.

Rayl, E.A., Moroson, B.A. and Beardsley, G.P. (1996) The human purH gene product, 5-aminoimidazole-4-carboxamide ribonucleotide formyltransferase/IMP cyclohydrolase. Cloning, sequencing, expression, purification, kinetic analysis, and domain mapping. *J Biol Chem* **271**: 2225-2233.

Reed, R., Holmes, D., Weyers, J. and Jones, A. (2007) *Practical skills in biomolecular sciences*, Pearson Education Limited, Essex, England.

Reichling, L.J., Riddle, S.M., Mei, B., Bruinsma, R., Goossens, T.A., Huwiler, K.G., Maffitt, M., Newport, A.M., Qian, X.D., Ruttimann-Johnson, C. and Vogel, K.W. (2008) Homogenous fluorescent assays for characterizing small-molecule activators of AMP-activated protein kinase (AMPK). *Curr Chem Genomics* **1**: 34-42.

Reinhold, D., Goihl, A., Wrenger, S., Reinhold, A., Kuhlmann, U.C., Faust, J., Neubert, K., Thielitz, A., Brocke, S., Tager, M., Ansorge, S. and Bank, U. (2009) Role of dipeptidyl peptidase IV (DP IV)-like enzymes in T lymphocyte activation: investigations in DP IV/CD26-knockout mice. *Clinical Chemistry and Laboratory Medicine* **47**: 268-74.

Ren, H., Wang, L., Bennett, M., Liang, Y., Zheng, X., Lu, F., Li, L., Nan, J., Luo, M., Eriksson, S., Zhang, C. and Su, X.D. (2005) The crystal structure of human adenylate kinase 6: An adenylate kinase localized to the cell nucleus. *Proc Natl Acad Sci U S A* **102**: 303-8.

Rettig, W.J., Garin-Chesa, P., Beresford, H.R., Oettgen, H.F., Melamed, M.R. and Old, L.J. (1988) Cell-surface glycoproteins of human sarcomas: differential expression in normal and malignant tissues and cultured cells. *Proc Natl Acad Sci U S A* **85**: 3110-4.

Rezaul, K., Wu, L., Mayya, V., Hwang, S.I. and Han, D. (2005) A systematic characterization of mitochondrial proteome from human T leukemia cells. *Mol Cell Proteomics* **4**: 169-81.

Richter, B., Bandeira-Echtler, E., Bergerhoff, K. and Lerch, C. (2008) Emerging role of dipeptidyl peptidase-4 inhibitors in the management of type 2 diabetes. *Vasc Health Risk Manag* **4**: 753-68.

Richter, C., Schweizer, M., Cossarizza, A. and Franceschi, C. (1996) Control of apoptosis by the cellular ATP level. *FEBS Letters* **378**: 107-110.

Rodrigues, H.M., Jungel, A., Gay, R.E. and Gay, S. (2009) Innate immunity, epigenetics and autoimmunity in rheumatoid arthritis. *Molecular Immunology* **47**: 12-18.

Sambrook, J., Fritsch, E.F. and Maniatis, T. (1989) *Molecular cloning: a laboratory manual*, Cold Spring Harbor Laboratory Press, USA.

Sanner, K., Conner, P., Bergfeldt, K., Dickman, P., Sundfeldt, K., Bergh, T., Hagenfeldt, K., Janson, P.O., Nilsson, S. and Persson, I. (2009) Ovarian epithelial neoplasia after hormonal infertility treatment: long-term follow-up of a historical cohort in Sweden. *Fertil Steril* **91**: 1152-8.

Santamaria, I., Velasco, G., Pendas, A.M., Fueyo, A. and Lopez-Otin, C. (1998) Cathepsin Z, a novel human cysteine proteinase with a short propeptide domain and a unique chromosomal location. *J Biol Chem* **273**: 16816-23.

- Santos, A.M., Jung, J., Aziz, N., Kissil, J.L. and Pure, E. (2009) Targeting fibroblast activation protein inhibits tumor stromagenesis and growth in mice. *J Clin Invest* **119**: 3613-3625.
- Scanlan, M.J., Raj, B.K., Calvo, B., Garin-Chesa, P., Sanz-Moncasi, M.P., Healey, J.H., Old, L.J. and Rettig, W.J. (1994) Molecular cloning of fibroblast activation protein α , a member of the serine protease family selectively expressed in stromal fibroblasts of epithelial cancers. *Proc Natl Acad Sci U S A* **91**: 5657-5661.
- Schafer, Z.T., Grassian, A.R., Song, L., Jiang, Z., Gerhart-Hines, Z., Irie, H.Y., Gao, S., Puigserver, P. and Brugge, J.S. (2009) Antioxidant and oncogene rescue of metabolic defects caused by loss of matrix attachment. *Nature* **461**: 109-113.
- Schlauderer, G.J. and Schulz, G.E. (1996) The structure of bovine mitochondrial adenylate kinase: comparison with isoenzymes in other compartments. *Protein Sci* **5**: 434-441.
- Schmidt, A., Wu, H., MacKenzie, R.E., Chen, V.J., Bewly, J.R., Ray, J.E., Toth, J.E. and Cygler, M. (2000) Structures of three inhibitor complexes provide insight into the reaction mechanism of the human methylenetetrahydrofolate dehydrogenase/cyclohydrolase. *Biochemistry* **39**: 6325-6335.
- Schmidt, O., Pfanner, N. and Meisinger, C. (2010) Mitochondrial protein import: from proteomics to functional mechanisms. *Nat Rev Mol Cell Biol* **11**: 655-667.
- Schricker, R., Angermayr, M., Strobel, G., Klinke, S., Korber, D. and Bandlow, W. (2002) Redundant mitochondrial targeting signals in yeast adenylate kinase. *J Biol Chem* **277**: 28757-28764.
- Scott, A.M., Wiseman, G., Welt, S., Adjei, A., Lee, F.T., Hopkins, W., Divgi, C.R., Hanson, L.H., Mitchell, P., Gansen, D.N., Larson, S.M., Ingle, J.N., Hoffman, E.W., Tanswell, P., Ritter, G., Cohen, L.S., Bette, P., Arvay, L., Amelsberg, A., Vlock, D., Rettig, W.J. and Old, L.J. (2003) A Phase I dose-escalation study of sibrotuzumab in patients with advanced or metastatic fibroblast activation protein-positive cancer. *Clin Cancer Res* **9**: 1639-1647.
- Šedo, A. and Malik, R. (2001) Dipeptidyl peptidase IV-like molecules: homologous proteins or homologous activities? *Biochim Biophys Acta* **1550**: 107-116.
- Shimokawa, T., Matsushima, S., Tsunoda, T., Tahara, H., Nakamura, Y. and Furukawa, Y. (2006) Identification of TOMM34, which shows elevated expression in the majority of human colon cancers, as a novel drug target. *Int J Oncol* **29**: 381-386.
- Sideris, D.P., Petrakis, N., Katrakili, N., Mikropoulou, D., Gallo, A., Ciofi-Baffoni, S., Banci, L., Bertini, I. and Tokatlidis, K. (2009) A novel intermembrane space-targeting signal docks cysteines onto Mia40 during mitochondrial oxidative folding. *J Cell Biol* **187**: 1007-1022.

Staudt, N.D., Aicher, W.K., Kalbacher, H., Stevanovic, S., Carmona, A.K., Bogoyo, M. and Klein, G. (2010) Cathepsin X is secreted by human osteoblasts, digests CXCL-12 and impairs adhesion of hematopoietic stem and progenitor cells to osteoblasts. *Haematologica* **95**: 1452-1460.

Stefansson, B. and Brautigan, D.L. (2006) Protein phosphatase 6 subunit with conserved Sit4-associated protein domain targets IkappaBepsilon. *J Biol Chem* **281**: 22624-22634.

Stefansson, B. and Brautigan, D.L. (2007) Protein phosphatase PP6 N terminal domain restricts G1 to S phase progression in human cancer cells. *Cell Cycle* **6**: 1386-1392.

Strobel, G., Zollner, A., Angermayr, M. and Bandlow, W. (2002) Competition of spontaneous protein folding and mitochondrial import causes dual subcellular location of major adenylate kinase. *Mol Biol Cell* **13**: 1439-1448.

Sulda, M.L. (2009) *Investigation of biological targets for prognostication and therapy in B-cell chronic lymphocytic leukaemia*, School of Biological Sciences, Flinders University.

Sun, H., Luo, X., Montalbano, J., Jin, W., Shi, J., Sheikh, M.S. and Huang, Y. (2010) DOC45, a novel DNA damage-regulated nucleocytoplasmic ATPase that is overexpressed in multiple human malignancies. *Mol Cancer Res* **8**: 57-66.

Syed, V., Ulinski, G., Mok, S.C., Yiu, G.K. and Ho, S.M. (2001) Expression of gonadotropin receptor and growth responses to key reproductive hormones in normal and malignant human ovarian surface epithelial cells. *Cancer Res* **61**: 6768-6776.

Taghizadeh, R.R. and Sherley, J.L. (2008) CFP and YFP, but not GFP, provide stable fluorescent marking of rat hepatic adult stem cells. *J Biomed Biotechnol* **2008**: 453590.

Tanabe, T., Yamada, M., Noma, T., Kajii, T. and Nakazawa, A. (1993) Tissue-specific and developmentally regulated expression of the genes encoding adenylate kinase isozymes. *J Biochem* **113**: 200-207.

Tanaka, S., Murakami, T., Horikawa, H., Sugiura, M., Kawashima, K. and Sugita, T. (1997) Suppression of arthritis by the inhibitors of dipeptidyl peptidase IV. *Intl J Immunopharmacol* **19**: 15-24.

Tanaka, S., Murakami, T., Nonaka, N., Ohnuki, T., Yamada, M. and Sugita, T. (1998) Anti-arthritic effects of the novel dipeptidyl peptidase IV inhibitors TMC-2A and TSL-225. *Immunopharmacology* **40**: 21-6.

Tang, H.-K., Tang, H.Y., Hsu, S.C., Chu, Y.R., Chien, C.H., Shu, C.H. and Chen, X. (2009) Biochemical properties and expression profile of human prolyl dipeptidase DPP9. *Arch Biochem Biophys* **485**: 120-127.

Tanswell, P., Garin-Chesa, P., Rettig, W.J., Welt, S., Divgi, C.R., Casper, E.S., Finn, R.D., Larson, S.M., Old, L.J. and Scott, A.M. (2001) Population pharmacokinetics of antifibroblast activation protein monoclonal antibody F19 in cancer patients. *Br J Clin Pharmacol* **51**: 177-180.

Taylor, A.L., Kudlow, B.A., Marrs, K.L., Gruenert, D.C., Guggino, W.B. and Schwiebert, E.M. (1998) Bioluminescence detection of ATP release mechanisms in epithelia. *Am J Physiol-Cell Ph* **275**: C1391-C1406.

Tibbetts, A.S. and Appling, D.R. (2000) Characterization of two 5-aminoimidazole-4-carboxamide ribonucleotide transformylase/inosine monophosphate cyclohydrolase isozymes from *Saccharomyces cerevisiae*. *J Biol Chem* **275**: 20920-20927.

Turk, B., Turk, D. and Turk, V. (2012) Protease signalling: the cutting edge. *EMBO J* **31**: 1630-1643.

Vander Heiden, M.G., Cantley, L.C. and Thompson, C.B. (2009) Understanding the Warburg Effect: The Metabolic Requirements of Cell Proliferation. *Science* **324**: 1029-1033.

Vander Heiden, M.G., Chandel, N.S., Schumacker, P.T. and Thompson, C.B. (1999) Bcl-x(L) prevents cell death following growth factor withdrawal by facilitating mitochondrial ATP/ADP exchange. *Mol Cell* **3**: 159-167.

Vasey, P.A., Shulman, L.N., Campos, S., Davis, J., Gore, M., Johnston, S., Kirn, D.H., O'Neill, V., Siddiqui, N., Seiden, M.V. and Kaye, S.B. (2002) Phase I trial of intraperitoneal injection of the E1B-55-kd-gene-deleted adenovirus ONYX-015 (dl1520) given on days 1 through 5 every 3 weeks in patients with recurrent/refractory epithelial ovarian cancer. *J Clin Oncol* **20**: 1562-1569.

Vaughan, S., Coward, J.I., Bast, R.C., Jr., Berchuck, A., Berek, J.S., Brenton, J.D., Coukos, G., Crum, C.C., Drapkin, R., Etemadmoghadam, D., Friedlander, M., Gabra, H., Kaye, S.B., Lord, C.J., Lengyel, E., Levine, D.A., McNeish, I.A., Menon, U., Mills, G.B., Nephew, K.P., Oza, A.M., Sood, A.K., Stronach, E.A., Walczak, H., Bowtell, D.D. and Balkwill, F.R. (2011) Rethinking ovarian cancer: recommendations for improving outcomes. *Nat Rev Cancer* **11**: 719-725.

Villa, H., Perez-Pertejo, Y., Garcia-Estrada, C., Reguera, R.M., Requena, J.M., Tekwani, B.L., Balana-Fouce, R. and Ordonez, D. (2003) Molecular and functional characterization of adenylate kinase 2 gene from *Leishmania donovani*. *Eur J Biochem* **270**: 4339-4347.

VilSBoll, T., Krarup, T., Sonne, J., Madsbad, S., Volund, A., Juul, A.G. and Holst, J.J. (2003) Incretin secretion in relation to meal size and body weight in healthy subjects and people with type 1 and type 2 diabetes mellitus. *J Clin Endocrinol Metab* **88**: 2706-2713.

Wang, C. and Youle, R.J. (2009) The Role of Mitochondria in Apoptosis. *Ann Rev Genet* **43**: 95-118.

Wang, X.M., Yao, T.W., Nadvi, N.A., Osborne, B., McCaughan, G.W. and Gorrell, M.D. (2008) Fibroblast activation protein and chronic liver disease. *Front Biosci-Landmark* **13**: 3168-3180.

Wang, X.M., Yu, D.M., McCaughan, G.W. and Gorrell, M.D. (2005) Fibroblast activation protein increases apoptosis, cell adhesion, and migration by the LX-2 human stellate cell line. *Hepatology* **42**: 935-945.

Wasternack, C. (1980) Degradation of Pyrimidines and Pyrimidine Analogs Pathways and Mutual Influences. *Pharmacol Therapeut* **8**: 629-651.

Watanabe, K. and Kubo, S. (1982) Mitochondrial Adenylate Kinase from Chicken Liver. *Eur J Biochem* **123**: 587-592.

White, P.C., Chamberlain-Shea, H. and de la Morena, M.T. (2010) Sitagliptin treatment of patients with type 2 diabetes does not affect CD4+ T-cell activation. *J Diabetes Complications* **24**: 209-213.

Williams, Y.N., Baba, H., Hayashi, S., Ikai, H., Sugita, T., Tanaka, S., Miyasaka, N. and Kubota, T. (2003) Dipeptidyl peptidase IV on activated T cells as a target molecule for therapy of rheumatoid arthritis. *Clin Exp Immunol* **131**: 68-74.

Wilson, C.H. (2011) *Identifying the substrate degradome and roles of dipeptidyl peptidase (DP) 8 and DP9 in breast and ovarian cancer cell lines*, School of Biological Sciences, Flinders University.

Wilson, C.H., Indarto, D., Doucet, A., Pogson, L.D., Pitman, M.R., McNicholas, K., Menz, R.I., Overall, C.M. and Abbott, C.A. (2013) Identifying Natural Substrates for Dipeptidyl Peptidases 8 and 9 Using Terminal Amine Isotopic Labeling of Substrates (TAILS) Reveals in Vivo Roles in Cellular Homeostasis and Energy Metabolism. *J Biol Chem* **288**: 13936-13949.

Wu, Y., Dong, Y., Song, P. and Zou, M.H. (2012) Activation of the AMP-activated protein kinase (AMPK) by nitrated lipids in endothelial cells. *PLoS One* **7**: e31056.

Yaginuma, Y. and Westphal, H. (1992) Abnormal structure and expression of the p53 gene in human ovarian carcinoma cell lines. *Cancer Res* **52**: 4196-4199.

Yan, S., Marguet, D., Dobers, J., Reutter, W. and Fan, H. (2003) Deficiency of CD26 results in a change of cytokine and immunoglobulin secretion after stimulation by pokeweed mitogen. *Eur J Immunol* **33**: 1519-1527.

Yao, T.W., Kim, W.S., Yu, D.M., Sharbeen, G., McCaughan, G.W., Choi, K.Y., Xia, P. and Gorrell, M.D. (2011) A novel role of dipeptidyl peptidase 9 in epidermal growth factor signaling. *Mol Cancer Res* **9**: 948-959.

Yazbeck, R., Howarth, G.S. and Abbott, C.A. (2009) Dipeptidyl peptidase inhibitors, an emerging drug class for inflammatory disease? *Trends Pharmacol Sci* **30**: 600-607.

Yokota, H., Fernandez-Salguero, P., Furuya, H., Lin, K., McBride, O.W., Podschun, B., Schnackerz, K.D. and Gonzalez, F.J. (1994) cDNA cloning and chromosome mapping of human dihydropyrimidine dehydrogenase, an enzyme associated with 5-fluorouracil toxicity and congenital thymine uraciluria. *J Biol Chem* **269**: 23192-23196.

Yoshioka, S., King, M.L., Ran, S., Okuda, H., MacLean, J.A., 2nd, McAsey, M.E., Sugino, N., Brard, L., Watabe, K. and Hayashi, K. (2012) WNT7A regulates tumor growth and progression in ovarian cancer through the WNT/beta-catenin pathway. *Mol Cancer Res* **10**: 469-482.

Yu, D.M.T., Ajami, K., Gall, M.G., Park, J., Lee, C.S., Evans, K.A., McLaughlin, E.A., Pitman, M.R., Abbott, C.A., McCaughan, G.W. and Gorrell, M.D. (2009) The In Vivo Expression of Dipeptidyl Peptidases 8 and 9. *J Histochem Cytochem* **57**: 1025-1038.

Yu, D.M.T., Wang, X.M., McCaughan, G.W. and Gorrell, M.D. (2006) Extraenzymatic functions of the dipeptidyl peptidase IV-related proteins DP8 and DP9 in cell adhesion, migration and apoptosis. *FEBS J* **273**: 2447-2460.

Yu, D.M.T., Yao, T.W., Chowdhury, S., Nadvi, N.A., Osborne, B., Church, W.B., McCaughan, G.W. and Gorrell, M.D. (2010) The dipeptidyl peptidase IV family in cancer and cell biology. *FEBS J* **277**: 1126-1144.

Zang, R., Li, D., Tang, I.-C., Wang, J.X. and Yang, S.-T. (2012) Cell-based assays in high-throughput screening for drug discovery. *Int J Biotech Well Indus* **1**: 31-51.

Zeimet, A.G. and Marth, C. (2003) Why did p53 gene therapy fail in ovarian cancer? *Lancet Oncol* **4**: 415-422.

Zhang, X., Ling, M.-T., Feng, H., Wong, Y.C., Tsao, S.W. and Wang, X. (2004) Id-1 stimulates cell proliferation through activation of EGFR in ovarian cancer cells. *Brit J Cancer* **91**: 2042-2047.

Zhao, Y., Jiang, Z., Zhao, T., Ye, M., Hu, C., Zhou, H., Yin, Z., Chen, Y., Zhang, Y., Wang, S., Shen, J., Thaker, H., Jain, S., Li, Y., Diao, Y., Chen, Y., Sun, X., Fisk, M.B. and Li, H. (2013) Targeting insulin resistance in type 2 diabetes via immune modulation of cord blood-derived multipotent stem cells (CB-SCs) in stem cell educator therapy: phase I/II clinical trial. *BMC Med* **11**: 160.

Zhao, Y., Jiang, Z.S. and Guo, C.S. (2011) New hope for type 2 diabetics: Targeting insulin resistance through the immune modulation of stem cells. *Autoimmun Rev* **11**: 137-142.

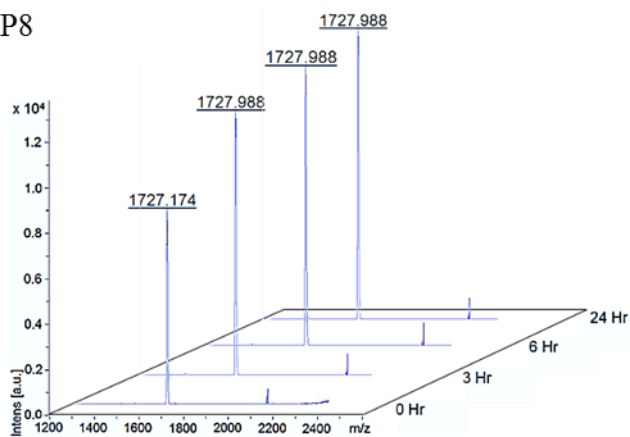
Zhu, H., Zhou, Z.M., Lu, L., Xu, M., Wang, H., Li, J.M. and Sha, J.H. (2005) Expression of a novel dipeptidyl peptidase 8 (DPP8) transcript variant, DPP8-v3, in human testis. *Asian J Androl* **7**: 245-255.

Zou, H., Henzel, W.J., Liu, X., Lutschg, A. and Wang, X. (1997) Apaf-1, a Human Protein Homologous to *C. elegans* CED-4, Participates in Cytochrome c-Dependent Activation of Caspase-3. *Cell* **90**: 405-413.

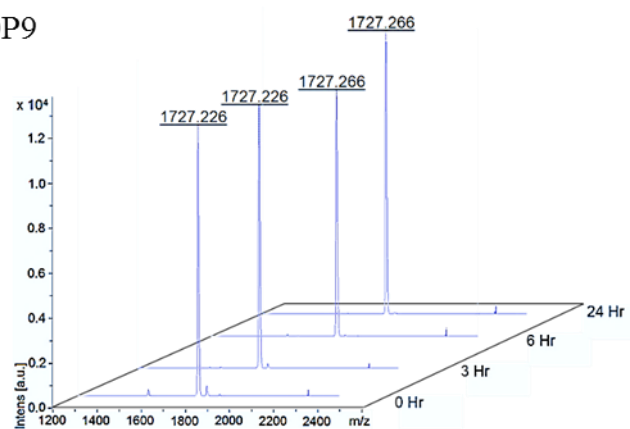
Zou, M.H., Kirkpatrick, S.S., Davis, B.J., Nelson, J.S., Wiles, W.G.t., Schlattner, U., Neumann, D., Brownlee, M., Freeman, M.B. and Goldman, M.H. (2004) Activation of the AMP-activated protein kinase by the anti-diabetic drug metformin in vivo. Role of mitochondrial reactive nitrogen species. *J Biol Chem* **279**: 43940-43951.

8. APPENDICES

A. DP8



B. DP9



C. DP4

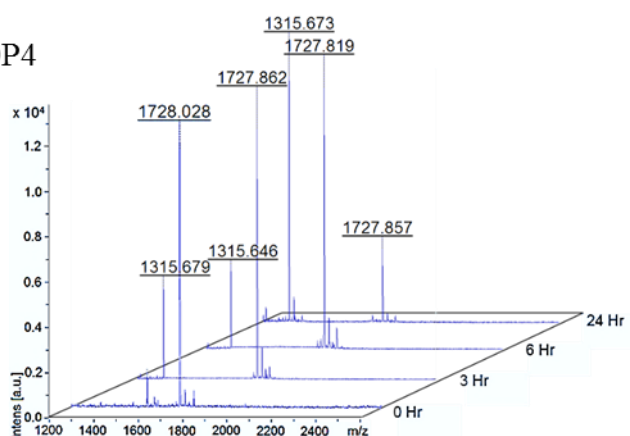
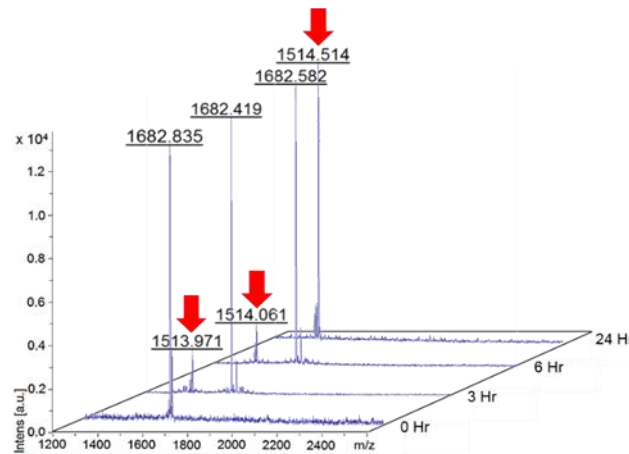
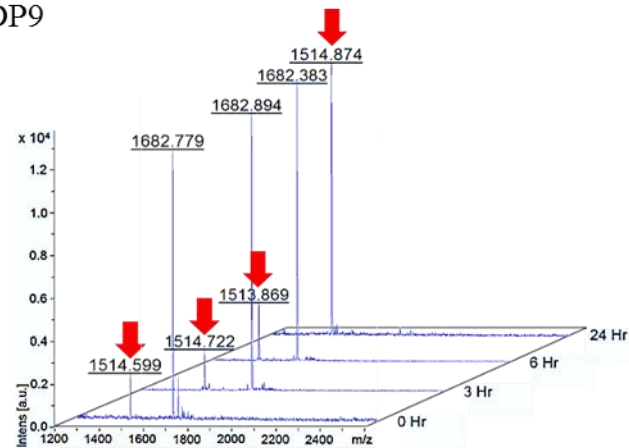


Figure 8.1. DP8, DP9 and DP4 cleavage activity towards the N terminus acetyl-CoA acetyltransferase. There was no cleaved peptide product after 24h incubation with DP8, DP9. Uncleaved peptide has molecular mass 1727.09 Da. After 3 h DP4 cleaved this peptide (1315 Da). Data represents three independent experiments.

A. DP8



B. DP9



C. DP4

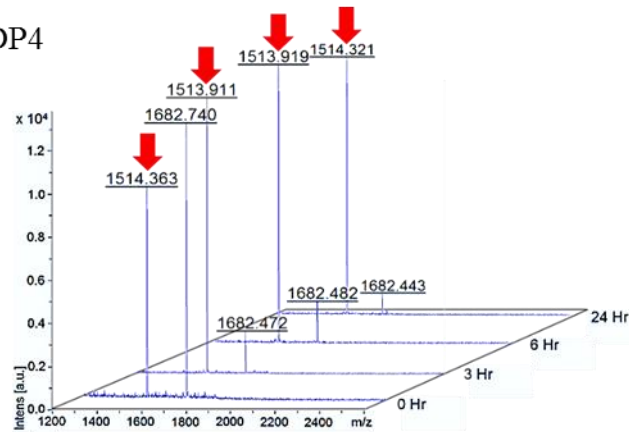
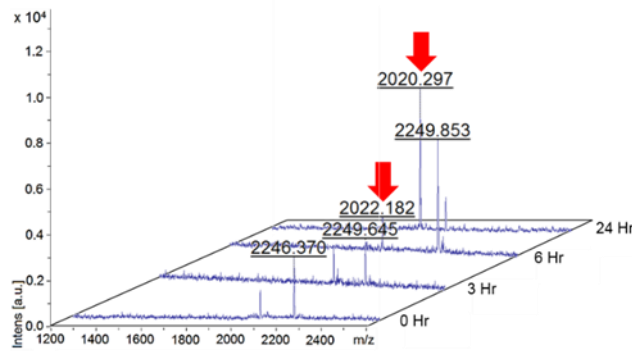
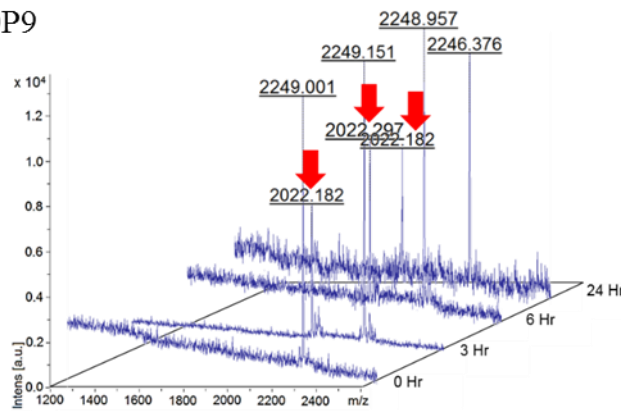


Figure 8.2. DP8, DP9 and DP4 cleavage activity towards the N terminus of AK2. A cleaved peptide product (around 1515 Da) was indicated by red arrows and uncleaved peptide has molecular mass 1681.89 Da. The first cleaved peptide was observed after 3h incubation with DP8 and 0h incubation with DP9. 30% of this peptide was cleaved by DP8 and this peptide was completely cleaved DP9 after 24h incubation. By contrast, the peptide was directly cleaved by DP4 after 0h incubation and this peptide was completely cleaved after 24h incubation. Data represents three independent experiments.

A. DP8



B. DP9



C. DP4

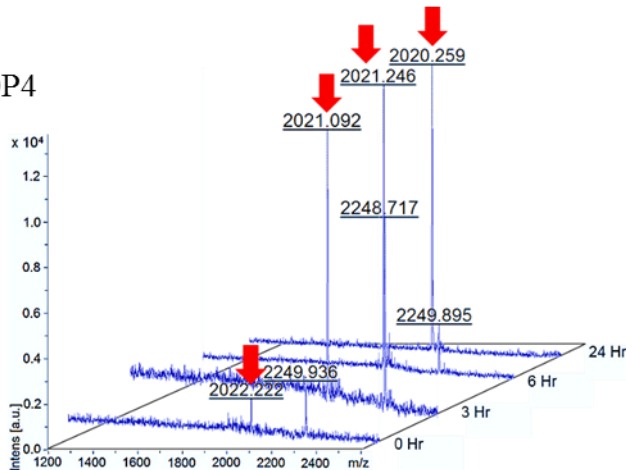


Figure 8.3. DP8, DP9 and DP4 cleavage activity towards the N terminus of calreticulin. A cleaved peptide product (around 2020 Da) was indicated by red arrows and uncleaved peptide has molecular mass 2245.45 Da. The first cleaved peptide was observed after 24h incubation with DP8 and 3h incubation with DP9. Around 80% of this peptide was cleaved by DP8 and this peptide was cleaved DP9 less than a half after 24h incubation. By contrast, the peptide was directly cleaved by DP4 after 0h incubation and this peptide was completely cleaved after 24h incubation. Data represents three independent experiments.

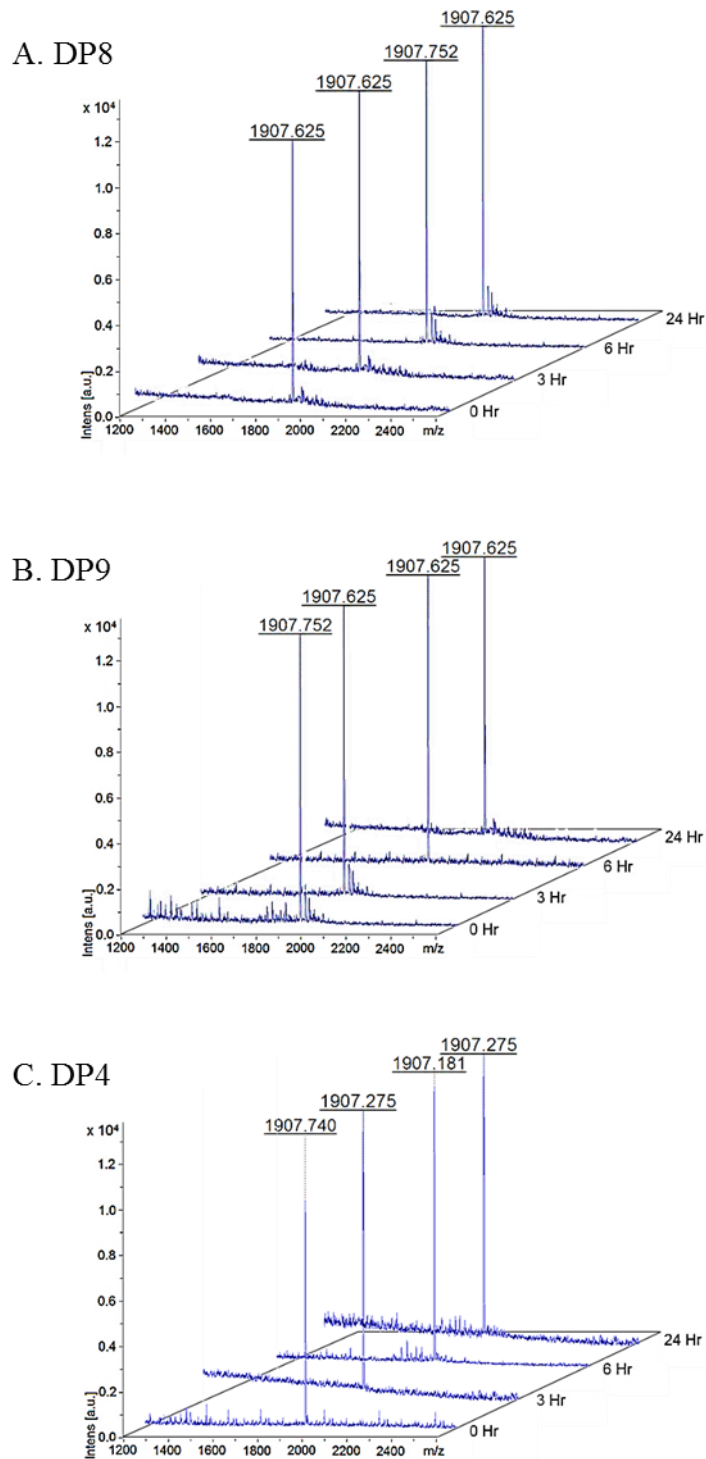


Figure 8.4. DP8, DP9 and DP4 cleavage activity towards the N terminus of collagen-binding protein 2 (Serpín H-1). There was no cleaved peptide after 24h incubation with DP8, DP9 and DP4. Uncleaved peptide has molecular mass 1907.21 Da. Data represented three independent experiments.

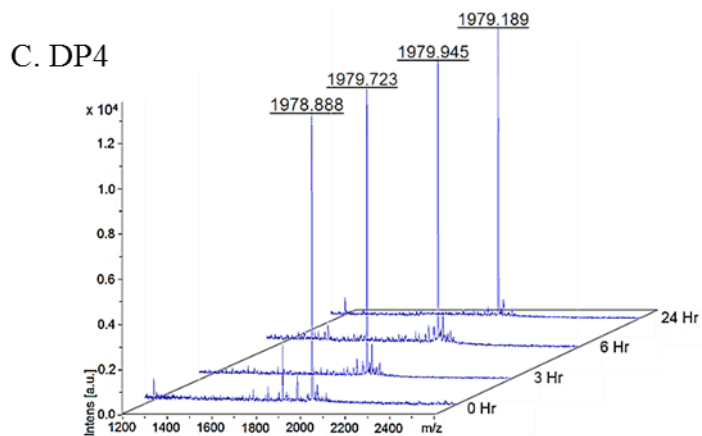
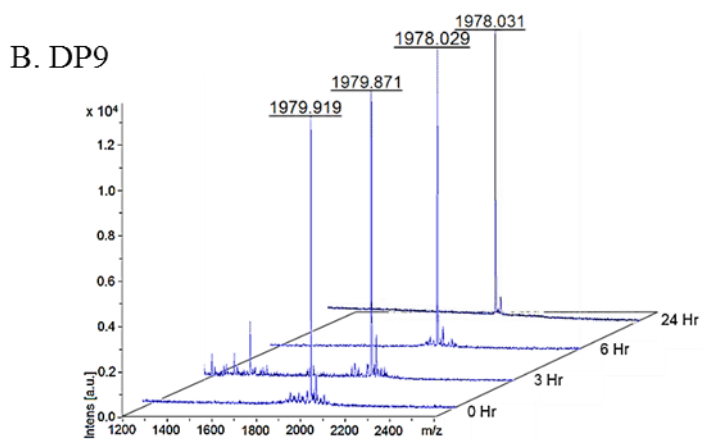
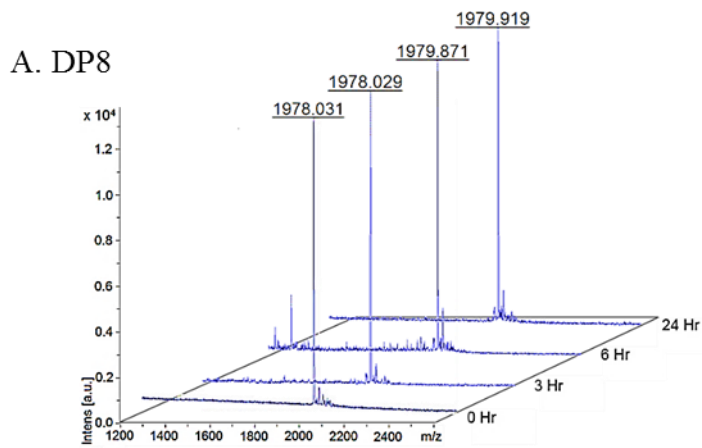


Figure 8.5. DP8, DP9 and DP4 cleavage activity towards the N terminus of endoplamin. There was no cleaved peptide after 24h incubation with DP8, DP9 and DP4. Uncleaved peptide has molecular mass 1978.03 Da. Data represents three independent experiments.

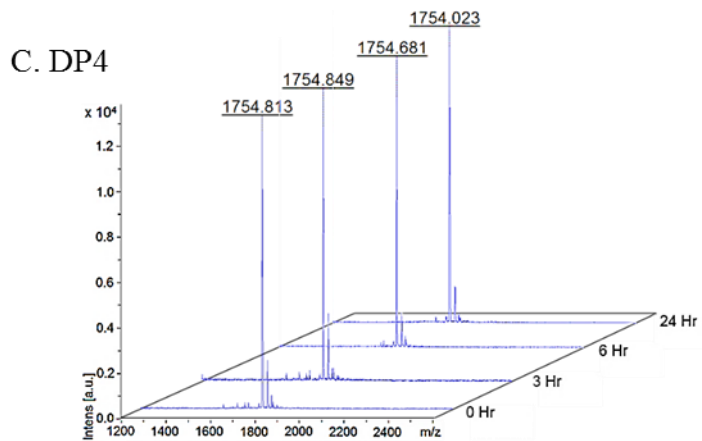
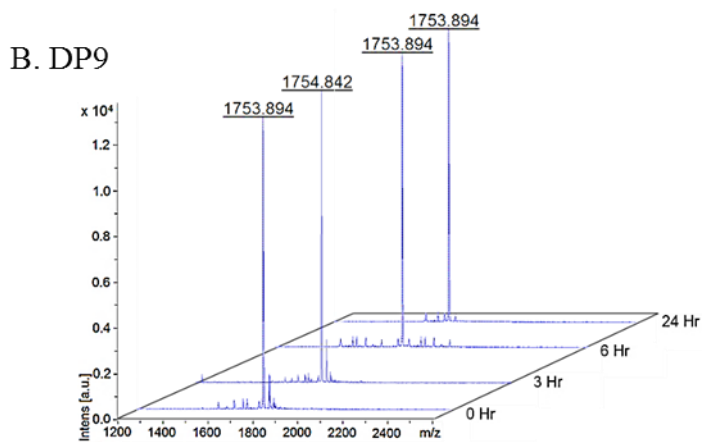
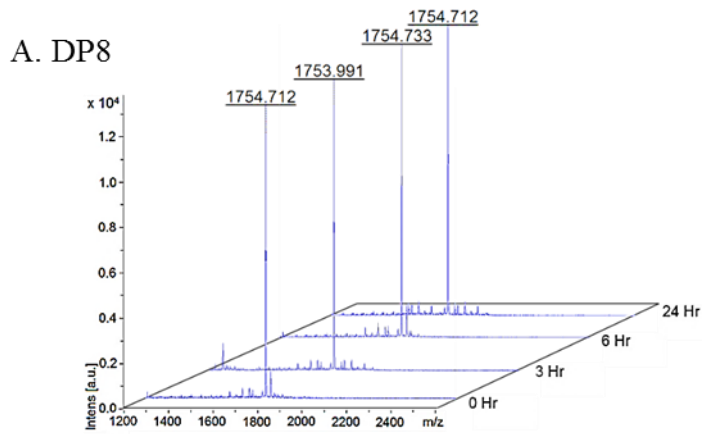


Figure 8.6. DP8, DP9 and DP4 cleavage activity towards the N terminus of enoyl-CoA hydratase. No cleaved peptide product (around 1596 Da) after 24h incubation with DP8 and DP9 and uncleaved peptide has molecular mass 1753.99Da. Data represents two independent experiments.

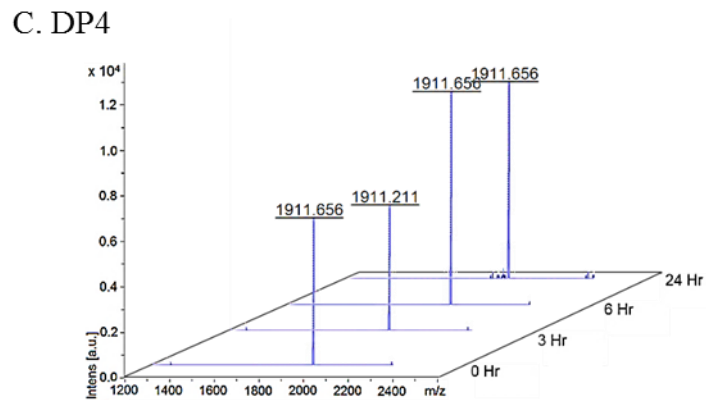
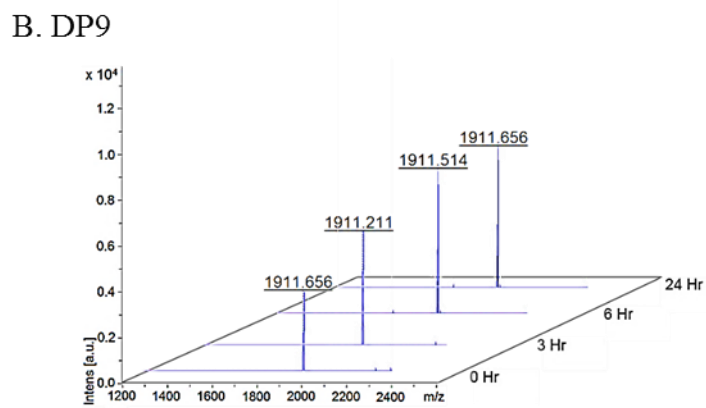
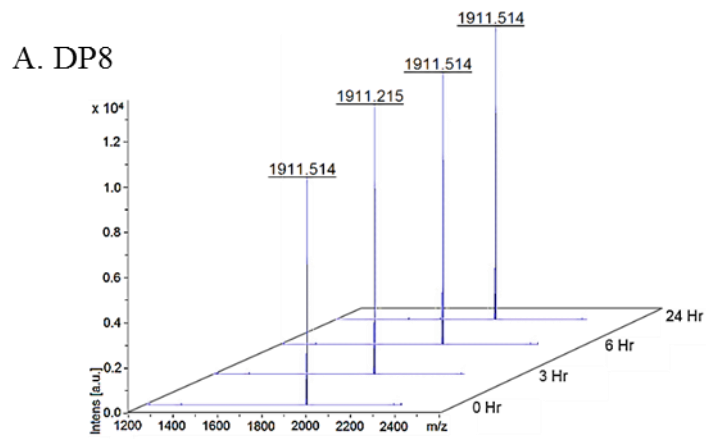


Figure 8.7. DP8, DP9 and DP4 cleavage activity towards the N terminus of heat shock 70 kDa protein 1L. There was no cleaved peptide after 24h incubation with DP8, DP9 and DP4. Uncleaved peptide has molecular mass 1911.21 Da. Data represented two independent experiments.

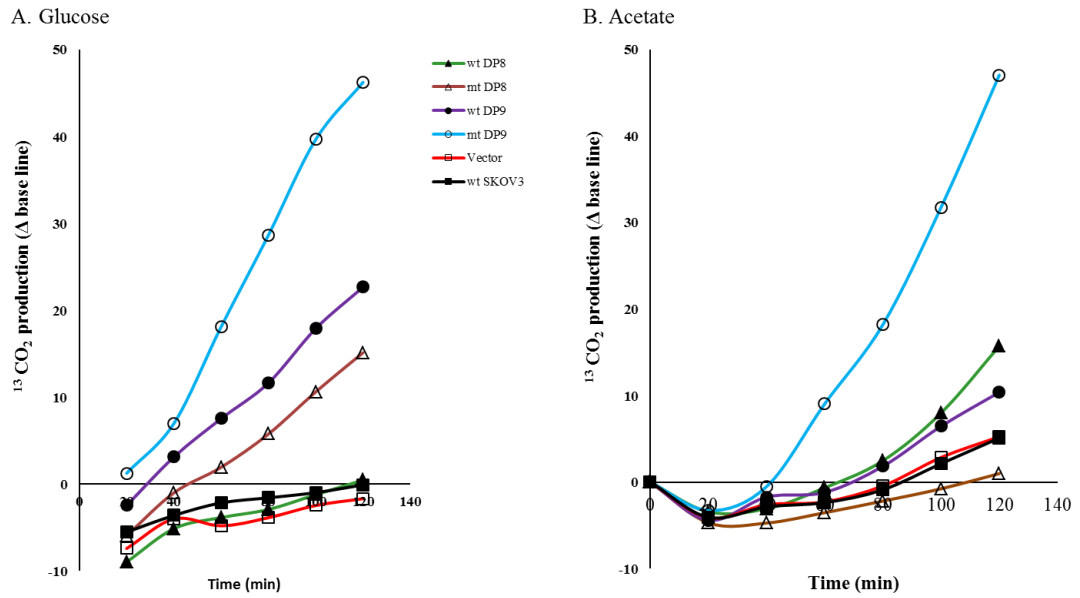


Figure 8.8. Glucose and fatty acid metabolism in SKOV3 cells with DP8 and DP9 overexpression. (A) 1×10^7 cells were incubated with 2 mM glucose $1\text{-}^{13}\text{C}$ in 40 ml DMEM. (B) 1×10^7 cells were incubated with 2 mM sodium acetate $1\text{-}^{13}\text{C}$ in 40 ml RPMI. CO_2 production was measured every 20 min for 120 min and data were presented as means from two independent experiments.

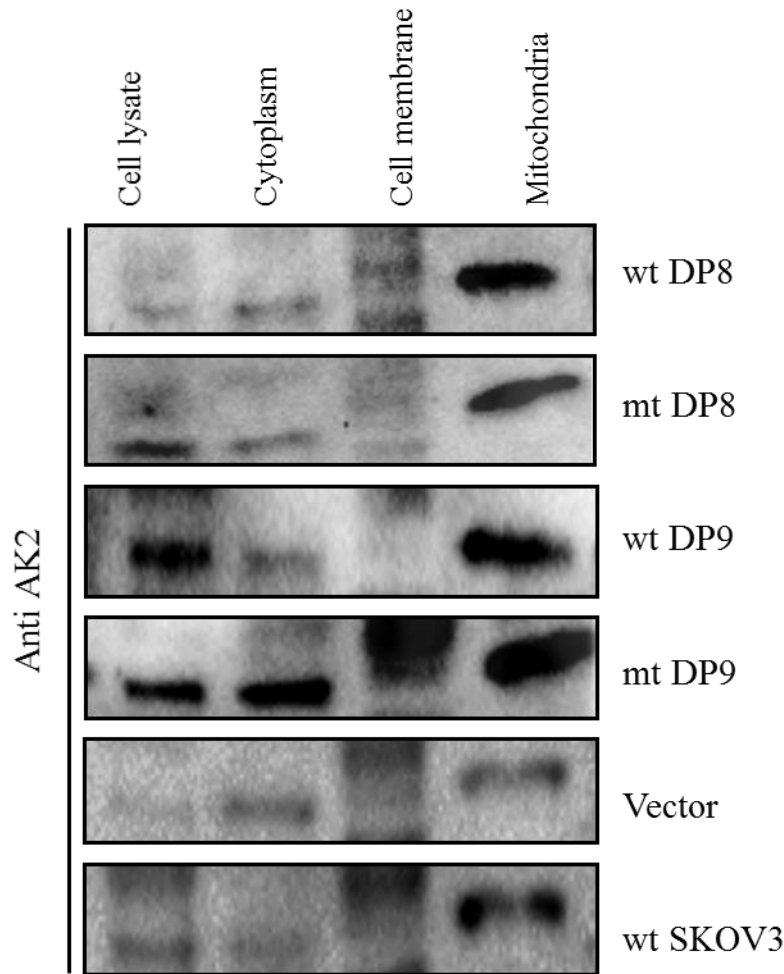


Figure 8.9. Protein expression of AK2 in cell fractions from SKOV3 cells with wt and mt DP8/DP9 overexpression. 25 μ g of total proteins of cell lysate, cell membrane, cytoplasm and purified mitochondria were separated using 10% SDS-PAGE and electro-transferred on to PVDF membrane. Blotted membranes then analysed in immunoblots using anti AK2 antibody. The band intensity was quantified using Bio-Rad Image lab™ software.

Identifying Natural Substrates for Dipeptidyl Peptidases 8 and 9 Using Terminal Amine Isotopic Labeling of Substrates (TAILS) Reveals *in Vivo* Roles in Cellular Homeostasis and Energy Metabolism^{*[5]♦}

Received for publication, December 18, 2012, and in revised form, March 4, 2013. Published, JBC Papers in Press, March 21, 2013, DOI 10.1074/jbc.M112.445841

Claire H. Wilson^{‡§1,2}, Dono Indarto^{‡¶1,3}, Alain Doucet[§], Lisa D. Pogson^{‡¶}, Melissa R. Pitman^{‡2}, Kym McNicholas[‡], R. Ian Menz[‡], Christopher M. Overall^{§4,5}, and Catherine A. Abbott^{‡¶4,6}

From the [‡]School of Biological Sciences and [¶]Flinders Centre for Innovation in Cancer, Flinders University, Adelaide, South Australia 5001, Australia and the [§]Departments of Biochemistry and Molecular Biology and Oral Biological and Medical Sciences, Centre for Blood Research and Faculty Dentistry, University of British Columbia, Vancouver, British Columbia V6T 1Z3, Canada

Background: Biological roles for intracellular dipeptidyl peptidases 8 and 9 are unknown.

Results: By degradomics, 29 new *in vivo* substrates were identified (nine validated) for DP8/DP9, including adenylate kinase 2 and calreticulin.

Conclusion: These substrates indicate roles for DP8 and DP9 in metabolism and energy homeostasis.

Significance: Being the first proteomics screen for DP8/DP9 substrates, unexpected new cellular roles were revealed.

Dipeptidyl peptidases (DP) 8 and 9 are homologous, cytoplasmic N-terminal post-proline-cleaving enzymes that are anti-targets for the development of DP4 (DPP4V/CD26) inhibitors for treating type II diabetes. To date, DP8 and DP9 have been implicated in immune responses and cancer biology, but their pathophysiological functions and substrate repertoire remain unknown. This study utilizes terminal amine isotopic labeling of substrates (TAILS), an N-terminal positional proteomic approach, for the discovery of *in vivo* DP8 and DP9 substrates. *In vivo* roles for DP8 and DP9 in cellular metabolism and homeostasis were revealed via the identification of more than 29 candidate natural substrates and pathways affected by DP8/DP9 overexpression. Cleavage of 14 substrates was investigated *in vitro*; 9/14 substrates for both DP8 and DP9 were confirmed by

MALDI-TOF MS, including two of high confidence, calreticulin and adenylate kinase 2. Adenylate kinase 2 plays key roles in cellular energy and nucleotide homeostasis. These results demonstrate remarkable *in vivo* substrate overlap between DP8/DP9, suggesting compensatory roles for these enzymes. This work provides the first global investigation into DP8 and DP9 substrates, providing a number of leads for future investigations into the biological roles and significance of DP8 and DP9 in human health and disease.

Dipeptidyl peptidase 8 (DP8/DPP8/dipeptidyl peptidase IV-related protein 1 (DPRP-1)) and DP9 (DPP9/DPRP-2) are highly conserved and ubiquitously expressed intracellular exopeptidases of the serine protease SC clan S9b subfamily (which includes (DPP4/DPIV/DPP4V/CD26 EC 3.4.14.5)) that share 61% identity at the amino acid level in humans (1–4). Studies utilizing nonselective DP⁷ inhibitors (5) and more selective DP8/DP9 inhibitors (6–8) have suggested an important immunological role for DP8/DP9. DP8/DP9 have also been implicated in the allergic response of the lung (9) and inflammatory bowel disorders (10). *In vitro* studies have demonstrated non-enzymatic roles for DP8 and DP9 in cell migration, proliferation, and apoptosis (11). In cancer, increased DP8 mRNA has been found in chronic lymphocytic leukemia (12) and DP9 mRNA in testicular cancer (3), and increased levels of DP8/DP9 mRNA, protein, and enzymatic activity have been observed in human meningiomas (13). Ubiquitous but differential expression of DP8/DP9 has been observed in breast and ovarian carcinoma cell lines (14), and a study has identified DP8/DP9 as survival factors for the Ewing sarcoma family of tumors (15). Despite these findings, the mechanism(s) of DP8/DP9

* This work was supported in part by an anonymous philanthropic grant (to C. A. A.), Canadian Institutes of Health Research Grant MOP-37937 (to C. M. O.), an infrastructure grant from the Michael Smith Research Foundation (University of British Columbia Centre for Blood Research), and by the British Columbia Proteomics Network (to C. M. O.).

♦ This article was selected as a Paper of the Week.

✂ Author's Choice—Final version full access.

[5] This article contains supplemental Figs. S1–S5 and Tables S1–S10.

¹ Supported by a Trevor Prescott Freemasons Memorial Scholarship (The Masonic Foundation, Australia), a Flinders University Overseas Field Trip Grant to visit the Overall Laboratory (February 2007 to August 2008), and a Flinders University Research Scholarship (Flinders University, Australia).

² Present address: Centre for Cancer Biology, SA Pathology, Adelaide, South Australia, 5000, Australia.

³ Employee of the Faculty of Medicine, Sebelas Maret University, Surakarta 57126, Indonesia. Supported by a Directorate General of Higher Education Ph.D. scholarship from the Indonesian Government.

⁴ Both authors are senior authors.

⁵ To whom proteomics correspondence should be addressed: University of British Columbia, Centre for Blood Research and Faculty of Dentistry, 4.401 Life Sciences Institute, 2350 Health Sciences Mall, Vancouver, British Columbia V6T 1Z3, Canada. Tel.: 604-822-2958; Fax: 604-822-7742; E-mail: chris.overall@ubc.ca.

⁶ To whom main correspondence should be addressed: School of Biological Sciences, Flinders University, GPO BOX 2100, Adelaide, SA, 5001, Australia. Tel.: 61-88201078; Fax: 61-882012030; E-mail: cathy.abbott@flinders.edu.au.

⁷ The abbreviations used are: DP, dipeptidyl peptidase; EGFP, enhanced green fluorescent protein; IPI, International Protein Index; TAILS, terminal amine isotopic labeling of substrates.

function in these events has yet to be identified, and their exact biological roles remain unknown. Uncovering protease substrates greatly assists in revealing the functions of proteases *in vivo* and their significance in pathophysiological processes (16, 17).

In vitro, both DP8 and DP9 cleave the well known DP4 substrates neuropeptide Y(1–36), glucagon-like peptide-1(7–36), glucagon-like peptide-2(1–33), and peptide YY(1–36) (18, 19). *In vitro*, DP8 cleavage of chemokine stromally derived factor 1 (CXCL12)- α/β , interferon- γ -inducible protein, and interferon-inducible T cell α -chemoattractant, also known DP4 substrates, has been demonstrated (20). However, as DP8 and DP9 are intracellular enzymes, it is unlikely that these secreted substrates will be of physiological relevance *in vivo*. Clues for their *in vivo* roles come from studies blocking DP8/DP9 or DP1V expression, which leads to neuropeptide Y-driven cell death within the Ewing sarcoma family of tumors cells (15). To date, the first and only *in vivo* substrate identified for DP9 is the antigenic peptide renal ubiquitous-1(34–42) with DP9 proteolysis preventing major histocompatibility complex class I cell surface antigen presentation (21). Besides these initial studies, no comprehensive effort has been made to identify the *in vivo* substrates of DP8 and DP9 on a system-wide scale.

This study used a positional N-terminal proteomics approach, terminal amine isotopic labeling of substrates (TAILS), to identify the substrate degradome of DP8 and DP9. TAILS is focused around the isolation of protein and peptide N termini for proteomic identification of neo-N termini resulting from proteolytic events (22). This method was recently used to detect cleavage events *in vivo* in inflamed mouse skin (23). Stable human ovarian cancer (SKOV3) cell lines expressing enzyme-active and catalytically inactive forms of DP8 and DP9 were generated, and their cytoplasmic proteomes were isolated and analyzed by TAILS. A number of candidate substrates were identified and confirmed, including two of biological interest, calreticulin and adenylate kinase 2. This work reveals the involvement of DP8 and DP9 in cellular energy homeostasis pathways in this ovarian cancer cell line.

EXPERIMENTAL PROCEDURES

All chemicals were purchased from Sigma unless stated otherwise.

Stable Cell Culture and Flow Cytometry—SKOV3 cells were maintained (14) with G418 addition (500 $\mu\text{g}/\text{ml}$) to stable transfectants. FuGENE[®] 6 (Roche Diagnostics) was used to stably transfect cells with constructs of pEGFPN1 (Clontech) alone or with wild-type human DP8_(882 aa) and DP9_(863 aa, short form) (where aa is amino acid) or catalytically inactive mutants DP8(S739A) and DP9(S729A) (11). Clonal cell lines were generated by single cell sorting of transfected parental cells using a FACSAria (Pharmingen) with initial supplementation of growth medium with 0.5 \times hybridoma fusion cloning supplement (Roche Diagnostics) and gentamicin (16 mg/ml). Stable EGFP-expressing transfectants were monitored using a FACScan (Pharmingen).

Isolation of Cytoplasmic Proteomes—Cells were grown to confluence in three T175 flasks, washed with PBS (three times, 10 ml) to remove serum proteins, and then incubated for 3 h in 15 ml of phenol red-free, serum-free DMEM (Invitrogen). Cells

were washed with ice-cold PBS, detached with 0.2% (w/v) EDTA/PBS, and then resuspended in ice-cold PBS. Cells ($0.5\text{--}2 \times 10^7$) pooled from three flasks were pelleted by centrifugation ($1500 \times g$, 5 min), resuspended in homogenization buffer (50 mM HEPES, pH 7.2, 200 mM NaCl, 10 mM CaCl₂) containing protease inhibitors (0.2 mM PMSF, 10 μM E64, 1 μM pepstatin A, and 1 mM EDTA), and then gently lysed by nitrogen cavitation (800 p.s.i., 30 min on ice) using a Parr Cell Disruptor (Parr Instrument Co.). Lysates were clarified by centrifugation ($1500 \times g$, 10 min, and 4 $^{\circ}\text{C}$), and then supernatants were subjected to ultracentrifugation (type 70.1 Ti rotor, $100,000 \times g$, 60 min at 4 $^{\circ}\text{C}$; Beckman Coulter Ultracentrifuge; Palo Alto, CA) for separation of membrane and cytosolic fractions. Cytosolic fractions were further clarified by additional ultracentrifugation ($100,000 \times g$, 30 min, 4 $^{\circ}\text{C}$). Protein concentrations were determined by micro-Bradford assay (Bio-Rad). Aliquots were made and stored at -70°C until TAILS proteome analysis.

TAILS—TAILS was performed using dimethylation labeling of primary amines of protein N termini and ϵ -amino acids of lysine side chains as described (22). In brief, equal quantities of cytosolic proteome (supplemental Table S1) from enzyme-active and catalytically inactive cell lines (both DP8 and DP9) were concentrated and purified by 12% (v/v final) TCA precipitation. Protein denaturation, reduction, and alkylation of cysteine residues was performed as described previously (22). Samples were isotopically labeled by dimethylation using formaldehyde as described previously (22) (supplemental Table S1). Residual formaldehyde was quenched; then heavy and light isotopically labeled samples were combined, concentrated, and purified by acetone precipitation and tryptically digested, and then labeled peptides were enriched by a negative selection step using a dendritic polyglycerol aldehyde polymer as described (22). Blocked N-terminal peptides (unbound) were physically separated from the polymer-captured peptides via 10-kDa Microcon centrifugation (Millipore, Bedford, MA) (22). Sample and wash flow-throughs were combined and then prepared for off-line strong cation exchange-HPLC fractionation or desalting (supplemental Table S1). Three biological replicates for both DP8 and DP9 were subjected to the TAILS process in three independent experiments.

Off-line Strong Cation Exchange-HPLC Fractionation and Peptide Desalting—Desalting and pre-fractionation of samples ($\sim 100 \mu\text{g}$) by strong cation exchange-HPLC, prior to LC-MS/MS analysis, was performed as described (24). N-terminal peptides not fractionated by strong cation exchange-HPLC (supplemental Table S1) were desalted using reverse phase-solid phase extraction via Sep-Pak[®] C₁₈ column (Waters, Milford, MA) according to the manufacturer's recommendations.

In-line Liquid Chromatography and Tandem-Mass Spectrometry—Peptide samples were analyzed by in-line reverse-phase nanospray LC-MS/MS using a C18 column (150-mm \times 100- μm column at a flow rate of 100–200 nl min^{-1}) coupled to a quadrupole time-of-flight QStar XL hybrid electrospray ionization mass spectrometer (Applied Biosystems/MDS-Sciex, Concord, Ontario, Canada) or a QStar Pulsar mass spectrometer (Applied Biosystems/MDS-Sciex, MDS-Sciex, Concord, Ontario, Canada). Samples were loaded, eluted, and separated on the C18 column, and MS data were acquired automatically

DP8 and DP9 Substrate Discovery

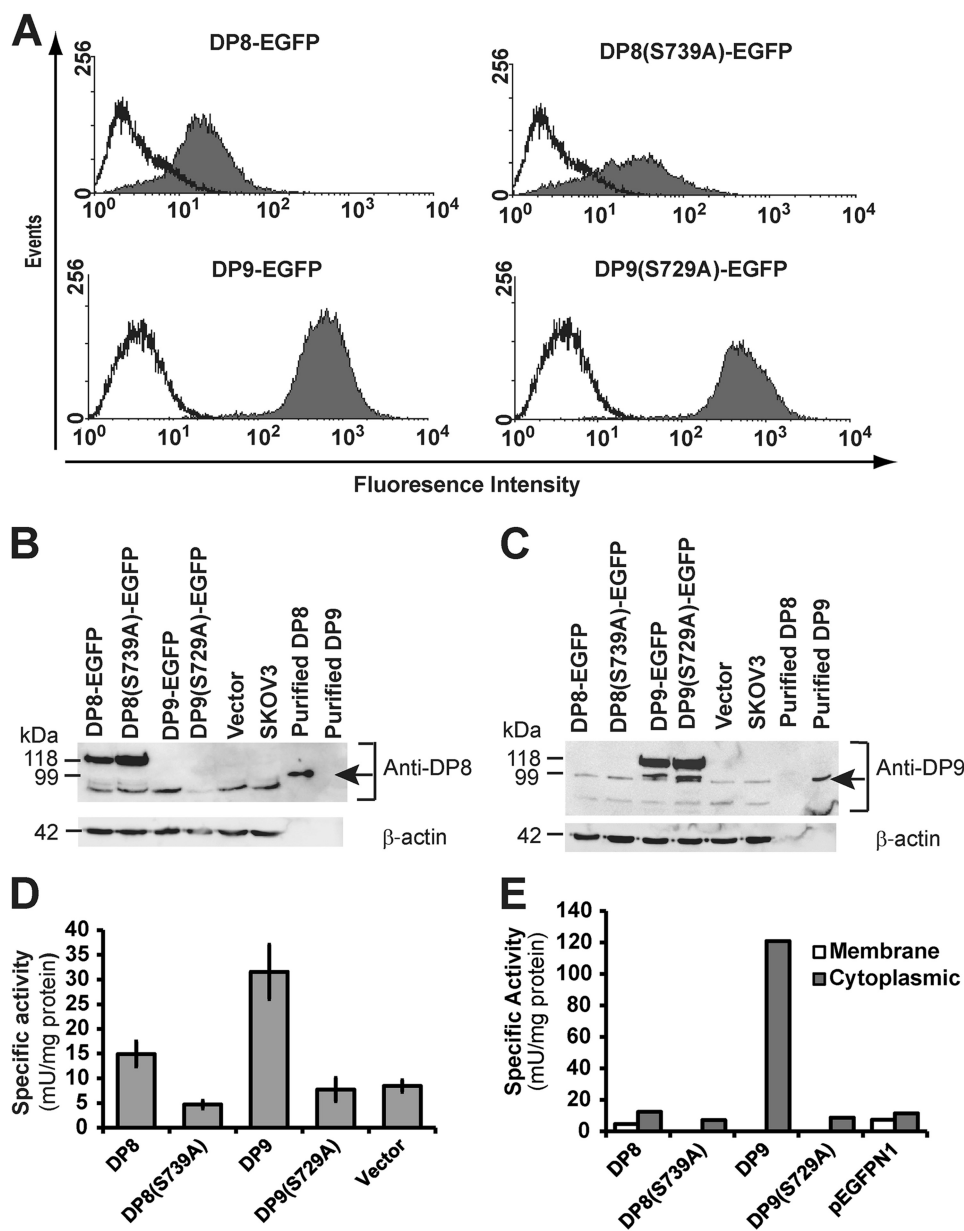


FIGURE 1. Characterization of stable wild-type and mutant DP8 and DP9 SKOV3 cell lines. *A*, cells transfected with wild-type (DP8-EGFP and DP9-EGFP) or mutant (DP8(S739)-EGFP and DP9(S729A)-EGFP) constructs (filled histograms) or nontransfected cells (open histograms) were analyzed by fluorescent flow cytometry on a FACScan. *B* and *C*, cell lysates (50 μ g) from DP8-EGFP, DP8(S739A)-EGFP, DP9-EGFP, DP9(S729A)-EGFP, vector-transfected, and nontransfected SKOV3 cells were analyzed by 8% (w/v) SDS-PAGE and immunoblotting for detection of DP8 (*B*) or DP9 (*C*). Recombinant purified DP8 and DP9 were included as controls and are indicated by arrows. For a loading control, β -actin was detected. *D* and *E*, specific activity against the synthetic DP substrate H-Ala-Pro-*p*-nitroanilide (0.5 mM) was determined in whole cells (*D*) and in membrane and soluble fractions (*E*). Values in *D* are expressed as means \pm S.E. ($n = 10$). Values in *E* are from a single experiment.

using Analyst QS version 1.1 software (Applied Biosystems/MDS-Sciex, Concord, ON, Canada) as described (25).

Mass Spectrometry Data Analysis—MS peak lists were searched by MASCOT (version 2.2, Matrix Science, London, UK) against the human International Protein Index (IPI) database (version 3.16, 62,322 entries, release date April, 2006). MASCOT searches of MS data were performed separately for heavy- and light-labeled peptides. Searches were performed using the following modifications: fixed carbamidomethylation of cysteines (+57.021 Da (Cys)), fixed heavy lysine (+34.0631 Da (Lys)), or light lysine (+28.0311 Da (Lys)); variable methionine oxidation (+15.995 Da (Met)), and fixed and variable

modifications of N termini with heavy formaldehyde (+34.0641 Da (N termini)), light formaldehyde (+28.0311 Da (N termini)), and acetylation (+42.011 Da (N termini)). The additional search criteria used were as follows: semi-ArgC cleavage specificity with up to three missed cleavages; a monoisotopic mass error window for the parent ion of 0.4 to 0.6 Da; peptide mass tolerance of 0.4 Da for MS/MS fragment ions; and the scoring scheme ESI-QUAD-TOF. Allowed peptide charge states were 1⁺, 2⁺, and 3⁺. Search results were analyzed using the Trans-Proteomic Pipeline (version 4.0 JETSTREAM revision 2, Build 200807011544 (MinGW)) (26) with PeptideProphet (27) sensitivity-error rate analysis. Quantification of

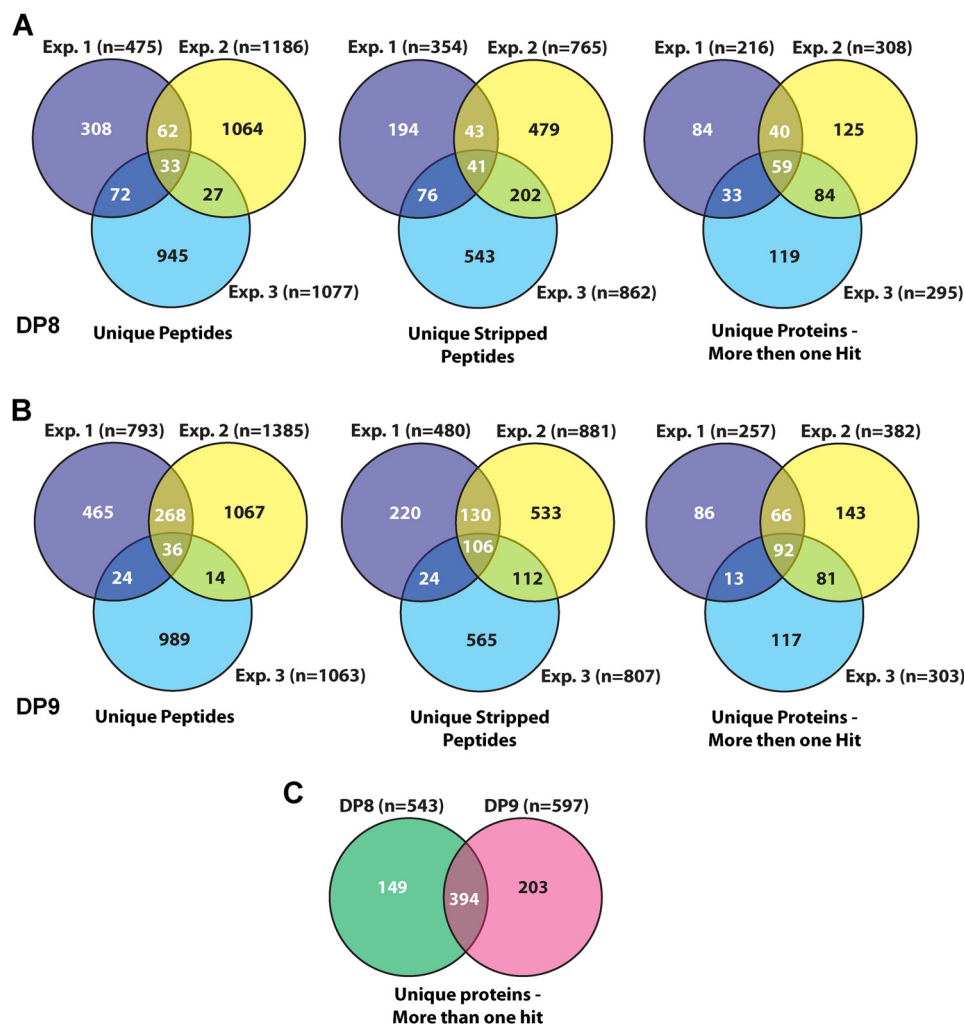


FIGURE 2. Summary of total peptides and proteins identified by TAILS analysis. *A* and *B*, three-way Venn diagrams of the number of unique peptides, unique stripped peptides, and unique proteins (identified by more than one spectra) identified by MASCOT searches in experiments (Exp.) 1, Exp. 2, and Exp. 3 for DP8 (*A*) and DP9 (*B*). *C*, two-way Venn diagram of unique proteins (identified by more than one hit) identified from all datasets for DP8 and DP9. The intersection of *C* displays the number of overlapping proteins identified in both the DP8 and DP9 datasets. The number of unique peptides for each experiment takes into account all possible modifications of a given peptide, including variable oxidation of methionine residues, although the number of unique stripped peptides for each experiment refers to unique peptides after the removal (stripping) of all possible modifications. The total number of unique proteins excludes any "single hit" proteins, *i.e.* a protein that is not identified by any other peptide/spectra in the dataset. All peptides were identified with $\geq 95\%$ confidence according to PeptideProphet. All MASCOT searches were performed against the human IPI database (version 3.16, 62,322 entries, release date 4/2006).

the ratio of heavy to light isotopically labeled peptides was achieved by using ASAPRatio (28) software. ASAPRatios were manually checked and edited, and CLIPPER was used to identify statistically significant changes in cleaved neo-N peptides (29).

DP8 and DP9 are exopeptidases with a strong preference for cleavage of N-terminal dipeptides mainly after a Pro residue in the P1 position ($\text{NH}_2\text{-P2-P1-P1}'\text{-P2}'\text{-}$). Because of this strict canonical specificity, datasets were also manually parsed to identify all peptides with a cleaved or noncleaved Pro residue in what would be the P1 position of a DP8/DP9 substrate. Pairs of peptides that differed in length by two amino acids at their N termini, but did not contain a Pro in P1, were also selected as candidate substrates.

Additional substrates and proteins that are altered (in expression or non-DP8/DP9 proteolysis) via DP8/DP9-affected pathways were identified from quantitative analysis of heavy/light (protease/control) isotope-labeled peptide abundance ratios.

Only peptides identified with $\geq 95\%$ confidence (PeptideProphet) were used for quantitative analysis. ASAPRatios were normalized by recentering the raw datasets around a median of one and then applying a natural logarithm transformation. This enabled the exclusion of obvious outliers and established a normal range for determining significance by using means and S.D. of the normalized data to determine 90% confidence intervals of the nontransformed data. This was achieved using the R statistical package. High and low ratio peptides were considered to be either substrates of DP8/DP9 or derived from proteins that were either differentially expressed or processed by an alternative protease to DP8/DP9.

Functional Annotation and Pathway Mapping—UniProt Knowledge Base (UniProtKB) accession numbers were mapped to protein IPI numbers. Functional annotation and biological pathway information were obtained from UniProtKB entries or by using the database for annotation, visualization and integrated discovery (DAVID), version 6.7 (30) (david.abcc.ncifcrf.

DP8 and DP9 Substrate Discovery

TABLE 1

Candidate DP8 and DP9 substrates

Peptides listed include the following peptides: (i) having a proline N-terminal to the MS/MS-identified peptide so that the peptide may have resulted from DP8/DP9 cleavage; (ii) peptides that contained a Pro in the P1 position; and (iii) peptides differing by two N-terminal dipeptide residues likely to have been removed by DP8/DP9 proteolysis. All individual peptides are listed for DP8 and DP9 in supplemental Tables S2 and S3, respectively. The MS/MS spectra for each of the peptides in the supplemental Tables can be found in the associated supplemental Tables S2 and S3 spectra files. #, number; #AA, number of amino acids in full-length protein; Seq. Pos., position of identified peptide in the full-length protein; -2AA, the two amino acids preceding the identified peptide, of these (-M) indicates initiator methionine; +1 AA, the first amino acid adjacent to the C-terminal end of the MS/MS-identified peptide; Exp, experiment number; Conf. is the confidence determined by Peptide Prophet modeling that the peptide identification was correctly assigned. Peptides in parentheses are those that have a lower confidence in spectra to peptide assignment, but their presence supports the protein being a substrate if identified from a separate high confidence peptide. Bold underlined text indicates the amino acid that DP8/DP9 will cleave at if the identified peptide is a *bona fide* substrate. Where more than one occurrence of a peptide was identified, only the highest confidence was reported in this table. Values for all peptides can be found in supplemental Tables S1 and S2.

UniProtKB Accession	Protein	#AA	Seq. Pos.	-2 AA	Identified Peptide	+1 AA	DP8			DP9			Localization	Biological Pathway			
							Exp.	Hits	Conf. (%)	Exp.	Hits	Conf. (%)					
P60709	Actin, cytoplasmic 1	375	103-116 101-116	HP	VLLTEAPLNPKANR	E				1	1	>96	Cytoplasm; cytoskeleton	Focal adhesion, Adherens junction, Tight junction, Leukocyte transendothelial migration, Regulation of actin cytoskeleton			
				EE	(HPVLLTEAPLNPKANR)	E				1	1	>50					
P62736	Actin, aortic smooth muscle	377	47-64 49-64	VM	VGMGQKDSYVGVDEAQSQR	G				1	2	100	Cytoplasm; Cytoskeleton	Vascular smooth muscle contraction			
				VG	VMVGMGQKDSYVGVDEAQSQR	G				1	4	100			2	2	100
P54819	Adenylate kinase 2, mitochondrial	239	4-17 2-17	AP	SVPAAEPEYPKGIR	A				1	2	>90	Mitochondrial intermembrane space	Purine metabolism, energy metabolism, nucleotide synthesis			
				-M	APSVPAAEPEYPKGIR	A	2	1	>75	2	1	>99			1	1	>99
							2	5	>99	2	5	>99			3	1	>99
Q8NI99	Angiopoietin-related protein 6 precursor	470	131-142	GA	EPAAALALLGER	V				152	1	>75	Extracellular space	Angiogenesis, cell differentiation (probable)			
							252	2	>95	252	2	>95					
P31939	Bifunctional purine biosynthesis protein PURH	592	2-22	-M	APGQLALFSVSKTGLVEFAR	N	1	1	100	3	2	100	Cytoplasm	Purine metabolism, IMP biosynthesis via de novo pathway One carbon pool by folate,			
							3	1	>95								
P11586	C-1-tetrahydrofolate synthase, cytoplasmic	934	2-16	-M	APAEILNGKEISAIQR	A	1	1	>95				Cytoplasm	Glyoxylate and dicarboxylate metabolism, One carbon pool by folate, tetrahydrofolate interconversion, purine biosynthesis, amino-acid biosynthesis			
							2	1	>99								
P27797	Calreticulin	417	20-36 18-36	EP	AVYFKEQFLDGGWTSR	W	2	2	>90	1	2	>99	Cytoplasm; Endoplasmic Reticulum; Plasma Membrane; Nucleus; Secreted	Antigen processing and presentation			
				VA	EPAVYFKEQFLDGGWTSR	W	1	4	100	1	13	100					
							2	5	100	2	4	>90			3	1	>95
Q9UBR2	Cathepsin Z/X	303	58-69	YL	SPADLPKSWDWR	N	1	1	>99	1	3	>85	Lysosome; Endoplasmic Reticulum; extracellular space	Lysosome, proteolysis			
							2	1	>90	2	1	>50					
Q8N888	CDNA FLJ39703 fis, clone SMINT2012195	145	56-78	RP	AGEEDAGGPERPGDVVNVVFDVDR	S				1	2	>99	Unknown	Not available			
Q12882	Dihydropyrimidine dehydrogenase [NADP+]	1025	4-21	AP	VLSKDSADIESILANPR	T	1	1	>85	1	1	100	Cytoplasm	Pyrimidine metabolism, beta-Alanine metabolism, Pantothenate and CoA biosynthesis, Drug metabolism			
Q16643	Drebrin	648	480-493	WP	GNGEGASTLQGEPR	A	252	2	>90	252	3	>90	Cytoplasm	Binds F-actin, cell differentiation, neurogenesis			
Q05639	Elongation factor 1-alpha 2	463	250-266 248-266	LP	(LQDVYKIGIGITVPVGR)	V				1	1	>65	Cytoplasm; Nucleus	Protein biosynthesis			
				LR	LPQLQDVYKIGIGITVPVGR	V				1	1	>80			352	2	100
Q9Y5Q0	Fatty acid desaturase 3	445	107-116	GP	LNAQLVEDFR	A	252	2	>85				Endoplasmic Reticulum Membrane	Electron transport, fatty acid biosynthesis/metabolism, lipid biosynthesis/metabolism			
P04075	Fructose-bisphosphate aldolase A	363	3-21 1-21 6-21 8-21	MP	YQYPALTEQKKEKLSIAHR	I	2	2	100	1	2	100	Cytoplasm	Glycolysis/Gluconeogenesis, Pentose phosphate pathway, Fructose and mannose metabolism			
				-	MPYQYPALTEQKKEKLSIAHR	I	2	1	100	2	2	100					
				YP	(ALTEQKKEKLSIAHR)	I				152	2	>90					
				AL	TEQKKEKLSIAHR	I				1	1	>95			2	2	>70
Q08380	Galectin-3-binding protein	585	456-475	RY	YPVQSFQTPQHPFLQDKR	V	2	2	>95				Extracellular	Cell adhesion			
O00214	Galectin-8	316	58-58	KP	RADVAHFHNPR	F				252	4	>95	Cytoplasm	Carbohydrate binding			
Q13151	Heterogeneous nuclear ribonucleoprotein A0	305	174-183	KA	VPKEDIYSGGGGGGSR	S	2	2	100				Nucleus	mRNA-binding component of ribonucleosomes			

gov). The TopFIND knowledge base was used to obtain functional insights to the cleaved substrates (31).

DP-specific Enzyme Assay—Diprollyl peptidase enzymatic activity was assayed using 0.5 mM H-Ala-Pro-*p*-nitroanilide (Bachem, Bubendorf, Switzerland) as described previously (14). Enzyme activity was expressed as milliunits/mg of protein,

where 1 unit of activity is defined as the amount of enzyme that cleaves 1 μ mol of substrate per min under the given assay conditions.

Western Blot Analysis—Protein extraction, SDS-PAGE, and Western blotting were performed as described previously (14) using primary antibodies for DP8 (RP1-DP8, Triple Point Bio-

TABLE 1—continued

UniProtKB Accession	Protein	#AA	Seq. Pos.	-2 AA	Identified Peptide	+1 AA	DP8			DP9			Localization	Biological Pathway
							Exp.	Hits	Conf. (%)	Exp.	Hits	Conf. (%)		
P10253	Lysosomal alpha-glucosidase	957	78-89	RA	VPTQCDVPPNSR	F	1	1	>99				Lysosome Membrane	Galactose metabolism, Starch and sucrose metabolism, Lysosome
O00754	Lysosomal alpha-mannosidase	1011	602-613	SW	SPALTIENEHIR	A				1	2	100	Lysosome	Other glycan degradation, Lysosome
P10619	Lysosomal protective protein (cathepsin A)	480	46-54	EA	APDQDEIQR	L	1	2	>99				Lysosome; Endoplasmic reticulum	Lysosome, Renin-angiotensin system
Q15785	Mitochondrial import receptor subunit TOM34	309	4-13	AP	(KFPDSVEELR)	A				1	1	>90	Cytoplasm; Mitochondrial outer membrane	Protein targeting and import of proteins to mitochondria, chaperone
P22894	Matrix metalloproteinase 8 (MMP8)	467	441-451	GP	RYYAFDLIAQR	V	2	2	>60				Cytoplasmic granule; secreted, extracellular space	Collagen degradation, proteolysis
Q9NTK5	Obg-like ATPase 1	396	2-18	-M	PPKKGDDGIKPPPIIGR	F	1	1	>99				Cytoplasm	ATP catabolism
Q06830	Peroxiredoxin-1	199	90-110	VN	TPKKQGGGLGPMNIPVSDPKR	T	2	2	>95				Cytoplasm	Oxidoreductase, cellular redox regulation, intracellular redox signaling, proliferation
P30044	Peroxiredoxin-5, mitochondrial	214	54-77	AM	APIKVGDAIPAVEVFEGEPGNKV N	L	1	1	100				Mitochondrial	Oxidoreductase, cellular redox regulation, intracellular redox signalling
P07737	Profilin-1	140	39-56	GK	TFVNIITPAEVGLVGKDR	S				1	1	>99	Cytoplasm; Cytoskeleton	Regulation of actin cytoskeleton, response to growth factor stimulus
			41-56	TE	VNIITPAEVGLVGKDR	S				1	1	100		
			53-56	VN	ITPAEVGLVGKDR	S				252	2	100		
										352	3	100		
										252	3	100		
P07602	Sap-mu-0 of Proactivator polypeptide precursor (prosaposin)	524	171-186	AP	FMANIPLLLYPQDGR	S				252	2	>85	Lysosome	Lysosomal degradation of sphingolipids
O00743	Serine/threonine-protein phosphatase 6	305	2-14	-M	APLDLDKYVEIAR	L				1	2	>95	Cytoplasm	Protein dephosphorylation, G1/S transition of mitotic cell cycle
							2	2	>99	2	2	>85		
Q53HE2	Triosephosphate isomerase	243	178-190	TA	TPQQAQEVHEKLR	G	2	1	>99	1	2	100	Cytoplasm	Glycolysis/Gluconeogenesis, Fructose and mannose metabolism, Inositol phos
			176-190	GK	TATPQQAQEVHEKLR	G	2	1	>99	1	1	100		
										2	1	>85		

logics Inc.), DP9 (RP1-DP9, Triple Point Biologics Inc.), β -actin (ab8227, Abcam, Cambridge, UK, or 011M4812, Sigma), calcitriculin (sc-6468, Santa Cruz Biotechnology Inc., Santa Cruz, CA), and adenylate kinase 2 (ab37594, Abcam).

In Vitro Validation of DP8 and DP9 Substrate Cleavage with MALDI-TOF MS Analysis—Recombinant human DP8_(882aa) and DP9_(892aa) were expressed and purified as described previously (20, 32). N-terminal peptides of 14 proteins identified by TAILS to be candidate substrates (Table 3) were synthesized to >95% purity by Genscript (Piscataway, NJ) or GL Biochem Ltd. (Shanghai, China). Peptides (10 μ M) were incubated with 1.7 milliunits of recombinant DP8 or DP9 in assay buffer: 50 mM Tris, 100 mM NaCl, pH 8.0, at 37 °C for up to 24 h. Calcitriculin and adenylate kinase 2 were also incubated in assay buffer alone or with DP8/DP9 in the presence of 10 μ M of the DP inhibitor, Val-Boro-Pro (PT-100/Talostat; obtained from Dr. Jonathon Cheng (Fox Chase Cancer Centre, Philadelphia) with approval from DARA BioSciences Inc., Raleigh, NC). At time points of 0, 1, 4, and 24 h, 5 μ l of each reaction was removed and stopped by the addition of 1% TFA. Peptides were desalted and cleaned by OMIX[®] C18 tip (Varian, Inc., Palo Alto, CA). Eluates were mixed 1:1 with α -cyano-3-hydroxycinnamic acid matrix solution (1% (w/v) α -cyano-3-hydroxycinnamic acid, 49.5% acetonitrile, 49.5% ethanol, 0.001% TFA) and spotted onto a standard stainless steel MALDI sample plate, and then masses of intact peptides and DP8/DP9 cleavage products were obtained by

MALDI-TOF MS analysis performed on a Waters Micromass[®] M@ALDI (Waters Micromass, Manchester, UK) or a Bruker Autoflex III MALDI MS/MS (Bruker, Billerica, MA). All cleavage experiments with MALDI-TOF analysis were performed in triplicate. MS spectra were processed using MassLynx 4.0 (Waters) software package.

Accession Information—All LC-MS/MS data (.wiff files) associated with this study may be downloaded from Proteome Commons.org Tranche using the following hash: YRRnIo-2jM9SRJ7vSBk7OG65e/3cVbIQ7ksECUIT97Doxwfg1YAGW-J5eHBqzMXog/IQFcGWzIS08gVKP/RqN+E1KLoVwAAAA-AAAAAYRg.

RESULTS

Generating Stable Clonal Cell Lines of Wild-type and Mutant DP8 and DP9—SKOV3 cells were stably transfected with constructs encoding enzymes DP8 and DP9, with a size of 882 and 863 residues, respectively, including the N-terminal β -propeller and C-terminal α/β -hydrolase domains. Clonal cell lines for both DP8 and DP9 were selected for equal expression of the active and inactive version of each enzyme in fusion with the fluorescent EGFP protein (Fig. 1A). DP8- and DP9-EGFP proteins were visualized by immunoblot (~118 kDa in mobility) confirming the heterologous expression of active and inactive proteases (Fig. 1B). All cell lines were found to express basal levels of endogenous DP8 and DP9 protein (~98 kDa in mobil-

DP8 and DP9 Substrate Discovery

ity) (Fig. 1B) that may contribute to background proteolysis and affect the discovery of substrates by TAILS. DP activity increased in the wild-type DP8- and DP9-transfected SKOV3 cells when compared with the catalytically inactive DP8(S739A), DP9(S729A), and vector-transfected controls (Fig. 1C). Enzymatic assays of fractionated clonal cell lines confirmed that this increase in DP activity is due to the overexpression of cytosolic DP8/DP9 (Fig. 1, D and E).

TAILS N-terminome Analysis of DP8 and DP9 Stable Cytoplasmic Proteomes—TAILS was performed on three isolations of cytoplasmic proteomes from both wild-type and catalytically inactive DP8- and DP9-stable SKOV3 cell lines. The total number of unique peptides and proteins identified within each experiment was determined (Fig. 2, A and B). Each TAILS experiment yielded 200–400 unique proteins that were identified from more than one N-terminal peptide occurrence, *i.e.* peptide/spectra (Fig. 2, A and B). The union of each DP8 TAILS experiment yielded 59 unique proteins (Fig. 2A), whereas the union of each DP9 TAILS experiment yielded 92 unique proteins (Fig. 2B). From all three experiments, a total of 543 unique proteins were identified for DP8, and 597 were identified for DP9, of which 394 proteins were common to both DP8 and DP9 (Fig. 2C).

Identification of Candidate DP8/DP9 Substrates by Parsing TAILS Data—A total of 22 and 21 proteins were identified by parsing for potential DP8 and DP9 substrates, respectively. Of these, 8/22 and 7/21 candidate substrates were uniquely identified for DP8 and DP9, respectively (Table 1). Most candidate substrates are localized to the cytoplasm or intracellular organelles (Table 1). Adenylate kinase 2 and calreticulin were two predominant proteins for which the most cleaved and non-cleaved peptides were identified for both DP8 and DP9 (Table 1). Approximately half of the peptides identified with the potential for DP8/DP9 cleavage were located at the N termini of the mature proteins as annotated in UniProtKB (Fig. 3, Table 1, and supplemental Figs. S2 and S3). Functional annotation and pathway mapping revealed the involvement of candidate substrates in biochemical pathways relating to lysosomal processes, carbohydrate metabolism, and nucleotide metabolism and synthesis (Table 1; supplemental Tables S6 and S7).

Identification of Candidate DP8/DP9 Substrates and DP8/DP9 Pathway-affected Proteins by Quantitative Analysis of TAILS Data—Quantitative analysis was only performed on datasets derived from the first two TAILS experiments for both DP8 and DP9 due to the poor recovery of labeled peptides from experiment 3 (data not shown). In total, 37 proteins were identified as potential DP8 substrates or DP8 pathway-affected proteins, and 55 proteins were identified as potential DP9 substrates or DP9 pathway-affected proteins; only 10 of these proteins were common to both DP8 and DP9 (supplemental Table S10). Of these, 17/37 and 10/55 proteins were identified as being candidate substrates of DP8 and DP9, respectively (Table 2), based on analysis of peptide positioning in the UniProtKB annotated protein sequences, *e.g.* peptides located at mature N termini. All other proteins identified (20 for DP8 and 45 for DP9) are listed in supplemental Table S10. Evidence of non-DP8/DP9 N- and C-terminal truncation of proteins was found (supplemental Table S10 and supplemental Figs. S3 and



FIGURE 3. Peptides of several candidate substrates identified by TAILS. Peptides identified by MS/MS are indicated by *bold underlined letters*. Light colored letters indicate precursor peptides of mature proteins or their initiator Met residues that are known to be removed as annotated in UniProtKB. The dipeptide residues identified as being cleaved, or as having the potential for cleavage, are outlined by a box. Where two peptides were identified by MS/MS as being the noncleaved DP8/DP9 precursor peptide (N-terminal dipeptide intact) and the DP8/DP9 cleavage product peptide (N-terminal dipeptide removed), an *arrow* is used to indicate the site of DP8/DP9 proteolysis. Peptides for C-1-tetrahydrofolate synthase and cytoplasmic and lysosomal protective protein were identified from manual parsing of the DP8 dataset. All other proteins were identified in both DP8 and DP9 datasets. The peptides corresponding to three of the potential cleavage sites indicated for fructose-bisphosphate aldolase A were only identified from manual parsing of the DP9 dataset (see Table 1). Full-length protein sequences of the above and other potential substrates can be found in supplemental Figs. S2 and S3.

S4), demonstrating that non-DP proteolytic pathways are altered by increasing DP8/DP9 activity. Interestingly, approximately half of the proteins identified for DP8 are mitochondrial, potentially occurring during mitochondrial turnover (Table 2 and supplemental Table S10). Functional annotation and pathway mapping revealed that many of the identified proteins play key roles in carbohydrate, nucleotide, and protein metabolism (supplemental Tables S8 and S9).

In Vivo Substrate Specificity of DP8 and DP9—Fig. 4 displays the frequency of residues in the P1 and P2 position of all DP8 and DP9 candidate substrates identified in this study. As expected, the majority of candidate substrates contain a Pro in the P1 position (Fig. 4, A and B) followed by an Ala in the P2 position (Fig. 4, C and D). The frequency of residues in the P1 and P2 position for the remaining candidate substrates was variable for both DP8 and DP9 (Fig. 4).

DP8 and DP9 cleave *in vitro* the N termini of adenylate kinase 2, calreticulin, and other peptides. *In vitro* validation of DP8/DP9 cleavage was performed for 14 candidate substrates, including the two most abundant substrates, adenylate kinase 2 and calreticulin (Table 3, Figs. 5 and 6, and supplemental Fig. S5). In total, cleavage of 9/14 substrates by both DP8 and DP9 was confirmed. No unique cleavage was identified for DP8 or DP9 demonstrating similar enzyme specificity and large substrate overlap between these enzymes.

TABLE 2

Candidate DP8 and DP9 substrates identified by quantitative analysis of TAILS data

Peptides were identified as significantly increased or decreased in the active DP8 EGFP or DP9-EGFP SKOV3 cells compared with the catalytically inactive forms. Individual peptides identified by MS/MS can be found for DP8 and DP9 in supplemental Tables S4 and S5, respectively. The MS/MS spectra for each of these peptides can be found in the associated supplemental Tables S4 and S5 spectra files. #, number; #AA, number of amino acids in full-length protein; Seq. Pos., position of identified peptide in the full-length protein; -2AA, the two amino acids preceding the identified peptide, of these (-M) indicates initiator methionine; +1AA, the first amino acid adjacent to the C-terminal end of the MS/MS-identified peptide; Exp., experiment number; Hits, number of spectra positively identified for each peptide; Ratio H/L, the isotopic heavy/light ratio. Ratios are expressed as means \pm S.D. Bold underlined text indicates the amino acid that DP8/DP9 will cleave at if the identified peptide is a *bona fide* substrate. Arrows (\downarrow / \uparrow) indicate whether the presence of peptide was significantly increased or decreased.

UniProtKB Accession	Protein	#AA	Seq. Pos.	-2 AA	Identified Peptide	+1 AA	DP8			DP9			Localization
							Exp.	Hits	Ratio H/L	Exp.	Hits	Ratio H/L	
P61981	14-3-3 protein gamma	247	2-19	-M	<u>V</u> DREQLVQKARLAEQAERY	Y				2	1	\downarrow 0.32	Cytoplasm
P42704	130 kDa leucine-rich protein	1402	60-77	LY	AIAAKEKDIQEESTFSSR	K	1 2	1 4	\downarrow 0.14 \downarrow 0.51 \pm 0.01				Mitochondria; Nucleus; Nucleus membrane
P24752	Acetyl-CoA acetyltransferase, mitochondrial	427	34-49	SY	<u>V</u> SKPTLKEVVIVSATR	T	1 2	1 3	\downarrow 0.18 1.65 \pm 0.10				Mitochondria
P62736	Actin, aortic smooth muscle	377	45-64	QG	<u>V</u> MVGMGQKDSYVGDEAQSQR	G	1 2	1 1	\downarrow 0.24 1.04	1 2	6 4	\uparrow 3.50 \pm 1.21 1.27 \pm 0.06	Cytoplasm; Cytoskeleton
			47-64	<u>V</u> M	VGMGQKDSYVGDEAQSQR	G				1	2	1.06 \pm 0.00	
			50-64	<u>G</u> M	GQKDSYVGDEAQSQR	G				1	1	\downarrow 0.37	
			231-256	<u>M</u> A	TAASSSSLEKSYELPDGQVITIGNER	F				1	1	\uparrow 6.01	
P54819	Adenylate kinase 2, mitochondrial	239	2-17	-M	<u>A</u> PSVPAAEPEYPKGIIR	A	1 2 3	1 4 1	\downarrow 0.17 1.47 \pm 0.15 \downarrow 0.22	1 2 3	1 4 1	\uparrow 2.44 \uparrow 3.04 \pm 0.37 0.22	Mitochondria; Mitochondrial inner membrane
			4-17	<u>A</u> P	SVPAAEPEYPKGIIR	A						0.63	
P31939	Bifunctional purine biosynthesis protein PURH	592	2-22	-M	<u>A</u> PGQLALFSVSDKTGLVEFAR	N	1 3	1 1	\downarrow 0.32 0.67				Cytoplasm
Q9UBR2	Cathepsin Z/X	303	58-69	YL	<u>S</u> PADLPKSWDWR	N	1 2	1 1	\downarrow 0.24 1.04				Lysosome
P11586	C-1-tetrahydrofolate synthase, cytoplasmic	935	2-17	-M	<u>A</u> PAEILNGKEISAQIR	A	2 1	1 1	\uparrow 2.45 0.82				Cytoplasm
P50454	Collagen-binding protein 2 (Serpin-H1)	418	19-46	<u>L</u> A	AEVKPPAAAAAPGTAELKSPAATLAER	S				2	1	\uparrow 2.87	Endoplasmic reticulum lumen
Q07021	Complement component 1, Q subcomponent-binding protein, mitochondrial	282	74-94	GS	<u>L</u> HTDGDKAFVDFLSDEIKEER	K	1 2 3	1 2 2	\downarrow 0.29 1.19 \pm 0.01 0.51 \pm 0.00				Mitochondrial matrix; Nucleus
P30084	Enoyl-CoA hydratase, mitochondrial	290	28-41	PF	<u>A</u> SGANFEYIIAEKR	G	1 2 3	2 9 2	\downarrow 0.25 \pm 0.00 1.01 \pm 0.12 0.72 \pm 0.00				Mitochondrial Matrix
P41091	Eukaryotic translation initiation factor 2 subunit 3	472	2-16	-M	<u>A</u> GGEAGVTLGQPHLSR	Q	2 1	1 1	\downarrow 0.05 1.08	1	1	\downarrow 0.11	Cytoplasm
P04075	Fructose-bisphosphate aldolase A	364	9-22	<u>A</u> L	TPEQKKELSDIAHR	I				1	1	\uparrow 3.81	Cytoplasm
			3-22	<u>M</u> P	YQYPALTPQKKELSDIAHR	I				1	1	0.70	
			2-22	- <u>M</u>	PYQYPALTPQKKELSDIAHR	I				1	2	\downarrow 0.19 \pm 0.00	
			1-22	-	MPYQYPALTPQKKELSDIAHR	I				2	1	0.89	
			32-43	<u>I</u> L	AADESTGSIAKR	L				2	2	0.56 \pm 0.00	
Q724H8	KDEL motif-containing protein 2	507	21-31	AA	<u>G</u> APEVLVSAPR	S	1	1	\downarrow 0.11				Endoplasmic reticulum
O00754	Lysosomal alpha-mannosidase	1011	602-613	<u>S</u> W	SPALTIENEHIR	A				2 1	1 2	\uparrow 4.46 \uparrow 2.62 \pm 0.25	Lysosome
Q15785	Mitochondrial import receptor subunit TOM34	309	2-13	-M	<u>A</u> PKFPDSVEELR	A	2	1	\uparrow 2.74				Cytoplasm; Mitochondrial outer membrane
Q9H1k1	NiFU-like N-terminal domain-containing protein	167	35-57	RL	<u>Y</u> HKKVVDHYENPR	N	1	1	\downarrow 0.14				Mitochondria; Cytoplasm; Nucleus
Q9NTK5	Obg-like ATPase 1	278	2-18	-M	<u>P</u> PKGGDGIKPPPIIGR	F	1	1	\downarrow 0.12	2	2	\downarrow 0.38 \pm 0.38	Cytoplasm
P36871	Phosphoglucosylase 1	562	2-23	-M	<u>V</u> KIVTVKTQAYQDQKPGTSGLR	K	1 2	1 4	\downarrow 0.15 1.05 \pm 0.04				Cytoplasm
P07737	Profilin-1	139	38-55	GK	<u>T</u> EVNITPAEVGVLVGKDR	S				1	1	\uparrow 4.01	Cytoplasm; Cytoskeleton
			40-55	<u>T</u> F	VNITPAEVGVLVGKDR	S				1	1	\downarrow 0.39	
Q99436	Proteasome subunit beta type 7	277	44-62	TG	<u>T</u> TIAGVVYKDGIVLGADTR	A	1 2	1 3	\downarrow 0.28 1.23 \pm 0.00				Cytoplasm; Nucleus; Proteasome
Q53HE2	Triosephosphate isomerase	249	176-190	GK	<u>T</u> ATPQQAQEVHEKLR	G	2	1	\downarrow 0.49	1	1	\uparrow 4.46	Cytoplasm
			178-190	<u>T</u> A	TPQQAQEVHEKLR	G	2	1	1.34	1	2	\uparrow 2.40 \pm 0.00	

DP8 and DP9 Substrate Discovery

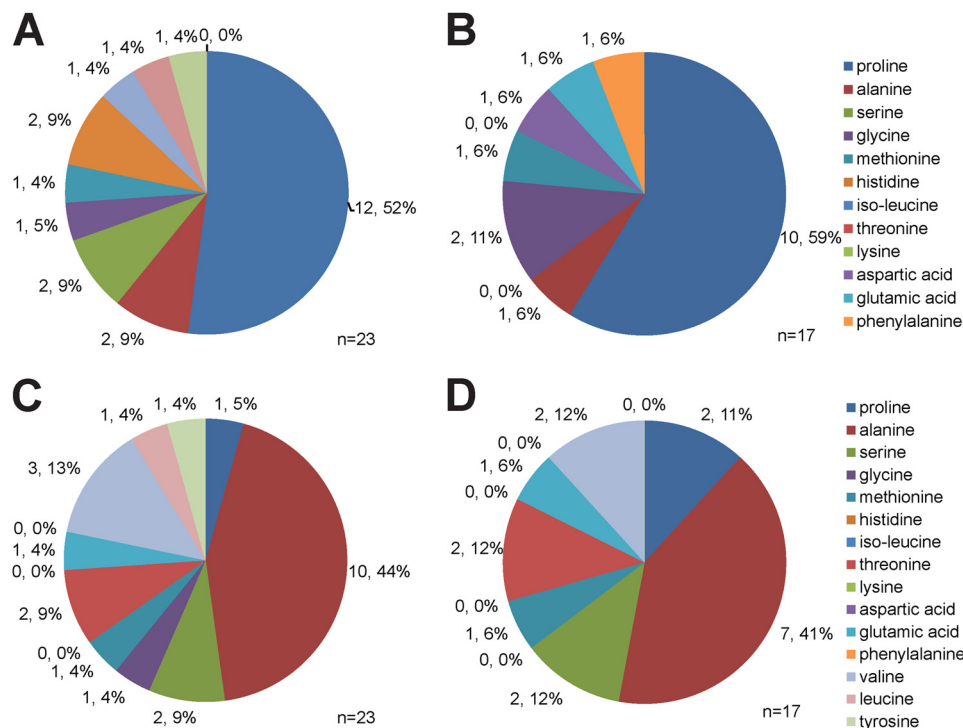


FIGURE 4. **Frequency distribution of residues in P1 and P2 position of DP8 and DP9 candidate substrates.** The frequency distribution of amino acids in the P1 (A and B) and P2 (C and D) position of candidate substrates identified in Table 3 are given for DP8 (A and C) and DP9 (B and D). The exact number of peptides in which each residue is found in the P1 or P2 position is given along with the percentage relating to frequency distribution.

TABLE 3

Confirmed cleavage of DP8 and DP9 substrates

For each substrate, 10 μM of the N-terminal oligopeptide was incubated with 1.7 milliunits of active, purified recombinant DP8 or DP9. Observed molecular mass (Da) was determined from MS spectra acquired 24 h after incubation, nc means not cleaved.

Substrate	Biological Pathway	NH ₂ -terminal oligopeptide	UniProtKB Accession	Molecular Mass (Da)	Expected Molecular Mass (Da) Post-Cleavage	Observed Molecular Mass (Da)	
						DP8	DP9
Acetyl-CoA acetyltransferase, mitochondrial	Fatty acid metabolism	VSKPTLKEVIVSATR	P24752	1727.09	1540.87	nc	nc
Adenylate kinase 2	Purine metabolism	APSVPAAEPEYPK GIR	P54819	1681.89	1512.79	1513.94	1514.01
Bifunctional purine biosynthesis protein PURH	Purine metabolism, One carbon pool by folate	APGQLALFVSDKTLVFEFAR	P31939	2206.55	2038.34	2039.4	2039.5
Calreticulin	Antigen processing and presentation	EPAVYFKEQLDGDGWTSR	P27797	2245.45	2017.95	2019.67	2019.81
Cathepsin Z/X	Lysosome, proteolysis	SPADLPKSWDWRNV DG	Q9UBR2	1843	1658.8	1659.9	1659.9
Collagen-binding protein 2 (Serpin H-1)	Response to unfolded protein	AEVKKPAAAAAPGTAELKSP	P50454	1907.21	1707	nc	nc
C-1-tetrahydrofolate synthase, cytoplasmic	Glyoxylate and dicarboxylate metabolism, One carbon pool by folate,	APAEILNGKEISAIQR	P11586	1709.98	1541.77	1542.8	1542.9
Dihydropyrimidine dehydrogenase [NADP+]	Pyrimidine metabolism,	APVLSKDSADIESILALNPR	Q12882	2109.43	1941.22	1942.3	1942.4
Endoplasmic	NOD-like receptor signaling pathway	DDEVVDVDTVEEDLGKSR	P14625	1978.03	1749.81	nc	nc
Enoyl-CoA hydratase, mitochondrial	Fatty acid metabolism	ASGANFEYIIAEKR GK	P30084	1753.99	1595.82	nc	nc
Heat shock 70 kDa protein 1L	Response to unfolded protein, antigen processing	ATAKGIAIGIDLGTYSYCVG	P34931	1911.21	1739.01	nc	nc
Mitochondrial import receptor subunit TOM34	Protein targeting and import, chaperone	APKFPDSVEELRAAG	Q15785	1586.78	1418.57	1419.6	1419.7
Obg-like ATPase 1	ATP catabolism	PPKGGDGIKPPPIIGR	Q9NTK5	1727.1	1532.86	1533.9	1533.90
Serine/threonine-protein phosphatase 6	Protein dephosphorylation, G1/S transition of mitotic cell cycle	APLDLDKYVEIARLCK	O00743	1847.22	1679.01	1680	1679.6

In comparison with DP8, DP9 more readily cleaved the N-terminal peptide of adenylate kinase 2 (Fig. 5A) demonstrating a probable higher affinity of recombinant DP9 for this substrate *in vitro*. Recombinant DP8 cleaved N-terminal peptides of adenylate kinase 2 and calreticulin with similar kinetics,

whereas DP9 displayed a faster rate of cleavage for the calreticulin N-terminal peptide compared with adenylate kinase 2 (Figs. 5A and 6A). Specificity of DP8/DP9 cleavage was confirmed by performing peptide catalysis reactions in the presence of the nonselective DP inhibitor, Val-Boro-Pro (PT-100/

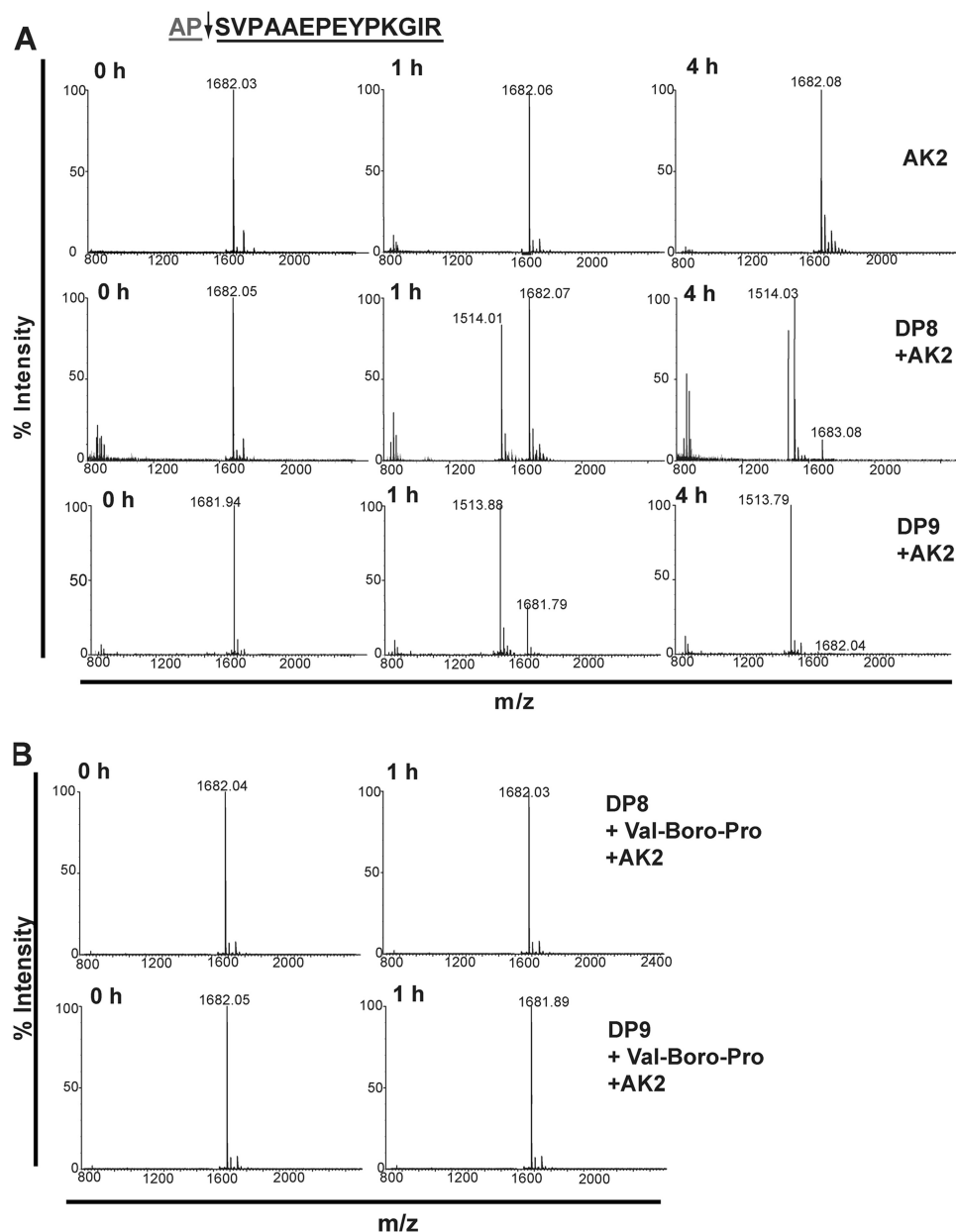


FIGURE 5. DP8 and DP9 cleave the N-terminal peptide of adenylate kinase 2 *in vitro*. The N-terminal peptide of mature adenylate kinase 2 is displayed. The *arrow* indicates the site of DP8/DP9 proteolysis with the *gray text* indicating the dipeptide that is removed following DP8/DP9 proteolysis. *A*, 10 μ M of the adenylate kinase 2 peptide was incubated alone or with 1.7 milliunits of active purified recombinant DP8 or DP9. Samples were collected and stopped with 1% TFA (v/v) final at 0, 1, and 4 h. MS spectra were acquired for noncleaved (m/z) and DP8/DP9-cleaved (m/z) peptides with a mass accuracy of 0.01 to 0.05% error. Theoretical masses of noncleaved and cleaved peptides are 1681.89 and 1512.79 Da, respectively. *B*, specificity of cleavage by DP8/DP9 of these peptides was confirmed by performing catalysis reactions in the presence of 10 μ M of the nonselective DP inhibitor, Val-Boro-Pro (PT-100/Talabostat). Displayed spectra are representatives from three independent cleavage experiments. AK2, adenylate kinase 2.

Talabostat) (Figs. 5B and 6B). Co-localization of DP8- and DP9-EGFP with both adenylate kinase 2 and calreticulin was demonstrated by confocal microscopy (Fig. 7A) confirming physical proximity between protease and substrate. No difference in the localization of either adenylate kinase 2 or calreticulin was detected between the active DP8- and DP9-EGFP cell lines compared with the catalytically inactive DP8(S739A)-EGFP and DP9(S729A)-EGFP cells (data not shown). Immunoblots demonstrated that full-length adenylate kinase 2 and calreticulin are not altered in their expression levels in the DP8- or DP9-EGFP SKOV3 cells lines (Fig. 7B) indicating

that DP8/DP9 proteolysis is unlikely to alter the stability of these two proteins.

DISCUSSION

This is the first cytosol-wide analysis of proteome regulation by DP8 and DP9. In contrast to other studies focused on individual substrates in *in vitro* assays (18, 20, 21), we have utilized TAILS (22), an N-terminally focused negative selection proteomics approach for the first time on a cytoplasmic proteome, to identify *in vivo* DP8 and DP9 substrates. In this study, stable transfected SKOV3 cells were used to identify 23 and 17

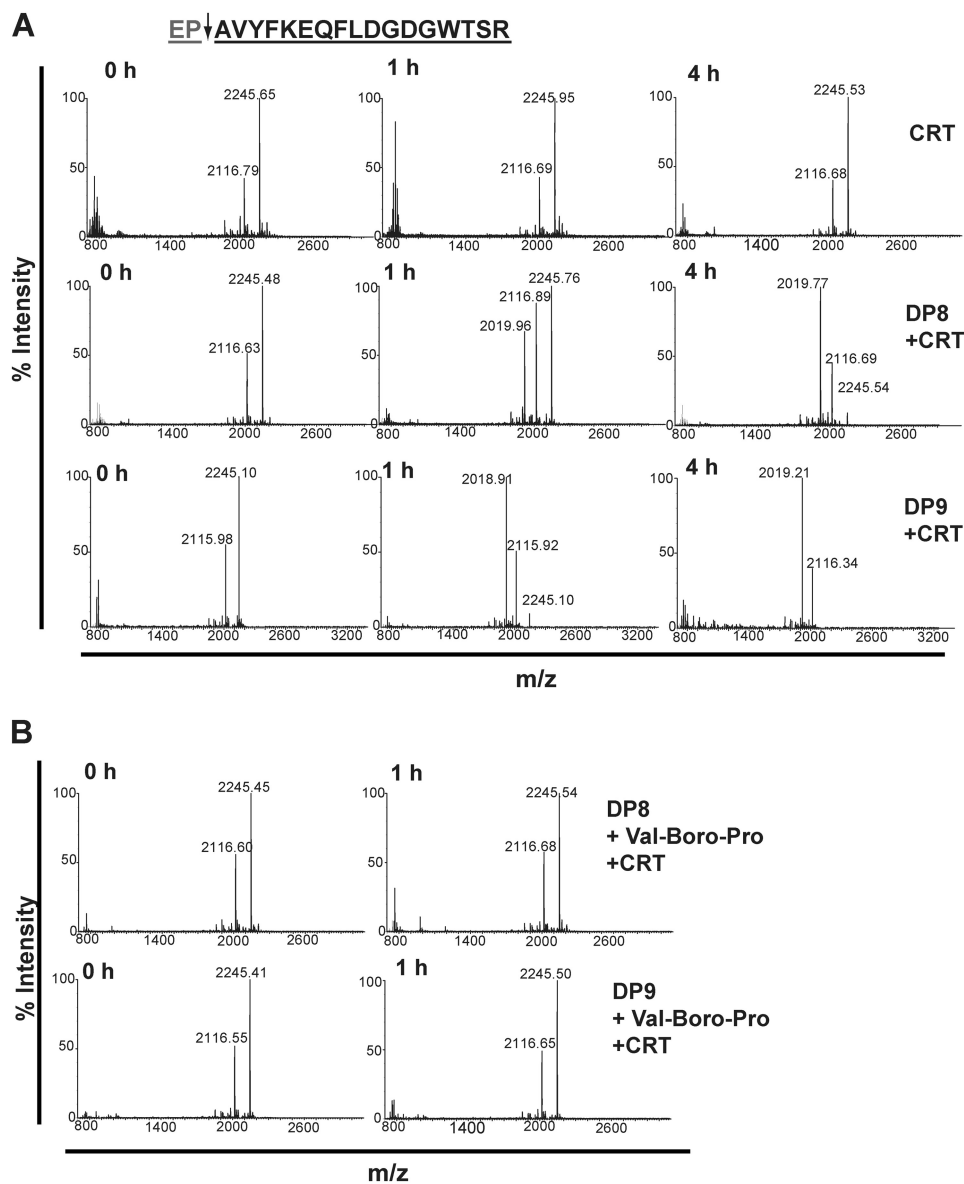


FIGURE 6. DP8 and DP9 cleave the N-terminal peptide of calreticulin *in vitro*. The N-terminal peptide of mature calreticulin is displayed. The *arrow* indicates the site of DP8/DP9 proteolysis, and the *gray text* indicates the dipeptide that is removed following DP8/DP9 proteolysis. *A*, 10 μM of the calreticulin was incubated alone or with 1.7 milliunits of active and purified recombinant DP8 or DP9. Samples were collected and stopped with 1% TFA (v/v) final at 0, 1, and 4 h. MS spectra were acquired for noncleaved (*m/z*) and DP8/DP9-cleaved (*m/z*) peptides with a mass accuracy of 0.01 to 0.05% error. Theoretical masses of noncleaved and cleaved peptides were 2245.45 and 2017.95 Da, respectively. *B*, specificity of cleavage by DP8/DP9 of these peptides was confirmed by performing catalysis reactions in the presence of 10 μM of the nonselective DP inhibitor, Val-Boro-Pro (PT-100/Talabostat). Displayed spectra are representatives from three independent cleavage experiments. *CRT*, calreticulin.

candidate substrates of DP8 and DP9 respectively; 14 of these were selected for *in vitro* validation. Adenylate kinase 2, calreticulin, and seven other substrates were validated as DP8/DP9 substrates. This quantitative analysis identified additional proteins involved in pathways regulated or affected by overexpression of DP8 (20 proteins) and DP9 (45 proteins) enzyme activity. Many of the proteins identified by quantitative analysis and those confirmed as DP8/DP9 substrates are involved in regulating cellular metabolism and energy homeostasis. Thus, this study for the first time reveals potential roles for DP8 and DP9 in cellular metabolic pathways, including glycolysis, gluconeogenesis, fatty acid metabolism, and nucleotide metabolism/biosynthesis. In addition, the involvement of calreticulin in the antigen processing and presentation is consistent with a role for

DP9 proteolysis in preventing cell surface presentation of the major histocompatibility complex class I antigen (21).

Many of the candidate substrates in Table 3 were identified only from peptides with the potential for DP8/DP9 cleavage, with little to no detection of the cleaved peptides. This is likely due to the cleaved peptides being of low abundance or may indicate their rapid degradation following DP8/DP9 truncation. For some targets, contradictory isotopic heavy/light ratios were identified, and discrepancies were observed with ratios between different datasets. These contradictory ratios are probably due to the endogenous enzyme levels of DP8 and DP9 present in all our cell lines. It is likely that background endogenous DP8/DP9 proteolysis also contributes to the identification of overlapping substrates of DP8 and DP9.

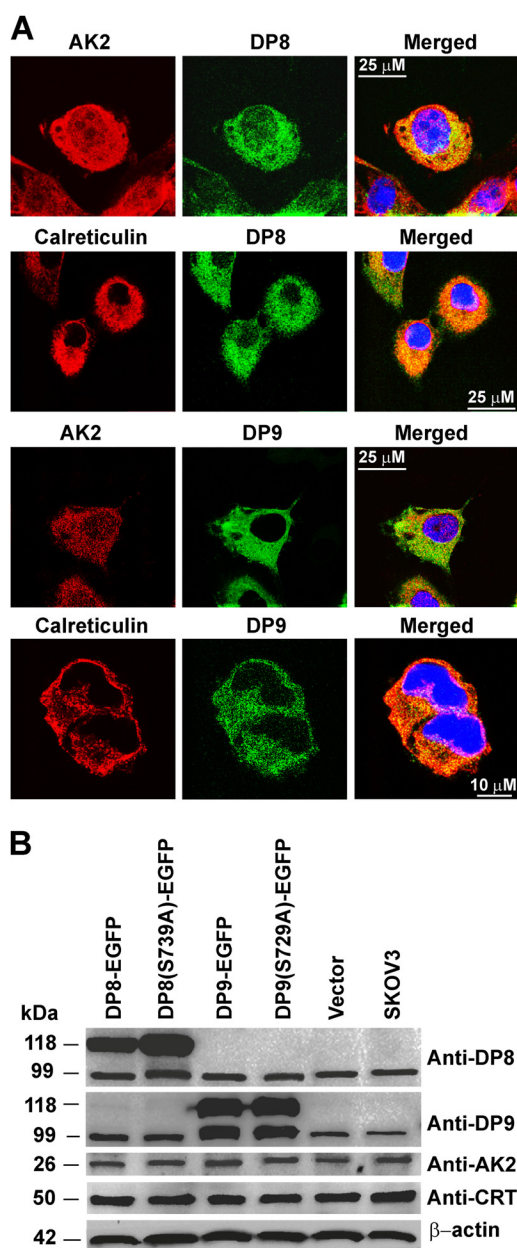


FIGURE 7. Expression and co-localization of adenylate kinase 2 and calreticulin with DP8 and DP9 in SKOV3 cells. *A*, DP8-EGFP- and DP9-EGFP SKOV3-expressing cells lines were analyzed by confocal microscopy and immunofluorescence using anti-calreticulin (1:50) and anti-adenylate kinase 2 (1:50) polyclonal antibodies. As labeled, *red panels* display adenylate kinase 2 or calreticulin, and *green panels* display DP8-EGFP or DP9-EGFP expression. Merged images are shown in the *far right-hand panels*. *B*, cell lysates (25 μ g) from DP8-EGFP, DP8(S739A)-EGFP, DP9-EGFP, DP9(S729A)-EGFP, vector-transfected, and nontransfected SKOV3 cells were analyzed by 10% (w/v) SDS-PAGE and immunoblotting using DP8 (1:5000), anti DP9 (1:5000), calreticulin (1:10,000), adenylate kinase 2 (1:5000), and β -actin (1:10,000) as a loading control. AK2, adenylate kinase 2; CRT, calreticulin.

In Vivo Substrate Specificity of DP8 and DP9—Candidate substrates identified in this study confirm *in vivo* the *in vitro* work of others demonstrating a preference for both DP8 and DP9 to cleave the post-prolyl bond (33–35), with a strong preference for substrates with an Ala in the P2 position followed by Val, Thr, Ser, or Pro residues. Our findings also reveal the potential for DP8/DP9 cleavage to occur after nontypical residues in the P1 position; however, all validated substrates con-

tained a Pro in P1 (Table 3). In addition an *in vivo* preference was observed for the potential cleavage of dipeptides from substrates with an Ala, Lys, Val, Thr, or Gly residue in what would be the P1' position. Roles for P1' and P2' residues in DP8 substrate specificity have been previously suggested following observations of DP8 *in vitro* cleavage of chemokines where DP8 kinetically favored cleavage of chemokines containing Ser in P2' and Leu and Val in P1' (20).

Identification of Noncytoplasmic Substrates—A number of DP8/DP9 substrates and pathway-affected proteins identified in this study are known to be localized in intracellular organelles. Approximately half of the identified DP8 substrate candidates are mature mitochondrial proteins for which a mitochondrial targeting sequence is absent (*e.g.* adenylate kinase 2) or has been removed. These findings suggest that in the DP8 cell lines, there may be increased mitochondrial turnover/degradation resulting in leakage of proteins from autophagosomes (as occurs for acetyl-CoA acetyltransferase (36)) suggesting that DP8 may play a role in mitochondrial homeostasis. Although it may be possible that some nuclear, mitochondrial, and other noncytoplasmic proteins are released upon cell lysis and thus accessible to DP8/DP9 cleavage, it is thought that this was not likely due to the gentle method of cell lysis used in this study, the rapid inclusion of protease inhibitors during lysis, and to the differences in localization of proteins between the DP8 and DP9 datasets.

Adenylate Kinase 2 and Calreticulin as Natural Endogenous DP8 and DP9 Substrates—Co-localization *in vivo* of a protease with its substrate is required for cleavage. By demonstrating this by co-localization studies, it supports the *in vivo* relevance of adenylate kinase 2 and calreticulin as natural substrates of DP8 and DP9. Although determination of the biological importance of the cleavage of adenylate kinase 2 and calreticulin by DP8/DP9 is difficult due to the pleiotropic effects of both adenylate kinase 2 and calreticulin (37), evidence for a potential biological role for DP8/DP9 processing in adenylate kinase 2 and calreticulin function exists in the literature. DP8 and DP9 may play a role in the post-translational modification of adenylate kinase 2, prior to its mitochondrial import, to produce a known variant lacking the N-terminal “MAP” sequence, which has a 2-fold higher activity than the major variant with the Ala-Pro dipeptide intact (38). DP8/DP9 proteolysis of adenylate kinase 2 may also occur following its apoptosis-induced release from the mitochondria, potentially altering its binding affinity to Fas-associated protein with death domain and activation of apoptosis via a novel pathway (39). Calreticulin is known to be retrotranslocated from the endoplasmic reticulum lumen to the cytoplasmic space after removal of its N-terminal signal peptide (residues 1–17) (40). In the cytosol, calreticulin has been shown to undergo post-translational arginylation of the exposed N-terminal aspartic acid residue (41, 42). Under stress conditions, arginylated calreticulin associates with stress granules in a calcium-dependent manner (41). Such a modification would make the N termini of cytosolic calreticulin inaccessible to DP8/DP9; however, under the basal conditions used in our study, no arginylated N-terminal peptides of calreticulin were identified in our datasets (data not shown). Indeed, we did identify DP8/DP9-cleaved N-terminal peptides of calreticulin.

DP8 and DP9 Substrate Discovery

Potentially, DP8/DP9 are involved in regulating the function and subcellular localization of cytoplasmic calreticulin in response to stress. In our study, under basal conditions, no change in calreticulin localization was observed following overexpression of active or catalytically inactive DP8 and DP9; however, under conditions of stress this may be altered.

The N-end rule specifies that the stability of a protein can be affected by the identity of its N-terminal residue (43). Although it is thought possible that DP8/DP9 may be involved in degradation of proline-containing proteins by affecting their stability upon N-terminal cleavage, no increase or decrease in the expression of full-length adenylate kinase 2 or calreticulin was observed in this study following overexpression of DP8 or DP9 (Fig. 7B).

In conclusion, this study has identified and validated a number of biologically important candidate *in vivo* substrates for both DP8 and DP9, both previously enigmatic proteases with only one *in vivo* substrate known. Furthermore, this work has highlighted roles for both of these proteases in cellular energy metabolism and homeostasis. Importantly, adenylate kinase 2 and calreticulin were identified and validated as substrates of both DP8 and DP9. Adenylate kinase 2 plays an important role in maintaining cellular energy homeostasis, and thus DP8/DP9 proteolysis may contribute to regulating cellular energy homeostasis through adenylate kinase 2. TAILS is a powerful proteomic approach for the discovery of protease substrates. The recent use of TAILS in *in vivo* analysis of tissue samples opens the possibility for similar analysis of DPs in the future. For the first time, we have applied TAILS to a cytoplasmic proteome and found the approach to be particularly well suited to the discovery of N-terminal substrates of the exopeptidases DP8 and DP9. This proteomic investigation has identified some unique but largely overlapping roles and substrates for DP8 and DP9, thus paving the way for ongoing investigations into the fundamental roles of DP8 and DP9 in cellular metabolism and homeostasis.

Acknowledgments—We thank Wei Chen, Susanne Perry, the University of British Columbia Centre for Blood Research Mass Spectrometry Suite, and the University of British Columbia Centre Proteomics Core Facility for mass spectrometry operation. We thank Dr. Denise Yu and Associate Professor Mark Gorrell (Centenary Institute, Sydney, Australia) for the pEGFPN1 constructs used for stable transfections. We thank Dr. Sheree Bailey for operation and assistance with flow cytometry performed in this study (Flinders Medical Centre, Adelaide, Australia). We thank the Flinders Analytical Laboratory (Flinders University) for access and use of their Mass Spectrometry Suite.

REFERENCES

1. Abbott, C. A., Yu, D. M., Woollatt, E., Sutherland, G. R., McCaughan, G. W., and Gorrell, M. D. (2000) Cloning, expression, and chromosomal localization of a novel human dipeptidyl peptidase (DPP) IV homolog, DPP8. *Eur. J. Biochem.* **267**, 6140–6150
2. Ajami, K., Abbott, C. A., McCaughan, G. W., and Gorrell, M. D. (2004) Dipeptidyl peptidase 9 has two forms, a broad tissue distribution, cytoplasmic localization, and DP-IV-like peptidase activity. *Biochim. Biophys. Acta* **1679**, 18–28
3. Yu, D. M., Ajami, K., Gall, M. G., Park, J., Lee, C. S., Evans, K. A., McLaughlin, E. A., Pitman, M. R., Abbott, C. A., McCaughan, G. W., and Gorrell, M. D. (2009) The *in vivo* expression of dipeptidyl peptidases 8 and 9. *J. Histochem. Cytochem.* **57**, 1025–1040
4. Olsen, C., and Wagtmann, N. (2002) Identification and characterisation of human DPP9, a novel homologue of dipeptidyl peptidase IV. *Gene* **299**, 185–193
5. Yazbeck, R., Howarth, G. S., and Abbott, C. A. (2009) Dipeptidyl peptidase inhibitors, an emerging drug class for inflammatory disease? *Trends Pharmacol. Sci.* **30**, 600–607
6. Lankas, G. R., Leiting, B., Roy, R. S., Eiermann, G. J., Beconi, M. G., Biftu, T., Chan, C. C., Edmondson, S., Feeney, W. P., He, H., Ippolito, D. E., Kim, D., Lyons, K. A., Ok, H. O., Patel, R. A., Petrov, A. N., Pryor, K. A., Qian, X., Reigle, L., Woods, A., Wu, J. K., Zaller, D., Zhang, X., Zhu, L., Weber, A. E., and Thornberry, N. A. (2005) Dipeptidyl peptidase IV inhibition for the treatment of type 2 diabetes: potential importance of selectivity over dipeptidyl peptidases 8 and 9. *Diabetes* **54**, 2988–2994
7. Reinhold, D., Goihl, A., Wrenger, S., Reinhold, A., Kühlmann, U. C., Faust, J., Neubert, K., Thielitz, A., Brocke, S., Täger, M., Ansorge, S., and Bank, U. (2009) Role of dipeptidyl peptidase IV (DP-IV)-like enzymes in T lymphocyte activation: investigations in DP-IV/CD26-knockout mice. *Clin. Chem. Lab. Med.* **47**, 268–274
8. Ansorge, S., Bank, U., Heimburg, A., Helmuth, M., Koch, G., Tadge, J., Lendeckel, U., Wolke, C., Neubert, K., Faust, J., Fuchs, P., Reinhold, D., Thielitz, A., and Täger, M. (2009) Recent insights into the role of dipeptidyl aminopeptidase IV (DPIV) and aminopeptidase N (APN) families in immune functions. *Clin. Chem. Lab. Med.* **47**, 253–261
9. Schade, J., Stephan, M., Schmiedl, A., Wagner, L., Niestroj, A. J., Demuth, H. U., Frerker, N., Klemann, C., Raber, K. A., Pabst, R., and von Hörsten, S. (2008) Regulation of expression and function of dipeptidyl peptidase 4 (DP4), DP8/9, and DP10 in allergic responses of the lung in rats. *J. Histochem. Cytochem.* **56**, 147–155
10. Yazbeck, R., Sulda, M. L., Howarth, G. S., Bleich, A., Raber, K., von Hörsten, S., Holst, J. J., and Abbott, C. A. (2010) Dipeptidyl peptidase expression during experimental colitis in mice. *Inflamm. Bowel Dis.* **16**, 1340–1351
11. Yu, D. M., Wang, X. M., McCaughan, G. W., and Gorrell, M. D. (2006) Extraenzymatic functions of the dipeptidyl peptidase IV-related proteins DP8 and DP9 in cell adhesion, migration, and apoptosis. *FEBS J.* **273**, 2447–2460
12. Sulda, M. L., Abbott, C. A., Macardle, P. J., Hall, R. K., and Kuss, B. J. (2010) Expression and prognostic assessment of dipeptidyl peptidase IV and related enzymes in B-cell chronic lymphocytic leukemia. *Cancer Biol. Ther.* **10**, 180–189
13. Stremenová, J., Mares, V., Lisá, V., Hilsner, M., Krepela, E., Vanicková, Z., Syrucek, M., Soula, O., and Sedo, A. (2010) Expression of dipeptidyl peptidase-IV activity and/or structure homologs in human meningiomas. *Int. J. Oncol.* **36**, 351–358
14. Wilson, C. H., and Abbott, C. A. (2012) Expression profiling of dipeptidyl peptidase 8 and 9 in breast and ovarian carcinoma cell lines. *Int. J. Oncol.* **41**, 919–932
15. Lu, C., Tilan, J. U., Everhart, L., Czarnecka, M., Soldin, S. J., Mendu, D. R., Jeha, D., Hanafy, J., Lee, C. K., Sun, J., Izycka-Swieszezewska, E., Toretzky, J. A., and Kitlinska, J. (2011) Dipeptidyl peptidases as survival factors in Ewing sarcoma family of tumors. *J. Biol. Chem.* **286**, 27494–27505
16. Overall, C. M., and Blobel, C. P. (2007) In search of partners: linking extracellular proteases to substrates. *Nat. Rev. Mol. Cell Biol.* **8**, 245–257
17. Lange, P. F., and Overall, C. M. (2013) Protein TAILS: when termini tell tales of proteolysis and function. *Curr. Opin. Chem. Biol.* **17**, 73–82
18. Bjelke, J. R., Christensen, J., Nielsen, P. F., Branner, S., Kanstrup, A. B., Wagtmann, N., and Rasmussen, H. B. (2006) Dipeptidyl peptidases 8 and 9: specificity and molecular characterization compared with dipeptidyl peptidase IV. *Biochem. J.* **396**, 391–399
19. Frerker, N., Wagner, L., Wolf, R., Heiser, U., Hoffmann, T., Rahfeld, J. U., Schade, J., Karl, T., Naim, H. Y., Alfalah, M., Demuth, H. U., and von Hörsten, S. (2007) Neuropeptide Y (NPY) cleaving enzymes: structural and functional homologues of dipeptidyl peptidase 4. *Peptides* **28**, 257–268
20. Ajami, K., Pitman, M. R., Wilson, C. H., Park, J., Menz, R. I., Starr, A. E., Cox, J. H., Abbott, C. A., Overall, C. M., and Gorrell, M. D. (2008) Stromal

- cell-derived factors 1 α and 1 β , inflammatory protein-10 and interferon-inducible T cell chemo-attractant are novel substrates of dipeptidyl peptidase 8. *FEBS Lett.* **582**, 819–825
21. Geiss-Friedlander, R., Parmentier, N., Möller, U., Urlaub, H., Van den Eynde, B. J., and Melchior, F. (2009) The cytoplasmic peptidase DPP9 is rate-limiting for degradation of proline-containing peptides. *J. Biol. Chem.* **284**, 27211–27219
 22. Kleifeld, O., Doucet, A., auf dem Keller, U., Prudova, A., Schilling, O., Kainthan, R. K., Starr, A. E., Foster, L. J., Kizhakkedathu, J. N., and Overall, C. M. (2010) Isotopic labeling of terminal amines in complex samples identifies protein N termini and protease cleavage products. *Nat. Biotechnol.* **28**, 281–288
 23. auf dem Keller, U., Prudova, A., Eckhard, U., Fingleton, B., and Overall, C. M. (2013) Systems-level analysis of proteolytic events in increased vascular permeability and complement activation in skin inflammation. *Sci. Signal.* **6**, rs2, 1–15
 24. Prudova, A., auf dem Keller, U., Butler, G. S., and Overall, C. M. (2010) Multiplex N-terminome analysis of MMP-2 and MMP-9 substrate degradomes by iTRAQ-TAILS quantitative proteomics. *Mol. Cell. Proteomics* **9**, 894–911
 25. Schilling, O., and Overall, C. M. (2008) Proteome-derived, database-searchable peptide libraries for identifying protease cleavage sites. *Nat. Biotechnol.* **26**, 685–694
 26. Keller, A., Eng, J., Zhang, N., Li, X. J., and Aebersold, R. (2005) A uniform proteomics MS/MS analysis platform utilizing open XML file formats. *Mol. Syst. Biol.* **1**, 2005.0017
 27. Keller, A., Nesvizhskii, A. I., Kolker, E., and Aebersold, R. (2002) Empirical statistical model to estimate the accuracy of peptide identifications made by MS/MS and database search. *Anal. Chem.* **74**, 5383–5392
 28. Li, X. J., Zhang, H., Ranish, J. A., and Aebersold, R. (2003) Automated statistical analysis of protein abundance ratios from data generated by stable-isotope dilution and tandem mass spectrometry. *Anal. Chem.* **75**, 6648–6657
 29. Keller, U. A., and Overall, C. M. (2012) CLIPPER: An add-on to the transproteomic pipeline for the automated analysis of TAILS N-terminomics data. *Biol. Chem.* **393**, 1477–1483
 30. Dennis, G., Jr., Sherman, B. T., Hosack, D. A., Yang, J., Gao, W., Lane, H. C., and Lempicki, R. A. (2003) DAVID: Database for annotation, visualization, and integrated discovery. *Genome Biol.* **4**, P3
 31. Lange, P. F., and Overall, C. M. (2011) TopFIND, a knowledge-base linking protein termini with function. *Nat. Methods* **8**, 703–704
 32. Pitman, M. R., Menz, R. I., and Abbott, C. A. (2010) Hydrophilic residues surrounding the S1 and S2 pockets contribute to dimerisation and catalysis in human dipeptidyl peptidase 8 (DP8). *Biol. Chem.* **391**, 959–972
 33. Chen, Y. S., Chien, C. H., Goparaju, C. M., Hsu, J. T., Liang, P. H., and Chen, X. (2004) Purification and characterization of human prolyl dipeptidase DPP8 in Sf9 insect cells. *Protein Expr. Purif.* **35**, 142–146
 34. Lee, H. J., Chen, Y. S., Chou, C. Y., Chien, C. H., Lin, C. H., Chang, G. G., and Chen, X. (2006) Investigation of the dimer interface and substrate specificity of prolyl dipeptidase DPP8. *J. Biol. Chem.* **281**, 38653–38662
 35. Tang, H. K., Tang, H. Y., Hsu, S. C., Chu, Y. R., Chien, C. H., Shu, C. H., and Chen, X. (2009) Biochemical properties and expression profile of human prolyl dipeptidase DPP9. *Arch. Biochem. Biophys.* **485**, 120–127
 36. Huth, W., Rolle, S., and Wunderlich, I. (2002) Turnover of matrix proteins in mammalian mitochondria. *Biochem. J.* **364**, 275–284
 37. Michalak, M., Groenendyk, J., Szabo, E., Gold, L. I., and Opas, M. (2009) Calreticulin, a multi-process calcium-buffering chaperone of the endoplasmic reticulum. *Biochem. J.* **417**, 651–666
 38. Schlauderer, G. J., and Schulz, G. E. (1996) The structure of bovine mitochondrial adenylate kinase: comparison with isoenzymes in other compartments. *Protein Sci.* **5**, 434–441
 39. Lee, H. J., Pyo, J. O., Oh, Y., Kim, H. J., Hong, S. H., Jeon, Y. J., Kim, H., Cho, D. H., Woo, H. N., Song, S., Nam, J. H., Kim, H. J., Kim, K. S., and Jung, Y. K. (2007) AK2 activates a novel apoptotic pathway through formation of a complex with FADD and caspase-10. *Nat. Cell Biol.* **9**, 1303–1310
 40. Afshar, N., Black, B. E., and Paschal, B. M. (2005) Retrotranslocation of the chaperone calreticulin from the endoplasmic reticulum lumen to the cytosol. *Mol. Cell. Biol.* **25**, 8844–8853
 41. Decca, M. B., Carpio, M. A., Bosc, C., Galiano, M. R., Job, D., Andrieux, A., and Hallak, M. E. (2007) Post-translational arginylation of calreticulin: a new isospecies of calreticulin component of stress granules. *J. Biol. Chem.* **282**, 8237–8245
 42. Carpio, M. A., López Sambrooks, C., Durand, E. S., and Hallak, M. E. (2010) The arginylation-dependent association of calreticulin with stress granules is regulated by calcium. *Biochem. J.* **429**, 63–72
 43. Varshavsky, A. (1996) The N-end rule: functions, mysteries, uses. *Proc. Natl. Acad. Sci. U.S.A.* **93**, 12142–12149